UNIFICATION AND PHYSICS BEYOND THE STANDARD MODEL

By

SAKI AHMED KHAN

Bachelor of Science (Hons.) in Physics
University of Dhaka
Dhaka, Bangladesh
2007

Diploma in Theoretical High Energy Physics
International Centre for Theoretical Physics
Trietse, Italy
2009

Submitted to the Faculty of the
Graduate College of the
Oklahoma State University
in partial fulfillment of
the requirements for
the Degree of
DOCTOR OF PHILOSOPHY
July, 2016

UNIFICATION AND PHYSICS BEYOND THE STANDARD MODEL

Dissertation Approved:

Rgnts Prof. Kaladi S. Babu

Dissertation Advisor

Rgnts Prof. Satyanarayan Nandi

Rgnts Prof. John W. Mintmire

Prof. Birne Binegar

ACKNOWLEDGMENTS

I would like to express my deepest appreciation to my thesis advisor and the chair of my graduate thesis committee, Prof. Kaladi S. Babu for his guidance, patience, endless support and inspiration. His valuable advice and constructive criticisms were absolute necessities for the materialization of my thesis. I feel myself honored to have an accomplished, knowledgeable and experienced mentor like him. His attitude towards research: lack of prejudice, his open-minded approach towards any intriguing idea irrespective of it being mainstream or non-mainstream, yet a clear preference to be rooted in realistic and well-motivated physics models; really inspired me to accept him as a mentor in the truest form. I am certain of his positive influence on me for the rest of my scientific career.

My sincere appreciation extends to Prof. Satya Nandi for his support and guidance during my doctoral study. His insights and suggestions were an integral part of my decision making process on multiple occasions. I would like to thank Prof. John W. Mintmire who was the Department Chair during my doctoral studies for his continual support by providing valuable advice along with highly appreciated teaching assistantships. This financial support has helped me complete my thesis without any additional stress.

I would like to thank all of my astute committee members, Prof. Kaladi babu, Prof. Satya Nandi, Prof. John Mintmire and Prof. Birne Binegar for their critical insights and invaluable suggestions in my research. Special thanks to all for the encouragement, collegial attitude and moral support for my graduate research. Heartfelt thanks for their valuable time to review my dissertation.

I would like to thank all the scientists who has collaborated and contributed in my research work. In particular, I want to acknowledge the collaborations with Dr. Ilia Gogoladze, Dr. Michal Malinsky, Dr. Takeshi Fukuyama and Dr. Zurab Tavartkiladze. I would like to thank Shaikh Saad who is one of my collaborator, my fellow graduate researcher and my old friend from back home. I would like to thank Dr. Ayon Patra for so many long discussions about research, teaching and other stuffs. Special thanks goes to all the fellow graduate students of department of physics specially the ones from the high energy physics group Dr. Durmus Karabacak and Dr. Julio Julio from whom I have learned a lot.

I would like to thank the department of physics for giving me the opportunity to pursue my

research work in this department. I am deeply grateful to faculty members, staff members and colleagues at the department for their unconditional supports and maintenance of a conducive environment. This has helped me tremendously to continue and finish my graduate work with passion and efficiency. I am morally indebted to the department for financial assistance throughout my graduate study and endorse me for various awards during this time. This has definitely heightened my confidence as a researcher as well as future mentor. My special thanks to the staff members of the department office for taking care of all my due paper works and helping me to carry on my graduate research with full attention. I would also like to thank Dr. Joseph Haley for his friendly advice, encouragements and critical insights that have aided in improving my professional and communication skills as a researcher.

Most importantly, I would like to thank my wife for her unconditional support and her belief in me. I would like to thank my daughter for her presence in my life which has been an eternal source of strength to confront any obstacle in life. I would like to remember my late father Sarwar Alam Khan and my late elder brother Shaafi Ahmed Khan for their endless love, absolute support and indubitable belief in me in pursuit of my research career. They have inspired me throughout their life as well as after and I am here today because of them. I thank my mother for her patience, perseverance and encouragement throughout this long journey filled with challenges.

Finally, I would like to thank everyone who has either supported or inspired me to accomplish my graduate research goal. [1]

[1] Acknowledgments reflect the views of the author and are not endorsed by committee members or Oklahoma State University

Name: Saki Khan

Date of Degree: JULY, 2015

Title of Study: UNIFICATION AND PHYSICS BEYOND THE STANDARD MODEL

Major Field: Physics

Abstract: In this dissertation, I study physics beyond the standard model of particle physics with a particular focus on unification. $SO(10)$ grand unified theories (GUTs) provide such a framework. Chapter 2 is devoted to construction of a minimal version of such models which has the potential to describe all physics below GUT energy scale. I study the evolution of gauge couplings in a minimal renormalizable $SO(10)$ model with threshold corrections and conclude that the model generally predicts an upper bound of few times 10^{35} yrs for proton lifetime, which is not too far from the present Super-Kamiokande limit of $\tau_p \gtrsim 1.4\times10^{34}$ yrs. The branching ratios for proton decay are also calculable with the leading modes being $p \to e^+\pi^0$ and $p \to \overline{\nu}\pi^+$. Chapter 3 involves the implication of a mechanism known as radiative electroweak symmetry breaking where loop corrections to the mass parameter of the Higgs triggers the electroweak symmetry breaking. Several simple extensions of Standard model have the proper ingredients to perform radiative electroweak symmetry breaking and they can have negative Higgs mass parameter in low energy while the mass parameter is positive at high energy. It is also shown that for each case, the potential remains bounded and the theory remains in perturbative regime. Chapter 4 is dedicated to the flavor puzzle of standard model where the maximal subgroup of global flavor group of fermions of SM has been gauged and subsequently broken down in such a manner that the flavor constraints are not violated. In such a model one can find a scalar particle of 750 GeV mass which can decay in the diphoton channel providing an explanation of the recently reported diphoton excess. In Chapter 5, I investigate several dark matter candidates in the context of $SO(10)$ GUT as the $\mathbb{Z}_2$ symmetry makes the dark matter absolutely stable. Such a $\mathbb{Z}_2$ symmetry is natural in $SO(10)$ GUTs as it shows up as a remnant of $B-L$ generator. Here I find that fermionic singlet together with a scalar singlet can be viable dark matter candidate. Other options like fermionic 10-plet with or without a fermionic singlet can also be suitable dark matter candidate and such scenarios should be experimentally detectable in near future.

TABLE OF CONTENTS

Chapter Page

1 INTRODUCTION 1

1.1 The Standard Model of Particle Physics 1

1.1.1 Structure of SM 2

1.1.2 Limitation of SM 6

1.1.3 Organisation of this Dissertation 13

REFERENCES 15

2 A MINIMAL NON-SUPERSYMMTRIC SO(10) MODEL: GAUGE COUPLING UNIFICATION, PROTON DECAY AND FERMION MASSES 18

2.1 Introduction 18

2.2 The Model 20

2.2.1 Choice of the Higgs sector 21

2.2.2 Associated Energy Scales 22

2.3 Running of gauge couplings using two loop Renormalization Group Equations 23

2.4 Threshold corrections 27

2.5 Proton Lifetime 31

2.6 The $54_H + 126_H$ Higgs Model for $SO(10)$ symmetry breaking 35

2.6.1 Details of Symmetry Breaking 37

2.6.2 Tree level mass spectrum 38

2.7 Yukawa sector of the model 43

2.8 Technical Details 45

2.9 Results with Benchmark points 47

2.10 Proton decay branching ratios 54

2.11 Axions as Dark Matter 58

2.12 Conclusion 61

REFERENCES 63

3 RADIATIVE ELECTROWEAK SYMMETRY BREAKING OF STANDARD MODEL EXTENSIONS **69**

3.1 Introduction . . . 69

3.2 Type-II seesaw neutrino mass model . . . 70

3.2.1 The model . . . 71

3.2.2 The stability conditions and the evolution of mass parameters . . . 72

3.2.3 Complete set of RGEs for Type-II neutrino mass model . . . 73

3.2.4 Solution to the RGEs . . . 74

3.3 Two-loop neutrino mass model . . . 74

3.3.1 The Model . . . 76

3.3.2 The stability conditions and the evolution of mass parameters . . . 77

3.3.3 Complete set of RGEs for Two-loop neutrino mass model . . . 78

3.3.4 Solution to the RGEs . . . 78

3.4 Inert doublet model . . . 79

3.4.1 The model . . . 80

3.4.2 The stability conditions and the evolution of mass parameters . . . 81

3.4.3 Complete set of RGEs for Inert doublet model . . . 82

3.4.4 Solution to the RGEs . . . 83

3.5 Extension of SM by a real scalar singlet . . . 84

3.5.1 The model . . . 84

3.5.2 The stability conditions and the evolution of the mass parameters . . . 85

3.5.3 Complete set of RGEs for Extension of SM with a scalar singlet . . . 86

3.5.4 Solution to the RGEs . . . 86

3.6 Vector-like fermion model . . . 87

3.6.1 The model . . . 88

3.6.2 The stability condition and the evolution of the mass parameters . . . 90

3.6.3 Complete set of RGEs for vector-like fermion model . . . 91

3.6.4 Solution to the RGEs . . . 92

3.7 Conclusion . . . 93

REFERENCES **94**

4 An $O(3)_L \times O(3)_R$ FLAVOR GAUGE SYMMETRY NEAR TEV SCALE **97**

4.0 Short Review of SM Flavor Physics . . . 97

4.1 Introduction . . . 99
4.2 The model(s) . . . 101
4.3 Model with a bi-fundamental . . . 102
4.3.1 The $O(3)_L \times O(3)_R$ flavor symmetry and the EW symmetry breaking . . . 103
4.3.2 The $D_{3L} \times D_{3R}$ flavor symmetry breaking . . . 106
4.3.3 The Yukawa Lagrangian . . . 108
4.4 Explaining the 750 GeV di-photon signal . . . 110
4.5 Model with the fundamentals . . . 112
4.6 Conclusion . . . 120

REFERENCES **121**

5 DARK MATTER IN SO(10) GUTs **122**
5.1 Introduction . . . 122
5.2 Discrete symmetries in $SO(10)$ . . . 123
5.3 DM candidates in $SO(10)$ GUTs . . . 124
5.4 The fermionic singlet DM in SO(10) GUTs . . . 125
5.4.1 The thermal abundance of singlet fermionic dark matter . . . 126
5.4.2 The extra scalar singlet . . . 128
5.5 The fermionic 10-plet DM in SO(10) GUTs . . . 129
5.6 Conclusion . . . 132

REFERENCES **133**

6 SUMMARY AND CONCLUSIONS **135**

LIST OF FIGURES

Figure Page

1.1 Standard Model: Particle content and interactions 4

1.2 Rotation curve of a typical spiral galaxy: predicted and observed. Dark matter can explain the 'flat' appearance of the velocity curve out to a large radius [24] 11

1.3 (a)The Bullet Cluster: Hubble Space Telescope image with overlays. The total projected mass distribution reconstructed from strong and weak gravitational lensing is shown in blue, while the X-ray emitting hot gas observed with Chandra X-ray Observatory is shown in red. (b)Mass density contours of the bullet cluster superimposed over photograph taken with Hubble Space Telescope. (Source: Wikipedia) 11

2.1 $SO(10)$ symmetry breaking pattern with a Higgs sector consisting of $54_H + 126_H + 10_H$. 22

2.2 Running of gauge couplings without threshold corrections using two-loop RGE. Pati-Salam symmetry with D parity is assumed as the intermediate scale. The dotted vertical lines correspond to the intermediate scale and the unification scale. 27

2.3 Running of gauge couplings with one-loop threshold corrections using two-loop RGE. This sample point corresponds to a case where some of the Higgs masses are taken to be two times the corresponding gauge boson mass determined without the threshold corrections and the others are one tenth of the scale. Special attention was given to the color triplet masses, so that they are heavier than 10^{13} GeV. In this extreme scenario, the mass of the leptoquark gauge boson (the one responsible of proton decay) is maximized. Then the scales were updated with an iteration process so that the scales correspond to the masses of the respective gauge bosons. 32

2.4 Proton lifetime (τ_p) as a function of the intermediate scale M_I for different levels of threshold corrections. The ratio of the mass of each Higgs boson to the corresponding gauge boson mass is kept in between $R = \{1/10, 1/20, 1/33\}$ and $R = 2$, with $R = \frac{M_{\text{Higgs boson}}}{\text{Corresponding gauge boson mass}}$. All the black points are phenomenologically viable ones. Orange points either go through gauge boson mediated proton decay with a lifetime shorter than the experimental limit (1.29×10^{34} yrs), or they correspond to scenarios where at least one of the color triplet Higgs boson acquires a mass less than 10^{13} GeV. From a conservative point of view, we decided to exclude points with light color triplet masses as they tend to contribute to proton decay at a dangerous level. 34

2.5 (a) Evolution of gauge couplings using one-loop RGE with threshold corrections determined by the scalar mass spectrum given in Table 2.3. The unification scale determined here is compatible with the current experimental limit on proton lifetime. The small black circles correspond to the various scalar masses changing the β function coefficients and inflicting changes in the slope of the graphs. The vertical dashed lines correspond to gauge boson masses that stay at intermediate scale and unification scale. (b) The region where the scalar bosons show up has been zoomed. 49

2.6 Evolution of gauge couplings using two-loop RGE with threshold corrections. The unification scale determined here is compatible with the current experimental limit on proton lifetime. The discontinuity in the running of the gauge couplings is due to the threshold corrections determined using the scalar mass spectrum given in Table 2.5. The vertical dashed lines correspond to the intermediate scale and unification scale. 54

2.7 Scatter plot for the proton lifetime (τ_p) vs. $\langle 126_H \rangle = \sigma$ generated using one-loop RGE. All the points correspond to proper gauge couplings unification and are compatible with realistic fermion masses and mixings. Only the black points comply with the current experimental limit of proton lifetime. 55

2.8 Scatter plot for proton lifetime (τ_p) as a function of the color octet mass ($M_{\phi_{10}}$) generated using one-loop RGE. All the points correspond to proper gauge couplings unification and compatible with realistic fermion masses and mixings. Only the black points comply with the current experimental limit on proton lifetime. Fine-tuning the octet mass to a lower energy scale does not create any internal inconsistency or phenomenological issue. But the extra fine-tuning does mean that one is deviating significantly from the extended survival hypothesis or equivalently minimal fine-tuning condition. That is why we consider highly fine-tuned octet mass which corresponds to a high a proton lifetime as not a likely scenario. 56

2.9 Proton Lifetime(τ_p) vs ratio of the $({}^{k_1}/_{k_2} - 1) \times 10^5$. The plot indicates that the ratio of ${}^{k_1}/_{k_2} = {}^{M_{(X',Y')}}/_{M_{(X,Y)}}$ varies less than 0.02% (0.005%) over the whole (phenomenologically viable) parameter space. 58

2.10 The region in the parameter space where cold ADM saturates the dark matter abundance. 60

3.1 Diagrammatic representation of Type-II seesaw 71

3.2 One loop running of the parameters of Type-II seesaw model upto Plank scale. The black dashed line in Fig. 3.2a corresponds to the scale, $\mu_r = \mu_\Delta$. 75

3.3 Feynman Diagram responsible for neutrino mass generation at two-loop level. 76

3.4 One loop running of the parameters of Two-loop neutrino mass model upto Planck scale. The black dashed line corresponds to the scale, $\mu_r = \mu_0$. Here μ_0 is the energy scale corresponding to the lightest of the newly introduced particles. In this sample point $\mu_o = \mu_k$. 80

3.5 Diagrammatic representation of neutrino mass generation in the scotogenic model . 82

3.6 One loop running of the parameters of Inert doublet model upto Planck scale. The black dashed line corresponds to the scale, $\mu_r = \mu_2$. 85

3.7 One loop running of the parameters of SM with an extension by a real scalar singlet upto Planck scale. The black dashed line corresponds to the scale, $\mu_r = \mu_s$. 87

3.8 Running of the SM Higgs quatic coupling in the extension of SM by a real scalar singlet. 88

3.9 One loop running of the couplings and mass parameters of vector-like fermion model. The black dashed line corresponds to the scale, $\mu_r = \mu_s$. 93

4.1 Feynman diagram for effective quartic coupling 107

4.2 Feynman diagram for the correction of strange and bottom quark masses 109

4.3 Production of 750 GeV scalar. 110
4.4 Decay of ψ_{11} field to di-photon. 111
4.5 Decay width for the process $\boldsymbol{S} \to \gamma\gamma$ for the cases (i) when four charged scalars contribute in Eq. (4.36) (left) and (ii) when all the charged scalars contribute (right). The vev of ψ_{11} is fixed to 100 GeV. 112
4.6 Production cross section $\times$ the branching ratio for the cases (i) when four charged scalars contribute in Eq. (4.36) (left) and (ii) when all the charged scalars contribute (right). The vev of ψ_{11} is fixed to 100 GeV. 112

5.1 Feynman diagram for loop correction to the mass of $\psi(1,3,0)$ from $\mathbf{45_F}$ 125
5.2 Feynman diagram of DM decaying into SM particles 129
5.3 Feynman diagram of radiative correction to dark matter mass, where dark matter is a fermionic weak doublet 130
5.4 Feynman diagram of color triplet from 10_F decaying into DM 130

LIST OF TABLES

Table Page

2.1 Decomposition of the scalar representations with respect to various $SO(10)$ subgroups. The "scale" indicates expectation based on extended survival hypothesis. The Higgs multiplets in red (or bold) are the massless Goldstone bosons which are absorbed by the corresponding gauge bosons. 24

2.2 Sample parameters and vev's to generate a benchmark point using one-loop RGE. The initial parameter and the vev values were updated through the iteration processes described in the text, and the listed values correspond to the final stable point. . . . 50

2.3 Sample scalar mass spectrum corresponding to the benchmark point generated using one-loop RGE. The value of the parameters and vev's used to generate the spectrum is given in Table 2.2. 51

2.4 Sample parameters and vev's to generate benchmark point using two-loop RGE. The initial parameters and the vev's were updated through the iteration processes described in the text, and the listed values correspond to the final stable point. 52

2.5 Sample scalar mass spectrum corresponding to the benchmark point generated using two-loop RGE. The value of the parameters and vev's used to generate the spectrum is given in Table 2.4. 53

2.6 The branching ratio of proton decay by gauge mediated $d = 6$ operator. 58

3.1 Quartic coupling and mass parameter values for the sample point used for the Type-II seesaw model in Fig. 3.2. 75

3.2 Quartic and Yukawa coupling and mass parameter values for the sample point used for the Two-loop neutrino mass model in Fig. 3.4 79

3.3 Quartic coupling and mass parameter values for the sample point used for the Inert doublet model in Fig. 3.6 84

3.4 Quartic coupling and mass parameter values for the sample point used for the extension of SM by a real scalar singlet in Fig. 3.7 87

3.5 Particle content of the vector-like fermion model 89

3.6 Quartic coupling and mass parameter values for the sample point used for the vector-like fermion model in Fig. 3.9 93

4.1 List of flavored fermions of SM 97

5.1 List of irreducible representation of $SO(10)$ 123

5.2 The $SO(10)$, Lorentz and the $B - L$ parity quantum numbers in the simple $SO(10)$ GUT models under consideration. The matter singlet at the bottom is the DM candidate as the combination of the statistics with the $\mathbb{Z}_2^{B-L}$ parity make it absolutely stable. 126

5.3 The basic scattering/annihilation processes underwent by 1_F in the early Universe under the supervision of the Lagrangian (5.5). 126

CHAPTER 1

INTRODUCTION

1.1 The Standard Model of Particle Physics

The Standard Model (SM) emerged in the early seventies [1, 2, 3] when particle physics was being struck by a new generation of conundrums, specially the four fermion weak interaction theory encountering incurable divergences and the failure to apply perturbation theory to strong interaction to do any practical calculation. The foundation of SM was based upon the understanding of symmetry, both global (like Lorentz symmetry) and local (like gauge symmetry), and renormalizability of quantum field theory.

The journey towards one of the most successful models of particle physics began with the slow understanding of symmetry principles. While Lorentz invariance of space and time indicated the simplicity of nature at the deepest level, it was realized that different interactions were governed by different internal symmetries among which most were not even exact. But it was not this "Global" symmetry, but the "Local" symmetry that proved to be the most powerful one. Under this $U(1)$ Gauge (local) transformations the electric field experiences a phase change that can vary independently at different space-time points, while the electromagnetic vector potential undergoes a corresponding gauge transformation [4]. This was the crucial idea upon which Quantum Electrodynamics was developed. In the seminal paper, published in 1954, Yang and Mills extended this idea to non-Abelian groups like $SU(2)$ [5]. The implication of Yang-Mills theory in the field of weak or strong interaction was impeded by the fact that gauge symmetry forbids the gauge bosons to possess any mass, while presence of any massless gauge boson would give rise to some new long range force which was ruled out by cosmological consideration alone.

The concept of spontaneous symmetry breaking that there can be symmetries of the Lagrangian which are not respected by the vacuum itself became the savior. For every generator of the global symmetry group broken spontaneously there exist a massless boson, known as "Goldstone boson" [6]. But the most interesting and important feature of this concept is that when the symmetry is a local one, the Goldstone boson turns into the helicity zero part of a gauge boson, which in

turn becomes massive [7]. So, in SM we need a scalar particle known as Higgs, which is a doublet under $SU(2)$ group. It is this scalar field whose non-zero vacuum expectation value (vev) broke the symmetry spontaneously and gave masses to the gauge bosons. It is not enough to give masses to the gauge boson only. In SM, the fermions, the leptons and the quarks also acquire masses through Yukawa interactions with this Higgs boson. This important ingrediant of SM was discovered in the Large Hadron Collider (LHC) in 2012 [8, 9].

About the issue of renormalizability, it was t'Hooft in 1971 who used path integration to define a gauge (known as t'Hooft Gauge) in which the theory was eventually proven to be renormalizable in all orders of perturbation [10]. In the strong interaction sector, in 1973 Gross, Wilczek and Politzer independently found that the non-Abelian gauge theories have a remarkable property currently known as Asymptotic Freedom [11, 12]. The absence of both free quarks and gluons are explained by a strange property of strong interaction known as color confinement, which states that color charged particles cannot be isolated singularly, and therefore cannot be directly observed.

Then almost for three decades the SM was brushed and polished by a great number of theoretical and experimental efforts. It managed to give many successful predictions like existence of neutral currents and the masses of $W^{\pm}$ and Z bosons which were tested by experiments. The enormous success of the standard model indicates the fact that the ultimate theory of particle physics should not be very different from what we currently have. Even though we have strong reason to go beyond SM, we can never discard this wonderful theory.

1.1.1 Structure of SM

The symmetry group (G_{SM}) under which the SM is invariant is given by

$$G_{SM} = SU(3)_C \times SU(2)_L \times U(1)_Y \tag{1.1}$$

which is spontaneously broken into the group G_{BR}

$$G_{BR} = SU(3)_C \times U(1)_Q \tag{1.2}$$

So every field of the SM is associated with a gauge transformation:

$$\psi \to V\psi; \qquad \phi \to V\phi; \qquad A_\mu \to VA_\mu V^\dagger - \frac{i}{g}(\partial_\mu V)V^\dagger \tag{1.3}$$

where $V = e^{i\alpha^a T^a} e^{i\beta^b R^b} e^{i\gamma Y}$. T^a's ($a = 1 \cdots 8$) are the generators of color gauge group $SU(3)_C$. The strong force is mediated by gluons which transform under the adjoint representation of $SU(3)_C$ while

the (anti) fermions (like (anti)quarks) transforming under (anti) fundamental representation respond to strong force. Particles immune to strong force like leptons transform as singlets under $SU(3)_C$ group. R^b's are the three generators of $SU(2)_L$ which correspond to three gauge bosons mediating weak force. Y is the generator of the Abelian group U(1) known as "Hypercharge". The hypercharge assignment is dictated by the corresponding electrical charge by the relation, $Q = I_{3L} + Y$ where I_{3L} is the third component of isospin of the group $SU(2)_L$. The kinetic terms of the gauge bosons are given by:

$$\mathcal{L}_{gb} = -\frac{1}{4}B_{\mu\nu}B^{\mu\nu} - \frac{1}{2}W^b_{\mu\nu}W^{b\mu\nu} - \frac{1}{2}G^a_{\mu\nu}G^{a\mu\nu} \tag{1.4}$$

where

$$F^a_{\mu\nu} = \partial_\mu A^a_\nu - \partial_\nu A^a_\mu + g f^{abc} A^b_\mu A^c_\nu. \tag{1.5}$$

Here $F^a_{\mu\nu}$ is the field strength tensor for the corresponding gauge field $A_m u^a$. g is the gauge coupling and f^{abc}'s are the structure constants of the gauge groups.

The fermion fields of the SM along with their SM quantum numbers are denoted by:

$$\begin{gathered} Q_{iL}(3,2,{}^1\!/_6) = \begin{pmatrix} u_{iL} \\ d_{iL} \end{pmatrix}; \qquad \ell_{iL}(1,2,-{}^1\!/_2) = \begin{pmatrix} \nu_{iL} \\ e_{iL} \end{pmatrix}; \\ u_{iR}(\overline{3},1,-{}^2\!/_3); \qquad d_{iR}(\overline{3},1,{}^1\!/_3); \qquad e_{iR}(1,1,1); \end{gathered} \tag{1.6}$$

where $i = 1-3$ denotes the generation and

$Q_L \rightarrow$ Left-handed quark doublet; $\quad \ell_L \rightarrow$ Left-handed lepton doublet

$u_R \rightarrow$ right-handed up-type quark singlet; $\quad d_R \rightarrow$ right-handed down-type quark singlet

$e_R \rightarrow$ right-handed charged lepton singlet

A very important feature of the fermion content of SM is that the left- and right-chiral components belong to different representation of the weak group $SU(2)_L$. One aspect of this distinction between left- and right-components is preventing the Lagrangian from containing an explicit mass term as it fails to be gauge invariant. To see this explicitly one can write gauge transformation of a fermion ψ which has a mass m:

$$m\overline{\psi}\psi = m\left(\overline{\psi_L}\psi_R + \overline{\psi_R}\psi_L\right) \rightarrow \; m\left(\overline{\psi_L}V_L^\dagger V_R\psi_R + \overline{\psi_R}V_R^\dagger V_L\psi_L\right). \tag{1.7}$$

This term is not gauge invariant as for a model with chiral fermion ie. for which left and right components of the fermion are not in the same representation, $V_L^\dagger V_R \neq 1$. So, the fermion part of the SM Lagrangian can be written as:

$$\mathcal{L}_f = \sum_f \; i\,\overline{f}\gamma_\mu D^\mu f \tag{1.8}$$

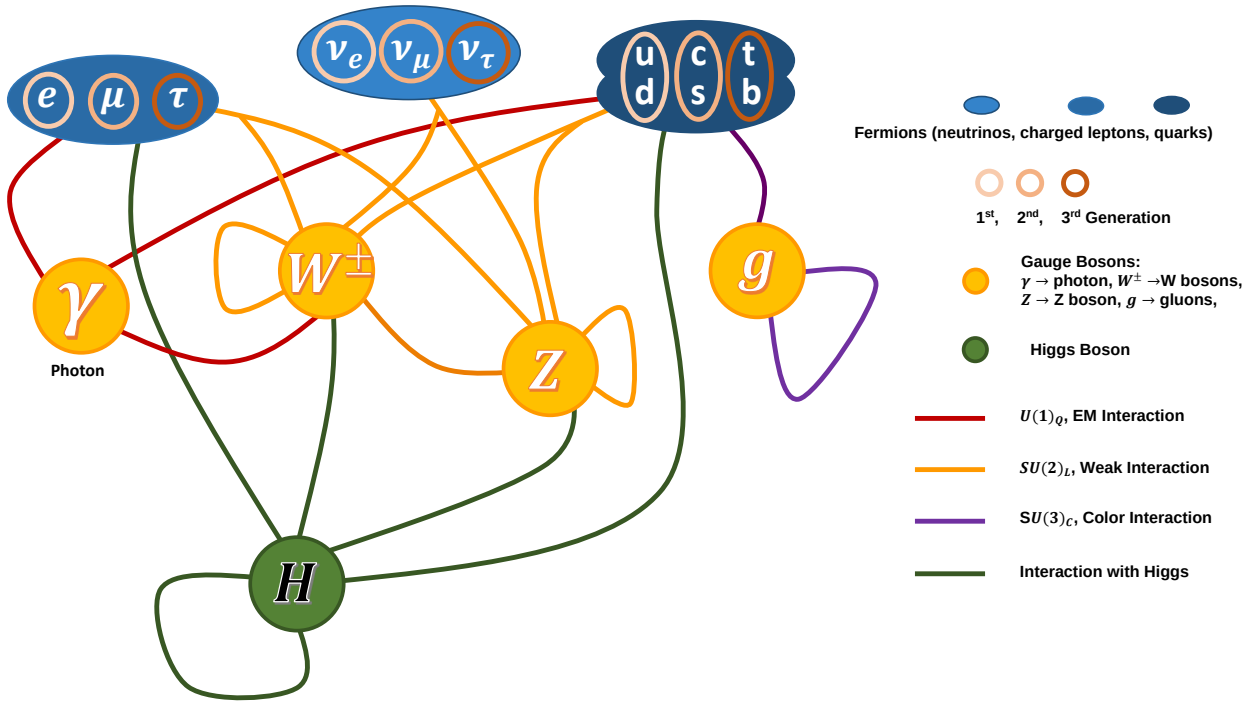

Figure 1.1: Standard Model: Particle content and interactions

where D^μ is the covariant derivative and is given by:

$$D^\mu \rightarrow \partial^\mu + ig_1 Y B^\mu + ig_2 A^\mu + ig_3 G^\mu. \tag{1.9}$$

Explicit mass terms for the gauge bosons are also not invariant under gauge transformation and is absent from Eq. (1.4). So, the gauge bosons in such a model have to be massless, which is not an issue for the case of massless photon or gluons, but the massive gauge bosons $W^\pm$ and Z for the weak interaction create a major dilemma.

To circumvent the apparent lack of mass in the theory, SM takes advantage of spontaneous symmetry breaking with the Higgs mechanism. A complex spin zero scalar field known as the "Higgs boson" which transform as

$$H(1, 2, 1/2) = \begin{pmatrix} H^+ \\ H^0 \end{pmatrix} \tag{1.10}$$

under SM gauge group is introduced to generate masses of all particles. The Higgs boson adds a potential to the SM Lagrangian which unlike chiral fermions contains explicit mass term.

$$V(H) = -\mu^2 H^\dagger H + \lambda (H^\dagger H)^2 \tag{1.11}$$

Spontaneous symmetry breaking happens when the mass parameter of such a mass term is negative as the minimum of the potential gets shifted to a non-zero value ($\langle H \rangle \equiv \sqrt{\frac{\mu^2}{2\lambda}} = \frac{v}{\sqrt{2}}$) and the vacuum fails to respect the corresponding gauge symmetry. v is known as the vacuum expectation value (vev) of the scalar field which breaks the symmetry $SU(2)_L \times U(1)_Y$ down to $U(1)_Q$. As the broken symmetry is gauged one, the three corresponding generators (two off-diagonal ones from $SU(2)_L$ and a linear combination of the diagonal generator of $SU(2)_L$ and $U(1)_Y$) absorb three components of the scalar doublet (complex charged component and the imaginary part of the neutral component) to generate massive $W^{\pm}$ and Z weak bosons. So, in unitary gauge the Higgs boson becomes

$$H = \begin{pmatrix} H^+ \\ H^0 \end{pmatrix} \rightarrow \frac{1}{\sqrt{2}} \begin{pmatrix} 0 \\ h + v \end{pmatrix}. \tag{1.12}$$

As the interaction terms between the fermions and Higgs scalar (known as Yukawa terms) are gauge invariant ($\overline{\psi_L} H \psi_R \rightarrow \overline{\psi_L} V_L^\dagger V_L H \psi_R) = \overline{\psi_L} H \psi_R$), they are added to the SM Lagrangian. Upon symmetry breaking when the Higgs boson develops a vev, the fermions ends up having a mass term proportional to the vev. For example, for the charged lepton case:

$$\mathbf{Y}^e_{ij} \overline{\ell^i_L} H e^j_R = \mathbf{Y}^e_{ij} \begin{pmatrix} \overline{\nu^i_L} & \overline{e^i_L} \end{pmatrix} \frac{1}{\sqrt{2}} \begin{pmatrix} 0 \\ (h+v) \end{pmatrix} e^j_R = \frac{\mathbf{Y}^e_{ij} v}{\sqrt{2}} \overline{e^i_L} e^j_R + \frac{\mathbf{Y}^e_{ij}}{\sqrt{2}} h \overline{e^i_L} e^j_R \tag{1.13}$$

where $\mathbf{Y}$ is a dimensionless Yukawa coupling. And we see that the fermions obtain mass terms. The whole Yukawa sector of the SM Lagrangian is given by:

$$\mathcal{L}_Y = \mathbf{Y}^u_{ij} \overline{Q^i_L} \tilde{H} u^j_R + \mathbf{Y}^d_{ij} \overline{Q^i_L} H d^j_R + \mathbf{Y}^e_{ij} \overline{\ell^i_L} H e^j_R + h.c. \tag{1.14}$$

For the case of the mass terms for the gauge bosons, one needs to expand the kinetic term of the Higgs boson with the shifted Higgs field. The Higgs part of the SM Lagrangian is given as,

$$\mathcal{L}_H = \frac{1}{2} (D^\mu H)^\dagger (D_\mu H) - V(H) \tag{1.15}$$

where D^μ is given by Eq. (1.9) and the potential $V(H)$ is given by Eq. (1.11). Expanding the kinetic part, mass terms for the $W^{\pm}$, Z and photon (A) yield

$$m_W = \frac{gv}{2}, \qquad m_Z = \frac{v\sqrt{g_1^2 + g_2^2}}{2} = \frac{m_W}{\cos\theta_W}, \qquad m_A = 0 \tag{1.16}$$

where Z_μ and A_μ are the mass eigenstates of W^3_μ and B_μ and the mixing angles between them is related to the gauge couplings by $\tan\theta_W = g_1/g_2$.

So, the full Lagrangian of the Standard Model is given by:

$$\begin{aligned}\mathcal{L}_{SM} =& \mathcal{L}_{gb} + \mathcal{L}_f + \mathcal{L}_H + \mathcal{L}_Y \\ =& -\frac{1}{4}B_{\mu\nu}B^{\mu\nu} - \frac{1}{2}W^b_{\mu\nu}W^{b\mu\nu} - \frac{1}{2}G^a_{\mu\nu}G^{a\mu\nu} + \sum_f i\,\overline{f}\gamma_\mu D^\mu f \\ &+ \frac{1}{2}(D^\mu H)^\dagger (D_\mu H) - (-\mu^2 H^\dagger H + \lambda(H^\dagger H)^2) \\ &+ \mathbf{Y}^u_{ij}\overline{Q^i_L}\tilde{H}u^j_R + \mathbf{Y}^d_{ij}\overline{Q^i_L}Hd^j_R + \mathbf{Y}^e_{ij}\overline{\ell^i_L}He^j_R + h.c.\end{aligned} \tag{1.17}$$

The success of SM has been repeatedly assured by numerous electroweak precision experiments ever since it was first proposed. The existence of particles like massive $W^\pm$-boson, Z-boson, charm (c)-quark, top (t)-quark were all predicted by the SM before they were experimentally observed. It was not only the prediction of the existence of the massive gauge bosons, the theoretical calculation of the masses themselves also turned out to be impeccable. SM's prediction about anomalous magnetic moment of the electron pans out to be accurate upto an order of one part in a billion. SM is able to explain the details of Charge-Parity (CP) violation and mass splitting observed in the neutral K-mesons. The ultimate triumph of SM comes with the discovery of the Higgs boson at Large Hadron Collider (LHC) in 2002 which was predicted almost half a century ago.

1.1.2 Limitation of SM

In spite of all the successes of the SM, recent discoveries and observations have compelled us to think beyond Standard Model (BSM). We have realized that the SM might not be the ultimate structure of the nature. But there can be no denying of the success of SM. These facts inspire us to think along the line that the SM might be a remnant of some higher symmetry and the "ultimate" model reduces to the familiar SM or a model which appears very analogous to it.

We dedicate much of this dissertation to study such limitations of the SM and build models with higher symmetries to address these issues. Thus before delving into the physics of BSM, one needs to know the most important shortcomings of the SM such as neutrino oscillations, dark matter and strong CP problem. There are also criticisms about SM which are of aesthetic in nature, but by no means can be taken lightly as they often provide crucial guidance to fabricate models with higher symmetries. These include issues like charge quantization, the fact that SM contains quite a few free parameters with no apparent relationship between them and the existence of several (three to be precise) copies of the same particles differing only by masses where the reason for such repetition is absent. Experimental observations like dark energy or theoretical issues like quantum gravity are

also unexplained by SM, but these topics will be out of scope of this dissertation and we will refrain ourselves from discussing any details about them.

We now briefly discuss some of the aforementioned difficulties of SM which can be explained in the framework of the BSM physics that will be considered in this dissertation.

Charge Quantization

One of the amazing phenomenon of nature is the equality of the electric charge of electron and proton. Both from cosmological and astrophysical considerations (the absence of electrostatic forces between galaxies) and laboratory considerations (study of neutral materials), it has been concluded that the charge difference between proton and electron is below one part in 10^{21} [2], ie.

$$\left|1 - \frac{Q_e}{Q_p}\right| < 10^{-21}. \tag{1.18}$$

In SM, the electron (which is a lepton) and quarks are placed in different multiplets. As the proton consists of two up-type and a down-type quarks, the charge of proton and that of electron should not necessarily be co-related at all. In SM, the hypercharge is assigned in such a way that the electric charge coincides with the phenomenological ones without any theoretical motivation or underlying principle. One should also note that this specific hypercharge assignment also keeps the SM anomaly free.

Neutrino oscillation

In the late sixties, Homestake Experiment first detected the effects of neutrino oscillation by observing a deficit in the flux of solar neutrinos [14]. After that numerous experiments with solar, atmospheric and reactor neutrinos have provided definitive evidence of neutrino oscillations and a comprehensive picture began to emerge [15, 16, 17, 18]. Neutrino oscillation is a phenomenon where a neutrino with a specific lepton flavor can be later detected to have a different flavor while it propagates through space and it occurs due to the non-zero neutrino masses and mixings. In the language of quantum field theory, the lepton flavor eigenstates of neutrinos $(\nu_e, \nu_\mu, \nu_\tau)$ are the linear combinations of the mass eigenstates of neutrinos (ν_1, ν_2, ν_3):

$$\nu_{\ell L}(x) = \sum_j U_{\ell j} \nu_{jL}(x); \qquad \ell = e, \mu, \tau \tag{1.19}$$

where U is the neutrino mixing matrix, also known as the Pontecorvo-Maki-Nakagawa-Sakata (PMNS) matrix.

A global analysis of the experiments gives rather precise determination of the oscillation parameters as [2]:

$$\begin{aligned}
\Delta m^2_{21} &= 7.54^{+0.26}_{-0.22}\times 10^{-5}\text{eV}^2 \\
\Delta m^2_{31} &= \begin{cases} +2.43^{+0.06}_{-0.06}\times 10^{-3}\text{eV}^2 & \text{for normal hierarchy} \\ -2.34^{+0.10}_{-0.09}\times 10^{-3}\text{eV}^2 & \text{for inverted hierarchy} \end{cases} \\
\sin^2\theta_{12} &= 0.308 \pm 0.017 \\
\sin^2\theta_{23} &= \begin{cases} 0.437^{+0.033}_{-0.023} & \text{for normal hierarchy} \\ 0.455^{+0.039}_{-0.031} & \text{for inverted hierarchy} \end{cases} \\
\sin^2\theta_{13} &= \begin{cases} 0.0234^{+0.0020}_{-0.0019} & \text{for normal hierarchy} \\ 0.0240^{+0.0019}_{-0.0022} & \text{for inverted hierarchy} \end{cases}
\end{aligned} \tag{1.20}$$

where $\Delta m^2_{ij} = m^2_i - m^2_j$. Neutrino experiments are not still sensitive to the sign of Δm^2_{31} and hence two possibilities exist. Normal hierarchy refers to the case where $m_1 < m_2 < m_3$ and inverted hierarchy is one for which $m_3 < m_1 < m_2$.

In SM neutrino remains massless, as even with the Higgs boson and its vev, SM lacks a Lagrangian term which can generate neutrino mass at renormalizable level (ie. mass dimension $d = 4$ operator is absent). One can write a Yukawa term that can lead to neutrino mass by allowing higher dimensional terms which is clearly suppressed by a new scale (M) of physics yet to be discovered:

$$\mathcal{L}_Y(d=5) \supset \mathbf{Y}_\nu \frac{(\ell^T_L C\, i\,\sigma_2 H)(H^T\, i\,\sigma_2 \ell_L)}{M}. \tag{1.21}$$

When electroweak symmetry is spontaneously broken, the Higgs H get a vev v and neutrino ends up getting a Majorana mass term

$$\mathcal{L}_Y \supset \mathbf{m}_\nu \nu^T_L C \nu_L \qquad \text{with} \qquad \mathbf{m}_\nu = \mathbf{Y}_\nu \frac{v^2}{M}. \tag{1.22}$$

If $M \gg v$, neutrinos are naturally lighter than the charged fermions. But the new physics scale M requires physics beyond SM. The wide range of possibilities can be classified into three major catagories. In the first case, neutrinos may be simple Dirac fermions. For such a case one considers the neutrino as a four-component spinor and $\nu_{L,R}$ are the left and right-handed chiral projection. Then neutrino acquires a Dirac mass just like any other fermions after electroweak symmetry breaking via a mass term in the Yukawa part of the Lagrangian with the help of newly introduced

right-handed (RH) neutrino. The term in the Lagrangian can be written as:

$$\mathcal{L}_Y \supset \mathbf{Y}_\nu v \overline{\nu_L} \nu_R + h.c. = \mathbf{m}_D \overline{\nu_L} \nu_R + h.c. \tag{1.23}$$

But the smallness of the neutrino mass ($\mathbf{m}_D$) or neutrino Yukawa coupling ($\mathbf{Y}_\nu$) remains a mystery and one needs to venture into the realm of extra dimension(s) to seek for answer. The RH neutrinos can have Majorana masses and smallness of the masses arises from some sort of seesaw mechanism occurring at a very high energy (the new scale M). The Majorana mass term for the right-handed neutrinos can be written as

$$\mathcal{L}_M = \mathbf{m}_R \nu_R^T C^{-1} \nu_R \tag{1.24}$$

where $\mathbf{m}_R$ is the Majorana mass matrix. The SM Lagrangian along with the Dirac mass term for neutrino is invariant under a global $U(1)$ symmetry known as lepton number which gets broken by the Majorana mass term by two units. Observation of such $\Delta L = 2$ processes like neutrinoless double β decay can be a strong indication of the Majorana character of neutrinos. Similar $\Delta L = 2$ type of operators become essential to explain one of the biggest mysteries of the universe - the asymmetry between matter and anti-matter - via a process known as leptogenesis.

Using the Dirac and Majorana mass term from the Lagrangian, the neutrino mass matrix becomes:

$$\mathbf{M}_\nu = \begin{pmatrix} 0 & \mathbf{m}_D \\ \mathbf{m}_D^T & \mathbf{m}_R \end{pmatrix} \tag{1.25}$$

and the light neutrino mass is given by

$$\mathbf{m}_\nu = \mathbf{m}_D \, \mathbf{m}_R^{-1} \mathbf{m}_D^T. \tag{1.26}$$

Here $\mathbf{m}_R$ often corresponds to the scale of new physics mentioned in Eq. (1.21) and for the cases where $\mathbf{m}_R \gg \mathbf{m}_D$, the light neutrino mass gets naturally suppressed. This mechanism is known as Type I seesaw mechanism for neutrino mass generation [19].

Instead of the RH neutrino, a scalar triplet, $\Delta_L(1,3,1)$ can play the same role and introduce tiny mass for neutrino. The Yukawa Lagrangian for the new triplet is given by:

$$\mathcal{L}_Y(\Delta) = \mathbf{Y}_\Delta^{ij} \ell_i^T C i\sigma_2 \Delta_L \ell_j + h.c. \tag{1.27}$$

where $i, j = 1 - 3$ are the generation indices. And the scalar Δ_L gets an induced vev through the potential terms :

$$V(\Delta) = \mu H^T \sigma_2 \Delta_L^* H + M_\Delta^2 \mathrm{Tr}(\Delta_L^\dagger \Delta_L). \tag{1.28}$$

The neutrino mass turns out to be:

$$\mathbf{m}_\nu = \mathbf{Y}_\Delta \langle \Delta \rangle = \mathbf{Y}_\Delta \frac{\mu v^2}{M_\Delta^2} \qquad \text{with} \qquad \langle \Delta \rangle \simeq \frac{\mu v^2}{M_\Delta^2}. \tag{1.29}$$

One expects μ to be order of M_Δ and if $M_\Delta \gg v$, neutrinos are naturally light. Such a method to generate tiny neutrino mass is known as Type-II seesaw.

Type-III seesaw mechanism is carried out by a weak triplet fermion $T_F(1,3,0)$, where the Lagragian term is given by,

$$\mathcal{L}_Y(T_F) = \mathbf{Y}_T \ell^T C \sigma_2 \sigma \cdot T_F H + M_T T_F C T_F \tag{1.30}$$

And when $M_T \gg v$, one gets tiny neutrino mass:

$$\mathbf{m}_\nu = \mathbf{Y}_T^T \frac{1}{M_T} \mathbf{Y}_T v^2 \tag{1.31}$$

A third alternative is that the neutrino masses are generated by loop corrections, hence the masses are suppressed by the loop factors. In these type of BSM cases, neutrino masses are forbidden at tree level by some symmetry and are generated at one or higher loop level. The first proposal of this type of radiative neutrino mass models are Zee model [20] (based on one-loop mass generation) and the Zee-Babu model [21] (based on two-loop mass generation).

Dark Matter

The existence of Dark Matter (DM) is one of the most astounding revelations of the twentieth century. It undoubtedly pervades the universe at a rate much higher than the ordinary baryonic matter. The total mass-energy of the known universe contains 4.9% ordinary matter, 26.8% dark matter and the rest is contributed by dark energy [1].

One of the earliest, yet perhaps still the most convincing evidence of DM came from the measurement of galactic rotation curves [23]. This astronomical observation revealed that rotational velocities of various luminous objects specially at the outer rims of the galaxies are much higher than one would expect if they were only affected by the gravitational force of other visible objects. This implies the existence of a dark halo with a mass density which falls with a inverse square law upto certain distance. Another particularly compelling astronomical example involves the bullet cluster (1E0657-558) which passed through another cluster [25]. During the collision while galaxies in the clusters proceeded on ballistic trajectories and stars easily passed each other, the hot gas forming most of the clusters' baryonic mass was shocked and decelerated. Using gravitational lensing techniques and measurement of the baryons by optical, infrared and X-ray data, the mass of the

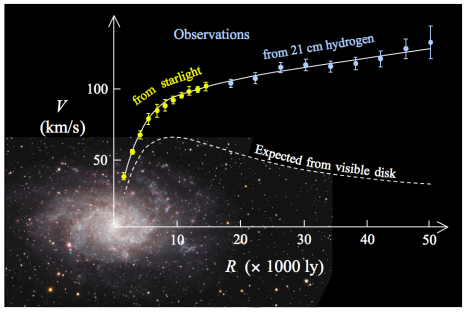

Figure 1.2: Rotation curve of a typical spiral galaxy: predicted and observed. Dark matter can explain the 'flat' appearance of the velocity curve out to a large radius [24]

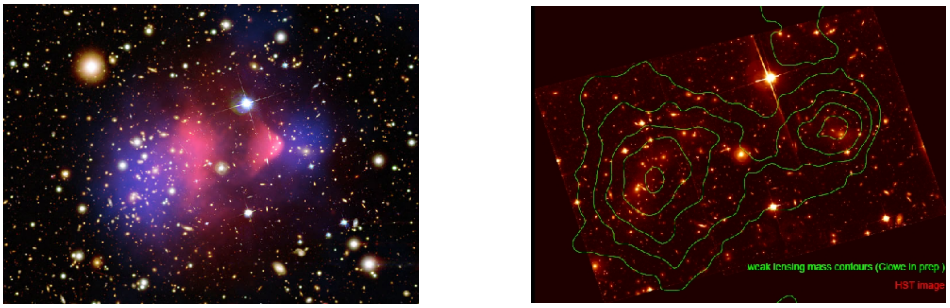

(a) (b)

Figure 1.3: (a)The Bullet Cluster: Hubble Space Telescope image with overlays. The total projected mass distribution reconstructed from strong and weak gravitational lensing is shown in blue, while the X-ray emitting hot gas observed with Chandra X-ray Observatory is shown in red. (b)Mass density contours of the bullet cluster superimposed over photograph taken with Hubble Space Telescope. (Source: Wikipedia)

stars (and any possible unknown substance that (almost) did not interact during the collision) was measured separated from the gas. This observation revealed that the mass of the clusters is made of 1% of baryons observable in optical and infrared data, 11% of baryons observable in X-ray data and the remaining 88% in DM component.

The currently most accurate determination of the critical density of DM comes from the global fits of cosmological parameters. For example, using measurements of the anisotropy of the Cosmic microwave background (CMB) and of the patial distribution of galaxies, we find that the density of cold, non-baryonic dark matter is:

$$\Omega_{DM} h^2 \sim 0.1186 \pm 0.0020 \tag{1.32}$$

where h is the Hubble constant in units of 100km/(s.Mpc), while the baryonic matter density is

given by

$$\Omega_{BM}h^2 \sim 0.02226 \pm 0.00023. \tag{1.33}$$

Even though more than 80% of the energy density of matter in the universe is composed of such non-baryonic dark matter, SM of particle physics cannot explain this observation as it lacks any candidate for such (dark) matter.

Strong CP problem

The violation of CP-symmetry in weak sector is a well established phenomenon which has been experimentally seen in the Neutral Kaon, K and B meson systems. As the complicated QCD vacuum structure admits a Lagrangian term $\mathcal{L}_\theta$, one would expect such CP violation in the strong sector too, where the term is given by

$$\mathcal{L}_\theta = \frac{\theta g_3^2}{32\pi^2} G^a_{\mu\nu} \tilde{G}^{a\mu\nu} \tag{1.34}$$

where $\tilde{G}^{a\mu\nu} = 1/2\ \epsilon^{\mu\nu\alpha\beta}\ G^a_{\alpha\beta}$ is the dual field strength for the gluon. The physically observable parameter $\overline{\theta}$ is a combination of θ and the phases of the quark masses and is given as:

$$\overline{\theta} = \theta + \text{Arg}[\text{Det}(M_q)] \tag{1.35}$$

where M_q is the quark mass matrix.

The most stringent constraint on the value of $\overline{\theta}$ is provided by the neutron electric dipole moment experiment which says $\overline{\theta} < 10^{-10}$ [26] [27]. A fundamental dimensionless parameter appearing in the SM Lagrangian should naturally be of the order one. The lack of explanation of the apparent minuscule value of the $\overline{\theta}$ parameter is known as Strong CP problem.

Flavor Puzzle

SM Lagrangian contains 19 parameters among which the three gauge couplings belong to the gauge sector, two of them (Higgs quartic coupling and Higgs mass-parameter) belong to the Higgs sector and the remaining 14 parameters (six quark masses, three charged lepton masses, three quark mixing angles, one weak CP violating phase, one strong CP violating term which is intimately related with quark masses) deal with the masses and mixings of the quarks and leptons. This is known as the flavor sector. If we consider neutrino oscillations we have to introduce nine more parameters (three neutrino masses, three mixing angles and three CP violating phases), all of which belong to flavor

sector.

Numerous experiments have provided abundant information on the numerical values of these parameters to an astonishing degree of precision. Still any fundamental understanding of the origin of these parameters is yet to emerge. Questions regarding the number of generations of fermions and the strong hierarchy between the charged fermions spanning some six orders of magnitude while top Yukawa is of order one are yet to be answered. This lack of understanding is often referred to "flavor puzzle".

1.1.3 Organisation of this Dissertation

This dissertation studies physics beyond the standard model with a particular focus on unification. This class of models beyond the standard model addresses some of these puzzles mentioned in the previous subsection. This dissertation is organized as follows. In chapter 2, we study a minimal version of renormalizable non-supersymmetric $SO(10)$ grand unified model. At first we argue that the minimal realistic version consists a symmetry breaking sector with Higgs fields in the $\mathbf{54_H + 126_H + 10_H}$ representations. This model admits a single intermediate scale associated with Pati-Salam symmetry along with a discrete parity. We study the gauge couplings unification of the model with threshold corrections and show that contrary to the popular belief the model successfully unifies the couplings at a high enough energy scale which is compatible with the current experimental bound on proton lifetime. Moreover this analysis is done while keeping the Yukawa sector of the model realistic which consists of only two matrices in family space and leads to a predictive scenario for quark and lepton masses and mixings. We introduce Pecci-Quinn global symmetry for a three-fold reason. It simultaneously keeps the Yukawa sector predictive, solves the strong CP problem and also provides a suitable dark matter candidate. The most exciting aspect of the model turns out to be that the model generally predicts an upper bound of few times 10^{35} yrs for proton lifetime, which is not too far from the present Super-Kamiokande limit of $\tau_p \gtrsim 1.4 \times 10^{34}$ yrs [36].

In Chapter 3, we study a general mechanism of electroweak symmetry breaking by evolution of mass parameter of the theory known as "Radiative Electroweak Symmetry Breaking". Even though the mechanism fails to work in SM due to the dominance of gauge coupling contributions to the evolution of Higgs mass parameter, the mechanism is quite successful in various extensions of SM. For this, we write down the complete set of renormalization group equations (RGEs) for various models and also determine the boundedness conditions for the potential. With these sets of equations we evolve all the couplings and mass parameters of the model while keeping track of boundedness con-

ditions all the way. We only consider the solutions which are in the perturbative regime. By this method, we show that for various simple extensions of SM, one can break the eletroweak symmetry radiatively, as there exists solutions to the RGEs that allow negative electroweak mass parameter at low energy while it becomes positive at high energy.We showed that such a radiative electroweak symmetry breaking can occur for SM extensions like Type-II seesaw model, radiative neutrino mass model and the inert doublet model. Even the simplest extension of SM by a real scalar singlet can perform such a radiative symmetry breaking and under suitable condition the electroweak vacuum becomes stable upto planck scale. We have also analyzed a variant of quark seesaw model which was originally based on a left-right symmetric model and introduces TeV scale vector-like fermions. The model can accommodate a scalar of 750 GeV which is the potential candidate particle for the recently reported excess at around 750 GeV diphoton invariant mass, but with a signal strength lower than initially reported down.

In Chapter 4, we construct a flavor model by gauging a maximal subgroup of the global flavor group possessed by the SM fermions. This flavor gauge group $O(3)_L \times O(3)_R$ is spontaneously broken down to $D_{3L} \times D_{3R}$ group. In this D_3 preserving limit, the first and the second generations of fermions are treated in the same manner while the third generation gets seperated. This attractive feature is supported by flavor constraints if the symmetry is further broken down by a smaller order. We study various possibilities of such breaking and find that for certain scalar sector used for symmetry breaking one can explain the recently reported excess in the 750 GeV diphoton invariant mass. We show that such a model can produce the right order of production crosssection $\times$ Branching ratio ≈ 3 fb while the decay width is of the order of 5 GeV.

In Chapter 5, we study various possibilities of dark matter candidate in the context of $SO(10)$ grand unified theories (GUTs). At first we show that $SO(10)$ GUT can provide an excellent framework to provide a well-motivated $\mathbb{Z}_2$ symmetry which is a remnant of $B-L$ generator. We show that even though the singlet fermion is the simplest case and is absolutely stable due to the $\mathbb{Z}_2$ symmetry, it fails to be viable dark matter as it is very weakly coupled to the SM sector. The introduction of a singlet scalar can elevate such an issue and provide a Higgs portal to SM particles. We also discuss other attarctive cases like fermionic 10-plet with or without the singlet fermion. In Chapter 6, we conclude the dissertation.

REFERENCES

[1] S. L. Glashow, Nucl. Phys. **22**, 579 (1961). doi:10.1016/0029-5582(61)90469-2

[2] S. Weinberg, Phys. Rev. Lett. **19**, 1264 (1967). doi:10.1103/PhysRevLett.19.1264

[3] A. Salam, Conf. Proc. C **680519**, 367 (1968).

[4] V. Fock, Z. Phys. **39**, 226 (1926) [Surveys High Energ. Phys. **5**, 245 (1986)]. doi:10.1007/BF01321989 H. Weyl, Z. Phys. **56**, 330 (1929) [Surveys High Energ. Phys. **5**, 261 (1986)]. doi:10.1007/BF01339504 F. London, Z. Phys. **42**, 375 (1927) [Surveys High Energ. Phys. **5**, 253 (1986)]. doi:10.1007/BF01397316

[5] C. N. Yang and R. L. Mills, Phys. Rev. **96**, 191 (1954). doi:10.1103/PhysRev.96.191

[6] J. Goldstone, Nuovo Cim. **19**, 154 (1961). doi:10.1007/BF02812722

[7] P. W. Higgs, Phys. Lett. **12**, 132 (1964). doi:10.1016/0031-9163(64)91136-9 P. W. Higgs, Phys. Rev. Lett. **13**, 508 (1964). doi:10.1103/PhysRevLett.13.508 P. W. Higgs, Phys. Rev. **145**, 1156 (1966). doi:10.1103/PhysRev.145.1156 T. W. B. Kibble, Phys. Rev. **155**, 1554 (1967). doi:10.1103/PhysRev.155.1554 G. S. Guralnik, C. R. Hagen and T. W. B. Kibble, Phys. Rev. Lett. **13**, 585 (1964). doi:10.1103/PhysRevLett.13.585 F. Englert and R. Brout, Phys. Rev. Lett. **13**, 321 (1964). doi:10.1103/PhysRevLett.13.321

[8] [ATLAS Collaboration], ATLAS-CONF-2012-093.

[9] CMS Collaboration [CMS Collaboration], CMS-PAS-HIG-12-020.

[10] G. 't Hooft, Nucl. Phys. B **35**, 167 (1971). doi:10.1016/0550-3213(71)90139-8

[11] D. J. Gross and F. Wilczek, Phys. Rev. Lett. **30**, 1343 (1973). doi:10.1103/PhysRevLett.30.1343

[12] H. D. Politzer, Phys. Rev. Lett. **30**, 1346 (1973). doi:10.1103/PhysRevLett.30.1346

[13] K. A. Olive *et al.* [Particle Data Group Collaboration], Chin. Phys. C **38**, 090001 (2014). doi:10.1088/1674-1137/38/9/090001

[14] R. Davis, Jr., D. S. Harmer and K. C. Hoffman, Phys. Rev. Lett. **20**, 1205 (1968). doi:10.1103/PhysRevLett.20.1205

[15] Y. Fukuda *et al.* [Super-Kamiokande Collaboration], Phys. Rev. Lett. **81**, 1562 (1998) doi:10.1103/PhysRevLett.81.1562 [hep-ex/9807003]. Y. Fukuda *et al.* [Super-Kamiokande Collaboration], Phys. Rev. Lett. **82**, 2644 (1999) doi:10.1103/PhysRevLett.82.2644 [hep-ex/9812014]. W. W. M. Allison *et al.* [Soudan-2 Collaboration], Phys. Lett. B **449**, 137 (1999) doi:10.1016/S0370-2693(99)00056-8 [hep-ex/9901024]. S. Fukuda *et al.* [Super-Kamiokande Collaboration], Phys. Rev. Lett. **85**, 3999 (2000) doi:10.1103/PhysRevLett.85.3999 [hep-ex/0009001]. M. Ambrosio *et al.* [MACRO Collaboration], Phys. Lett. B **517**, 59 (2001) doi:10.1016/S0370-2693(01)00992-3 [hep-ex/0106049].

[16] B. T. Cleveland, T. Daily, R. Davis, Jr., J. R. Distel, K. Lande, C. K. Lee, P. S. Wildenhain and J. Ullman, Astrophys. J. **496**, 505 (1998). doi:10.1086/305343 J. N. Abdurashitov *et al.* [SAGE Collaboration], Phys. Rev. C **60**, 055801 (1999) doi:10.1103/PhysRevC.60.055801 [astro-ph/9907113]. W. Hampel *et al.* [GALLEX Collaboration], Phys. Lett. B **447**, 127 (1999). doi:10.1016/S0370-2693(98)01579-2 Q. R. Ahmad *et al.* [SNO Collaboration], Phys. Rev. Lett. **87**, 071301 (2001) doi:10.1103/PhysRevLett.87.071301 [nucl-ex/0106015]. Q. R. Ahmad *et al.* [SNO Collaboration], Phys. Rev. Lett. **89**, 011301 (2002) doi:10.1103/PhysRevLett.89.011301 [nucl-ex/0204008]. S. Fukuda *et al.* [Super-Kamiokande Collaboration], Phys. Lett. B **539**, 179 (2002) doi:10.1016/S0370-2693(02)02090-7 [hep-ex/0205075].

[17] K. Eguchi *et al.* [KamLAND Collaboration], Phys. Rev. Lett. **90**, 021802 (2003) doi:10.1103/PhysRevLett.90.021802 [hep-ex/0212021]. T. Araki *et al.* [KamLAND Collaboration], Phys. Rev. Lett. **94**, 081801 (2005) doi:10.1103/PhysRevLett.94.081801 [hep-ex/0406035].

[18] D. G. Michael *et al.* [MINOS Collaboration], Phys. Rev. Lett. **97**, 191801 (2006) doi:10.1103/PhysRevLett.97.191801 [hep-ex/0607088]. P. Adamson *et al.* [MINOS Collaboration], Phys. Rev. Lett. **101**, 131802 (2008) doi:10.1103/PhysRevLett.101.131802 [arXiv:0806.2237 [hep-ex]].

[19] P. Minkowski, Phys. Lett. B **67**, 421 (1977). doi:10.1016/0370-2693(77)90435-X M. Gell-Mann, P. Ramond and R. Slansky, Conf. Proc. C **790927**, 315 (1979) [arXiv:1306.4669 [hep-th]]. R. N. Mohapatra and G. Senjanovic, Phys. Rev. Lett. **44**, 912 (1980). doi:10.1103/PhysRevLett.44.912

[20] A. Zee, Phys. Lett. B **93**, 389 (1980) Erratum: [Phys. Lett. B **95**, 461 (1980)]. doi:10.1016/0370-2693(80)90349-4, 10.1016/0370-2693(80)90193-8

[21] K. S. Babu, Phys. Lett. B **203**, 132 (1988). doi:10.1016/0370-2693(88)91584-5

[22] P. A. R. Ade *et al.* [Planck Collaboration], Astron. Astrophys. **571**, A1 (2014) doi:10.1051/0004-6361/201321529 [arXiv:1303.5062 [astro-ph.CO]].

[23] V. C. Rubin and W. K. Ford, Jr., Astrophys. J. **159**, 379 (1970). doi:10.1086/150317

[24] E. Corbelli and P. Salucci, Mon. Not. Roy. Astron. Soc. **311**, 441 (2000) doi:10.1046/j.1365-8711.2000.03075.x [astro-ph/9909252].

[25] D. Clowe, A. Gonzalez and M. Markevitch, Astrophys. J. **604**, 596 (2004) doi:10.1086/381970 [astro-ph/0312273]. M. Markevitch *et al.*, Astrophys. J. **606**, 819 (2004) doi:10.1086/383178 [astro-ph/0309303].

[26] V. Baluni, Phys. Rev. D **19**, 2227 (1979). doi:10.1103/PhysRevD.19.2227 R. J. Crewther, P. Di Vecchia, G. Veneziano and E. Witten, Phys. Lett. B **88**, 123 (1979) Erratum: [Phys. Lett. B **91**, 487 (1980)]. doi:10.1016/0370-2693(80)91025-4, 10.1016/0370-2693(79)90128-X C. A. Baker *et al.*, Phys. Rev. Lett. **97**, 131801 (2006) doi:10.1103/PhysRevLett.97.131801 [hep-ex/0602020].

[27] M. A. B. Beg and H.-S. Tsao, Phys. Rev. Lett. **41**, 278 (1978). doi:10.1103/PhysRevLett.41.278 R. N. Mohapatra and G. Senjanovic, Phys. Lett. B **79**, 283 (1978). doi:10.1016/0370-2693(78)90243-5 K. S. Babu and R. N. Mohapatra, Phys. Rev. D **41**, 1286 (1990). doi:10.1103/PhysRevD.41.1286 S. M. Barr, D. Chang and G. Senjanovic, Phys. Rev. Lett. **67**, 2765 (1991). doi:10.1103/PhysRevLett.67.2765 R. N. Mohapatra and A. Rasin, Phys. Rev. Lett. **76**, 3490 (1996) doi:10.1103/PhysRevLett.76.3490 [hep-ph/9511391]. R. Kuchimanchi, Phys. Rev. Lett. **76**, 3486 (1996) doi:10.1103/PhysRevLett.76.3486 [hep-ph/9511376]. R. N. Mohapatra, A. Rasin and G. Senjanovic, Phys. Rev. Lett. **79**, 4744 (1997) doi:10.1103/PhysRevLett.79.4744 [hep-ph/9707281]. K. S. Babu, B. Dutta and R. N. Mohapatra, Phys. Rev. D **65**, 016005 (2002) doi:10.1103/PhysRevD.65.016005 [hep-ph/0107100].

[28] H. Nishino *et al.* [Super-Kamiokande Collaboration], Phys. Rev. D **85**, 112001 (2012) [arXiv:1203.4030 [hep-ex]].

CHAPTER 2

A MINIMAL NON-SUPERSYMMTRIC SO(10) MODEL: GAUGE COUPLING UNIFICATION, PROTON DECAY AND FERMION MASSES

2.1 Introduction

The desire to achieve true unification of the strong, weak and electromagnetic forces under one simple non-abelian gauge group gave birth to the idea of Grand Unified Theories (GUTs) [1, 2, 3, 4]. The absence of an abelian factor in such unified theories readily quantizes electric charges, an observational feature left unexplained in the Standard Model (SM), which has served as one of the primary motivations of GUTs [3]. Yet, the initially introduced minimal $SU(5)$ model fails to unify the three gauge couplings [5]. The $SU(3)$-color and $SU(2)$-weak gauge couplings meet around 10^{16} GeV while the $U(1)$-hypercharge gauge coupling meets $SU(2)$ gauge coupling at a much lower energy scale of 10^{13} GeV, which is too low to comply with the experimental limits on proton lifetime. Of course, such an issue is absent in a low energy supersymmtric (SUSY) $SU(5)$ GUT where the three gauge couplings merge to a common value around 2×10^{16} GeV[1] [5].

The discovery of a Standard Model-like Higgs boson became the crowning event of the first run of LHC [6]. The triumph of SM and the absence of any compelling evidence (such as signals for new particles or exotic phenomena) of physics beyond SM in the LHC data, are making a large portion of the physics community rethink about the next step in the field. Supersymmetry (SUSY), one of the most elegant and successful solutions of the hierarchy problem [7] along with the WIMP (Weakly Interacting Massive Particle) scenario for dark matter, has been the most widely studied candidate of physics beyond SM at the TeV scale. Even though there is absolutely no reason to abandon the hopes of finding the necessary traces of new physics to solve such issues in the second run of LHC, one should also entertain the possibility that the hierarchy problem may simply be "solved" by fine-tuning. There exists a variety of approaches to justify such fine-tuning [8, 9]. One might invoke the anthropic principle, which has been much talked about in the field of cosmology [10] as the observed value of the cosmological constant Λ poses an unsolved naturalness problem of larger magnitude [11].

[1] In supersymmetry GUTs, the rate for proton decay $\Gamma(p \to \overline{\nu} K^+)$ arising from color triplet Higgsino exchange has to comply with experimental limits, which is a non-trivial task for SUSY GUT model building.

If one considers a universe with domains which can have different values of some of the underlying parameters like the Higgs boson mass, it has been argued that the observed values of the masses are reasonably typical of the anthropically allowed ranges [12]. One can look for answers in the much more debatable idea of infinite number of universes (multiverse) continuously created by quantum fluctuations and we happen to live in a very unlikely one [13]. In string theory landscape picture, our universe might be just one example out of 10^{500} possible solutions [14]. Or the "hierarchy problem" may very well be an artificially created one in quantum field theories which necessarily require regularization of infinities. Despite the philosophical point of view one might adopt, the lack of hard evidence of new physics sparked the revival of a class of BSMs (Beyond Standard Models) known as non-SUSY Grand Unified Theories, which ignores the hierarchy problem while trying to remain consistent with all the phenomenological constraints and predicting their own experimental signatures [8, 15, 16, 17, 18, 19, 9, 9].

$SO(10)$ grand unified theory [21] is undoubtedly the best motivated candidate in the above-mentioned class of models. Instead of taking help from supersymmetry to unify all the three gauge couplings, it relies on the fact that the rank-5 $SO(10)$ group can accommodate one or more intermediate scales between the unified scale and the weak scale [22, 23, 24, 25, 26, 27, 28]. As the gauge group structure changes (for example, $U(1)$ is usually embedded in $SU(2)_R$) above the intermediate scale, so does the running of the gauge couplings, allowing for the possibility of unification of all three gauge couplings. The fact that $SO(10)$ GUT is naturally free of anomalies [21] and that it unifies one generation of fermions (both leptons and quarks) into a 16-dimensional spinorial representation (16_F) only enhance the beauty of the model. This is due to the fact that the $SO(10)$ symmetry includes quark-lepton symmetry ($SU(4)_C$) [2] and the left-right symmetry ($SU(2)_L \times SU(2)_R$) [29]. Unlike $SU(5)$, the 16_F representation also includes a right-handed neutrino and provides an appealing explanation of small neutrino masses and oscillations through the seesaw mechanism [2, 31]. This setup has all the ingredients to explain the observed baryon asymmetry of the universe either by leptogenesis [32, 33] or by $B - L$ violating decays of new scalar states [34, 35].

Our goal in this paper is to construct the most minimal non-supersymmetric $SO(10)$ model. We shall be guided by simplicity and minimality, while being consistent with proton lifetime bound [36, 37], staying in agreement with the fermion masses and mixings [18], providing axion as a suitable candidate for dark matter while solving the strong CP problem [38]. The model should be able to address the issue of the instability of the electroweak vacuum[2] with SM singlet(s) and other particles

[2]The study of the stability of the SM eletroweak vacuum has shown that for a Higgs mass of 125.5 ± 0.5 GeV the Higgs quartic coupling of SM becomes negative around $(10^{10} - 10^{11})$ GeV energy scale [39] , indicating that we

lying inside the Higgs sector of the model. Inflation might be generated by a gravitationally coupled SM singlet(s) outside the model, or SM singlet(s) already present in the model may do the trick.

Search for such a minimal, yet realistic, unified model is highly non-trivial as the constraints provided by phenomenology are quiet demanding. After going through the process of selecting the Higgs sector, we end up with a symmetry breaking pattern:

$$SO(10) \xrightarrow{54_H} SU(4)_C \times SU(2)_L \times SU(2)_R \times D \xrightarrow{126_H} SU(3)_C \times SU(2)_L \times U(1)_Y \xrightarrow{10_H} SU(3)_C \times U(1)_{em}.$$

From the viewpoint of minimal Higgs sector, this symmetry breaking chain is the simplest, employing a single real 54_H, a complex 126_H and a complex 10_H. Even though earlier works [26, 27, 28, 42] may have prematurely sentenced this model as an unrealistic candidate for its failure to provide a high enough energy scale of gauge coupling unification to be compatible with proton lifetime limits, we decided to analyze the model more carefully before passing out the final verdict. Our detailed analysis of the model included the threshold corrections coming from the scalar and gauge boson sectors with complete mass spectrum. We also include effects of introducing the PQ-symmetry and its breaking by a singlet scalar, requiring compatibility with realistic and predictable Yukawa sector, and fine-tuning the hierarchy issue in the Higgs doublet sector.

We find from an explicit computation of the Higgs boson masses obtained by analyzing the Higgs potential of the model for the first time, that indeed compatibility with proton lifetime can be achieved. Rather than assuming the heavy Higgs bosons to have masses spread over an order of magnitude either way from the intermediate or GUT scale that has been employed traditionally, we chose the fundamental couplings of the Higgs potential to vary within a reasonable range, which provides more stringent constraints.

2.2 The Model

In this section we present our logic for choosing the symmetry breaking sector and describe qualitatively the emergence of an intermediate scale. After establishing the symmetry breaking pattern, we determine the energy scales associated with each Higgs multiplet in such a way that the arrangement is in agreement with phenomenological constraints.

might be living in a metastable universe. The electroweak vacuum can be stabilized by the threshold effect of a single scalar with vacuum expectation value close to the instability energy scale [40, 41]. Such a scalar arises naturally in our framework as a remnant of the PQ symmetry breaking.

2.2.1 Choice of the Higgs sector

The representations of the Higgs bosons primarily dictate the breaking of any higher gauge symmetry group down to lower ones [43]. Various low dimensional scalar representations - $10_H, 16_H, 45_H, 54_H$, 120_H, 126_H,$144_H, 210_H$-plets - have been used to break the $SO(10)$ group. Depending on the choice of the Higgs, it is possible to find multiple distinct breaking chains all of which end up in the SM symmetry. In this work, we are guided by the philosophy of minimality while staying within the perimeter of phenomenological constraints. As minimal non-supersymmtric $SU(5)$ (with no light exotics) corresponds to a proton lifetime which has been already ruled out by Super-Komiakande [36], between the two maximal subgroup of $SO(10)$ that contains SM, namely $SU(5) \times U(1)_X$ and $SU(4)_C \times SU(2)_L \times SU(2)_R$, the latter one is preferred in the breaking chain.

A simple choice of Higgs sector consisting 45_H+16_H tends to break $SO(10)$ to $SU(5)$. Alternative breaking channels fail to possess a gauge hierarchy at tree level in which $SU(2)_L \times SU(2)_R \times U(1)$ or $SU(4)_C$ makes an appearance resulting in a tachyonic mass spectrum [44, 45, 46]. The same comment holds for the Higgs system consisting of $45_H + 126_H$. Recently quantum salvation of these type of models has been shown by assuming that loop level contribution to the Higgs masses surpass the tree level ones [47]. In a series of papers, the details of these type of models were discussed [16]. While interesting, we view such models as not the very minimal, at least in the technical sense, since loop corrections are essential to stabilize the tree level potential.

The next choice is naturally 54_H+16_H. But the absence of any non-trivial cross-coupling between 54_H and 16_H promotes the global symmetry to $SO(10) \times SO(10)$ in this case. 54_H breaks one of them down to Pati-Salam (PS) symmetry with D-parity[3] ($SU(4)_C \times SU(2)_L \times SU(2)_R \times D$) while 16_H breaks the other $SO(10)$ to $SU(5)$ corresponding to a larger symmetry breaking which leaves an unwanted extra massless Goldstone boson in the $\left\{(3, 2, \frac{1}{6}) + h.c.\right\}$ representation of the SM gauge symmetry.[4]

[3]D-parity is a discrete symmetry residing in the $SO(10)$ group which behaves similar to parity (P) or charge conjugation (C) operator, at least in the case of fermions (for example, $D(4, 1, 2)_{PS} = (\overline{4}, 2, 1)_{PS}$ or simply $q \to q^C$). For the scalar sector, the effect of D-parity is a little different from C or P. For example, both 54_H and 210_H lead to the maximal little groups being the Pati-Salam group, as both possess a Pati-Salam singlet $(1, 1, 1)_{PS}$. Yet the singlet in 54_H is "D-even", $D(1, 1, 1)_{PS} = (1, 1, 1)_{PS}$, in contrast to the singlet in 210_H which is "D-odd", $D(1, 1, 1)_{PS} = -(1, 1, 1)_{PS}$. So, if one breaks $SO(10)$ with the vacuum expectation value (vev) of 54_H, D-parity is intact and one ends up getting $g_L = g_R$ at the energy scale associated with right-handed gauge boson ($W_R^{\pm}$), unlike the case of breaking initiated by the vev of 210_H. As this discrete symmetry was used for the first time to decouple the Parity and $SU(2)_R$ breaking scales, it earned the name "D-parity" [48].

[4]It will be interesting to study quantum salvation of such a model. We note, however, that generating large Majorana neutrino masses in this case would require introduction of new $SO(10)$ singlet fermions, which would make

In contrast, Higgs sector consisting a real 54_H and a complex 126_H along with a complex 10_H has all the properties that one needs to build a successful and predictive non-supersymmetric minimal $SO(10)$ GUT. In this case the symmetry breaking pattern is as shown in Fig. 2.1.

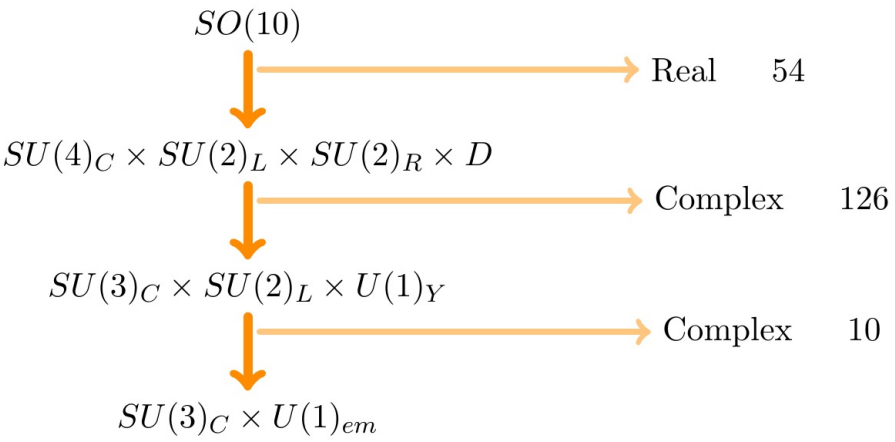

Figure 2.1: $SO(10)$ symmetry breaking pattern with a Higgs sector consisting of $54_H + 126_H + 10_H$.

In this breaking chain,

(i) A real 54_H breaks the $SO(10)$ symmetry to the Pati-Salam symmetry with D-parity.

(ii) A complex 126_H breaks the Pati-Salam symmetry to the Standard Model.

(iii) A complex 10_H is used to perform the electroweak scale breaking.

Even though a real 10_H is good enough to break the last stage of symmetry, a complex 10_H has been used here as the complex version is needed along with the complex 126_H to reproduce realistic fermion masses as argued in Ref. [8]. The decomposition of the Higgs fields under the Pati-Salam (PS) group $(SU(4)_C \times SU(2)_L \times SU(2)_R)$, the Standard Model group $(SU(3)_C \times SU(2)_L \times U(1)_Y)$ and $SU(5) \times U(1)_X$ are given in the Table 2.1.

2.2.2 Associated Energy Scales

In general, there are five possible energy scales associated with the left-right decomposition of any $SO(10)$ model, namely: (i) M_U for $SO(10) \to SU(4)_C \times SU(2)_L \times SU(2)_R$, (ii) M_C for $SU(4)_C \to SU(3)_C \times U(1)_{B-L}$, (iii) M_R for $SU(2)_R \to U(1)_R$, (iv) M'_R for $U(1)_R \times U(1)_{B-L} \to U(1)_Y$ and (v) M_W for $SU(2)_L \times U(1)_Y \to U(1)_{em}$ [46]. In this minimal model, all three scales besides M_U and M_W merge together and we will call the energy scale $M_C = M_R = M'_R \equiv M_I$, the intermediate scale. The presence of only one intermediate scale (M_I) in between unified scale (M_U) and the eletroweak scale (M_W) makes the model highly constrained and predictive.

the model not so minimal.

Extended Survival Hypothesis: To ascertain the energy scales of all the Higgs multiplets, we evoke the philosophy known as "Extended Survival Hypothesis". This is an extension of Georgi's "Survival Hypothesis" for fermions [49] which states "the representation that is invariant of the gauge group do acquire super-large mass". It was later extended to include scalar particles by the hypothesis: "Higgs acquire the maximum mass compatible with the symmetry breaking."[50, 51]. Here we will employ a more relaxed version of the hypothesis by stating that "Higgs multiplets remain at the maximum energy scale compatible with the symmetry breaking and phenomenological constraints." This is essentially a hypothesis of minimal fine-tuning.

According to this hypothesis, all the components of the 54_H remain at the unification scale, M_U. The 126_H decomposes as $\Sigma_1(6,1,1)_{PS} \oplus \Sigma_2(10,3,1)_{PS} \oplus \Sigma_3(\overline{10},1,3)_{PS} \oplus \Sigma_4(15,2,2)_{PS}$ under PS symmetry. As the PS symmetry is broken at the intermediate scale M_I by the vacuum expectation value of $\langle \Sigma_3(\overline{10},1,3)_{PS} \rangle$, all the components of $\Sigma_3(10,1,3)_{PS}$ must remain at M_I. Due to the D-parity, the $\Sigma_2(10,3,1)_{PS}$ multiplet also remains at M_I. To reproduce all the realistic fermion masses and mixings, the $\Sigma_4(15,2,2)_{PS}$ needs to stay at the intermediate scale M_I. This is due to the fact that if $\Sigma_4(15,2,2)_{PS}$ lives at the unification scale, the induced electroweak vev of $\Sigma_4(15,2,2)_{PS}$ will get suppressed by the square of the ratio of intermediate scale and unification scale. In general such a small induced vev fails to correct the mass relations generated by only one complex 10_H Higgs [52]. These bad mass relations include $V_{CKM} = \mathbb{1}$ and $m_u : m_c : m_t = m_d : m_s : m_b = m_e : m_\mu : m_\tau$. These wrong relations can be appropriately modified if the induced vev's are in the right order. Induced vev of order m_b is needed for $\Sigma_4(15,2,2)_{PS}$ and a suppression of $({}^{M_I}/_{M_U})^2 \sim 10^{-4}$ will be insufficient. Hence the need for $\Sigma_4(15,2,2)_{PS}$ being at M_I. As 126_H and 54_H have only one non-trivial cross coupling, the $\Sigma_1(6,1,1)_{PS}$ multiplet does not have enough freedom to be at the unification energy scale M_U and will be brought down to M_I. This is a consequence of explicit Higgs potential analysis. In short, the whole 126_H has to be at the intermediate scale, M_I.

The weak scale breaking in this model is achieved by a complex 10_H. So, only one of the doublets of SM needs to be at the weak scale. The other doublet needs to stay at the intermediate scale for the same reason as $\Sigma_4(15,2,2)_{PS}$. The rest of the multiplets (the color triplets) from 10_H will acquire masses of the order of the unification scale M_U.

2.3 Running of gauge couplings using two loop Renormalization Group Equations

In general, the three gauge couplings of the SM do not coincide at a single point when extrapolated using the SM renormalization group equation to high energy. But if a specific GUT, like the one

$SO(10)$	$SU(4)_C \times SU(2)_L \times SU(2)_R$	$SU(3)_C \times SU(2)_L \times U(1)_Y$	$SU(5) \times U(1)_X$	Scale
10	$H_T(6,1,1)$	$T_1(3,1,-\frac{1}{3})$	$(5,-2)$	M_U
		$T_2(\overline{3},1,+\frac{1}{3})$	$(\overline{5},+2)$	M_U
	$H_D(1,2,2)$	$H_1(1,2,-\frac{1}{2})$	$(5,-2)$	M_W
		$H_2(1,2,+\frac{1}{2})$	$(\overline{5},+2)$	M_I
54	$\zeta_1(1,3,3)$	$\zeta_{11}(1,3-1)$	$(15,-4)$	M_U
		$\zeta_{12}(1,3,0)$	$(24,0)$	M_U
		$\zeta_{13}(1,3,+1)$	$(\overline{15},+4)$	M_U
	$\zeta_2(6,2,2)$	$\zeta_{21}(3,2,-\frac{5}{6})$	$(24,0)$	$\boldsymbol{M_U}$
		$\zeta_{22}(3,2,+\frac{1}{6})$	$(15,-4)$	$\boldsymbol{M_U}$
		$\zeta_{23}(\overline{3},2,-\frac{1}{6})$	$(15,-4)$	$\boldsymbol{M_U}$
		$\zeta_{24}(\overline{3},2,+\frac{5}{6})$	$(24,0)$	$\boldsymbol{M_U}$
	$\zeta_3(20',1,1)$	$\zeta_{31}(\overline{6},1,+\frac{2}{3})$	$(\overline{15},+4)$	M_U
		$\zeta_{32}(6,1,-\frac{2}{3})$	$(15,-4)$	M_U
		$\zeta_{33}(8,1,0)$	$(24,0)$	M_U
	$\zeta_0(1,1,1)$	$\zeta_{00}(1,1,0)$	$(24,0)$	M_U
126	$\Sigma_1(6,1,1)$	$\Sigma_{11}(3,1,-\frac{1}{3})$	$(45,-2)$	M_U
		$\Sigma_{12}(\overline{3},1,+\frac{1}{3})$	$(\overline{5},+2)$	M_U
	$\Sigma_2(10,3,1)$	$\Sigma_{21}(1,3,-1)$	$(\overline{15},-6)$	M_I
		$\Sigma_{22}(3,3,-\frac{1}{3})$	$(45,-2)$	M_I
		$\Sigma_{23}(6,3,+\frac{1}{3})$	$(\overline{50},+2)$	M_I
	$\Sigma_3(\overline{10},1,3)$	$\Sigma_{31}(1,1,0)$	$(1,+10)$	$\boldsymbol{M_I}$
		$\Sigma_{32}(1,1,+1)$	$(10,+6)$	$\boldsymbol{M_I}$
		$\Sigma_{33}(1,1,+2)$	$(\overline{50},+2)$	M_I
		$\Sigma_{34}(\overline{3},1,+\frac{4}{3})$	$(10,+6)$	M_I
		$\Sigma_{35}(\overline{3},1,+\frac{1}{3})$	$(\overline{50},+2)$	M_I
		$\Sigma_{36}(\overline{3},1,-\frac{2}{3})$	$(45,-2)$	$\boldsymbol{M_I}$
		$\Sigma_{37}(\overline{6},1,-\frac{4}{3})$	$(\overline{50},+2)$	M_I
		$\Sigma_{38}(\overline{6},1,-\frac{1}{3})$	$(45,-2)$	M_I
		$\Sigma_{39}(\overline{6},1,+\frac{2}{3})$	$(\overline{15},-6)$	M_I
	$\Sigma_4(15,2,2)$	$\Sigma_{41}(1,2,-\frac{1}{2})$	$(\overline{5},+2)$	M_I
		$\Sigma_{42}(1,2,+\frac{1}{2})$	$(45,-2)$	M_I
		$\Sigma_{43}(3,2,+\frac{7}{6})$	$(\overline{50},+2)$	M_I
		$\Sigma_{44}(3,2,+\frac{1}{6})$	$(10,+6)$	M_I
		$\Sigma_{45}(\overline{3},2,-\frac{1}{6})$	$(\overline{15},-6)$	M_I
		$\Sigma_{46}(\overline{3},2,-\frac{7}{6})$	$(45,-2)$	M_I
		$\Sigma_{47}(8,2,-\frac{1}{2})$	$(\overline{50},+2)$	M_I
		$\Sigma_{48}(8,2,+\frac{1}{2})$	$(45,-2)$	M_I

Table 2.1: Decomposition of the scalar representations with respect to various $SO(10)$ subgroups. The "scale" indicates expectation based on extended survival hypothesis. The Higgs multiplets in red (or bold) are the massless Goldstone bosons which are absorbed by the corresponding gauge bosons.

under study, requires some Higgs bosons and gauge bosons other than the SM ones at a scale below M_U and the newly introduced bosons have substantial effects on the beta functions, then it might be possible to assign suitable masses to these bosons and achieve unification of couplings. After specifying the Higgs sector of the model and the symmetry breaking pattern, one needs to run the couplings of the gauge groups with the appropriate beta functions and determine the status of the unification of the model under study.

The two-loop renormalization group equations (RGE) for the gauge couplings can be written as:

$$\frac{d\alpha_i^{-1}(\mu)}{d\ln\mu} = -\frac{a_i}{2\pi} - \sum_j \frac{b_{ij}}{8\pi^2\alpha_j^{-1}(\mu)} \tag{2.1}$$

where i, j indices refer to different subgroups of the unified gauge group at the energy scale μ and

$$\alpha_i^{-1} = \frac{4\pi}{g_i^2}. \tag{2.2}$$

The β-function up to two-loop order is given by [53]

$$\begin{aligned}\beta(g) = \mu\frac{dg}{d\mu} &= -\frac{g^3}{(4\pi)^2}\left\{\frac{11}{3}C_2(G) - \frac{4}{3}\kappa S_2(F) - \frac{1}{6}\eta S_2(S)\right\} \\ &\quad -\frac{g^5}{(4\pi)^4}\left\{\frac{34}{3}\left[C_2(G)\right]^2 - \kappa\left[4C_2(F) + \frac{20}{3}C_2(G)\right]S_2(F)\right. \\ &\quad \left. -\left[2C_2(S) + \frac{1}{3}C_2(G)\right]\eta S_2(S)\right\}. \end{aligned} \tag{2.3}$$

Here S_2 and C_2 denote the Dynkin indices of the representations with the appropriate multiplicity factors (one has to be careful about whether the representation is complex or real) and the quadratic Casimir of a given representation. $\kappa = 1, \frac{1}{2}$ for Dirac and Weyl fermions and $\eta = 1, 2$ for real and complex scalar fields. G, F and S stand for gauge multiplets, fermions and scalars.
From the β-function expression we get,

$$a_i = -\frac{11}{3}C_2(G_i) + \frac{4}{3}\kappa S_2(F_i) + \frac{1}{6}\eta S_2(S_i) \tag{2.4}$$

$$\begin{aligned} b_{ij} &= -\frac{34}{3}\left[C_2(G_i)\right]^2\delta_{ij} + \kappa\left[4C_2(F_j) + \frac{20}{3}\delta_{ij}C_2(G_i)\right]S_2(F_i) \\ &\quad +\eta\left[2C_2(S_j) + \frac{1}{3}\delta_{ij}C_2(G_i)\right]S_2(S_i). \end{aligned} \tag{2.5}$$

The one-loop and two-loop β-function coefficients for the Standard Model (valid for $M_W \leq \mu \leq M_I$), and the Pati-Salam symmetry group with D-parity (valid for $M_I \leq \mu \leq M_U$) are found to be

$$a_{SM} = \begin{pmatrix} -7 \\ -\frac{19}{6} \\ \frac{41}{10} \end{pmatrix}; \qquad b_{SM} = \begin{pmatrix} -26 & \frac{9}{2} & \frac{11}{10} \\ 12 & \frac{35}{6} & \frac{9}{10} \\ \frac{44}{5} & \frac{27}{10} & \frac{199}{50} \end{pmatrix}; \tag{2.6}$$

$$a_{PS} = \begin{pmatrix} 1 \\ \frac{26}{3} \\ \frac{26}{3} \end{pmatrix}; \qquad b_{PS} = \begin{pmatrix} \frac{1209}{2} & \frac{249}{2} & \frac{249}{2} \\ \frac{1245}{2} & \frac{779}{3} & 48 \\ \frac{1245}{2} & 48 & \frac{779}{3} \end{pmatrix}. \tag{2.7}$$

Here we have used the intermediate scale scalar spectrum of Table 2.1, along with the intermediate gauge symmetry $SU(4)_C \times SU(2)_L \times SU(2)_R \times D$.

The appropriate matching conditions for two-loop RGE, when a simple gauge group $\mathcal{G}$ spontaneously breaks down into subgroups $\mathcal{G}_i$'s, is given by [54]

$$\frac{1}{\alpha_i(\mu)} = \frac{1}{\alpha_G(\mu)} - \frac{\lambda_i(\mu)}{12\pi}, \tag{2.8}$$

where

$$\begin{aligned} \lambda_i(\mu) \;=\; & \overbrace{(C_G - C_i)}^{\lambda_i^G} - 21 \overbrace{Tr\left(t_{iV}^2 \ln \frac{M_V}{\mu}\right)}^{\lambda_i^V} \\ & + \underbrace{Tr\left(t_{iS}^2 P_{GB} \ln \frac{M_S}{\mu}\right)}_{\lambda_i^S} + 8 \underbrace{Tr\left(t_{iF}^2 \ln \frac{M_F}{\mu}\right)}_{\lambda_i^F}. \end{aligned} \tag{2.9}$$

Here V, F and S denote respectively vector, fermion and scalar particles that are integrated out at the matching scale μ; C_G and C_i denote the quadratic Casimir invariants of the groups $\mathcal{G}$ and $\mathcal{G}_i$; $t_{i\{V,F,S\}}$'s are the generators of the lower symmetry $\mathcal{G}_i$ for the representations in which the heavy - Gauge bosons, fermions, scalar bosons - appear; P_{GB} is a projection operator which projects out all the Goldstone bosons.

Equipped with all these RGE's and matching conditions given above, it becomes straightforward to determine the intermediate scale M_I and the unification scale M_U for our model. Let us first find out these scales completely ignoring the threshold corrections stemming from the gauge bosons and unknown masses of the Higgs particles. In this scenario, we assume that all the Higgs and gauge boson masses are degenerate with masses equal to either M_I or M_U as dictated by the extended survival hypothesis. For the group $U(1)_Y$ the appropriate matching condition is given by

$$\frac{1}{\alpha_{1Y}(\mu)} = \frac{3}{5}\left(\frac{1}{\alpha_{2R}(\mu)} - \frac{C_{2R}}{12\pi}\right) + \frac{2}{5}\left(\frac{1}{\alpha_{4C}(\mu)} - \frac{C_{4C}}{12\pi}\right). \tag{2.10}$$

As input at $\mu = M_Z$, we use

$$\begin{aligned} \alpha_{1Y}^{-1} &= {}^3\!/_5\, \alpha_{em}^{-1}(1 - \sin^2\theta); & \alpha_{2L}^{-1} &= \alpha_{em}^{-1} \sin^2\theta; \\ M_Z &= 91.1876 \text{ GeV}; & \alpha_{em}^{-1} &= 127.940; \\ \sin^2\theta &= 0.23126; & \alpha_{3c} &= 0.1185. \end{aligned} \tag{2.11}$$

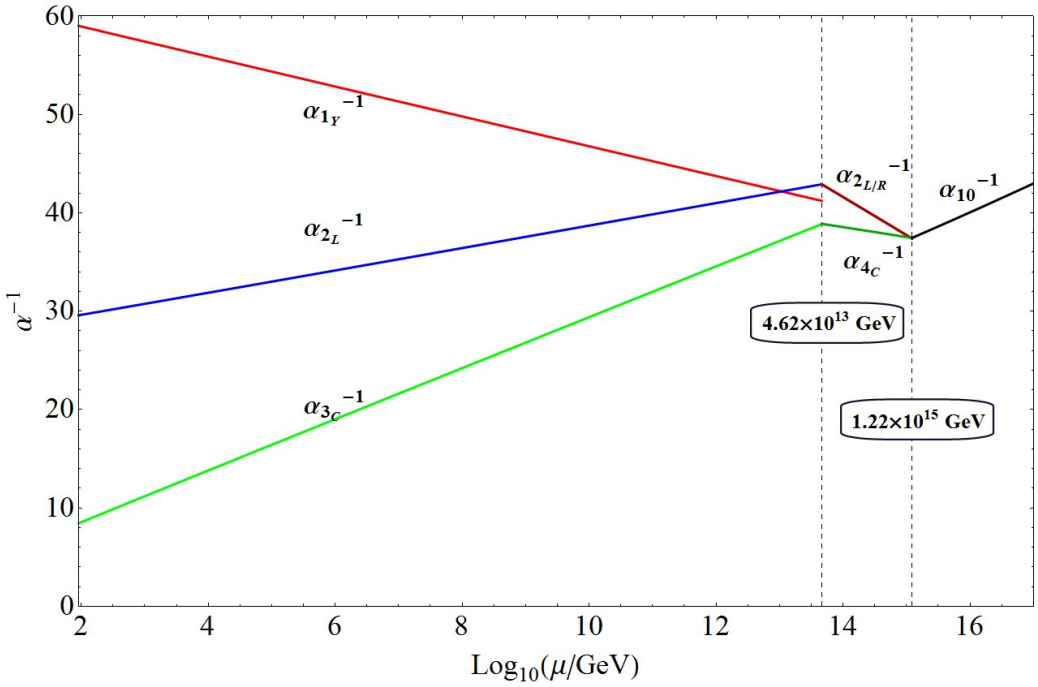

Figure 2.2: Running of gauge couplings without threshold corrections using two-loop RGE. Pati-Salam symmetry with D parity is assumed as the intermediate scale. The dotted vertical lines correspond to the intermediate scale and the unification scale.

By solving the two-loop RGE numerically, one obtains the intermediate scale to be 4.62×10^{13} GeV and the unification scale to be 1.22×10^{15} GeV. Such a unification scale is obviously ruled out by the current bound on proton lifetime, $\tau_p(p \to e^+\pi^0) > 1.29 \times 10^{34}$ yrs which requires $M_U \gtrsim (5 \sim 7) \times 10^{15}$ GeV [36]. It is this feature that has made the model less studied. But as we show in the next section, threshold corrections arising from the scalar sector at M_I and M_U can nicely rectify the situation and make the model consistent and still testable.

2.4 Threshold corrections

A fundamental limitation of all GUTs is the lack of underlying physics required to predict the masses of Higgs bosons and thus the threshold corrections associated with them. To improve the situation somewhat, one can always go through the tedious process of writing down the whole Lagrangian for the $SO(10)$ model and then derive the scalar particle mass spectrum in terms of the couplings and vev's of the $SO(10)$ Lagrangian. In such a scenario, the couplings and vev's are only constrained by the phenomenology and perturbitivity arguments.

Even though the scale of the physics, masses of the gauge bosons and the Higgs bosons should

be around the same order of energy, nothing dictates that they should all be exactly the same. On a stronger note, one can say that even though some of them can be degenerate, it is unlikely that all of them are. And this distribution of masses and vev's generates the threshold corrections. This becomes a very important factor for Higgs bosons belonging to a large representation such as 126_H. The predictions of the model derived while ignoring the threshold corrections becomes unreliable.

Here we proceed to take account of these corrections and study the resulting modification of the values of M_I and M_U. At first we include the threshold corrections in a very generic manner. At this stage, we assume that all the Higgs masses are independent and they are selected in a completely random manner. The only constraint that we put on the Higgs masses is due to the extended survival hypothesis. We kept the ratio, R of Higgs boson mass and the corresponding gauge boson masses to be between $R = \{1/10, 1/20, 1/33\}$ and $R = 2$. While ignoring any relations between the scalar masses, this analysis gives us the maximum threshold correction to the energy scales in terms of the spread of the distribution of scalar masses.

Defining the Pati-Salam Scale M_{PS}

Low energy experimental data fixes the initial points for the running of the gauge couplings while demand of unification puts a couple of constraints on the evolution. These determine two unique scales of the model. Let us consider the running of the three gauge couplings up to a scale Λ_i which is higher than the heaviest component of 126_H but lighter than any component of 54_H. For such a situation we have:

$$\begin{aligned}
\alpha_{3C}^{-1}(M_Z) &= \alpha_{4C}^{-1}(\Lambda_i) + \frac{a_{3C}}{2\pi}\ln\left[\frac{\Lambda_i}{M_Z}\right] - \frac{\lambda_{3C}^i}{12\pi};\\
\alpha_{2L}^{-1}(M_Z) &= \alpha_{2L}^{-1}(\Lambda_i) + \frac{a_{2L}}{2\pi}\ln\left[\frac{\Lambda_i}{M_Z}\right] - \frac{\lambda_{2L}^i}{12\pi};\\
\alpha_{1Y}^{-1}(M_Z) &= \frac{3}{5}\alpha_{2R}^{-1}(\Lambda_i) + \frac{2}{5}\alpha_{4C}^{-1}(\Lambda_i) + \frac{a_{1y}}{2\pi}\ln\left[\frac{\Lambda_i}{M_Z}\right] - \frac{\lambda_{1Y}^i}{12\pi}.
\end{aligned} \tag{2.12}$$

With the notation $\eta_j^a = ln\frac{M_j}{M_a}$; j being any Higgs multiplet and $a = i, u$ being intermediate scale (M_I) or unification scale (M_U) respectively:

$$\begin{aligned}
\lambda_{3C}^{iS} &= \eta_{\Sigma_{11}}^i + \eta_{\Sigma_{12}}^i + 3\eta_{\Sigma_{22}}^i + 15\eta_{\Sigma_{23}}^i + \eta_{\Sigma_{34}}^i + \eta_{\Sigma_{35}}^i + 5\eta_{\Sigma_{37}}^i + 5\eta_{\Sigma_{38}}^i + 5\eta_{\Sigma_{39}}^i\\
&\quad +2\eta_{\Sigma_{43}}^i + 2\eta_{\Sigma_{44}}^i + 2\eta_{\Sigma_{45}}^i + 2\eta_{\Sigma_{46}}^i + 12\eta_{\Sigma_{47}}^i + 12\eta_{\Sigma_{48}}^i;\\
\lambda_{2L}^{iS} &= \eta_{H_2}^i + 4\eta_{\Sigma_{21}}^i + 12\eta_{\Sigma_{22}}^i + 24\eta_{\Sigma_{23}}^i + \eta_{\Sigma_{41}}^i + \eta_{\Sigma_{42}}^i + 3\eta_{\Sigma_{43}}^i + 3\eta_{\Sigma_{44}}^i + 3\eta_{\Sigma_{45}}^i\\
&\quad +3\eta_{\Sigma_{46}}^i + 8\eta_{\Sigma_{47}}^i + 8\eta_{\Sigma_{48}}^i;
\end{aligned}$$

$$\begin{aligned}
\lambda_{1Y}^{iS} &= \frac{1}{5}\left(3\eta_{H_2}^i + 2\eta_{\Sigma_{11}}^i + 2\eta_{\Sigma_{12}}^i + 18\eta_{\Sigma_{21}}^i + 6\eta_{\Sigma_{22}}^i + 12\eta_{\Sigma_{23}}^i + 24\eta_{\Sigma_{33}}^i + 32\eta_{\Sigma_{34}}^i + 2\eta_{\Sigma_{35}}^i\right. \\
&\quad +64\eta_{\Sigma_{37}}^i + 4\eta_{\Sigma_{38}}^i + 16\eta_{\Sigma_{39}}^i + 3\eta_{\Sigma_{41}}^i + 3\eta_{\Sigma_{42}}^i + 49\eta_{\Sigma_{43}}^i + \eta_{\Sigma_{44}}^i + \eta_{\Sigma_{45}}^i + 49\eta_{\Sigma_{46}}^i \\
&\quad \left. +24\eta_{\Sigma_{47}}^i + 24\eta_{\Sigma_{48}}^i\right); \\
\lambda_{3C}^{iV} &= \eta_{PSV}^i; \quad \lambda_{2L}^{iV} = 0; \quad \lambda_{1Y}^{iV} = \frac{8}{5}\eta_{PSV}^i + \frac{6}{5}\eta_{W_R}^i; \quad \lambda_{3C}^{iG} = 1; \quad \lambda_{2L}^{iG} = 0; \quad \lambda_{1Y}^{iG} = \frac{14}{5}. \qquad (2.13)
\end{aligned}$$

Here PSV is the Pati-Salam gauge boson$(\overline{3}, 1, -\frac{2}{3})$ and W_R is the right-handed $W_R^{\pm}(1, 1, -1)$. The coefficients of the η's are the Dynkin indices of the representations of the respective gauge group together with the multiplicity factors. For the case of hypercharge GUT-compatible normalization has been used. Along with Eq. (2.13) we find the following equation:

$$\left(5\alpha_{1Y}^{-1} - 3\alpha_{2L}^{-1} - 2\alpha_{3C}^{-1}\right)(M_Z) = \frac{1}{2\pi}\left\{-2 + \ln\frac{M_{PS}^{44}}{M_Z^{44}}\right\} \qquad (2.14)$$

where

$$M_{PS} = \left(\frac{M_{PSV}^{21} M_{W_R}^{21} M_{\Sigma_{22}}^6 M_{\Sigma_{23}}^{15} M_{\Sigma_{38}} M_{\Sigma_{44}}^2 M_{\Sigma_{45}}^2 M_{\Sigma_{47}}^4 M_{\Sigma_{48}}^4}{M_{\Sigma_{21}} M_{\Sigma_{33}}^4 M_{\Sigma_{34}}^5 M_{\Sigma_{37}}^9 M_{\Sigma_{39}} M_{\Sigma_{43}}^6 M_{\Sigma_{46}}^6}\right)^{1/44}.$$

Here M_{PSV} is the mass of the Pati-Salam gauge boson$(\overline{3}, 1, -\frac{2}{3})$ and M_{W_R} is the mass of right-handed $W_R^{\pm}(1, 1, -1)$. Eq. (2.14) completely determines the "Pati-Salam Scale (M_{PS})" in terms of low energy experimental data, which will be the intermediate scale unless otherwise mentioned.

Using one-loop RGE, we find the intermediate scale (Pati-Salam scale) to be:

$$M_{PS}^{1-loop} = M_Z\, e^{\frac{C_{ps}}{44}} = 5.33 \times 10^{13}\ GeV$$

where

$$C_{ps} = 2\pi\left(5\alpha_{1Y}^{-1}(M_Z) - 3\alpha_{2L}^{-1}(M_Z) - 2\alpha_{3C}^{-1}(M_Z)\right) + 2$$

and we have used the data given in Eq. (2.11). To reduce the error coming from the fact that this definition does not use two-loop RGE running, we can run the SM gauge couplings at two-loop level up to the energy $\approx 10^{12}$ GeV. In that case, we find that $M_{PS} = 4.67 \times 10^{13}$ GeV which is very close to the value obtained by using two-loop RGE running up to unification scale.

Analytically it is tricky to define the Pati-Salam/intermediate scale at the two-loop level. Nevertheless, as the scales should not depend on the threshold corrections, one can evolve the couplings at two-loop level assuming all the scalar and gauge bosons to be degenerate at the respective scales. In that case, the unification constraint and low energy data fix the scale to be $M_{PS} = 4.62 \times 10^{13}$ GeV. This indicates an important fact that, if we consider two-loop RGE up to an energy scale $\approx 10^{12}$ GeV and then analyze the rest of the evolution (up to the unification scale) at one-loop level, the error introduced should not change the result drastically. The two-loop effects cannot accumulate a large

amount of corrections in the process of running by only three orders of magnitude in energy scale from $(10^{12} - 10^{15})$ GeV.

Defining the unification scale M_U

After defining the PS Scale, we can forget about the threshold corrections at the intermediate scale and use the new-found PS scale for any calculation needed for determining the unification scale. So, starting from the Pati-Salam scale we can write a new set of RGE for the couplings at an energy scale Λ_u higher than the energy scale corresponding to all the scalar particle masses as:

$$\begin{aligned}
\alpha_{4C}^{-1}(M_{PS}) &= \alpha_U^{-1}(\Lambda_u) + \frac{a_{4C}}{2\pi}\ln\left[\frac{\Lambda_u}{M_{PS}}\right] - \frac{\lambda_{4C}^u}{12\pi};\\
\alpha_{2L}^{-1}(M_{PS}) &= \alpha_U^{-1}(\Lambda_u) + \frac{a_{2L}}{2\pi}\ln\left[\frac{\Lambda_u}{M_{PS}}\right] - \frac{\lambda_{2L}^u}{12\pi};\\
\alpha_{2R}^{-1}(M_{PS}) &= \alpha_U^{-1}(\Lambda_u) + \frac{a_{2R}}{2\pi}\ln\left[\frac{\Lambda_u}{M_{PS}}\right] - \frac{\lambda_{2R}^u}{12\pi}.
\end{aligned} \tag{2.15}$$

Here

$$\lambda_{4C}^{uS} = 2\eta_{H_T} + 8\eta_{\zeta_3}; \qquad \lambda_{2L}^{uS} = 6\eta_{\zeta_1}; \qquad \lambda_{2R}^{uS} = 6\eta_{\zeta_1};$$

$$\lambda_{4C}^{uV} = 4\eta_{uV}; \quad \lambda_{4C}^{uG} = 4; \quad \lambda_{2L}^{uV} = 6\eta_{uV}; \quad \lambda_{2L}^{uG} = 6; \quad \lambda_{2R}^{uV} = 64\eta_{uV}; \quad \lambda_{2R}^{uG} = 6 \tag{2.16}$$

where the notation uV corresponds to the leptoquark gauge boson at the unification scale (M_U). Using these equations, we find:

$$\alpha_{4C}^{-1}(M_{PS}) - \alpha_{2L}^{-1}(M_{PS}) = \frac{1}{6\pi}\left\{1 - \ln\frac{M_U^{23}}{M_{PS}^{23}}\right\} \tag{2.17}$$

where

$$M_U = \left(\frac{M_{uV}^{21} M_{H_T} M_{\zeta_3}^4}{M_{\zeta_1}^3}\right)^{\frac{1}{23}}. \tag{2.18}$$

Just like the Pati-Salam scale, we can define a unification scale (M_U) completely fixed by the Pati-Salam scale:

$$M_U^{1-loop} = M_{PS}\, e^{\frac{C_u}{23}} = 2.4 \times 10^{15}\ GeV \tag{2.19}$$

where

$$C_u = 1 - 6\pi\left(\alpha_{4C}(M_{PS}) - \alpha_{2L}(M_{PS})\right).$$

Similarly to the Pati-Salam scale, if one runs SM gauge couplings at two-loop level to an energy scale of 10^{12} GeV, the unification scale becomes $M_U = 1.36 \times 10^{15}$ GeV. And at two-loop level we find $M_U^{2-loop} = 1.22 \times 10^{15}$ GeV. Again, this small discrepancy in M_U is due to the fact that the latter one is a two-loop gauge coupling evolution up to the unification scale while the previous one is two-loop level up to an energy level of 10^{12} GeV.

Threshold corrections at the unification scale

After defining the scales and finding out the scales of all the Higgs bosons (given in Table 2.1), it is straightforward to calculate analytically the threshold corrections for the one-loop running of the gauge couplings [55]. Numerically it is possible to improve the process, by using two-loop RGE (Eq. (2.1)) and one-loop threshold correction formulas given in Eqs. (2.8), (2.13), (2.16).

It is obvious that the masses of the gauge bosons will depend on the randomness adopted for the heavy Higgs masses due to the unification constraints given by Eqs. (2.14), (2.17). Guided by the extended survival hypothesis, we decided to allow the ratio of the mass of each Higgs boson to the corresponding gauge boson mass to be between $R = \{1/10, 1/20, 1/33\}$ and 2, with $R = \dfrac{M_{\text{Higgs boson}}}{\text{Corresponding gauge boson mass}}$. We study three cases where $R^{-1} = 10, 20$ and 33. The upper limit of 2 comes from the fact that we do not want to risk the perturbitivity of the model.

For a random sample of Higgs masses lying within the pre-selected range, one finds out the one-loop threshold corrections. Then using two-loop RGE for running of the gauge couplings and the unification constraints one determines the masses of the gauge bosons. Using the newly obtained gauge boson masses as updated scales, one repeats the process. After a few iterations, one ends up with a two-loop RGE of gauge couplings with one-loop threshold corrections with intermediate scale and unification scale at the corresponding gauge boson masses. Fig. 2.3 is a sample of such running of gauge couplings using two loop RGE and one loop threshold corrections.

To find out the pattern of the Higgs boson masses allowed by the current experimental bound, one needs to find out the proton lifetime in terms of the masses of the leptoquark gauge boson and the unified gauge coupling.

2.5 Proton Lifetime

Gauge mediated proton decay: In non-supersymmetric GUTs, the primary mode of proton decay is $p \to e^+\pi^0$. This gauge induced $d = 6$ operator predicts a proton lifetime of the order of $\tau_p \approx {M^4_{(X,Y)}}/{(g^4 m_p^5)}$, where $M_{(X,Y)}$ is the mass of the leptoquark (known as X, Y gauge boson), $g^2 \approx \dfrac{4\pi}{35}$ is the coupling at unification energy and m_p is the mass of the proton.

We have calculated the rates for proton decay using a more detailed version of the lifetime formula which includes the relevant hadronic matrix elements of operators and also renormalization effect of the operator in going from GUT energy scale to $\mu = 1$ GeV. The proton lifetime formula in $SO(10)$

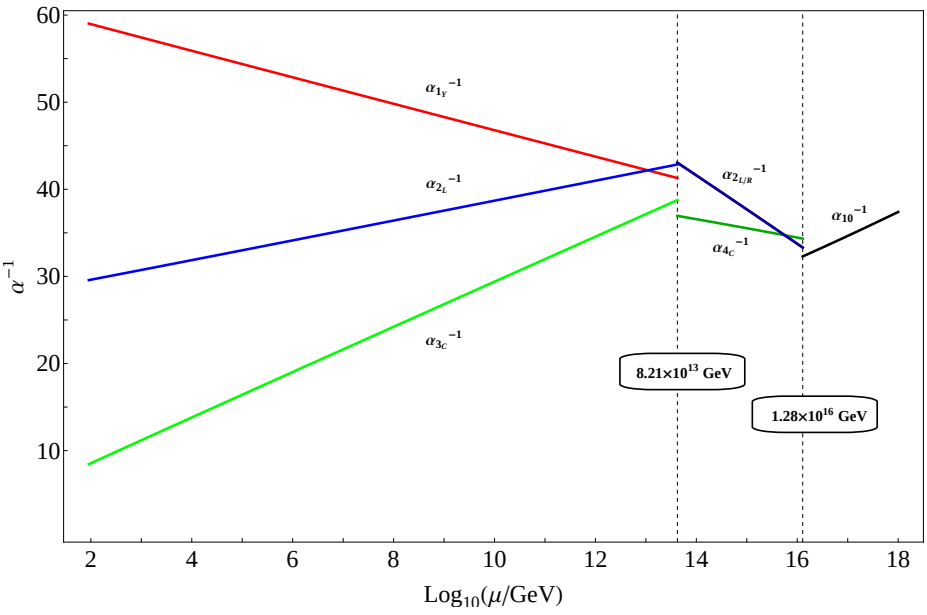

Figure 2.3: Running of gauge couplings with one-loop threshold corrections using two-loop RGE. This sample point corresponds to a case where some of the Higgs masses are taken to be two times the corresponding gauge boson mass determined without the threshold corrections and the others are one tenth of the scale. Special attention was given to the color triplet masses, so that they are heavier than 10^{13} GeV. In this extreme scenario, the mass of the leptoquark gauge boson (the one responsible of proton decay) is maximized. Then the scales were updated with an iteration process so that the scales correspond to the masses of the respective gauge bosons.

models is [56, 57, 58, 17]:

$$\tau_P = \left[\frac{\pi}{4} \frac{m_p \alpha_U^2}{f_\pi^2} |\alpha_H|^2 R_L^2 (1+F+D)^2 \left(A_{SR}^2 \left(\frac{1}{M_{(X,Y)}^2} + \frac{1}{M_{(X',Y')}^2} \right)^2 + \frac{4A_{SL}^2}{M_{(X,Y)}^4} \right) \right]^{-1} \tag{2.20}$$

where $R_L = 1.36$ is the two-loop long-range running effect on the effective proton decay operator [59], $\alpha_H \simeq -0.01 GeV^3$ [60] denotes the relevant hadronic matrix element defined by $\alpha_H u_L^p(\vec{k}) \equiv \epsilon_{\alpha\beta\gamma} \langle 0| d_R^\alpha u_R^\beta u_L^\gamma |p(\vec{k})\rangle$, $D = 0.8$ and $F = 0.47$ are chiral Lagrangian parameters [60], $f_\pi = 130.7$ MeV is the pion decay constant and g_G is the gauge coupling constant at the unification scale. $M_{(X,Y)}$ and $M_{(X',Y')}$ are the masses of the corresponding gauge bosons, $(X,Y)(3,2,+5/6)$ and $(X',Y')(3,2,-1/6)$. $A_{SL(R)}$ is the short-range left-handed (right-handed) renormalization factors of the proton decay operator corresponding to the running from the scale $\mu = M_U$ to M_Z, passing through the intermediate scale M_I and given by [61, 62, 63, 64]

$$A_{SL(R)} = \prod_{i=1}^{n} \prod_{sc}^{M_Z \le m_{sc} < M_U} \left[\frac{\alpha_i(m_{sc+1})}{\alpha_i(m_{sc})} \right]^{\frac{\gamma_{L(R)(sc)i}}{a_i(m_{sc+1} - m_{sc})}}$$

where

$$\gamma_{L(M_Z)} = \left\{\frac{23}{20}, \frac{9}{4}, 2\right\}; \quad \gamma_{R(M_Z)} = \left\{\frac{11}{20}, \frac{9}{4}, 2\right\}; \quad \gamma_{L/R(M_{PS})} = \left\{\frac{15}{4}, \frac{9}{4}, \frac{9}{4}\right\}.$$

And a_i's are the one-loop beta-function coefficients given in Eqs (2.6) -(2.7) and the relevant scales (sc) are M_U, M_{PS}, M_Z $(sc = 1, 2, 3)$.

As the $SO(10)$ model under scrutiny has a realistic and predictive Yukawa sector, the fermion masses and mixings can be determined by some fitting algorithm [18, 9]. After one gets the explicit numerical values for the fermion masses and mixings, it is trivial to determine the branching ratios of various proton decay channels. The issue will be discussed in details in Sec. 2.10 after we analyze the Yukawa sector of the model.

Higgs boson mediated proton decay: The Higgs boson induced $d = 6$ proton decay operator has the potential to play a vital role in the proton lifetime determination if certain scalar color triplets $T(3, 1, -1/3)$ become light enough. As mentioned earlier, not all the dangerous Higgs color triplets are at the unification scale. A couple of them slide down to the intermediate scale due to the fact that the 54 and 126 plet of $SO(10)$ have only one non-trivial cross coupling which is fine-tuned to keep the $(15, 2, 2)_{PS}$ at the intermediate scale.

In general, Higgs boson induced $d = 6$ operators are suppressed by the first generation Yukawa couplings.($\tau_p \approx {}^{m_T^4}/_{|Y_u Y_d|^2 m_p^5}$) [58]. As, in the SM, $(Y_u Y_d) \approx 10^{-10}$, in all cases we took a conservative lower limit and kept all the Higgs color triplet $T(3, 1, -1/3)$ mass, $m_T > 10^{13}$ GeV, so that they do not contribute significantly to proton decay.

Proton lifetime and threshold corrections: Proton lifetime is very sensitive to the mass of the leptoquark gauge boson which in turn depends on the randomness adopted for the heavy Higgs masses. After we find out the masses of the gauge bosons and the unified gauge coupling using one-loop threshold corrections and two-loop RGE running of the gauge couplings, we can use Eq. (2.20) to determine proton lifetime.

From our numerical analysis, we find that one can maximize proton lifetime by maximizing the masses of the following Higgs bosons: $\Sigma_{21}, \Sigma_{22}, \Sigma_{23}, \Sigma_{33}, \Sigma_{34}, \Sigma_{41}, \Sigma_{42}, \Sigma_{43}$, Σ_{44}, Σ_{45}, Σ_{46}, H_2, $\zeta_{11}, \zeta_{12}, \zeta_{13}$ and by minimizing: $T_1, T_2, \Sigma_{11}, \Sigma_{12}, \Sigma_{35}, \Sigma_{37}, \Sigma_{38}, \Sigma_{39}, \Sigma_{47}, \Sigma_{48}$, ζ_{31}, ζ_{32}, ζ_{33}. In such a maximal/minimal arrangement, the proton lifetime can go as large as:

$$\begin{aligned} \tau_{max} &= 1.45 \times 10^{35} \text{ yrs}; \qquad R^{-1} = 10, \\ \tau_{max} &= 9.85 \times 10^{35} \text{ yrs}; \qquad R^{-1} = 20, \\ \tau_{max} &= 3.91 \times 10^{36} \text{ yrs}; \qquad R^{-1} = 33. \end{aligned} \tag{2.21}$$

We have plotted in Fig. 2.4 proton lifetime as a function of the intermediate scale M_I which has

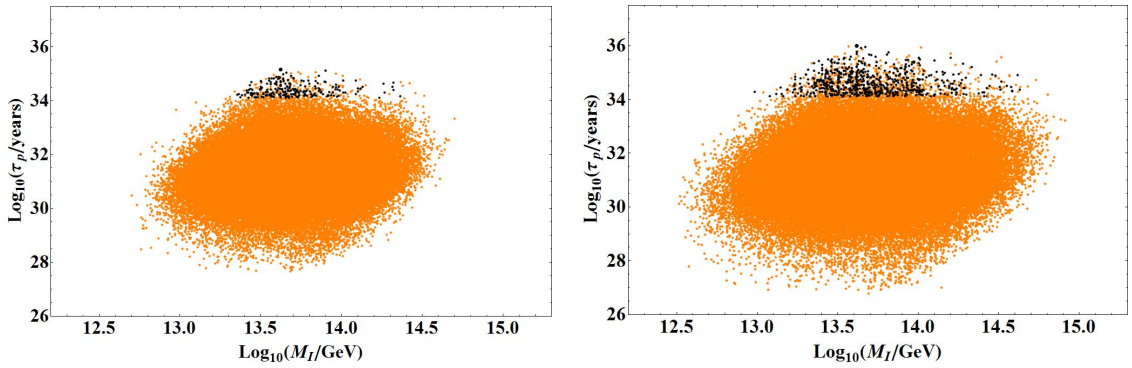

(a) $R^{-1} = 10$ (b) $R^{-1} = 20$

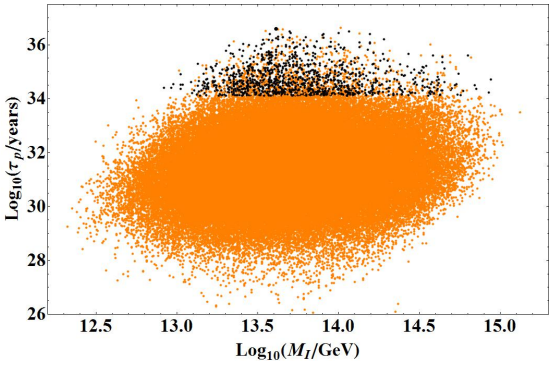

(c) $R^{-1} = 33$

Figure 2.4: Proton lifetime (τ_p) as a function of the intermediate scale M_I for different levels of threshold corrections. The ratio of the mass of each Higgs boson to the corresponding gauge boson mass is kept in between $R = \{1/10, 1/20, 1/33\}$ and $R = 2$, with $R = \frac{M_{\text{Higgs boson}}}{\text{Corresponding gauge boson mass}}$. All the black points are phenomenologically viable ones. Orange points either go through gauge boson mediated proton decay with a lifetime shorter than the experimental limit (1.29×10^{34} yrs), or they correspond to scenarios where at least one of the color triplet Higgs boson acquires a mass less than 10^{13} GeV. From a conservative point of view, we decided to exclude points with light color triplet masses as they tend to contribute to proton decay at a dangerous level.

been picked up as the mass of the PS gauge boson with random distribution of Higgs boson masses. The Higgs boson masses were randomly chosen among the corresponding scale and the extreme (minimum and maximum) values. All the black points correspond to phenomenologically viable points, while the orange points are excluded due to the proton lifetime experimental bound. The maximum proton lifetime in each case is marked by a larger black point. The points above the current lifetime limit ($\tau_p = 1.29 \times 10^{34} yrs$), yet orange in the scatter plot (in Fig. 2.4) are due to the fact that those points corresponds to cases where at least one of the Higgs color triplets becomes lighter than the conservative lower limit of 10^{13} GeV on their masses.

2.6 The $54_H + 126_H$ Higgs Model for $SO(10)$ symmetry breaking

In this section we analyze the breaking of $SO(10)$ symmetry down to the SM. We consider $SO(10)$ model with Higgs sector including a real 54_H (a rank two symmetric tensor, denoted by Φ_{ij}), a complex 126_H (a rank five totally antisymmteric tensor, denoted by Σ_{ijklm}) and a complex 10_H (a vector representation, denoted by ϕ_i). Being non-supersymmetric, the model inherits a couple of crucial deficiencies, namely failure to address the hierarchy issue and the lack of an automatic dark matter candidate. As the hierarchy problem is one of "naturalness", in this model we invoke fine-tuning to bring the Higgs doublet to the weak scale and fulfill the phenomenological constraints. The loss of the dark matter candidate can be easily remedied by introducing an additional Pecci-Quinn (PQ) $U(1)_{PQ}$ symmetry to the $SO(10)$ framework. It should be stressed that in this upgraded framework, along with the dark matter candidate, one simultaneously solves the strong CP problem - the absence of CP violation in the strong interaction sector.

The assigned PQ-charges of the various fields in the model are as follows:

$$\boldsymbol{16_F} \to e^{-i\alpha}\boldsymbol{16_F}; \quad \boldsymbol{10_H} \to e^{-2i\alpha}\boldsymbol{10_H}; \quad \boldsymbol{126_H} \to e^{2i\alpha}\boldsymbol{126_H}; \quad \boldsymbol{S_H} \to e^{-4i\alpha}\boldsymbol{S_H}. \tag{2.22}$$

As $\langle 126_H \rangle$ can only break a linear combination of the $U(1)_X$ and $U(1)_{PQ}$, one singlet (S_H) Higgs has been introduced to break the other linear combination so that only one $U(1)_Y$ is left unbroken above the weak scale [65]. With the newly introduced singlet field one can write the general potential for the model $SO(10) \times U(1)_{PQ}$ as

$$V = V(\Phi, \Sigma) + V(\Phi, \Sigma, \phi) + V(S) \tag{2.23}$$

where

$$
\begin{aligned}
V(\phi,\Sigma) &= -\frac{\mu^2}{2}\Phi_{ij}\Phi_{ij}+\frac{c}{3}\Phi_{ij}\Phi_{jk}\Phi_{ki}+\frac{a}{4}\Phi_{ij}\Phi_{ij}\Phi_{kl}\Phi_{kl}+\frac{b}{2}\Phi_{ij}\Phi_{jk}\Phi_{kl}\Phi_{li}-\frac{\nu^2}{2\cdot 5!}\Sigma_{ijklm}\Sigma^*_{ijklm}\\
&+\frac{\lambda_0}{2!^2 5!^2}\Sigma_{ijklm}\Sigma^*_{ijklm}\Sigma_{nopqr}\Sigma^*_{nopqr}+\frac{\lambda_2}{4!^2}\Sigma_{ijklm}\Sigma^*_{ijkln}\Sigma_{opqrm}\Sigma^*_{opqrn}\\
&+\frac{\lambda_4}{3!^2 2!^2}\Sigma_{ijklm}\Sigma^*_{ijkno}\Sigma_{pqrlm}\Sigma^*_{pqrno}+\frac{\lambda'_4}{3!^2}\Sigma_{ijklm}\Sigma^*_{ijkno}\Sigma_{pqrln}\Sigma^*_{pqrmo}\\
&+\frac{\alpha}{2!5!}\Phi_{ij}\Phi_{ij}\Sigma_{pqrlm}\Sigma^*_{pqrlm}+\frac{\beta}{3!}\Phi_{ij}\Phi_{kl}\Sigma_{mnoik}\Sigma^*_{mnojl},\\
V(\Phi,\Sigma,\phi) &= -\xi_0^2\phi_i\phi_i^*+\xi_1\phi_i\phi_i^*\phi_j\phi_j^*+\xi_2\phi_i\phi_i\phi_j^*\phi_j^*+\xi_3\Phi_{i,j}\phi_i\phi_j^*+\frac{\gamma_1}{4!}\Sigma_{ijklm}\Sigma^*_{ijkln}\phi_m\phi_n^*\\
&+\frac{\gamma_2}{4!}\Sigma_{ijklm}\Sigma^*_{ijkln}\phi_n\phi_m^*+\frac{\eta_0}{2}\Phi_{ij}\Phi_{ij}\phi_k\phi_k^*+\frac{\eta_1}{(3!)^2(2!)^2}\Sigma_{ijklm}\Sigma^*_{ijkpq}\Sigma^*_{lmpqn}\phi_n\\
&+\frac{\eta_1^*}{(3!)^2(2!)^2}\Sigma^*_{ijklm}\Sigma_{ijkpq}\Sigma_{lmpqn}\phi_n^*+\eta_2\Phi_{ij}\Phi_{ik}\phi_j\phi_k^*+\frac{\eta_3}{4!}\Sigma_{ijklm}\Sigma_{ijkln}\phi_m\phi_n\\
&+\frac{\eta_3^*}{4!}\Sigma^*_{ijklm}\Sigma^*_{ijkln}\phi_m^*\phi_n^*,\\
V(S) &= -\mu_s^2SS^*+\chi_1\left(SS^*\right)^2+\chi_2\Sigma_{ijklm}\Sigma^*_{ijklm}SS^*+\chi_3\Phi_{ij}\Phi_{ij}SS^*+\frac{\chi_4}{4!}\Sigma_{ijklm}\Sigma_{ijkln}\Phi_{ij}S\\
&+\frac{\chi_4^*}{4!}\Sigma^*_{ijklm}\Sigma^*_{ijkln}\Phi_{ij}S^*+\chi_5\phi_i\phi_i^*SS^*+\chi_6\phi_i\phi_iS^*+\chi_6^*\phi_i^*\phi_i^*S.
\end{aligned}
$$

In the potential, terms like $\Sigma^4, (\Sigma^*)^4$ are absent due to the PQ symmetry. Notice that the potential has four complex couplings, namely $\eta_1, \eta_3, \chi_4, \chi_6$. Among them, η_3 does not appear in the minimization condition and the mass spectrum. The other three couplings (η_1, χ_4, χ_6) can be made real by redefinitions of the fields Σ, S, ϕ respectively. This results in a vev structure of the potential $(\langle V\rangle)$ which is completely devoid of any complex couplings. In short, this means that we can always find a solution where all the vev's of the fields are real and we will deal with such a case.

In the model, the cubic coupling, c of 54_H^3 is imperative for the desired symmetry breaking scenario. It has been shown in Ref. [43] that if one tries to break $SO(10)$ with a 54_H in the absence of this cubic term, it only breaks it down to either $SO(5)\times SO(5)$ or $SO(9)$.

As the 10_H is complex, $126_H\cdot\overline{126}_H\cdot 10_H\cdot 10_H^*$ has two linearly independent couplings (γ_1,γ_2). In the potential (Eq. (2.23)), the trivial coupling is the linear sum of the two. So, one finds that, the mass spectrum of the non-singlet Higgs only depends on the difference of the couplings $(\gamma_1-\gamma_2)$.

The term $126_H\cdot\overline{126}_H\cdot 126_H\cdot 10_H$ with the coefficient η_1 is important for the fermion mass fitting, as this is the term which generates the induced vev's (κ_u,κ_d) for the electroweak doublets contained in the 126_H, or more precisely in the $(15,2,2)_{PS}$ [52]. If the vev's of the two complex doublets in 10_H are denoted by v_u, v_d then

$$\kappa_{u,d}\sim\eta_1\left(\frac{\langle 126_H\rangle^2}{M^2_{(15,2,2)_{PS}}}\right)v_{u,d} \tag{2.24}$$

2.6.1 Details of Symmetry Breaking

$SO(10)$ symmetry spontaneously breaks down to $SU(4)_C \times SU(2)_L \times SU(2)_R \times D$ when the 54_H acquires a non-zero vacuum expectation value given by

$$\langle 54 \rangle = diagonal \left({}^{-2}\!/_{5}, {}^{-2}\!/_{5}, {}^{-2}\!/_{5}, {}^{-2}\!/_{5}, {}^{-2}\!/_{5}, {}^{-2}\!/_{5}, {}^{3}\!/_{5}, {}^{3}\!/_{5}, {}^{3}\!/_{5}, {}^{3}\!/_{5} \right) \omega_s$$

where $\omega_s \sim M_U$. The vev of the SM singlet from 54_H is $\langle S_{54} \rangle = -\sqrt{\frac{12}{5}}\omega_s$. The $SU(4)_C \times SU(2)_L \times SU(2)_R \times D$ is broken down to SM model gauge group with the added $U(1)_{PQ'}$ (unbroken combination of $U(1)_X \times U(1)_{PQ}$) by the vev of 126_H, denoted by $\langle \Sigma_{2,4,6,8,10} \rangle = \frac{\sigma}{4\sqrt{2}}$, or in terms of SM Singlet in 126 as $\langle S_{126} \rangle = \frac{\sigma}{\sqrt{2}}$. Lastly, the singlet S_H acquires a vev (denoted by $\langle S_S \rangle = \frac{v_s}{\sqrt{2}}$) which breaks the extra $U(1)_{PQ'}$ and we get SM plus an axion at low energy. One linear combination of the two complex $SU(2)_L$ doublets of complex 10_H and the two complex $SU(2)_L$ doublets of 126_H remains massless at this stage. This linear combination is the field that acquires a vev and breaks the electroweak symmetry. We will denote the vev's of the two complex doublets in the 10_H as v_u, v_d and the two complex doublets in the $(15, 2, 2)_{PS}$ in 126_H get the induced vev's denoted by κ_u, κ_d.

In short, the high scale vev's acquired by the SM singlet contained in the Higgs 54_H, 126_H and S_H are as follows:

$$\langle S_{54} \rangle = -\sqrt{\frac{12}{5}}\omega_s; \qquad \langle S_{126} \rangle = \frac{\sigma}{\sqrt{2}}; \qquad \langle S_S \rangle = \frac{v_s}{\sqrt{2}}. \tag{2.25}$$

In this notation the vacuum expectation value of the potential (V) becomes:

$$\begin{aligned} \langle V \rangle = &-\frac{6}{5}\mu^2\omega_s^2 + \frac{4}{25}c\omega_s^3 + \frac{36}{25}a\omega_s^4 + \frac{42}{125}b\omega_s^4 - \frac{\nu^2}{2}\sigma^2 + \lambda_0\sigma^4 + \frac{3}{5}\alpha\omega_s^2\sigma^2 - \frac{3}{5}\beta\omega_s^2\sigma^2 \\ &- \frac{\mu_s^2}{2}v_s^2 + \frac{\chi_1}{4}v_s^4 + \frac{\chi_2}{4}\sigma^2 v_s^2 + \frac{3}{5}\chi_3\omega_s^2 v_s^2. \end{aligned} \tag{2.26}$$

Here the weak scale vev's are ignored as they are at least 10^{-8} times smaller than the smallest vev (namely v_s). It is very much possible to keep the electroweak scale vev's in the equations and do all the corresponding calculations. At the end of the calculation, one will realize that the weak scale vev's will only correspond to the mass splitting of the electroweak multiplets and that will correspond to an order of 10^2 GeV. Besides the SM doublet, all other scalar fields will acquire masses at the order of 10^{10} GeV or higher. So, for the sake of simplicity, we shall ignore corrections of order of 10^2 GeV, which is well justified.

Minimizing $\langle V \rangle$ with respect to the parameters ω_s, σ, v_s, the following relations can be obtained:

$$\begin{aligned}
\mu^2 =& \frac{12}{5} a\omega_s^2 + \frac{14}{25} b\omega_s^2 + \frac{c}{5}\omega_s + \frac{\alpha}{2}\sigma^2 - \frac{\beta}{2}\sigma^2 + \frac{\chi_3}{2} v_s^2 \\
\nu^2 =& \frac{6}{5}\alpha\omega_s^2 - \frac{6}{5}\beta\omega_s^2 + \lambda_0\sigma^2 \frac{\chi_2}{2} v_s \\
\mu_s^2 =& \chi_1 v_s + \frac{\chi_2}{2}\sigma^2 + \frac{6}{5}\chi_3\omega_s^2.
\end{aligned} \tag{2.27}$$

These minimization conditions are used in determining the masses of the various Higgs multiplets in the next subsection.

2.6.2 Tree level mass spectrum

One can go ahead and analyze the potential in its full glory (for example, using the methods described in Ref. [66]) and determine the whole scalar mass spectrum. The gauge boson mass spectrum is determined by constructing the covariant derivative and then analyzing the kinetic part of the Lagrangian, as usual.

Gauge boson mass spectrum

One needs to consider the properly normalized fields and analyze the kinetic part of the Lagrangian to obtain the mass spectrum of all the gauge bosons. In the case of the gauge bosons, besides the usual leptoquark gauge bosons $(X, Y)(3, 2, {}^{-5}/_{6})$, $(X', Y')(3, 2, {}^{+1}/_{6})$ and the Pati-Salam gauge boson $(\overline{3}, 1, {}^{-2}/_{3})$ and their conjugates, the heavy $(1, 1, \pm 1)$ particle corresponds to the right handed $W_R^{\pm}$. One of the $(1, 1, 0)$ corresponds to the Z' of the $U(1)_R$ and other one to the weak scale Z-boson which remains massless until the electroweak symmetry is broken. We find these masses to be:

$$\begin{aligned}
M_A^2(3, 2, -\frac{5}{6}) =& g_U^2\omega_s^2; \\
M_A^2(3, 2, +\frac{1}{6}) =& g_U^2\omega_s^2 + g_I^2\sigma^2; \\
M_A^2(\overline{3}, 1, -\frac{2}{3}) =& g_I^2\sigma^2; \\
M_A^2(1, 1, -1) =& g_I^2\sigma^2; \\
M_A^2(1, 1, 0) =& \begin{pmatrix} 3 & \sqrt{6} \\ \sqrt{6} & 2 \end{pmatrix} g_I^2\sigma^2.
\end{aligned} \tag{2.28}$$

Here the quantum numbers listed are under SM group $SU(3)_C \times SU(2)_L \times U(1)_Y$. One should notice that the determinant of the mass matrix for the gauge boson $(1, 1, 0)$ is zero and the eigenvalues of the matrix are $\{5, 0\}$. The zero eigenvalue corresponds to the Z-boson of mass 91 GeV.

Scalar Boson Mass Spectrum

The determination of the scalar mass spectrum is a little bit involved compared to the gauge boson mass spectrum, mainly due to presence 126_H which is represented by a rank-five totally antisymmetric tensor. But as shown in Ref. [66], one can identify the sub-multiplets inside the full multiplet in a systematic way and insert the vev's for the SM singlets to obtain the scalar mass spectrum.

Going through the straightforward, yet tedious calculation, one gets the following mass spectrum:

$$
\begin{aligned}
&M^2(1,3,0) = \frac{8}{5} b\omega_s^2 + c\omega_s; \\
&M^2(8,1,0) = \frac{2}{5} b\omega_s^2 - c\omega_s; \\
&M^2(3,3,-\frac{1}{3}) = 4\left(3\lambda_2 + 3\lambda_4 + 4\lambda_4'\right)\sigma^2; \\
&M^2(6,3,+\frac{1}{3}) = 8\left(\lambda_2 + \lambda_4 + 4\lambda_4'\right)\sigma^2; \\
&M^2(3,2,-\frac{5}{6}) = 0; \\
&M^2(\overline{3},1,-\frac{2}{3}) = 0; \\
&M^2(1,1,-1) = 0 \\
&M^2(1,1,+2) = 8\left(\lambda_2 + \lambda_4 + 4\lambda_4'\right)\sigma^2; \\
&M^2(\overline{3},1,+\frac{4}{3}) = 4\left(3\lambda_2 + 3\lambda_4 + 4\lambda_4'\right)\sigma^2; \\
&M^2(\overline{6},1,-\frac{4}{3}) = 8\left(\lambda_2 + \lambda_4 + 4\lambda_4'\right)\sigma^2; \\
&M^2(\overline{6},1,-\frac{1}{3}) = 4\left(3\lambda_2 + 3\lambda_4 + 4\lambda_4'\right)\sigma^2; \\
&M^2(1,3,-1) = \begin{pmatrix} \frac{8}{5} b\omega_s^2 + c\omega_s + \frac{1}{2}\beta\sigma^2 & 2\chi_4\sigma v_s \\ 2\chi_4\sigma v_s & 8\left(2\lambda_2 + 3\lambda_4 + 2\lambda_4'\right)\sigma^2 \end{pmatrix}; \\
&M^2(\overline{6},1,+\frac{2}{3}) = \begin{pmatrix} \frac{2}{5} b\omega_s^2 - c\omega_s + \frac{1}{2}\beta\sigma^2 & 2\chi_4\sigma v_s \\ 2\chi_4\sigma v_s & 8\left(2\lambda_2 + 3\lambda_4 + 2\lambda_4'\right)\sigma^2 \end{pmatrix}; \\
&M^2(3,2,+\frac{7}{6}) = \begin{pmatrix} 4\left(3\lambda_2 + 3\lambda_4 + 4\lambda_4'\right)\sigma^2 + \beta\omega_s^2 & -2\sqrt{2}\chi_4\omega_s v_s \\ -2\sqrt{2}\chi_4\omega_s v_s & 8\left(\lambda_2 + \lambda_4 + 2\lambda_4'\right)\sigma^2 + \beta\omega_s^2 \end{pmatrix}; \\
&M^2(8,2,-\frac{1}{2}) = \begin{pmatrix} 4\left(3\lambda_2 + 3\lambda_4 + 4\lambda_4'\right)\sigma^2 + \beta\omega_s^2 & -2\sqrt{2}\chi_4\omega_s v_s \\ -2\sqrt{2}\chi_4\omega_s v_s & 8\left(\lambda_2 + \lambda_4 + 2\lambda_4'\right)\sigma^2 + \beta\omega_s^2 \end{pmatrix};
\end{aligned}
$$

$$M^2(3,2,+\frac{1}{6}) = \begin{pmatrix} 8\left(2\lambda_2+3\lambda_4+2\lambda_4'\right)\sigma^2+\beta\omega_s^2 & 2\sqrt{2}\chi_4\omega_s v_s & -2\chi_4\sigma v_s \\ 2\sqrt{2}\chi_4\omega_s v_s & \beta\omega_s^2 & \frac{1}{\sqrt{2}}\beta\sigma\omega_s \\ -2\chi_4\sigma v_s & \frac{1}{\sqrt{2}}\beta\sigma\omega_s & \frac{1}{2}\beta\sigma^2 \end{pmatrix};$$

$$M^2(3,1,-\frac{1}{3}) = \begin{pmatrix} 4\left(3\lambda_2+3\lambda_4+4\lambda_4'\right)\sigma^2+4\beta\omega_s^2 & 4\sqrt{2}\chi_4\omega_s v_s & 0 & 0 & 0 \\ 4\sqrt{2}\chi_4\omega_s v_s & 8\left(\lambda_2+\lambda_4+2\lambda_4'\right)\sigma^2+4\beta\omega_s^2 & 16\sqrt{2}\lambda_4'\sigma^2 & 0 & 4\eta_1\sigma^2 \\ 0 & 16\sqrt{2}\lambda_4'\sigma^2 & 8\left(\lambda_2+\lambda_4\right)\sigma^2 & 0 & 4\sqrt{2}\eta_1\sigma^2 \\ 0 & 0 & 0 & A1 & \sqrt{2}\chi_6 v_s \\ 0 & 4\eta_1\sigma^2 & 4\sqrt{2}\eta_1\sigma^2 & \sqrt{2}\chi_6 v_s & B1 \end{pmatrix};$$

$$M^2(1,2,-\frac{1}{2}) = \begin{pmatrix} 8\left(\lambda_2+\lambda_4-2\lambda_4'\right)\sigma^2+\beta\omega_s^2 & 2\sqrt{2}\chi_4\omega_s v_s & 0 & 4\sqrt{3}\eta_1\sigma^2 \\ 2\sqrt{2}\chi_4\omega_s v_s & 4\left(3\lambda_2+3\lambda_4+4\lambda_4'\right)\sigma^2+\beta\omega_s^2 & 0 & 0 \\ 0 & 0 & A2 & \sqrt{2}\chi_6 v_s \\ 4\sqrt{3}\eta_1\sigma^2 & 0 & \sqrt{2}\chi_6 v_s & B2 \end{pmatrix};$$

$$M^2(1,1,0) = \begin{pmatrix} \frac{1}{10}c\omega_s+\frac{12}{5}a\omega_s^2+\frac{14}{25}b\omega_s^2 & -\sqrt{\frac{3}{5}}(\alpha-\beta)\sigma\omega_s & -\sqrt{\frac{3}{5}}\chi_3\omega_s v_s \\ -\sqrt{\frac{3}{5}}(\alpha-\beta)\sigma\omega_s & \frac{1}{4}\lambda_0\sigma^2 & \frac{1}{2}\chi_2\sigma v_s \\ -\sqrt{\frac{3}{5}}\chi_3\omega_s v_s & \frac{1}{2}\chi_2\sigma v_s & \chi_1 v_s^2 \end{pmatrix}.$$

$$M^2(1,1,0) = 0$$

$$M^2(1,1,0) = 0 \tag{2.29}$$

Here in the color triplet and $SU(2)_L$ doublet matrices, we have defined

$$\begin{aligned} A1 =& -\frac{2}{5}\xi_3\omega_s+\frac{6}{5}\eta_0\omega_s^2+\frac{4}{25}\eta_2\omega_s^2+\gamma_1\sigma^2+\frac{1}{2}\chi_5 v_s^2+m^2 \\ B1 =& -\frac{2}{5}\xi_3\omega_s+\frac{6}{5}\eta_0\omega_s^2+\frac{4}{25}\eta_2\omega_s^2+\gamma_2\sigma^2+\frac{1}{2}\chi_5 v_s^2+m^2 \\ A2 =& \frac{3}{5}\xi_3\omega_s+\frac{6}{5}\eta_0\omega_s^2+\frac{9}{25}\eta_2\omega_s^2+\gamma_1\sigma^2+\frac{1}{2}\chi_5 v_s^2+m^2 \\ B2 =& \frac{3}{5}\xi_3\omega_s+\frac{6}{5}\eta_0\omega_s^2+\frac{9}{25}\eta_2\omega_s^2+\gamma_2\sigma^2+\frac{1}{2}\chi_5 v_s^2+m^2 \end{aligned}$$

The mass matrices are spanned in the following bases:

$$(1,3,-1) \to \{(1,3,-1)_{\zeta_1},(1,3,-1)_{\Sigma_{21}}\}$$

$$(\overline{6},1,-2/3) \to \left\{(\overline{6},1,-2/3)_{\zeta_3},(\overline{6},1,-2/3))_{\Sigma_{39}}\right\}$$

$$(3,2,+7/6) \to \left\{(3,2,+7/6)_{\Sigma_{46}^*},(3,2,+7/6)_{\Sigma_{43}}\right\}$$

$$(8,1,-1/2) \to \left\{(8,1,-1/2)_{\Sigma_{48}^*},(8,1,-1/2)_{\Sigma_{47}}\right\}$$

$$(3,2,+1/6) \to \left\{(3,2,+1/6)_{\Sigma^*_{45}}, (3,2,+1/6)_{\Sigma_{44}}, (3,2,+1/6)_{\zeta_2}\right\}$$

$$(3,1,-1/3) \to \left\{(3,1,-1/3)_{\Sigma_{11}}, (3,1,-1/3)_{\Sigma^*_{12}}, (3,1,-1/3)_{\Sigma^*_{35}}, (3,1,-1/3)_{T_1}, (3,1,-1/3)_{T^*_2}\right\}$$

$$(1,2,-1/2) \to \left\{(1,2,-1/2)_{\Sigma_{41}}, (1,2,-1/2)_{\Sigma^*_{42}}, (1,2,-1/2)_{H_1}, (1,2,-1/2)_{H^*_2}\right\}$$

A few remarks are in order about the mass spectrum:

- From the mass spectrum of the Higgs bosons, we find that there are 34 massless states, which correspond to the broken generators of $SO(10)$ plus the imaginary part of the singlet (S) which corresponds to the axion. These 33 Goldstone bosons are eaten up by the 33 massive gauge bosons whose mass spectrum is given in Eq. (2.28).

- From the mass spectrum, it is obvious that $\Sigma_{22}(3,3,-1/3)$, $\Sigma_{38}(\overline{6},1,-1/3)$, $\Sigma_{42}(1,2,+1/2)$, $\Sigma_{46}(\overline{3},2,-7/6)$, $\Sigma_{48}(8,2,+1/2)$ and $\Sigma_{11}(3,1,-1/3)$ are degenerate except for the presence of contribution coming 54_H vev (ω_s) for the Higgs $\Sigma_{42}, \Sigma_{46}, \Sigma_{48}$ and Σ_{11}. The degeneracy comes from the fact that all these Higgs bosons are inside the $(45,2)$under $SU(5) \times U(1)_X$. As $\Sigma_3(\overline{10},1,3)$ acquires a vev, minimization condition removes the ω_s contribution from Σ_{38} and due to the D-parity, Σ_{22} is also missing the ω_s contribution to its mass.

- Similar arguments apply for masses of $\Sigma_{23}(6,3,+1/3)$, $\Sigma_{33}(1,1,+2)$, $\Sigma_{35}(\overline{3},1,+1/3)$, $\Sigma_{37}(\overline{6},1,-4/3)$, $\Sigma_{43}(3,2,+7/6)$ and $\Sigma_{47}(8,2,-1/2)$ where Σ_{43} and Σ_{47} are the only ones having contribution from ω_s.

- The rank of the matrix $M^2(3,2,+1/6)$ is two, where the massless eigenstate corresponds to the Goldstone boson of the theory, which gets eaten up by the (X',Y') gauge boson. The other massless Goldstone bosons from $(3,2,-5/6)$ are absorbed by the (X,Y) gauge boson.

- In the absence of the singlet (S_H), most of the mass matrices reduce to diagonal forms, indicating no mixing between many fields, even though they possess the same gauge quantum numbers. This is again due to the fact that the corresponding SM fields reside in a different $SU(5)$ multiplet. For example, one of the $(8,2,-1/2)$ lives in the $(\overline{50},+2)$ and a second one is in the $(45,-2)$ under $SU(5)\times U(1)_X$. There is non-trivial mixing in the mass matrix of $(3,2,+1/6)$ due to non-trivial quartic coupling β which generates term like $(24,0)(1,+10)(15,-4)(\overline{15},-6)$ written under $SU(5) \times U(1)_X$.

- In the doublet mass matrix only one of the doublets from 126_H gets mixed up directly (due to the coupling η_1) with one of the doublets from 10_H-plet as they both are from $(\overline{5},+2)$ of $SU(5) \times U(1)_X$. Besides this term, the two Higgs doublets in 126_H get mixed due to the

presence of the couplings from the singlet-potential ($V(S)$). Same type of mixing happens between the two Higgs doublet in 10_H. So, all the doublet fields mix with each other. This property of the doublet mass matrix is of utmost importance to generate realistic fermion masses.

- One should remember that in $SO(10)$ models without the PQ-symmetry, due to the presence of the term $126\cdot126\cdot54$ in the Lagrangian, one will end up getting all the off-diagonal mixing term at the SM level Lagrangian. Even though one gets a well-mixed doublet mass matrix, in that case one ends up with an extra set of Yukawa couplings and the theory loses predictivity. The inclusion of the PQ-symmetry gets rid of the extra Yukawa couplings and at the same time, gets rid of the usual mixing terms in the scalar mass spectra. But, at the end, the couplings in the singlet part of the potential ($V(S)$), which breaks the PQ-symmtery, reintroduces those mixing terms in the mass matrices. This makes the singlet vev important as in the doublet mass matrix it shows up in the off-diagonal terms and in the Yukawa sector the off diagonal elements cannot be ignored while reproducing realistic fermion masses and mixings.

- As one of the electroweak doublets and the color antitriplets of 126_H live in $(\overline{5},+2)$ of $SU(5)\times U(1)_X$ and one of the electroweak doublets and color triplets of 10_H live in $(5,2)$, the mixing term in doublet mass matrix and triplet mass matrix should be the same ($4\sqrt{3}\eta_1\sigma^2$). The apparent dissimilarity in the triplet matrix is due to the basis in which the triplet mass matrix is written. By a simple rotation of the triplet mass matrix one can show that mixing term is indeed given by $4\sqrt{3}\eta_1\sigma^2$ and in that basis, there is no mixing between the triplet from $(\overline{50},+2)$ and triplet from 10_H-plet. Besides these ones, other terms in the doublet and triplet matrices differ in a significant way and fine-tuning the doublet determinant to zero does not set the determinant of the triplet mass matrix to zero. While not unexpected, this condition is crucial for consistent phenomenology.

- The presence of the quartic coupling β ensures a mass contribution from the $\langle 126_H\rangle$ for the fields from 54_H. But such a contribution is missing from the multiplet which resides in the 24_H-plet of $SU(5)$. This can be easily explained under a situation where the $\langle 126_H\rangle > \langle 54_H\rangle$ and the model goes through $SU(5)$. Now that the SM singlet of 54_H is in the 24_H-plet (under $SU(5)$) and the minimization condition removes the contribution from $\langle 126_H\rangle$, SM muliplet $(8,1,0)$ and $(1,3,0)$ end up with no mass contribution from $\langle 126_H\rangle$. For the same reason only (X',Y') gauge bosons have mass contribution from the $\langle 126_H\rangle$, but not (X,Y) gauge bosons.

2.7 Yukawa sector of the model

The burning question about the search of the minimal Yukawa sector can be addressed under this minimal $SO(10)$ model with PQ-symmetry. In $SO(10)$ grand unified theory, each generation of fermions belong to a 16-dimensional spinorial representation, whose masses arise from the renormalizable Yukawa couplings with Higgs fields ($\overline{16} \times \overline{16} = 10 + \overline{126} + 120$). In the minimal model described here, the Yukawa part of the Lagrangian is given as:

$$\mathcal{L} = 16_F \left(Y_{10} 10_H + Y_{\overline{126}} \overline{126}_H \right) 16_F \tag{2.30}$$

where $Y_{10}, Y_{\overline{126}}$ are complex symmetric matrices in the generation space. A complex 10_H in general brings an extra set of Yukawa couplings. But in this case $U(1)_{PQ}$ symmetry forbids $16_F 10_H^* 16_F$ couplings, see Eq. (2.22). Besides providing a candidate for dark matter while solving the strong CP problem, the PQ-symmetry also affects the Yukawa sector making it realistic and predictive [8]. Notice that here, both $10_H(\phi)$ and $126_H(\Sigma)$ are complex in nature and each of them carries two $SU(2)_L$ Higgs doublets. It is assumed that only one linear combination of these electroweak doublets remains massless before electroweak symmetry breaking and acquires electroweak vev. This corresponds to the minimal fine-tuning as dictated by extended survival hypothesis. For such a case, the quark and lepton mass matrices become:

$$\begin{aligned} M_u &= h v_u + f \kappa_u; & M_d &= h v_d + f \kappa_d; \\ M_\nu^D &= h v_u - 3 f \kappa_u; & M_l &= h v_d - 3 f \kappa_d; \\ & & M_\nu^M &= f \sigma. \end{aligned} \tag{2.31}$$

Here, $M_{u,d,l}$ is the up-type quark, down-type quark and lepton mass matrix, M_ν^D is the Dirac neutrino matrix and M_ν^M is the Majorana mass matrix. These expressions can be rewritten in a more compact form which is more popular for a fit to masses and mixing angles:

$$\begin{aligned} M_u &= r(H + sF); & M_d &= H + F; \\ M_\nu^D &= r(H - 3sF); & M_l &= H - 3F; \\ & & M_\nu^M &= r_R^{-1} F \end{aligned} \tag{2.32}$$

where $H = h v_d$, $F = f \kappa_d$ are complex symmetric matrices and $r = {}^{v_u}/_{v_d}$, $s = {}^{\kappa_u}/_{(r\kappa_d)}$, $r_R = {}^{\kappa_d}/_{\sigma}$ are dimonsionless parameter.

An ample amount of literature has been devoted to find the best fit values of the parameters for various general minimal and non-minimal SO(10) Yukawa structures [67, 68, 69, 70, 71, 72, 73, 18, 9,

74]. Then the minimal model described in this work can reproduce a realistic fermion mass spectrum, if the model has enough freedom to have $r \approx 69$ and $s \approx 0.36 - 0.04i$ with some uncertainty [18]. Here, we can see that s is almost real, exactly what is needed for this model. At this point, we do realize that a small deviation in the parameter of a delicate χ^2 - analysis used in the fit of fermion masses and mixings has the potential to make the χ^2_{min} shift. Under such scenario, one can always redo the χ^2-analysis and minimize the χ^2. Besides adjusting the input mass matrices (for example, lepton and down-type quark mass matrices M_l, M_d), the process has the potential to change the vev ratios (r, s) as in this minimal model there is no phase associated with s. Yet as the phase of the s parameter is already small, we do not expect a large change in the fitting of fermion masses and mixings and we also emphasis the fact that the model has enough freedom to accommodate such a change.

So, one needs to verify and make sure that the doublet mass matrix has enough freedom to remain positive-definite and produce the appropriate vev ratios while not leading to light eigenvalues in the triplet mass matrix.

From the structure of the doublet mass matrix ($\mathcal{D}$), we see that the massless SM Higgs doublet h_{SM} becomes

$$h_{SM} = \alpha_H H_u + \beta_H H_d^* + \alpha_h h_u + \beta_h h_d^* \tag{2.33}$$

where H_u and H_d are the up-type and down-type doublet in $(15, 2, 2)_{PS}$ of 126_H and h_u and h_d are the up-type and down-type doublet living in the complex 10_H. For such a case we have

$$\begin{aligned}
&\mathcal{D}_{11}\alpha_H + \mathcal{D}_{12}\beta_H + \mathcal{D}_{14}\beta_d = 0;\\
&\mathcal{D}_{12}\alpha_H + \mathcal{D}_{22}\beta_H = 0;\\
&\mathcal{D}_{33}\alpha_h + \mathcal{D}_{34}\beta_h = 0;\\
&\mathcal{D}_{14}\alpha_H + \mathcal{D}_{34}\alpha_h + \mathcal{D}_{44}\beta_h = 0;\\
&\mathcal{D}_{11}\mathcal{D}_{22}\mathcal{D}_{33}\mathcal{D}_{44} + \mathcal{D}_{12}^2\mathcal{D}_{34}^2 - \mathcal{D}_{22}\mathcal{D}_{33}\mathcal{D}_{14}^2 - \mathcal{D}33\mathcal{D}_{44}\mathcal{D}_{12}^2 - \mathcal{D}_{11}\mathcal{D}_{22}\mathcal{D}_{34}^2 = 0.
\end{aligned} \tag{2.34}$$

As $r = {}^{\alpha_h}/_{\beta_h} > 0$ and $\mathcal{D}_{22} > 0$, we must have $\mathcal{D}_{12} < 0$. Similar argument implies $\mathcal{D}_{34} < 0$. Again one can show from the above mentioned set of equations that

$$\mathcal{D}_{11} = \frac{\mathcal{D}_{14}^2}{\mathcal{D}_{44} - r^2\mathcal{D}_{33}} - \frac{\mathcal{D}_{12}}{s} > 0 \tag{2.35}$$

Now, without any loss of generality, one can take the sign of β_h to be positive, then $\alpha_h > 0$ and α_H and β_H are of the same sign. For the case, $\alpha_H > 0$, if $\mathcal{D}_{14} > 0$ then only valid solution lies for $\left|\frac{\mathcal{D}_{14}^2}{\mathcal{D}_{44} - r^2\mathcal{D}_{33}}\right| < \left|\frac{\mathcal{D}_{12}}{s}\right|$. In contrast, if $\mathcal{D}_{14} < 0$, there is no such constraint. Similarly, for the case

$\alpha_H < 0$, the case $\mathcal{D}_{14} < 0$ gets the added condition. These conditions reduce the parameter space of the model significantly and need to be considered when one starts the process of random selection of sample points for the Higgs cubic and quartic couplings.

2.8 Technical Details

Due to the richness in the mass matrices in the scalar mass spectrum, one fails to come up with simple mass relations for the Higgs sector. All the couplings coming from the $SO(10)$-potential (Eq. (2.23)) need to be in the perturbative range. So, it is obvious that instead of the scalar masses, one should start from the couplings and vev's of the theory and calculate the mass spectrum of scalars and gauge bosons. Now, for a realistic model one needs to take into account the unification of the couplings and all the phenomenological constraints imposed by proton decay, realistic fermion mass spectrum and dark matter abundance.

To produce a sample scalar mass spectrum for the Higgs (10_H, 54_H, 126_H, S_H), first the vev's were picked to be $\omega_s \sim \left(10^{15} - 10^{16}\right)$ GeV, $\sigma \sim \left(10^{13} - 10^{14}\right)$GeV, $v_s \sim \left(10^{10} - 10^{12}\right)$GeV. The range of the intermediate scale and unification scale vev's are decided from the scatter plot generated before the scalar mass spectrum was determined (see Fig.2.4). As the singlet vev (v_s) breaks the PQ-symmetry, it corresponds to the axion decay constant f_a and the range taken for v_s is compatible with all the axion search experiments and astrophysical bounds. In the numerical analysis, one also sees that the above-mentioned range for v_s is also preferred by the doublet mass matrix. The dimensionless couplings are chosen randomly in the range of $[-1, 1]$ with the exception of the coupling b which was chosen from $[-2, 2]$ due to the poor availability of realistic parameter space in the more restrictive range. The couplings with positive mass dimensions were chosen either to be close to the corresponding scale or lower than the scale, so that the potential does not develop any unwanted minimum.

With the scalar masses fixed, the gauge boson masses were determined by the unification constraints and using the RGE the unified coupling at the unification scale was calculated. This unified coupling and the pre-assumed vev's also give the gauge boson masses which generally do not coincide with the previous ones determined from the unification conditions. To solve this an iteration process was used, until the difference between gauge boson masses calculated from these two methods becomes negligible.

The running of the gauge couplings can be done mainly in three ways:

1. One can run the SM gauge couplings at one-loop level, all the way to the unification scale

while updating the beta function coefficients whenever one encounters a scalar or gauge boson. The uncertainty coming from the one-loop running can be reduced if we run the SM gauge couplings at the two-loop level until we introduce the heavy scalar particles. The full two-loop running for computing the threshold corrections is not done due to the unknown two-loop connecting formula at the scale of symmetry breaking.

2. One can do a one-loop running of the SM gauge couplings until one hits a energy scale corresponding to the Pati-Salam gauge boson $(\overline{3}, 1, -2/3)$. Beyond that energy scale, it is the gauge couplings of the Pati-Salam model that is considered to be evolving until we reach a energy scale corresponding to the leptoquark gauge boson (X, Y). Under such type of running, unification is achieved after we have crossed the threshold of all the scalars and gauge multiplets of the theory. This program introduces some uncertainty due to the mass splittings of the submultiplets due to the lower order vev's. This may become important due to the vicinity of the intermediate and unification scales. To remedy the issue, while running the gauge couplings of higher symmetry, we only introduce the effects of a scalar particle in the beta functions, if that particle completes the multiplet of the higher symmetry. Finally, the uncertainty coming from the one-loop running can be reduced if we run the SM gauge couplings at the two-loop level until we introduce the first heavy scalar particles. Again, the full two-loop running was not done due to the unknown two-loop connecting formula of symmetry breaking.

3. One can also do a two-loop running where all the threshold correction is dumped in the intermediate and unification scales. Then one ends up with a discontinuity of the running of couplings corresponding to the threshold corrections. One should remember that in this case the scale at which the couplings become unified does not necessarily correspond to the mass of the leptoquark gauge bosons which mediate proton decay. One can chose the scale to be the intermediate scale and unification scale determined initially without any threshold corrections. In the following part of the paper, we picked the vev's as the corresponding scales.

The following steps were taken to produce the benchmark points:

- To produce the initial results, a set of random numbers (within a reasonable range) was generated in the 24-dimensional parameter space. Using the mass spectrum, all the Higgs boson masses were calculated and the gauge boson masses were determined by Eqs. (2.14), (2.17). One-loop running of the SM gauge couplings was performed to determine the initial status of the unification. At this level, strict unification is not achieved and the data set does not reproduce a realistic fermion mass spectrum. Also the gauge boson masses do not

necessarily correspond to the one calculated from gauge boson mass spectrum. Each of those points is selected individually and updated so that all the points satisfy the consistency checks and phenomenological constraints.

- After the initial random choice of parameters, one needs to impose the constraints imposed by the doublet mass matrix and realistic fermion mass spectrum. One needs to update the initial parameter values to generate one massless Higgs doublet and keep the vev ratios fixed to at $r \approx 69, s \approx 0.36$ [18].

- By performing a gauge coupling evolution, the gauge boson masses are updated so that we achieve $SU(2)_L$ and $SU(2)_R$ unification at Pati-Salam scale and perfect unification at the GUT scale. As the vev ω_s corresponding to the gauge boson mass and the one corresponding to scalar masses do not necessary coincide, an iteration process was run to rectify the situation.

- Due to the iteration process, the vev's of the theory get updated. As the doublet mass matrix, which is required to satisfy multiple conditions, is highly sensitive to the vev's, one needs to update the parameter space to ensure that availability of the massless Higgs doublet and keep the vev ratios fixed.

- This update of parameter space requires update of the vev's by iteration process described earlier so that gauge boson masses remain consistent. These updates of vev's and coupling parameters need to be iterated until the error is within an acceptable limit.

- At every step one also has to keep checking the positive-definiteness of all the eigenvalues of all mass matrices and pay special attention to the triplet mass matrix so that the lowest lying color triplet does not become much lighter than 10^{13} GeV.

2.9 Results with Benchmark points

In this section we present our procedure to pick a couple of benchmark points. Going through the procedure and constraints described in the previous section, we can identify sample points satisfying all the phenomenological constraints which would then become true candidates from the large parameter space. For that purpose, one can ease the process by including the conditions required to ensure the stability of the vacuum and positive-definiteness of all the scalar masses along with the issue of realistic fermion mass spectrum.

For example: being the only non-trivial coupling of $54^2 \cdot 126 \cdot \overline{126}$, β needs to be fine-tuned so that $(15, 2, 2)_{PS}$ stays in the intermediate scale. The conditions translates as $\beta\omega_s^2 \approx \sigma^2$, making

$\beta \lesssim \sigma^2/\omega_s^2 \approx 10^{-4}$, while positive-definiteness of the mass matrix of $(3,2,+1/6)$ says $\beta > 0$. Again, from the masses of $(1,3,0)$ and $(8,1,0)$, we can say that $b > 0$ for $\omega_s > 0$. Besides the condition described in Eq. (2.34), the couplings λ_2, λ_4 and λ_4' also have to maintain the following constraints among themselves to keep all other mass matrices positive-definite:

$$\begin{aligned}
3\lambda_2 + 3\lambda_4 + 4\lambda_4' &> 0; \\
\lambda_2 + \lambda_4 + 4\lambda_4' &> 0; \\
2\lambda_2 + 3\lambda_4 + 2\lambda_4' &> 0; \\
\lambda_2 + \lambda_4 &> 0; \\
8(\lambda_2 + \lambda_4 + 2\lambda_4')\sigma^2 + 4\beta\omega_s^2 &> 0; \\
8(\lambda_2 + \lambda_4 - 2\lambda_4')\sigma^2 + \beta\omega_s^2 &> 0.
\end{aligned}$$

After going through the process described before and keeping track of all the consistency checks and phenomenological constraints, one can produce an ample amount of benchmark points. One can adopt a one-loop RGE evolution while updating the beta functions as one arrives at the threshold of each scalar multiplet. Or one can adopt a two-loop RGE evolution while keeping all the threshold corrections at the corresponding scale. In the next couple of subsections we present our results for each cases.

Benchmark point using one-loop RGE

For the first case we consider the evolution of gauge couplings using one-loop RGE and include the effect of a scalar multiplet in the beta coefficients at the threshold energy scale corresponding to its mass. The benchmark point we select is given in Table 2.2 and corresponding mass spectrum is given in Table 2.3.

For such a sample point, the RGE evolution produces a unification corresponding to a (X,Y) gauge boson mass compatible with the current proton lifetime. For this benchmark point, the (X,Y) gauge bosons have a mass of 7.82×10^{15} GeV. Using Eq. (2.20) we find out the proton lifetime to be 5.72×10^{34} yrs, which is permitted by the current experimental limit, but reachable in the next upgrade of proton decay detectors. Also the vev ratios are capable of reproducing fermion mass spectrum as, $r = 69, s = 0.36, r_R \approx 10^{-14}$ as demanded by the fermion mass fitting shown in Ref. [18].

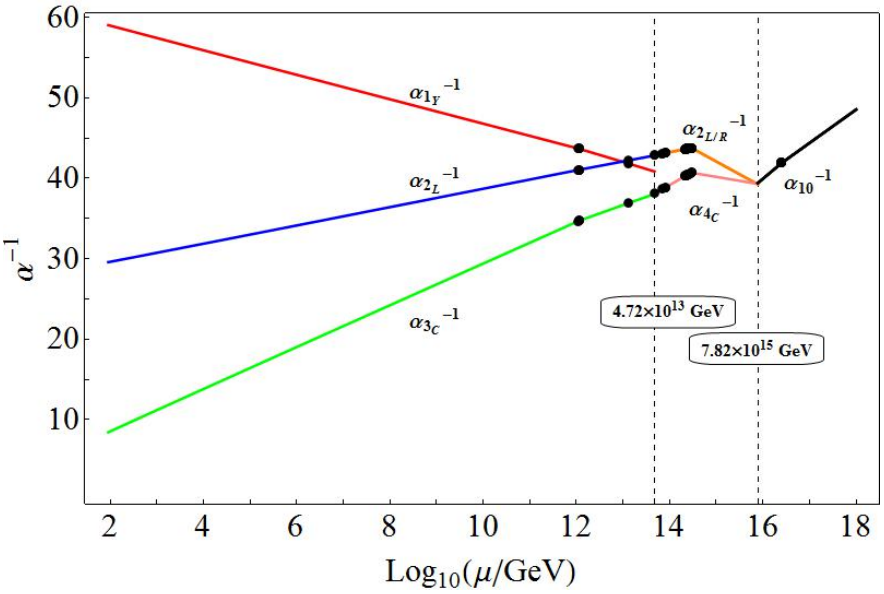

(a)

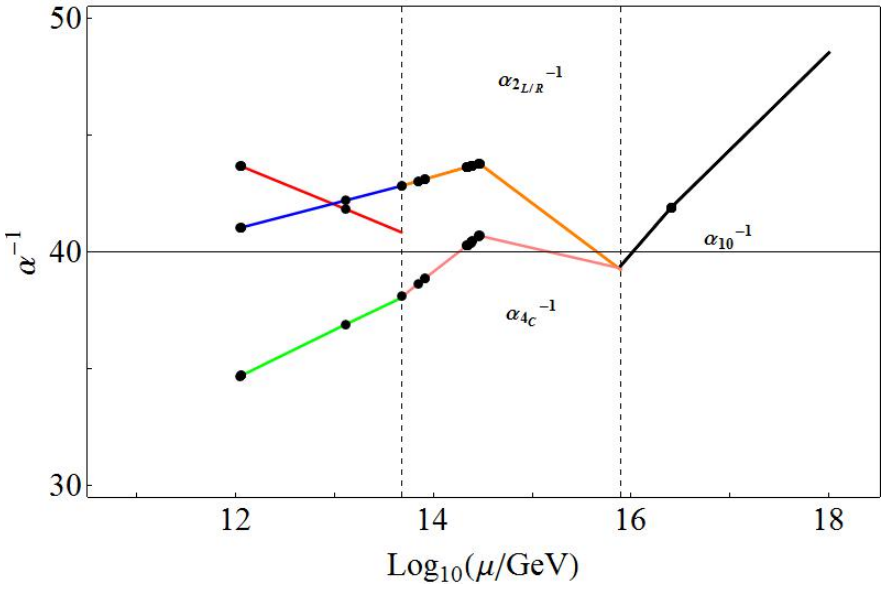

(b)

Figure 2.5: (a) Evolution of gauge couplings using one-loop RGE with threshold corrections determined by the scalar mass spectrum given in Table 2.3. The unification scale determined here is compatible with the current experimental limit on proton lifetime. The small black circles correspond to the various scalar masses changing the β function coefficients and inflicting changes in the slope of the graphs. The vertical dashed lines correspond to gauge boson masses that stay at intermediate scale and unification scale. (b) The region where the scalar bosons show up has been zoomed.

Parameter	Value	Parameter	Value
b	1.70	a	0.31
λ_2	-0.17	λ_0	0.90
λ_4	0.48	α	-0.23
λ_4'	0.17	χ_1	0.10
β	1.25×10^{-5}	χ_2	0.12
η_1	-0.002	χ_3	-0.01
η_2	0.90	c	9.36×10^{15} GeV
χ_4	-0.55	ξ_3	-3.15×10^{14} GeV
χ_5	0.32	χ_6	-2.67×10^{14} GeV
γ_1	-0.38	v_s	9.36×10^{10} GeV
γ_2	0.52	σ	8.65×10^{14} GeV
η_0	-0.15	ω_s	1.38×10^{16} GeV

Table 2.2: Sample parameters and vev's to generate a benchmark point using one-loop RGE. The initial parameter and the vev values were updated through the iteration processes described in the text, and the listed values correspond to the final stable point.

Benchmark point using two-loop RGE

After updating the sample point at one-loop level, so that it satisfies all the consistency checks and phenomenological constraints, one can upgrade the procedure to two-loop level, while including all the threshold corrections at the corresponding scales. For such a scenario, the vev's have been chosen to play the role of scales. The sample point for the two-loop case is given in Table 2.4 and the corresponding sample scalar mass spectrum is given in Table 2.5.

Again for such a sample point, the RGE evolution produces a unification scale corresponding to a (X, Y) gauge boson mass compatible with the current proton lifetime. In this benchmark point, the (X, Y) gauge boson has a mass of 7.11×10^{15} GeV. Using Eq. (2.20) we find out the proton lifetime to be 2.21×10^{34} yrs, which is permitted by the current experimental limit, but reachable in the next upgrade of proton decay detectors. Also the vev ratios are capable of reproducing fermion mass sprectrum as, $r = 69, s = 0.36, r_R \approx 10^{-14}$ as demanded by the fermion mass fitting shown in

Multiplet	Mass [GeV]	Multiplet	Mass [GeV]
$(1,3,0)$	2.54×10^{16}	$(8,1,0)$	1.11×10^{12}
$(3,3,-\frac{1}{3})$	2.17×10^{14}	$(6,3,+\frac{1}{3})$	2.42×10^{14}
$(1,1,+2)$	2.42×10^{14}	$(\overline{3},1,+\frac{4}{3})$	2.17×10^{14}
$(\overline{6},1,-\frac{4}{3})$	2.42×10^{14}	$(\overline{6},1,-\frac{1}{3})$	2.17×10^{14}
$(1,3,-1)$	2.54×10^{16}	$(\overline{6},1,+\frac{2}{3})$	1.13×10^{12}
	2.91×10^{14}		2.91×10^{14}
$(3,2,+\frac{7}{6})$	2.47×10^{14}	$(8,2,-\frac{1}{2})$	2.47×10^{14}
	2.22×10^{14}		2.22×10^{14}
$(3,2,+\frac{1}{6})$	4.83×10^{13}	$(1,2,-\frac{1}{2})$	2.23×10^{14}
	2.95×10^{14}		8.12×10^{13}
$(3,1,-\frac{1}{3})$	2.86×10^{14}		1.13×10^{12}
	2.37×10^{14}		≈ 0
	8.22×10^{14}	$(1,1,0)$	1.66×10^{16}
	6.99×10^{13}		3.90×10^{13}
	1.28×10^{13}		2.69×10^{10}

Table 2.3: Sample scalar mass spectrum corresponding to the benchmark point generated using one-loop RGE. The value of the parameters and vev's used to generate the spectrum is given in Table 2.2.

Ref. [18].

Even though it is desirable to generate Fig. 2.5 and Fig. 2.6 from the same sample point, numerically that becomes a difficult task. Even if one starts with the same sample point, due to the updates of parameters and vev coming from the fine-tuning of the doublet mass matrix and iteration process to reduce the error in determining the gauge boson masses (details are described in Sec. 2.8), one ends up with similar, yet not exactly the same sample point. But the uncertainty involved in the process only corresponds to error comparable to higher order loop corrections, and one can claim with enough confidence that final verdict based on such benchmark points is phenomenologically

Parameter	Value	Parameter	Value
b	1.70	a	0.31
λ_2	-0.17	λ_0	0.90
λ_4	0.49	α	-0.23
λ_4'	0.17	χ_1	0.10
β	1.25×10^{-5}	χ_2	0.12
η_1	-0.002	χ_3	-0.12
η_2	-0.73	c	8.50×10^{15} GeV
χ_4	-0.60	ξ_3	1.83×10^{15} GeV
χ_5	0.32	χ_6	-2.67×10^{14} GeV
γ_1	-0.38	v_s	9.36×10^{10} GeV
γ_2	0.52	σ	8.56×10^{13} GeV
η_0	-0.15	ω_s	1.25×10^{16} GeV

Table 2.4: Sample parameters and vev's to generate benchmark point using two-loop RGE. The initial parameters and the vev's were updated through the iteration processes described in the text, and the listed values correspond to the final stable point.

viable in all aspects.

One can keep repeating the process and generate multiple points which are phenomenologically viable in all aspects. A scatter plot with such points is shown in the Fig. 2.7. One major characteristics of the scatter plot with threshold corrections generated using the scalar boson mass spectrum is the distribution of the points, which indicates that the intermediate scale (σ) does not change much even though the scalar masses are generated with random parameters. This characteristic was missing when the scatter plot was generated with threshold corrections without considering the mass relationship coming into play from scalar mass spectrum. In the absence of such relationships, one can pick the scalar masses completely independently and push the intermediate or unification scale in either direction. But because of the mass relations, due to the fewer number of parameters in $SO(10)$ Lagrangian, one looses such freedom. Selecting one scalar mass in such a way that it will raise the scale fixes mass of another scalar which may tend to lower the scale. Due to the

Multiplet	Mass [GeV]	Multiplet	Mass [GeV]
$(1,3,0)$	2.31×10^{16}	$(8,1,0)$	1.11×10^{12}
$(3,3,-\frac{1}{3})$	2.18×10^{14}	$(6,3,+\frac{1}{3})$	2.42×10^{14}
$(1,1,+2)$	2.42×10^{14}	$(\overline{3},1,+\frac{4}{3})$	2.18×10^{14}
$(\overline{6},1,-\frac{4}{3})$	2.42×10^{14}	$(\overline{6},1,-\frac{1}{3})$	2.18×10^{14}
$(1,3,-1)$	2.31×10^{16}	$(\overline{6},1,+\frac{2}{3})$	1.13×10^{12}
	2.92×10^{14}		2.92×10^{14}
$(3,2,+\frac{7}{6})$	2.47×10^{14}	$(8,2,-\frac{1}{2})$	2.47×10^{14}
	2.22×10^{14}		2.22×10^{14}
$(3,2,+\frac{1}{6})$	2.96×10^{14}	$(1,2,-\frac{1}{2})$	2.23×10^{14}
	4.38×10^{13}		8.12×10^{13}
$(3,1,-\frac{1}{3})$	2.83×10^{14}		1.13×10^{12}
	2.35×10^{14}		≈ 0
	8.22×10^{13}	$(1,1,0)$	1.66×10^{16}
	7.06×10^{13}		3.90×10^{13}
	1.28×10^{13}		2.69×10^{10}

Table 2.5: Sample scalar mass spectrum corresponding to the benchmark point generated using two-loop RGE. The value of the parameters and vev's used to generate the spectrum is given in Table 2.4.

large number of scalar particles in the intermediate scale, the scale tends not to slide much in either direction. But the value of the gauge couplings at the scale do vary from sample to sample. Similar stationary properties are absent for the case of threshold corrections at the unification scale and one is able to raise the scale high enough to make the proton live long enough to escape the current experimental limit.

Proton lifetime however cannot be raised too much. If one respects the extended survival hypothesis, the upper bound on proton lifetime in this minimal model becomes a few times 10^{35} yrs. So there is a good possibility of discovering proton decay at Super-Kamiokande and the next generation

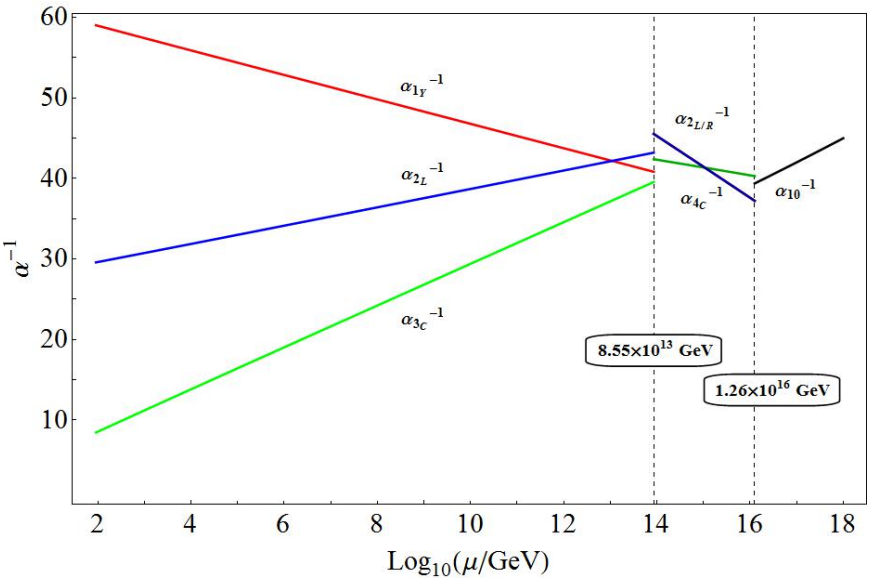

Figure 2.6: Evolution of gauge couplings using two-loop RGE with threshold corrections. The unification scale determined here is compatible with the current experimental limit on proton lifetime. The discontinuity in the running of the gauge couplings is due to the threshold corrections determined using the scalar mass spectrum given in Table 2.5. The vertical dashed lines correspond to the intermediate scale and unification scale.

experiments.

If one analyzes the scalar mass spectrum carefully, one realizes the fact that all the scalar masses have to remain in the vicinity of intermediate scale and unification scale. One can only introduce extra fine-tuning in the color octet $(8, 1, 0)$ mass and lower it down without spoiling the whole scenario. This is because its mass is not closely tied to the masses of other scalars and this color octet field does not mediate proton decay. By doing so, one also raises the predicted proton lifetime up to 10^{37} yrs which is beyond the reach of next generation proton decay detectors. This is not a likely scenario, since it could mean deviating significantly from the extended survival or equivalently minimal fine-tuning condition.

2.10 Proton decay branching ratios

As the color triplets Higgs in the model are always kept heavier than 10^{13} GeV, the primary source of proton decay is due to $d = 6$ gauge boson mediating effective operators which are given by

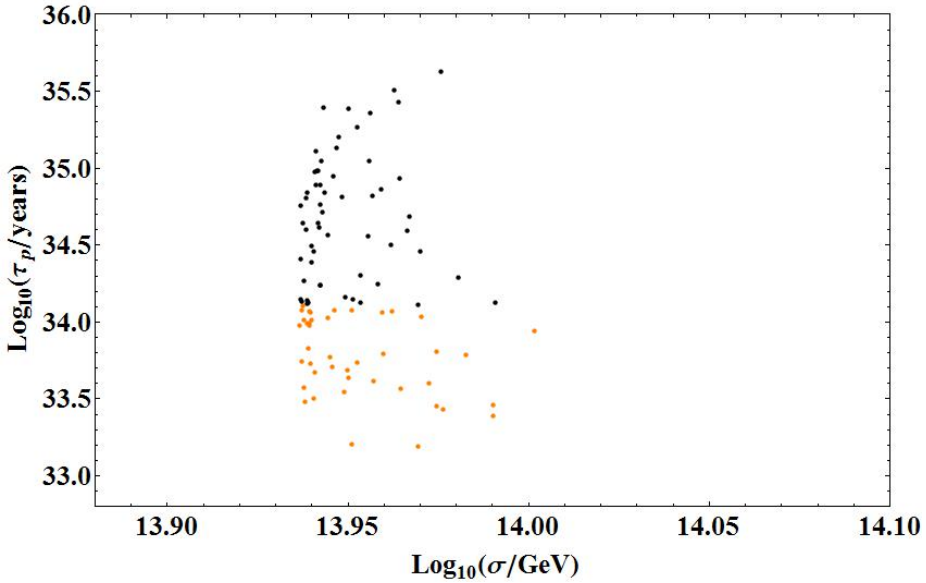

Figure 2.7: Scatter plot for the proton lifetime (τ_p) vs. $\langle 126_H \rangle = \sigma$ generated using one-loop RGE. All the points correspond to proper gauge couplings unification and are compatible with realistic fermion masses and mixings. Only the black points comply with the current experimental limit of proton lifetime.

[75, 63, 76, 57, 58]

$$\begin{aligned}
\mathcal{O}_I^{B-L} &= k_1^2\ \epsilon_{ijk}\ \epsilon_{\alpha\beta}\ \overline{u_{ia\,L}^C}\ \gamma^\mu\ Q_{j\alpha aL}\ \overline{e_{b\ L}^C}\ \gamma_\mu\ Q_{k\beta bL};\\
\mathcal{O}_{II}^{B-L} &= k_1^2\ \epsilon_{ijk}\ \epsilon_{\alpha\beta}\ \overline{u_{ia\,L}^C}\ \gamma^\mu\ Q_{j\alpha aL}\ \overline{d_{kb\,L}^C}\ \gamma_\mu\ L_{\beta bL};\\
\mathcal{O}_{III}^{B-L} &= k_2^2\ \epsilon_{ijk}\ \epsilon_{\alpha\beta}\ \overline{d_{ia\,L}^C}\ \gamma^\mu\ Q_{j\beta aL}\ \overline{u_{kb\,L}^C}\ \gamma_\mu\ L_{\alpha bL};\\
\mathcal{O}_{IV}^{B-L} &= k_2^2\ \epsilon_{ijk}\ \epsilon_{\alpha\beta}\ \overline{d_{ia\,L}^C}\ \gamma^\mu\ Q_{j\beta aL}\ \overline{\nu_{b\ L}^C}\ \gamma_\mu\ Q_{k\alpha bL}.
\end{aligned} \tag{2.36}$$

Here, $k_1 = {}^{g_u}/_{(\sqrt{2}M_{(X,Y)})}$ and $k_2 = {}^{g_u}/_{(\sqrt{2}M_{(X',Y')})}$, $Q_L = (u_L, d_L)$ and $L_L = (\nu_L, e_L)$. The indices i, j, k are color indices, a, b are family indices and α, β are $SU(2)_L$ indices. The effective operators in physical basis becomes,

$$\begin{aligned}
\mathcal{O}(e_\alpha^C, d_\beta) &= c(e_\alpha^C, d_\beta)\ \epsilon_{ijk}\ \overline{u_{i\ L}^C}\ \gamma^\mu u_{jL}\ \overline{e_{\alpha\,L}^C}\ \gamma_\mu\ d_{k\beta L};\\
\mathcal{O}(e_\alpha, d_\beta^C) &= c(e_\alpha, d_\beta^C)\ \epsilon_{ijk}\ \overline{u_{i\ L}^C}\ \gamma^\mu u_{jL}\ \overline{d_{k\beta\,L}^C}\ \gamma_\mu\ e_{\alpha L};
\end{aligned}$$

$$\begin{aligned}
\mathcal{O}(\nu_l, d_\alpha, d_\beta^C) &= c(\nu_l, d_\alpha, d_\beta^C)\ \epsilon_{ijk}\ \overline{u_{i\ L}^C}\ \gamma^\mu\ d_{j\alpha L}\ \overline{d_{k\beta\,L}^C}\ \gamma_\mu\ \nu_{lL};\\
\mathcal{O}(\nu_l^C, d_\alpha, d_\beta^C) &= c(\nu_l^C, d_\alpha, d_\beta^C)\ \epsilon_{ijk}\ \overline{d_{i\beta\,L}^C}\ \gamma^\mu\ u_{jL}\ \overline{\nu_{l\ L}^C}\ \gamma_\mu\ d_{k\alpha L};
\end{aligned} \tag{2.37}$$

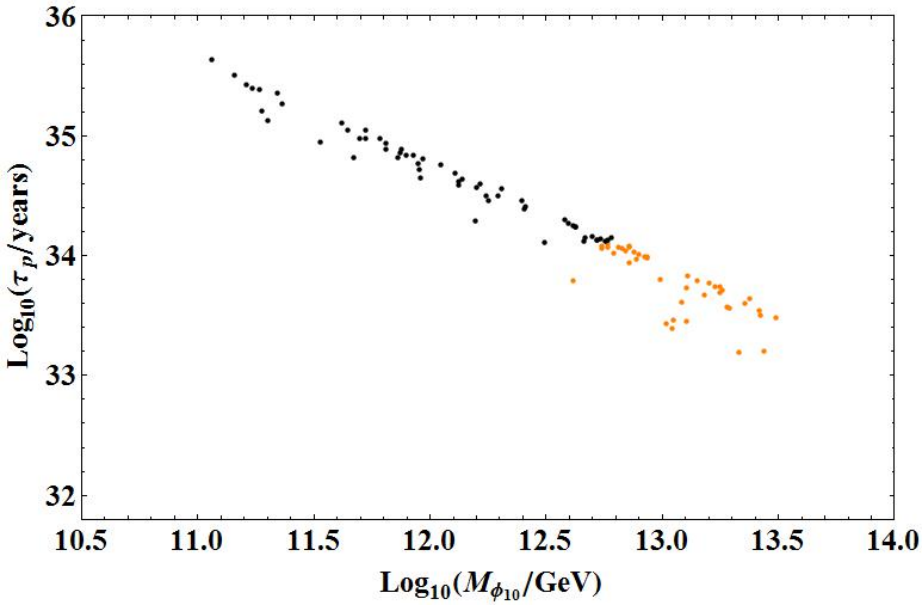

Figure 2.8: Scatter plot for proton lifetime (τ_p) as a function of the color octet mass ($M_{\phi_{10}}$) generated using one-loop RGE. All the points correspond to proper gauge couplings unification and compatible with realistic fermion masses and mixings. Only the black points comply with the current experimental limit on proton lifetime. Fine-tuning the octet mass to a lower energy scale does not create any internal inconsistency or phenomenological issue. But the extra fine-tuning does mean that one is deviating significantly from the extended survival hypothesis or equivalently minimal fine-tuning condition. That is why we consider highly fine-tuned octet mass which corresponds to a high a proton lifetime as not a likely scenario.

where

$$
\begin{aligned}
c(e^C_\alpha, d_\beta) &= k_1^2 \left[V_1^{11} V_2^{\alpha\beta} + (V_1 V_{UD})^{1\beta} \left(V_2 V_{UD}^\dagger \right)^{\alpha 1} \right]; \\
c(e_\alpha, d^C_\beta) &= k_1^2 V_1^{11} V_3^{\beta\alpha} + k_2^2 \left(V_4 V_{UD}^\dagger \right)^{\beta 1} \left(V_1 V_{UD} V_4^\dagger V_3 \right)^{1\alpha}; \\
c(\nu_l, d_\alpha, d^C_\beta) &= k_1^2 \left(V_1 V_{UD} \right)^{1\alpha} \left(V_3 V_{EN} \right)^{\beta l} + k_2^2 V_4^{\beta\alpha} \left(V_1 V_{UD} V_4^\dagger V_3 V_{EN} \right)^{1l}; \\
c(\nu^C_l, d_\alpha, d^C_\beta) &= k_2^2 \left[\left(V_4 V_{UD}^\dagger \right)^{\beta 1} \left(U_{EN}^\dagger V_2 \right)^{l\alpha} + V_4^{\beta\alpha} \left(U_{EN}^\dagger V_2 V_{UD}^\dagger \right)^{l1} \right]; \alpha = \beta \neq 2.
\end{aligned}
\tag{2.38}
$$

The mixing matrices are defined as : $V_1 = U_C^\dagger U$, $V_2 = E_C^\dagger D$, $V_3 = D_C^\dagger E$, $V_4 = D_C^\dagger D$, $V_{UD} = U^\dagger D$, $V_{EN} = E^\dagger N$ and $U_{EN} = E_C^\dagger N_C$, where U,D,E define the Yukawa coupling diagonalization so that

$$
\begin{aligned}
U_C^T Y_U U &= Y_U^{diag}; \qquad & D_C^T Y_D D &= Y_D^{diag}; \\
E_C^T Y_E E &= Y_E^{diag}; \qquad & N^T Y_N N &= Y_N^{diag}.
\end{aligned}
\tag{2.39}
$$

For the $SO(10)$ model with symmetric Yukawa couplings, the mixing matrices becomes $U_C = UK_u$, $D_C = DK_d$ and $E_C = EK_e$, where K_u, K_d and K_e are diagonal matrices containing three phases. The proton decay rate into different channels due to the presence of the gauge mediated $d = 6$ operators are given by [56, 57]:

$$\Gamma(p \to K^+\overline{\nu}) = \frac{\left(m_p^2 - m_K^2\right)^2}{8\pi m_p^3 f_\pi^2} R_L^2 A_S^2 \left|\alpha\right|^2 \sum_{i=1}^{3} \left| \frac{2m_p}{3m_B} D\, c\left(\nu_i, d, s^C\right) + \left[1 + \frac{m_p}{3m_B}\left(D + 3F\right)\right] c\left(\nu_i, s, d^C\right) \right|^2;$$

$$\Gamma\left(p \to \pi^+\overline{\nu}\right) = \frac{m_p}{8\pi f_\pi^2} R_L^2 A_S^2 \left|\alpha\right|^2 \left(1 + D + F\right) \sum_{i=1}^{3} \left|c\left(\nu_i, d, d^C\right)\right|^2;$$

$$\Gamma\left(p \to \eta e_\beta^+\right) = \frac{\left(m_p^2 - m_\eta^2\right)^2}{48\pi m_p^3 f_\pi^2} R_L^2 A_S^2 \left|\alpha\right|^2 \left(1 + D - 3F\right)^2 \left\{\left|c\left(e_\beta, d^C\right)\right|^2 + \left|c\left(e_\beta^C, d\right)\right|^2\right\};$$

$$\Gamma\left(p \to K^0 e_\beta^+\right) = \frac{\left(m_p^2 - m_K^2\right)^2}{8\pi m_p^3 f_\pi^2} R_L^2 A_S^2 \left|\alpha\right|^2 \left[1 + \frac{m_p}{m_B}\left(D - F\right)\right]^2 \left\{\left|c\left(e_\beta, s^C\right)\right|^2 + \left|c\left(e_\beta^C, s\right)\right|^2\right\};$$

$$\Gamma\left(p \to \pi^0 e_\beta^+\right) = \frac{m_p}{16\pi f_\pi^2} R_L^2 A_S^2 \left|\alpha\right|^2 \left(1 + D + F\right)^2 \left\{\left|c\left(e_\beta, d^C\right)\right|^2 + \left|c\left(e_\beta^C, d\right)\right|^2\right\}; \tag{2.40}$$

where, $\nu_i = \nu_e, \nu_\mu, \nu_\tau$ and $e_\beta = e, \mu$. Here m_B is the average baryon mass satisfying $m_B \approx m_\Sigma \approx \Lambda$. As the current (and most probably next generation) proton decay detectors are insensitive to the flavor of the neutrinos, proton decay rates are calculated by summing over all the flavors. For similar reason the chirality of the charged lepton is also summed over. Here, $A_S \approx 2$ is the average of the left-handed and right-handed short range renormalization factor.

Now if we consider the fermion masses and mixings given in the ref [18], using the vev ratio parameter values $r = 69$ and $s = 0.36$, the proton decay branching ratio due to gauge mediated $d = 6$ operator are given in the Table 2.6.

These branching ratios mainly depend on the ratio of the leptoquark gauge bosons ${}^{k_1}/_{k_2} = {}^{M_{(X',Y')}}/_{M_{(X,Y)}}$. From the gauge boson mass spectrum and the scatter plot (Fig. 2.9), it is clear that in this $SO(10)$ model, the branching ratios will not vary much within the phenomenologically viable parameter space. We see that the dominant modes are $p \to e^+\pi^0$ and $p \to \overline{\nu}\pi^+$, with roughly equal rates.

The proton decay branching ratios given in Table 2.6 is quite similar to the one given in Ref. [77] for the case of minimal $SO(10)$ with split supersymmetry. This is mainly due to the fact that the Yukawa sector is essentially the same (up to renormalization effects) and since $M_{(X,Y)} \backsimeq M_{(X',Y')}$ was assumed in Ref. [77].

Process	Branching ratio
$p \to \pi^0 e^+$	$\approx 47\%$
$p \to \pi^0 \mu^+$	$\approx 1.00\%$
$p \to \eta^0 e^+$	$\approx 0.20\%$
$p \to \eta^0 \mu^+$	$\approx 0.004\%$
$p \to K^0 e^+$	$\approx 0.16\%$
$p \to K^0 \mu^+$	$\approx 3.62\%$
$p \to \pi^+ \overline{\nu}$	$\approx 48\%$
$p \to K^+ \overline{\nu}$	$\approx 0.22\%$

Table 2.6: The branching ratio of proton decay by gauge mediated $d = 6$ operator.

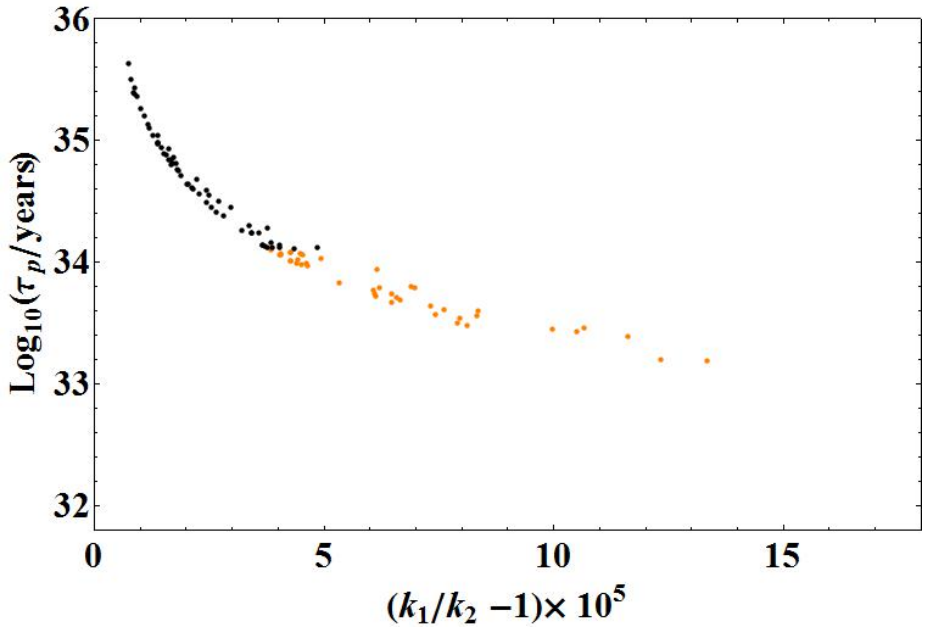

Figure 2.9: Proton Lifetime(τ_p) vs ratio of the $(k_1/k_2 - 1) \times 10^5$. The plot indicates that the ratio of $k_1/k_2 = M_{(X',Y')}/M_{(X,Y)}$ varies less than 0.02% (0.005%) over the whole (phenomenologically viable) parameter space.

2.11 Axions as Dark Matter

Introducing a Peccei-Quinn(PQ)-symmetry [38] in non-supersymmetric $SO(10)$ GUTs provides the perfect framework for the axionic dark matter which simultaneously solves the strong CP problem.

The PQ-symmetry affected the Higgs potential (by removing terms like 126^4) and also made the Yukawa sector realistic and predictive. Yet, the main contribution of the PQ-symmetry is to provide axion as dark matter candidate which can explain the entire dark matter abundance in the universe while also solving the strong CP problem.

The axion in the model is of DFSZ type [78, 79]. While the original DFSZ axion was mainly composed of a complex singlet field with an admixture of one up-type Higgs doublet and one down-type Higgs doublet, the axion in this model is mainly composed of the complex singlet field (S_H) with the admixture of two up-type Higgs doublets (H_u from 126_H and h_u from 10_H) and two down type Higgs doublets (H_d from 126_H and h_d from 10_H).

In the model, the PQ-symmetry is broken by the vev of the singlet S_H, and the scale is quiet independent of the intermediate (Pati-Salam) scale and unification scale. Even though the choice of v_s is mainly guided by the axion phenomenology, in the numerical analysis of the sample points we found out that the PQ-breaking scale stays around $\left(5 \times 10^{10} - 1 \times 10^{12}\right)$ GeV without any extra fine-tuning. In that case, the axion mass can be computed using

$$m_a = \frac{z^{1/2}}{1+z} \frac{f_\pi m_\pi}{f_a} \tag{2.41}$$

where $z = {}^{m_u}/_{m_d}$ and f_a is the axion decay constant. For the numerical analysis we took $m_\pi = 135$ MeV and $f_\pi \approx 130.7$ MeV and kept the range of $z = 0.35 - 0.60$ [80]. Then for $f_a = v_s$, we get m_a $(8-175)$ μeV, which is compatible with both the laboratory experimental limit and astrophysical bounds.

PQ-symmetry breaking before or during inflation

The cosmic mass density of axion field today is [81]

$$\Omega_a h^2 \approx 0.7 \left(\frac{f_a}{10^{12}\ GeV}\right)^{7/6} \left(\frac{\overline{\Theta}_i}{\pi}\right)^2, \tag{2.42}$$

where h is the present-day Hubble expansion parameter and $-\pi \geq \overline{\Theta}_i \geq \pi$ is the initial "misalignment angle". If the PQ-symmetry is broken before or during inflation, inflation expands a domain with some value of $\overline{\Theta}_i$ to a size larger than the present universe. In that case, $\overline{\Theta}_i$ can take any value and naturally should not be fine-tuned. Using the experimental limit $\Omega_a h^2 = 0.1199 \pm 0.0027$ [82], we can scan the parameter space in the α, f_a basis.

As the model allows the axion decay constant as low as 5×10^{10} GeV and as high as 10^{12} GeV, the misalignment angle can take any value beyond 1.26, ie $1.26 < \left|\overline{\Theta}_i\right| < \pi$. We also see that, for f_a smaller than 2.33×10^{11} GeV, axionic dark matter fails to explain the entirety of dark matter abundance.

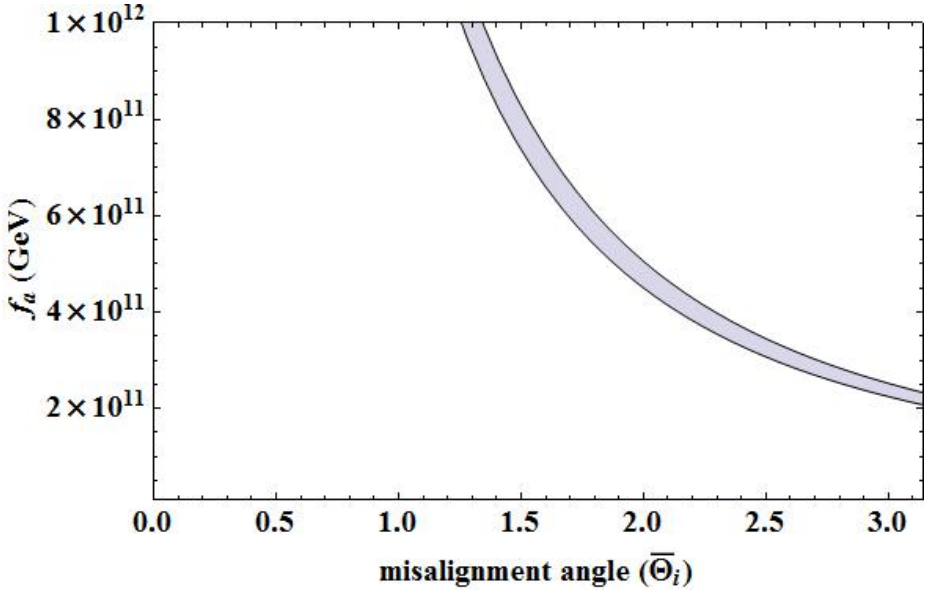

Figure 2.10: The region in the parameter space where cold ADM saturates the dark matter abundance.

From the recent Planck data, we find that if we assume that the PQ symmetry is broken during inflation and it is not restored by the quantum fluctuation of the inflation nor by thermal fluctuation in the case of a very efficient reheating stage and all of cold dark matter (CDM) consists of axions produced by the misalignment angle mechanism, the upper bound on the energy scale of inflation (H_{inf}) becomes[83]:

$$H_{inf} \leq 0.87 \times 10^7\ GeV \left(\frac{f_a}{10^{11}\ GeV}\right)^{0.408}. \tag{2.43}$$

This is due to the fact that the axion which already exists during inflation obtains large quantum fluctuations and produces isocurvature density perturbations which are stringently constrained by CMB observation. So, for low axion decay constant, we end up having an upper bound on the energy scale of inflation as low as 10^7 GeV.

PQ-symmetry breaking after inflation

Cosmological consequences of axions are different if the PQ-symmetry is broken after inflation. Unlike the previous case, universe does not settle into the same minimum when the axion acquires its mass at the QCD scale and ends up forming topological defects [84]. Now, the misalignment axion cold dark matter energy density is given by [85]

$$\Omega_{a,mis}h^2 = 2.07 \left(\frac{f_a}{10^{12}\ GeV}\right)^{7/6} \tag{2.44}$$

while

$$\Omega_a h^2 = 2.07(1+\alpha_{dec})\left(\frac{f_a}{10^{12}\ GeV}\right)^{7/6} \tag{2.45}$$

where $\alpha_{dec} = 0.164$ corresponds to the factor introduced due to the decay of topological defects like axionic strings [85]. Under such consideration, one finds that the Planck data corresponds to a axion mass $m_a \approx 80\ \mu$eV and axion decay constant $f_a \approx 8 \times 10^{10}$ GeV [85], which are perfectly admissible in the GUT under scrutiny.

2.12 Conclusion

The Standard Model emerged in the early seventies and since then it has been weathered by all sorts of experiments at various laboratories and colliders. Until now, it has given the best description of nature. Recent discoveries about dark matter, neutrino masses and mixings and old questions like charge quantization and baryogenesis demand physics beyond the SM, yet LHC data up to now has failed to provide any glimpse of such new physics. In the realm of unification models, the supersymmetric $SO(10)$ GUTs have been studied in depth in the past decades [86]. The crucial point about $SO(10)$ GUTs is that if we change our current attitude about fine-tuning, yet keep it at the minimal level by adopting philosophy like extended survival hypothesis, we realize that even without supersymmetry, $SO(10)$ symmetry has the potential to be the gauge symmetry of nature on its own right, at least up to the GUT scale ($\sim 10^{16}$ GeV). The absence of low energy supersymmetry might be the reality of our universe, taking away primary motivation to introduce supersymmetry. Thus it becomes mandatory to revisit the non-supersymmetric version of $SO(10)$ GUTs with a more open attitude.

The purpose of the paper was to search for the minimal non-supersymmetric $SO(10)$ grand unified model which can withstand the pressure of all the phenomenological constraints. Our aim was to address all possible issues (except gravity) either explicitly or by showing that the model has enough flexibility to accommodate the phenomena. We acknowledge that the minimality is not a universal and uniquely defined concept. In this work, the philosophy of minimality was applied in the choice Higgs representation and that resulted in a breaking pattern with minimal number of intermediate scale (namely one) making the model truly minimal and predictive.

Such a minimal model ended up relying on threshold corrections to escape from the wrath of experimental bounds on proton lifetime. The issue of threshold corrections deserves particular attention here. On one hand, one should not discard a model without taking into account the threshold corrections, on the other hand, one should not expect that threshold corrections can

rescue any model before performing detailed calculation.

The non-SUSY $SO(10)$ GUT presented here managed to unify the gauge couplings at a scale high enough to comply with the current experimental bound of proton lifetime. The Yukawa sector of the model provided a realistic description of fermion masses and mixings. The PQ-phase transition introduced axion as the dark matter candidate that can explain the dark matter abundance in the universe, while also solving the strong CP problem. Leptogenesis finds a natural place in $SO(10)$ with seesaw mechanism and the Yukawa sector of the model has the potential to procure the right amount. Physics of inflation may reside outside the scope of the model or within the model where one (or more) SM singlets already present may provide the necessary ingredients.

One should emphasis the claim that the SM spectrum is completed by the recently discovered light Higgs and LHC should fail to find any other new physics, as the next scale of physics lies at the energy scale of 10^{10} GeV. Before getting demoralized one also needs to realize that the model generally predicts a proton lifetime less than a few times 10^{35} yrs. So Super-Kamiokande or next generation proton decay detectors and axion search experiments has the potential to discover the essential phenomenological proof of the model.

REFERENCES

[1] J. C. Pati and A. Salam, Phys. Rev. Lett. **31**, 661 (1973).

[2] J. C. Pati and A. Salam, Phys. Rev. D **10**, 275 (1974) [Phys. Rev. D **11**, 703 (1975)].

[3] H. Georgi and S. L. Glashow, Phys. Rev. Lett. **32**, 438 (1974).

[4] H. Georgi, H. R. Quinn and S. Weinberg, Phys. Rev. Lett. **33**, 451 (1974).

[5] S. Dimopoulos, S. Raby and F. Wilczek, Phys. Rev. D **24**, 1681 (1981); L. E. Ibanez and G. G. Ross, Phys. Lett. B **105**, 439 (1981); M. B. Einhorn and D. R. T. Jones, Nucl. Phys. B **196**, 475 (1982); W. J. Marciano and G. Senjanovic, Phys. Rev. D **25**, 3092 (1982); P. Langacker and M. x. Luo, Phys. Rev. D **44**, 817 (1991); C. Giunti, C. W. Kim and U. W. Lee, Mod. Phys. Lett. A **6**, 1745 (1991); U. Amaldi, W. de Boer and H. Furstenau, Phys. Lett. B **260**, 447 (1991).

[6] S. Chatrchyan *et al.* [CMS Collaboration], Phys. Lett. B **716**, 30 (2012) [arXiv:1207.7235 [hep-ex]]; G. Aad *et al.* [ATLAS Collaboration], Phys. Lett. B **716**, 1 (2012) [arXiv:1207.7214 [hep-ex]]; G. Aad *et al.* [ATLAS and CMS Collaborations], Phys. Rev. Lett. **114**, 191803 (2015) [arXiv:1503.07589 [hep-ex]].

[7] E. Gildener, Phys. Rev. D **14**, 1667 (1976); M. J. G. Veltman, Acta Phys. Polon. B **12**, 437 (1981); E. Witten, Nucl. Phys. B **188**, 513 (1981); E. Witten, Phys. Lett. B **105**, 267 (1981).

[8] B. Bajc, A. Melfo, G. Senjanovic and F. Vissani, Phys. Rev. D **73**, 055001 (2006) [hep-ph/0510139].

[9] G. Altarelli and D. Meloni, JHEP **1308**, 021 (2013) [arXiv:1305.1001, arXiv:1305.1001 [hep-ph]].

[10] J. D. Barrow and F. J. Tipler, "The Anthropic Cosmological Principle", (Clarrendon, Oxford,1986); P. C. W. Davies, "The Accidental Universe" (Cambridge Univ. Press,Cambridge,1982); B. Carter, Philos. Trans. Roy. Soc. London A **310**, 347(1983).

[11] J. Frieman, M. Turner and D. Huterer, Ann. Rev. Astron. Astrophys. **46**, 385 (2008) [arXiv:0803.0982 [astro-ph]].

[12] V. Agrawal, S. M. Barr, J. F. Donoghue and D. Seckel, Phys. Rev. D **57**, 5480 (1998) [hep-ph/9707380].

[13] For a review, see A. H. Guth, J. Phys. A **40**, 6811 (2007) [hep-th/0702178 [HEP-TH]].

[14] M. R. Douglas and S. Kachru, Rev. Mod. Phys. **79**, 733 (2007) [hep-th/0610102]; M. R. Douglas, arXiv:1204.6626 [hep-th].

[15] S. Bertolini, L. Di Luzio and M. Malinsky, Phys. Rev. D **81**, 035015 (2010) [arXiv:0912.1796 [hep-ph]]; S. Bertolini, L. Di Luzio and M. Malinsky, J. Phys. Conf. Ser. **259**, 012098 (2010) [arXiv:1010.0338 [hep-ph]].

[16] S. Bertolini, L. Di Luzio and M. Malinsky, Phys. Rev. D **85**, 095014 (2012) [arXiv:1202.0807 [hep-ph]]; S. Bertolini, L. Di Luzio and M. Malinsky, AIP Conf. Proc. **1467**, 37 (2012) [arXiv:1205.5637 [hep-ph]]; M. Malinsky, S. Bertolini and L. Di Luzio, AIP Conf. Proc. **1534**, 293 (2012) [arXiv:1210.3789 [hep-ph]].

[17] S. Bertolini, L. Di Luzio and M. Malinsky, Phys. Rev. D **87**, no. 8, 085020 (2013) [arXiv:1302.3401 [hep-ph]].

[18] A. S. Joshipura and K. M. Patel, Phys. Rev. D **83**, 095002 (2011) [arXiv:1102.5148 [hep-ph]].

[19] F. Buccella, D. Falcone, C. S. Fong, E. Nardi and G. Ricciardi, Phys. Rev. D **86** (2012) 035012 [arXiv:1203.0829 [hep-ph]].

[20] Y. Mambrini, N. Nagata, K. A. Olive, J. Quevillon and J. Zheng, Phys. Rev. D **91**, no. 9, 095010 (2015) [arXiv:1502.06929 [hep-ph]].

[21] H. Georgi, in Particles and Fields, Ed. by C. Carlson (AIP, NY, 1975); H. Fritzsch and P. Minkowski, Annals Phys. **93**, 193 (1975).

[22] T. G. Rizzo and G. Senjanovic, Phys. Rev. Lett. **46**, 1315 (1981); T. G. Rizzo and G. Senjanovic, Phys. Rev. D **24**, 704 (1981) [Phys. Rev. D **25**, 1447 (1982)]; T. G. Rizzo and G. Senjanovic, Phys. Rev. D **25**, 235 (1982).

[23] see also, W. E. Caswell, J. Milutinovic and G. Senjanovic, Phys. Rev. D **26**, 161 (1982).

[24] J. M. Gipson and R. E. Marshak, Phys. Rev. D **31**, 1705 (1985).

[25] D. Chang, R. N. Mohapatra, J. Gipson, R. E. Marshak and M. K. Parida, Phys. Rev. D **31**, 1718 (1985).

[26] N. G. Deshpande, E. Keith and P. B. Pal, Phys. Rev. D **46**, 2261 (1993).

[27] N. G. Deshpande, E. Keith and P. B. Pal, Phys. Rev. D **47**, 2892 (1993) [hep-ph/9211232].

[28] S. Bertolini, L. Di Luzio and M. Malinsky, Phys. Rev. D **80**, 015013 (2009) [arXiv:0903.4049 [hep-ph]].

[29] R. N. Mohapatra and J. C. Pati, Phys. Rev. D **11**, 2558 (1975); G. Senjanovic and R. N. Mohapatra, Phys. Rev. D **12**, 1502 (1975); G. Senjanovic, Nucl. Phys. B **153**, 334 (1979).

[30] P. Minkowski, Phys. Lett. B **67**, 421 (1977); O. Sawada and A. Sugamoto, Tsukuba, Japan: Natl.Lab.High Energy Phys.(1979) 109 P.and Japan Natl Lab High Energy - KEK-79-18 (79,REC.JAN 80) 109p; S. Glashow, In *Cargese 1979, Proceedings, Quarks and Leptons* M. Gell-Mann, P. Ramond and R. Slansky, Conf. Proc. C **790927**, 315 (1979) [arXiv:1306.4669 [hep-th]]; R. N. Mohapatra and G. Senjanovic, Phys. Rev. Lett. **44**, 912 (1980).

[31] See also, J. Schechter and J. W. F. Valle, Phys. Rev. D **22**, 2227 (1980); J. Schechter and J. W. F. Valle, Phys. Rev. D **25**, 774 (1982).

[32] M. Fukugita and T. Yanagida, Phys. Lett. B **174**, 45 (1986).

[33] For a recent review, see S. Davidson, E. Nardi and Y. Nir, Phys. Rept. **466**, 105 (2008) [arXiv:0802.2962 [hep-ph]].

[34] K. S. Babu and R. N. Mohapatra, Phys. Rev. D **86**, 035018 (2012) [arXiv:1203.5544 [hep-ph]]; K. S. Babu and R. N. Mohapatra, Phys. Lett. B **715**, 328 (2012) [arXiv:1206.5701 [hep-ph]].

[35] K. S. Babu and R. N. Mohapatra, Phys. Rev. Lett. **109**, 091803 (2012) [arXiv:1207.5771 [hep-ph]];

[36] H. Nishino *et al.* [Super-Kamiokande Collaboration], Phys. Rev. D **85**, 112001 (2012) [arXiv:1203.4030 [hep-ex]].

[37] K. S. Babu *et al.*, "Working Group Report: Baryon Number Violation," arXiv:1311.5285 [hep-ph].

[38] R. D. Peccei and H. R. Quinn, Phys. Rev. Lett. **38**, 1440 (1977).

[39] J. A. Casas, J. R. Espinosa and M. Quiros, Phys. Lett. B **342**, 171 (1995) [hep-ph/9409458]; J. A. Casas, J. R. Espinosa and M. Quiros, Phys. Lett. B **382**, 374 (1996) [hep-ph/9603227]; G. Isidori, G. Ridolfi and A. Strumia, Nucl. Phys. B **609**, 387 (2001) [hep-ph/0104016];

C. P. Burgess, V. Di Clemente and J. R. Espinosa, JHEP **0201**, 041 (2002) [hep-ph/0201160]; G. Degrassi, S. Di Vita, J. Elias-Miro, J. R. Espinosa, G. F. Giudice, G. Isidori and A. Strumia, JHEP **1208**, 098 (2012) [arXiv:1205.6497 [hep-ph]].

[40] J. Elias-Miro, J. R. Espinosa, G. F. Giudice, H. M. Lee and A. Strumia, JHEP **1206**, 031 (2012) [arXiv:1203.0237 [hep-ph]].

[41] For example, A. Salvio, Phys. Lett. B **743**, 428 (2015) [arXiv:1501.03781 [hep-ph]].

[42] M. Abud, F. Buccella, D. Falcone and D. Falcone, Phys. Rev. D **86**, 073014 (2012) [arXiv:1207.4979 [hep-ph]].

[43] L. F. Li, Phys. Rev. D **9**, 1723 (1974).

[44] M. Yasue, Phys. Rev. D **24**, 1005 (1981).

[45] G. Anastaze, J. P. Derendinger and F. Buccella, Z. Phys. C **20**, 269 (1983).

[46] K. S. Babu and E. Ma, Phys. Rev. D **31**, 2316 (1985).

[47] S. Bertolini, L. Di Luzio and M. Malinsky, Phys. Rev. D **81**, 035015 (2010) [arXiv:0912.1796 [hep-ph]].

[48] D. Chang, R. N. Mohapatra and M. K. Parida, Phys. Rev. Lett. **52**, 1072 (1984).

[49] H. Georgi, Nucl. Phys. B **156**, 126 (1979).

[50] F. del Aguila and L. E. Ibanez, Nucl. Phys. B **177**, 60 (1981).

[51] R. N. Mohapatra and G. Senjanovic, Phys. Rev. D **27**, 1601 (1983).

[52] K. S. Babu and R. N. Mohapatra, Phys. Rev. Lett. **70**, 2845 (1993) [hep-ph/9209215].

[53] M. E. Machacek and M. T. Vaughn, Nucl. Phys. B **222**, 83 (1983).

[54] L. J. Hall, Nucl. Phys. B **178**, 75 (1981).

[55] R. N. Mohapatra and M. K. Parida, Phys. Rev. D **47**, 264 (1993) [hep-ph/9204234].

[56] M. Claudson, M. B. Wise and L. J. Hall, Nucl. Phys. B **195**, 297 (1982); S. Chadha and M. Daniel, Nucl. Phys. B **229**, 105 (1983).

[57] P. Fileviez Perez, Phys. Lett. B **595**, 476 (2004) [hep-ph/0403286].

[58] P. Nath and P. Fileviez Perez, Phys. Rept. **441**, 191 (2007) [hep-ph/0601023].

[59] T. Nihei and J. Arafune, Prog. Theor. Phys. **93**, 665 (1995) [hep-ph/9412325].

[60] Y. Aoki, C. Dawson, J. Noaki and A. Soni, Phys. Rev. D **75**, 014507 (2007) [hep-lat/0607002].

[61] A. J. Buras, J. R. Ellis, M. K. Gaillard and D. V. Nanopoulos, Nucl. Phys. B **135**, 66 (1978).

[62] J. R. Ellis, M. K. Gaillard and D. V. Nanopoulos, Phys. Lett. B **88**, 320 (1979).

[63] F. Wilczek and A. Zee, Phys. Rev. Lett. **43**, 1571 (1979).

[64] I. Dorsner and I. Mocioiu, Nucl. Phys. B **796**, 123 (2008) [arXiv:0708.3332 [hep-ph]].

[65] R. N. Mohapatra and G. Senjanovic, Z. Phys. C **17**, 53 (1983); R. Holman, G. Lazarides and Q. Shafi, Phys. Rev. D **27**, 995 (1983).

[66] C. S. Aulakh and A. Girdhar, Int. J. Mod. Phys. A **20**, 865 (2005) [hep-ph/0204097]; C. S. Aulakh and A. Girdhar, Nucl. Phys. B **711**, 275 (2005) [hep-ph/0405074].

[67] B. Bajc, G. Senjanovic and F. Vissani, PoS HEP **2001**, 198 (2001) [hep-ph/0110310].

[68] T. Fukuyama and N. Okada, JHEP **0211**, 011 (2002) [hep-ph/0205066].

[69] B. Bajc, G. Senjanovic and F. Vissani, Phys. Rev. Lett. **90**, 051802 (2003) [hep-ph/0210207].

[70] H. S. Goh, R. N. Mohapatra and S. P. Ng, Phys. Lett. B **570**, 215 (2003) [hep-ph/0303055].

[71] H. S. Goh, R. N. Mohapatra and S. P. Ng, Phys. Rev. D **68**, 115008 (2003) [hep-ph/0308197].

[72] S. Bertolini, M. Frigerio and M. Malinsky, Phys. Rev. D **70**, 095002 (2004) [hep-ph/0406117].

[73] K. S. Babu and C. Macesanu, Phys. Rev. D **72**, 115003 (2005) [hep-ph/0505200].

[74] A. Dueck and W. Rodejohann, JHEP **1309**, 024 (2013) [arXiv:1306.4468 [hep-ph]].

[75] S. Weinberg, Phys. Rev. Lett. **43**, 1566 (1979).

[76] L. F. Abbott and M. B. Wise, Phys. Rev. D **22**, 2208 (1980).

[77] B. Bajc, I. Dorsner and M. Nemevsek, JHEP **0811**, 007 (2008) [arXiv:0809.1069 [hep-ph]].

[78] M. Dine, W. Fischler and M. Srednicki, Phys. Lett. B **104**, 199 (1981).

[79] A. R. Zhitnitsky, Sov. J. Nucl. Phys. **31**, 260 (1980) [Yad. Fiz. **31**, 497 (1980)].

[80] J. Beringer *et al.* [Particle Data Group Collaboration], Phys. Rev. D **86**, 010001 (2012).

[81] P. Sikivie, Lect. Notes Phys. **741**, 19 (2008) [astro-ph/0610440].

[82] P. A. R. Ade *et al.* [Planck Collaboration], arXiv:1502.01589 [astro-ph.CO].

[83] P. A. R. Ade *et al.* [Planck Collaboration], Astron. Astrophys. **571** (2014) A22 [arXiv:1303.5082 [astro-ph.CO]].

[84] M. Kawasaki and K. Nakayama, Ann. Rev. Nucl. Part. Sci. **63**, 69 (2013) [arXiv:1301.1123 [hep-ph]].

[85] E. Di Valentino, E. Giusarma, M. Lattanzi, A. Melchiorri and O. Mena, Phys. Rev. D **90**, no. 4, 043534 (2014) [arXiv:1405.1860 [astro-ph.CO]].

[86] see for example, K. S. Babu, J. C. Pati and Z. Tavartkiladze, JHEP **1006**, 084 (2010) [arXiv:1003.2625 [hep-ph]].

CHAPTER 3

RADIATIVE ELECTROWEAK SYMMETRY BREAKING OF STANDARD MODEL EXTENSIONS

3.1 Introduction

Discovery of the Higgs boson at both the ATLAS and the CMS detectors became the moment of triumph for the Standard Model (SM) of particle physics [1]. Such a historic discovery together with decades of eletroweak precision data have well established the validity of SM. However, there is no verified explanation of the origin and the smallness of neutrino masses, no viable candidate for the elusive dark matter. Due to these unwavering issues, various extensions of SM have been proposed. The secret of neutrino masses may lie in some form of seesaw mechanism, where a SM singlet like right-handed neutrinos (Type-I) with large majorana masses cause the light neutrino masses [2, 3] or a SM weak scalar triplet (Type-II) with a tiny induced vev generate the small neutrino masses [3, 4, 5] or it might be a SM fermionic triplet (Type-III) [6] which manages to construct the non-renormalizable neutrino mass operator suppressed by its high mass scale. Then again, if neutrino masses are generated by one or loop processes, the masses will naturally be suppressed by the loop factors and such an extension of SM is both theoretically well motivated and phenomenologically viable [7].

Search for stable dark matter candidate have also been motivation for various extensions of SM. Some form of symmetry usually stabilizes the dark matter. Simple discrete symmetries like R-parity in supersymmetric models [3]can perform an excellent job of preventing the particle from decaying. Kaluza-Klein parity [4] in universal extra dimension models and T-parity in Littlest Higgs models [5] can also stabilize the lightest particle; turning them into promising dark matter candidate. Similar role is played by a $\mathbb{Z}_2$ symmetry for the case of Inert doublet models [6] or Scotogenic models [7]. Instead of being an adhoc symmetry, this $\mathbb{Z}_2$ symmetry can be the remnant of $B - L$ generator of $SO(10)$ grand unified theories (GUTs) [8].

$SO(10)$ GUTs provide one of the most lucrative frameworks, where one can incorporate many of the aforementioned extensions of SM along with the beautiful unified picture of SM gauge couplings.

Among the classes of $SO(10)$ GUTs supersymmetric versions have multiple features like successful unification of gauge couplings, natural dark matter candidate while it solves the gauge hierarchy problem based on the symmetry principle. In addition, supersymmetric models offer a mechanism for triggering electroweak symmetry breaking via radiative effects [14]. In this scenario, the positive mass parameter becomes negative in low energy due to the radiative loop corrections which dictate how the parameters evolve with scale. Such a radiative loop correction can also trigger the electroweak symmetry breaking in non-supersymmetric extensions of SM.

In many extensions of SM Higgs boson is a part of the larger multiplet, which breaks some higher symmetry. In such models consistency of the high scale symmetry breaking requires that the mass-squared parameter of all the physical scalar bosons remain positive at the higher symmetry breaking scale. Then one needs to introduce new multiplet to break the electroweak symmetry which introduces new particles and model might loose it minimality and predictivity. For such class of models one might employ radiative loop corrections to turn Higgs mass parameter negative at low energy from positive value it obtained at high energy and thus cause eletroweak symmetry breaking with the same multiplet. For example: a class of $SO(10)$ models with the symmetry breaking sectors containing $\overline{126}_H$ along with either a 45_H or a 210_H has been analyzed in Ref [15] where flavor mixing is induced by vector-like fermions in the $16 + \overline{16}$ representation. In such models, the doublets residing inside the $\overline{126}_H$ can easily trigger the electroweak symmetry breaking when the positive mass parameter required by the higher symmetry breaking turns negative at low energy due to radiative loop corrections. Similar arguments can be applied for the case where a single 144-representation breaks $SO(10)$ into SM [16] or trinification model with symmetry $SU(3)_C \times SU(3)_L \times SU(3)_R$ gets broken by the fields in $(1, 3, \overline{3})$-representation.

In this work, we considers some popular extensions of SM and from the full set of renormalization group equations (RGEs) we evolved the mass parameters relevant to the eletroweak symmetry breaking. We showed that for every case, the model possesses solutions which allow the electroweak symmetry breaking triggered by radiative corrections while the potential remains bounded all the way and the theory remains perturbative.

3.2 Type-II seesaw neutrino mass model

Seesaw mechanism is one of the most popular generic models adopted to explain the origin and the smallness of neutrino masses. While Type-I seesaw needs right-handed (RH) neutrinos which

are neutral under the Standard Model (SM) gauge group with large Majorana masses, the minimal Type-II seesaw mechanism requires the existence of a weak scalar triplet. The most natural source for such triplets is provided by the Left-Right symmetric theories which can be realized either at low energy or can be embedded in Grand Unified Theories (GUTs) like SO(10) or E6.

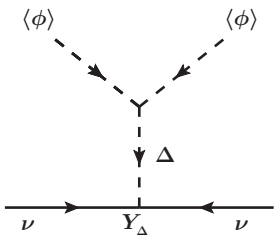

Figure 3.1: Diagrammatic representation of Type-II seesaw

3.2.1 The model

In this section, we consider the possibility that the weak scalar triplet is the only low-energy remnant of the new physics beyond the SM and the neutral component (Δ^0) acquires a very small vacuum expectation value ($\langle\Delta\rangle$) at low energy. The ordinary SM electroweak doublet $\phi(1,2,1/2)$ and the electroweak triplet $\Delta(1,3,1)$ are denoted by,

$$\phi = \begin{pmatrix} \phi^+ \\ \phi^0 \end{pmatrix}; \qquad \Delta = \frac{\sigma_i}{\sqrt{2}}\,\Delta_i = \begin{pmatrix} \Delta^+/\sqrt{2} & \Delta^{++} \\ \Delta^0 & \Delta^+/\sqrt{2} \end{pmatrix} \tag{3.1}$$

where σ_i's are the Pauli matrices. The most general renormalisable tree-level scalar potential is

$$\begin{aligned} V(\phi,\Delta) = {} & \mu_\phi^2\,\phi^\dagger\phi + \frac{\lambda_1}{2}\,(\phi^\dagger\phi)^2 + \mu_\Delta^2\,\mathrm{Tr}(\Delta^\dagger\Delta) + \frac{\lambda_2}{2}\left(\mathrm{Tr}(\Delta^\dagger\Delta)\right)^2 + \frac{\lambda_3}{2}\left[\left(\mathrm{Tr}(\Delta^\dagger\Delta)\right)^2 - \mathrm{Tr}(\Delta^\dagger\Delta\Delta^\dagger\Delta)\right] \\ & + \lambda_4\,\phi^\dagger\phi\,\mathrm{Tr}(\Delta^\dagger\Delta) + \lambda_5\,\phi^\dagger[\Delta^\dagger,\Delta]\phi + \left\{\frac{\mu}{\sqrt{2}}\,\phi^T\,i\sigma_2\,\Delta^\dagger\phi + h.c.\right\}. \end{aligned} \tag{3.2}$$

The weak triplet also generates a Majorana mass term for the neutrinos through the Yukawa term:

$$\mathcal{L}_Y \supset -\frac{(\mathbf{Y_\Delta})_{ij}}{\sqrt{2}}\,\ell_i^T C\,i\sigma_2\,\Delta\,\ell_j + h.c. \tag{3.3}$$

With the vacuum expectation value (vev) of the electroweak doublet $\langle\phi\rangle = v$, an effective dimension 5 operator generates the neutrino masses through the small but non-zero induced vev, $\langle\Delta\rangle = \dfrac{\mu v^2}{\sqrt{2}\mu_\Delta^2} \ll v$ when $v \ll \mu_\Delta$ and/or $\mu \ll 1$ as the electroweak triplet decouples. The neutrino mass matrix is

given by

$$\mathbf{m}_\nu \simeq \mathbf{Y_\Delta}\,\frac{\mu\, v^2}{2\mu_\Delta^2}. \tag{3.4}$$

One also needs to realize the fact that integrating out the heavy scalar triplet in the tree level approximation will also have an effect on the SM Higgs quartic coupling. The effective quartic coupling below the scale $\mu_r = \mu_\Delta$ is given by

$$\lambda_1^{\text{eff}} = \lambda_1 - \frac{\mu^2}{\mu_\Delta^2}. \tag{3.5}$$

This is the connecting formula for the Standard model quartic coupling λ_1 at the scale $\mu_r = \mu_\Delta$.

3.2.2 The stability conditions and the evolution of mass parameters

The stability conditions for the potential to be bounded from below are given by,

$$\begin{aligned}
&(i)\ \lambda_1 \geq 0; \quad \text{and} \quad \lambda_2 \geq 0 \\
&(ii)\ \lambda_2 + \frac{\lambda_3}{2} \geq 0 \quad \text{and} \quad \lambda_4 - \lambda_5 + 2\sqrt{2\lambda_1\lambda_2} \geq 0 \quad \text{and} \quad \lambda_4 - |\lambda_5| + \sqrt{2\lambda_1\lambda_2} \geq 0 \\
&(iii)\ \sqrt{2\lambda_1}(\lambda_2+\lambda_3) + 2\lambda_4\sqrt{\lambda_2} \geq 0 \\
&\qquad\qquad \text{or} \quad \lambda_2\lambda_3^2 + \lambda_3^3 - 4\lambda_1\lambda_3(\lambda_2+\lambda_3) + 2\lambda_3\lambda_4^2 - 4\lambda_2\lambda_5^2 - 2\lambda_3\lambda_5^2 \geq 0.
\end{aligned} \tag{3.6}$$

All the couplings of the Lagrangian have to maintain these stability conditions upto the energy scale of new physics like GUTs.

Using vertex corrections and the wave function renomalization factors, we can calculate the complete set of β-functions and Renomalization Group Equations (RGEs) [18, 17]. We have also determined the RGEs for the mass parameters of the model which were related to the anomalous dimensions (γ_m) of the scalar masses by

$$\gamma_m \equiv \frac{1}{2}\frac{d\ln(m^2)}{dt} \tag{3.7}$$

where $t = \ln\mu_r$ and μ_r is the running scale. So, the set of RGEs for the mass parameters is given by:

$$\begin{aligned}
16\pi^2\frac{d\mu_\phi^2}{dt} &= \left[-\frac{9}{10}g_1^2 - \frac{9}{2}g_2^2 + 3\lambda_1 + 2T\right]\mu_\phi^2 + 6\lambda_4\mu_\Delta^2 + 6|\mu|^2; \\
16\pi^2\frac{d\mu_\Delta^2}{dt} &= \left[\left(-\frac{18}{5}g_1^2 - 12g_2^2\right) + 8\lambda_1 + 2\lambda_2 + 2\text{Tr}\left(\mathbf{Y_\Delta^\dagger Y_\Delta}\right)\right]\mu_\Delta^2 + 4\lambda_4\mu_\phi^2 + 2|\mu|^2; \\
16\pi^2\frac{d\mu}{dt} &= \left[\lambda_1 + 4\lambda_4 - 8\lambda_5 - \frac{27}{10}g_1^2 - \frac{21}{2}g_2^2 + 2T + \text{Tr}\left(\mathbf{Y_\Delta^\dagger Y_\Delta}\right)\right]\mu;
\end{aligned} \tag{3.8}$$

where

$$T = \text{Tr}\left[\mathbf{Y_e^\dagger Y_e} + 3\mathbf{Y_d^\dagger Y_d} + 3\mathbf{Y_u^\dagger Y_u}\right]. \tag{3.9}$$

A complete set of RGEs for all the couplings of the Lagrangian is given as in Sec. 3.2.3. With this set of RGEs we proceed towards solution. We can already see that the contribution from the cubic coupling μ and quartic couplings like λ_4 has the potential to drive the positive mass parameter at high energy scale towards a negative value at lower energy scale to trigger the mechanism known as Radiative Eletroweak symmetry breaking (REWSB). For a TeV scale scalar triplet mass one realizes that to get the correct order of neutrino mass the cubic parameter μ needs to be very small ($\sim\ 10^{-5}$ GeV), which makes the contribution of μ term in the RGEs of mass parameters irrelevant.

3.2.3 Complete set of RGEs for Type-II neutrino mass model

The RGEs for the Yukawa couplings are given by:

$$\begin{aligned}
16\pi^2\frac{d\mathbf{Y}_d}{dt} =&\mathbf{Y_d}\left[\frac{3}{2}\mathbf{Y_d^\dagger Y_d}-\frac{3}{2}\mathbf{Y_u^\dagger Y_u}\right]+\mathbf{Y_d}\left[T-\frac{1}{4}g_1^2-\frac{9}{4}g_2^2-8\,g_3^2\right];\\
16\pi^2\frac{d\mathbf{Y}_u}{dt} =&\mathbf{Y_u}\left[\frac{3}{2}\mathbf{Y_u^\dagger Y_u}-\frac{3}{2}\mathbf{Y_d^\dagger Y_d}\right]+\mathbf{Y_u}\left[T-\frac{17}{20}g_1^2-\frac{9}{4}g_2^2-8\,g_3^2\right];\\
16\pi^2\frac{d\mathbf{Y}_e}{dt} =&\mathbf{Y_e}\left[\frac{3}{2}\mathbf{Y_e^\dagger Y_e}+\frac{3}{2}\mathbf{Y_\Delta^\dagger Y_\Delta}\right]+\mathbf{Y_e}\left[T-\frac{9}{4}g_1^2-\frac{9}{4}g_2^2\right];\\
16\pi^2\frac{d\mathbf{Y}_\Delta}{dt} =&\left[\frac{1}{2}\mathbf{Y_e^\dagger Y_e}+\frac{3}{2}\mathbf{Y_\Delta^\dagger Y_\Delta}\right]^T\mathbf{Y_\Delta}+\mathbf{Y_\Delta}\left[\frac{1}{2}\mathbf{Y_e^\dagger Y_e}+\frac{3}{2}\mathbf{Y_\Delta^\dagger Y_\Delta}\right]\\
&+\left[-\frac{3}{2}\left(\frac{3}{5}g_1^2+3g_2^2\right)+\mathrm{Tr}\left(\mathbf{Y_\Delta^\dagger Y_\Delta}\right)\right]\mathbf{Y_\Delta}.
\end{aligned}\tag{3.10}$$

The RGEs for the quartic couplings of the Lagrangians are given by

$$\begin{aligned}
16\pi^2\frac{d\lambda_1}{dt} =&12\lambda_1^2-3\lambda_1\left(3g_2^2+\frac{3}{5}g_1^2\right)+3g_2^4+\frac{3}{2}\left(\frac{3}{5}g_1^2+g_2^2\right)^2+4\lambda_1 T-8H+12\lambda_4^2+8\lambda_5^2;\\
16\pi^2\frac{d\lambda_2}{dt} =&-\frac{36}{5}g_1^2\lambda_2-24g_2^2\lambda_2+\frac{108}{25}g_1^4+18g_2^4+\frac{72}{5}g_1^2g_2^2+14\lambda_2^2+4\lambda_2\lambda_3+2\lambda_3^2+4\lambda_4^2+4\lambda_5^2\\
&+4\mathrm{Tr}\left(\mathbf{Y_\Delta^\dagger Y_\Delta}\right)\lambda_2-8\mathrm{Tr}\left(\mathbf{Y_\Delta^\dagger Y_\Delta Y_\Delta^\dagger Y_\Delta}\right);\\
16\pi^2\frac{d\lambda_3}{dt} =&-\frac{36}{5}g_1^2\lambda_3-24g_2^2\lambda_3+12g_2^4-\frac{144}{5}g_1^2g_2^2+3\lambda_3^2+12\lambda_2\lambda_3-8\lambda_5^2+4\mathrm{Tr}\left(\mathbf{Y_\Delta^\dagger Y_\Delta}\right)\lambda_3\\
&+8\mathrm{Tr}\left(\mathbf{Y_\Delta^\dagger Y_\Delta Y_\Delta^\dagger Y_\Delta}\right);\\
16\pi^2\frac{d\lambda_4}{dt} =&-\frac{9}{2}g_1^2\lambda_4-\frac{33}{2}g_2^2\lambda_4+\frac{27}{25}g_1^4+6g_2^4+\left[8\lambda_2+2\lambda_3+6\lambda_1+4\lambda_4+2T+2\mathrm{Tr}\left(\mathbf{Y_\Delta^\dagger Y_\Delta}\right)\right]\lambda_4+8\lambda_5^2;\\
16\pi^2\frac{d\lambda_5}{dt} =&-\frac{9}{2}g_1^2\lambda_5-\frac{33}{2}g_2^2\lambda_5-\frac{18}{5}g_1^2g_2^2+\left[2\lambda_2-2\lambda_3+2\lambda_1+8\lambda_4+2T+2\mathrm{Tr}\left(\mathbf{Y_\Delta^\dagger Y_\Delta}\right)\right]\lambda_5.
\end{aligned}$$

$$\begin{aligned}
\text{where}\qquad T=&\mathrm{Tr}\left[\mathbf{Y_e^\dagger Y_e}+3\mathbf{Y_d^\dagger Y_d}+3\mathbf{Y_u^\dagger Y_u}\right];\\
H=&\mathrm{Tr}\left[\mathbf{Y_e^\dagger Y_e Y_e^\dagger Y_e}+3\mathbf{Y_d^\dagger Y_d Y_d^\dagger Y_d}+3\mathbf{Y_u^\dagger Y_u Y_u^\dagger Y_u}\right].
\end{aligned}\tag{3.11}$$

The RGEs for the mass parameters are given by Eq.(3.8).

Beyond the energy scale corresponding to the mass of the triplet (μ_Δ) the SM gauge coupling

evolution also needs to be recalculated due to the triplet's contribution. While the weak triplet does not effect the evolution of the $SU(3)_C$ gauge coupling evolution, it does change the RGEs of the other gauge couplings. The RGEs for the gauge couplings are given by

$$16\pi^2 \frac{dg_i}{dt} = b_i \, g_i^3, \tag{3.12}$$

where $g_i = \{g_3, g_2, g_1\}$ are the three gauge couplings with the one loop β-function coefficient $b_i = \{-7, -5/2, 47/10\}$.

3.2.4 Solution to the RGEs

To analyze the evolution of the mass parameters, one needs to solve the set of RGEs which in turn requires one to define the relevant couplings at some energy scale. In this case, all the SM gauge couplings, Yukawa couplings and Higgs quartic couplings were evaluated at two-loop level upto the energy scale corresponding to the scalar triplet mass. After that the gauge couplings were evolved continuously but with the updated RGEs given in the set of RGEs in Eq.(3.12). The quartic coupling of the SM electroweak doublet Higgs has a discontinuity at the triplet energy scale due to the matching condition of the parameter given in Eq. (3.5). Above the energy scale μ_Δ, the full set of RGEs was used to evolve all the parameters of the model.

To generate a sample case, we specified the values of all the quartic couplings and mass parameters of the model at the low energy scale, $\mu_r = \mu_\Delta$, consistent with the stability conditions. Also the masses of neutrinos put a natural limit on the cubic coupling of the model because of Eq. (3.4) and this in turn makes the discontinuity in the Higgs quartic coupling λ_1 ignorable. To illustrate the phenomenon of radiative electroweak symmetry breaking in the Type-II seesaw model a sample point is given by Table 3.1. The sample point satisfies all the stability conditions and the mass parameter μ_ϕ^2 runs with a positive slope with the energy scale. Fig. 3.2 shows that the mass parameter becomes negative at low energy even though it is positive at high energy scale.

3.3 Two-loop neutrino mass model

Even before the experimental discovery of neutrino oscillation which is a clear indication of non-zero neutrino masses and mixings, the subject of neutrino mass generation has been an active arena of research. The wide range of possibilities can be classified into three major categories. In the first case, neutrinos may be simple Dirac fermions. For such a case the smallness of the mass remains a mystery and one needs to venture into the realm of extra dimension(s) to seek for answers. Neutrinos

Quartic couplings	values	Mass parameters	values
		$m_t(m_t)$	162.25 GeV
$\lambda_1(m_Z)$	0.258	$\mu_\Delta^2(\mu_\Delta)$	500^2 $(\text{GeV})^2$
$\lambda_1(\mu_\Delta)$	0.1887	$M_h(m_Z)$	125.1 GeV
$\lambda_2(\mu_\Delta)$	0.15	$v(m_Z)$	174.10 GeV
$\lambda_3(\mu_\Delta)$	0.45	$v(\mu_\Delta)$	171.45 GeV
$\lambda_4(\mu_\Delta)$	0.19	$\mu_\phi^2(m_Z)$	-88.72^2 $(\text{GeV})^2$
$\lambda_5(\mu_\Delta)$	0.10	$\mu_\phi^2(\mu_\Delta)$	-74.48^2 $(\text{GeV})^2$
		$\mu(\mu_\Delta)$	10^{-5} GeV

Table 3.1: Quartic coupling and mass parameter values for the sample point used for the Type-II seesaw model in Fig. 3.2.

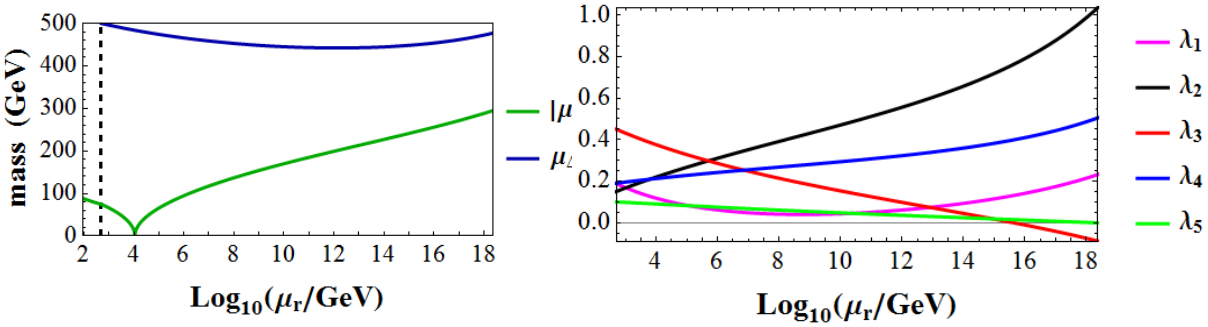

(a) Evolution of mass parameters

(b) Evolution of quartic couplings

Figure 3.2: One loop running of the parameters of Type-II seesaw model upto Plank scale. The black dashed line in Fig. 3.2a corresponds to the scale, $\mu_r = \mu_\Delta$.

may be Majorana particles and smallness of the masses is due to seesaw mechanism occurring at a very high energy with the help of a SM singlet like right-handed neutrino (Type-I) or a SM weak scalar triplet (Type-II) (discussed in Sec. 3.2) or a SM fermionic triplet (Type-III). A third alternative is that the neutrino masses are generated by loop correction, hence the masses are suppressed by the loop factors. In this scenario, the new physics responsible for the neutrino mass generation has the possibility of showing up at the Large Hadron Collider in the near future.

3.3.1 The Model

In this section we will consider the two-loop neutrino mass model which introduces a doubly charged (k^{++}) and a singly charged (h^+) scalars along with the SM particles [19]. In this model in attempt to generate non-zero neutrino mass, the lepton number conservation law is abandoned and as a result tiny Majorana mass arises through loop diagram at two-loop level. One of the salient features of the model requires one of the three neutrino masses to be zero. The model also admits both normal and inverted hierarchy of neutrino masses.

The new scalars under the SM gauge group $SU(3)_C \times SU(2)_L \times U(1)_Y$ are denoted by

$$h^+(1,1,1); \qquad\qquad k^{++}(1,1,2). \tag{3.13}$$

The gauge invariant Yukawa couplings that are allowed involving the new scalars are:

$$\mathcal{L}_Y \supset \mathbf{f}_{ab}\ \ell_a^i \ell_b^j \epsilon_{ij} h^+ + \mathbf{h}_{ab}\ e_a^c e_b^c k^{--} + h.c. \tag{3.14}$$

Here a, b are generation indices, i, j are $SU(2)_L$ indices with ϵ_{ij} being antisymmetric tensor. The Yukawa coupling matrix $\mathbf{f}$ is antisymmetric whereas the Yukawa matrix $\mathbf{h}$ is symmetric.
The scalar potential for the model is given by

$$\begin{aligned} V(\phi, h^+, k^{++}) = {} & \mu_\phi^2\ \phi^\dagger\phi + \mu_h^2\ h^+h^- + \mu_k^2\ k^{++}k^{--} - \left(\mu\ h^+h^+k^{--} + h.c.\right) + \frac{\lambda_1}{2}\ (\phi^\dagger\phi)^2 \\ & + \frac{\lambda_2}{2}\ (h^+h^-)^2 + \frac{\lambda_3}{2}\ (k^{++}k^{--})^2 + \lambda_4\ (\phi^\dagger\phi)(h^+h^-) + \lambda_5\ (\phi^\dagger\phi)(k^{++}k^{--}) \\ & + \lambda_6\ (h^+h^-)(k^{++}k^{--}). \end{aligned} \tag{3.15}$$

Using the lepton number violating Yukawa coupling $\mathbf{h}$, small neutrino mass matrix is generated by a two-loop process depicted in the feynman diagram (Fig. 3.3).

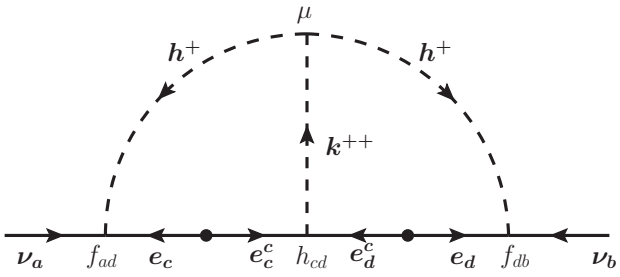

Figure 3.3: Feynman Diagram responsible for neutrino mass generation at two-loop level.

3.3.2 The stability conditions and the evolution of mass parameters

The boundedness conditions are given by [19],

$$\begin{aligned}
&(i)\ \lambda_1 \geq 0; \qquad \lambda_2 \geq 0; \qquad \lambda_3 \geq 0; \\
&(ii)\ \lambda_4 \geq -\sqrt{\lambda_1\lambda_2}; \qquad \lambda_5 \geq -\sqrt{\lambda_1\lambda_3}; \qquad \lambda_6 \geq -\sqrt{\lambda_2\lambda_3}; \\
&(iii)\ \lambda_4\sqrt{\lambda_3} + \lambda_6\sqrt{\lambda_1} + \lambda_5\sqrt{\lambda_2} + \sqrt{\lambda_1\lambda_2\lambda_3} \geq 0 \qquad \text{or} \qquad \det \boldsymbol{\lambda} \geq 0;
\end{aligned} \tag{3.16}$$

where

$$\boldsymbol{\lambda} = \begin{pmatrix} \lambda_1 & \lambda_4 & \lambda_5 \\ \lambda_4 & \lambda_2 & \lambda_6 \\ \lambda_5 & \lambda_6 & \lambda_3 \end{pmatrix}. \tag{3.17}$$

It has been shown that the model maintains perturbativity and boundedness for both normal and inverted case, if $|\mathbf{h}_{\mu\mu}| < 0.45$ and $|\mathbf{f}_{\mu\tau}| < \ 0.34$. For the antisymmetric Yukawa coupling matrix $\mathbf{f}$, the neutrino mixing angles provide two constraints reducing the number of free parameters to one. For the case of normal neutrino mass hierarchy the relation is given by:

$$\begin{aligned}
\epsilon &= \tan\theta_{12}\ \frac{\cos\theta_{23}}{\cos\theta_{13}} + \tan\theta_{13}\ \sin\theta_{23}\ e^{-i\delta}; \\
\epsilon' &= \tan\theta_{12}\ \frac{\sin\theta_{23}}{\cos\theta_{13}} - \tan\theta_{13}\ \cos\theta_{23}\ e^{-i\delta}.
\end{aligned} \tag{3.18}$$

And for the inverted mass hierarchy we have:

$$\epsilon = -\sin\theta_{23}\ \cot\theta_{13}\ e^{-i\delta}; \qquad \epsilon' = \cos\theta_{23}\ \cot\theta_{13}\ e^{-i\delta}. \tag{3.19}$$

where in both case the definition of ϵ and ϵ' is given as:

$$\epsilon \equiv \frac{\mathbf{f}_{e\tau}}{\mathbf{f}_{\mu\tau}}; \qquad \epsilon' \equiv \frac{\mathbf{f}_{e\mu}}{\mathbf{f}_{\mu\tau}}. \tag{3.20}$$

Similar to the previous case, we require the full set of RGEs for this model which includes the evolution of the gauge couplings, Yukawa couplings, quartic couplings and the mass parameters of the Lagrangian. While the complete set of the RGEs is listed in Sec. 3.3.3, the RGEs for the mass parameters of the Lagrangian are given by:

$$\begin{aligned}
16\pi^2\frac{d\mu_\phi^2}{dt} &= \mu_\phi^2\left(-\frac{9}{10}g_1^2 - \frac{9}{2}g_2^2 + 2T + 6\lambda_1\right) + 2\lambda_4\mu_h^2 + 2\lambda_5\mu_k^2; \\
16\pi^2\frac{d\mu_h^2}{dt} &= \mu_h^2\left(-\frac{18}{5}g_1^2 + 8\mathrm{Tr}(\mathbf{f}^\dagger\mathbf{f}) + 4\lambda_2\right) + 4\lambda_4\mu_\phi^2 + 2\lambda_6\mu_k^2 + 8\mu^2; \\
16\pi^2\frac{d\mu_k^2}{dt} &= \mu_k^2\left(-\frac{72}{5}g_1^2 + 4\mathrm{Tr}(\mathbf{h}^\dagger\mathbf{h}) + 4\lambda_3\right) + 4\lambda_5\mu_\phi^2 + 2\lambda_6\mu_h^2 + 4\mu^2; \\
16\pi^2\frac{d\mu}{dt} &= \mu\left(-\frac{54}{5}g_1^2 + 2\lambda_2 + 2\lambda_6 + 2\mathrm{Tr}(\mathbf{h}^\dagger\mathbf{h}) + 8\mathrm{Tr}(\mathbf{f}^\dagger\mathbf{f})\right).
\end{aligned} \tag{3.21}$$

3.3.3 Complete set of RGEs for Two-loop neutrino mass model

For the Two-loop neutrino mass model, among the gauge couplings only the hypercharge gauge coupling is modified due the additional scalar particles. So, the RGEs for the SM gauge couplings are given by,

$$16\pi^2 \frac{dg_i}{dt} = b_i g_i^3, \tag{3.22}$$

where $g_i = \{g_3, g_2, g_1\}$ are the three gauge couplings with the one loop β-function coefficient $b_i = \{-7, -{}^{19}/_{6}, {}^{51}/_{10}\}$

The RGEs for the Yukawa couplings are given by,

$$\begin{aligned} 16\pi^2 \frac{d\mathbf{h}}{dt} &= 4(\mathbf{h}\mathbf{h}^\dagger\mathbf{h}) + 4\mathbf{h}\mathrm{Tr}(\mathbf{h}^\dagger\mathbf{h}) - \frac{18}{5}g_1^2\mathbf{h} + \frac{1}{2}(\mathbf{h}\mathbf{Y}_\ell^\dagger\mathbf{Y}_\ell) + \frac{1}{2}(\mathbf{Y}_\ell^{\mathbf{T}}\mathbf{Y}_\ell^*\mathbf{h}); \\ 16\pi^2 \frac{d\mathbf{f}}{dt} &= 4(\mathbf{f}\mathbf{f}^\dagger\mathbf{f}) + 4\mathbf{f}\mathrm{Tr}(\mathbf{f}^\dagger\mathbf{f}) + \frac{1}{2}(\mathbf{f}\mathbf{Y}_\ell\mathbf{Y}_\ell^\dagger) + \frac{1}{2}(\mathbf{Y}_\ell^*\mathbf{Y}_\ell^{\mathbf{T}}\mathbf{f}) - \frac{3}{2}\mathbf{f}(-\frac{3}{5}g_1^2 + g_2^2). \end{aligned} \tag{3.23}$$

The RGEs for the quartic scalar couplings are given by

$$\begin{aligned} 16\pi^2 \frac{d\lambda_1}{dt} &= 12\lambda_1^2 + 2\lambda_4^2 + 2\lambda_5^2 - \lambda_1\left(9g_2^2 + \frac{9}{5}g_1^2\right) + \frac{9}{4}g_2^4 + \frac{27}{100}g_1^4 + \frac{9}{10}g_2^2g_1^2 + 4\lambda_1 T - 4H; \\ 16\pi^2 \frac{d\lambda_2}{dt} &= 10\lambda_2^2 + 4\lambda_4^2 + 2\lambda_6^2 - \frac{36}{5}\lambda_2 g_1^2 + \frac{108}{25}g_1^4 + 16\lambda_2\mathrm{Tr}(\mathbf{f}^\dagger\mathbf{f}) - 32\ \mathrm{Tr}(\mathbf{f}^\dagger\mathbf{f})^2; \\ 16\pi^2 \frac{d\lambda_3}{dt} &= 10\lambda_3^2 + 4\lambda_5^2 + 2\lambda_6^2 - \frac{144}{5}\lambda_2 g_1^2 + \frac{864}{25}g_1^4 + 16\lambda_3\mathrm{Tr}(\mathbf{h}^\dagger\mathbf{h}) - 64\ \mathrm{Tr}(\mathbf{h}^\dagger\mathbf{h})^2; \\ 16\pi^2 \frac{d\lambda_4}{dt} &= 6\lambda_1\lambda_4 + 4\lambda_2\lambda_4 + 2\lambda_5\lambda_6 + 4\lambda_4^2 - \lambda_4\left(\frac{9}{2}g_2^2 + \frac{45}{10}g_1^2\right) + \frac{27}{50}g_1^4 \\ &\quad + 2\lambda_4\left[4\mathrm{Tr}(\mathbf{f}^\dagger\mathbf{f}) + T\right] - 8\mathrm{Tr}\left(\mathbf{f}^\dagger\mathbf{f}\mathbf{Y}_\ell^\dagger\mathbf{Y}_\ell\right); \\ 16\pi^2 \frac{d\lambda_5}{dt} &= 6\lambda_1\lambda_5 + 4\lambda_3\lambda_5 + 2\lambda_4\lambda_6 + 4\lambda_5^2 - \lambda_5\left(\frac{9}{2}g_2^2 + \frac{153}{10}g_1^2\right) + \frac{108}{25}g_1^4 \\ &\quad + 2\lambda_5\left[4\mathrm{Tr}(\mathbf{h}^\dagger\mathbf{h}) + T\right] - 8\mathrm{Tr}\left(\mathbf{Y}_\ell^\dagger\mathbf{Y}_\ell\mathbf{h}^\dagger\mathbf{h}\right); \\ 16\pi^2 \frac{d\lambda_6}{dt} &= 4\lambda_2\lambda_6 + 4\lambda_3\lambda_6 + 4\lambda_4\lambda_5 + 4\lambda_6^2 - \frac{90}{5}\lambda_6 g_1^2 + \frac{432}{25}g_1^4 + 8\lambda_6\left[\mathrm{Tr}(\mathbf{f}^\dagger\mathbf{f}) + \mathrm{Tr}(\mathbf{h}^\dagger\mathbf{h})\right]. \end{aligned} \tag{3.24}$$

The RGEs for the mass parameters are given by Eq. (3.21).

3.3.4 Solution to the RGEs

To find the solution to the full set of RGEs, one requires to completely specify the values of all the parameters of the Lagrangian at some energy scale. Similar to the previous case, we specify the sample values at low energy scale while satisfying the necessary and sufficient conditions for the boundedness of the scalar potential.

For the sample case, we selected the normal mass hierarchy for no specific reason. Similar result can be found if the hierarchy is inverted. We used the set of two-loop RGEs for the SM case and ran

Quartic, Yukawa couplings	values	Mass paramters	values
$\lambda_1(M_Z)$	0.258	$m_t(m_t)$	162.25 GeV
$\lambda_1(\mu_0)$	0.1924	$M_h(m_Z)$	125.1 GeV
$\lambda_2(\mu_0)$	0.20	$v(m_Z)$	174.10 GeV
$\lambda_3(\mu_0)$	0.50	$v(\mu_0)$	171.21GeV
$\lambda_4(\mu_0)$	0.10	$\mu_h^2(\mu_0)$	800^2 $(\text{GeV})^2$
$\lambda_5(\mu_0)$	0.15	$\mu_k^2(\mu_0)$	450^2 $(\text{GeV})^2$
$\lambda_6(\mu_0)$	-0.25	$\mu(\mu_0)$	500GeV
$\lvert\mathbf{f}_{\mu\tau}\rvert(\mu_0)$	0.013	$\mu_\phi^2(m_Z)$	-88.72^2 $(\text{GeV})^2$
$\lvert\mathbf{h}_{\mu\mu}\rvert(\mu_0)$	0.4	$\mu_\phi^2(\mu_0)$	-75.09^2 $(\text{GeV})^2$

Table 3.2: Quartic and Yukawa coupling and mass parameter values for the sample point used for the Two-loop neutrino mass model in Fig. 3.4

upto the lightest newly introduced scalar particle (in the sample point $\mu_0 = \mu_k$) and from that point used the previously mentioned full set of RGEs to evolve the couplings and the mass parameters upto the Planck scale.

In the sample point the other values of the Yukawa couplings $\mathbf{f}$ can be calculated using Eq. (3.18) and the definitions in Eq. (3.20). For the case of the Yukawa couplings $\mathbf{h}$, we only kept the value of $|\mathbf{h}_{\mu\mu}|$ non-zero. It is obvious from Fig. 3.4 that the radiative correction manages to push the Higgs mass parameter in such a way that it acquires a negative value at low energy.

3.4 Inert doublet model

Inert doublet model is one of the most simple extensions of the SM, which can be treated as a special case of more general two Higgs doublet model. In the Inert doublet model, the potential has a $\mathbb{Z}_2$ symmetry that is unbroken by the vacuum state. Even though it was introduced in the 70s, it received a new influx of attention when the model was shown to be able to alleviate the LEP paradox, be able to address the issue of the smallness of the neutrino masses either via Type-I seesaw mechanism or via one loop radiative mechanism (also known as Scotogenic neutrino model),

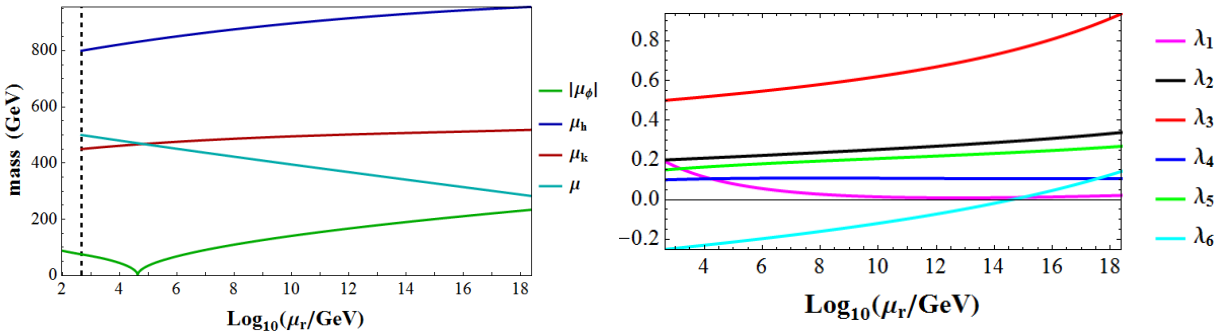

(a) Evolution of mass parameters

(b) Evolution of quartic couplings

Figure 3.4: One loop running of the parameters of Two-loop neutrino mass model upto Planck scale. The black dashed line corresponds to the scale, $\mu_r = \mu_0$. Here μ_0 is the energy scale corresponding to the lightest of the newly introduced particles. In this sample point $\mu_o = \mu_k$.

leptogenesis by including TeV scale right-handed neutrino. It has also been shown that electroweak symmetry breaking can be induced by loop effects.

3.4.1 The model

The model requires three right-handed neutrinos (N_i) along with inert scalar doublet (η) and the SM particles. All the newly introduced particles (also the RH neutrinos for the case of Scotogenic model) are charged under the additional $\mathbb{Z}_2$ parity symmetry while all the SM particles are neutral under this parity. The scalar doublet has the potential to be the DM of the model and for the case of Scotogenic model the RH neutrino may or may not be DM candidate depending on their masses. It is crucial to realize the importance of the survival of the $\mathbb{Z}_2$ symmetry as this symmetry protects the DM candidate from annihilation and in the scotogenic version the symmetry forbids the neutrino to acquire mass at the tree level.

The scalar potential of a general Inert doublet model can be written as:

$$\begin{aligned} V(\phi,\eta) = \mu_1^2\phi^\dagger\phi + \mu_2^2\eta^\dagger\eta + \frac{\lambda_1}{2}(\phi^\dagger\phi)^2 + \frac{\lambda_2}{2}(\eta^\dagger\eta)^2 + \lambda_3(\phi^\dagger\phi)(\eta^\dagger\eta) \\ + \lambda_4(\eta^\dagger\phi)(\phi^\dagger\eta) + \frac{\lambda_5}{2}\left[(\eta^\dagger\phi)^2 + h.c.\right] \end{aligned} \tag{3.25}$$

In the potential the mass parameters $\mu_i^2 (i = 1, 2)$ and the couplings $\lambda_i, (i = 1 - 4)$ must be real. λ_5 can also be taken to real without any loss of generality as the phase of the coupling can be absorbed by the redefinition of the η field.

3.4.2 The stability conditions and the evolution of mass parameters

One needs to be careful while identifying the solution to the set of RGEs. The parameters in the scalar potential have to satisfy the boundedness conditions at all energy scales which ensures that the potential is bounded from below all the way. The conditions are given as:

$$\lambda_1 \geq 0; \qquad \lambda_2 \geq 0; \qquad \lambda_3 \geq -\sqrt{\lambda_1 \lambda_2}; \qquad \lambda_3 + \lambda_4 - |\lambda_5| \geq -\sqrt{\lambda_1 \lambda_2}. \tag{3.26}$$

One can also find the physical scalar mass spectrum as:

$$\begin{aligned} m_h^2 &= 2\lambda_1 v^2; \\ m_\pm^2 &= m_2^2 + \lambda_3 v^2; \\ m_R^2 &= m_2^2 + v^2(\lambda_3 + \lambda_4 + \lambda_5); \\ m_I^2 &= m_2^2 + v^2(\lambda_3 + \lambda_4 - \lambda_5). \end{aligned} \tag{3.27}$$

where m_h is the mass of the SM Higgs boson, $m_\pm$ is the mass of the charged component of η doublet, m_R and m_I are the masses of the real and imaginary scalar component of the neutral component of the η doublet. About the issue of DM, we chose real part of neutral scalar η as the DM candidate. For this scenario, the charged component of the electroweak doublet η needs to be heavier than the neutral component. Also by keeping λ_5 negative and small, we get a slightly heavier pseudoscalar.

In the model the right-handed neutrinos get a direct majorana mass term $\frac{1}{2}\overline{N_R^i} M_{ij} N_R^{j^c} + h.c.$ which leads to masses M_i's (where $i = 1, 2, 3$) upon diagonalisation. In the regular Type-I seesaw version, the right-handed neutrino majorana masses needs to be around 10^9 GeV or higher to attain the right order of neutrino masses. But for the scotogenic version, the right-handed neutrino can be at the TeV scale as the suppression factor of the neutrino masses comes from the fact that the right-handed neutrinos are odd under the $\mathbb{Z}_2$ symmetry and the neutrino mass has to be generated at the loop level. A neutrino Yukawa coupling involving the newly introduced scalar η and the right-handed neutrinos in addition to the SM lepton doublets needs to be added. The term given by:

$$\mathcal{L}_Y \supset -\mathbf{h}_{ij} \overline{N_R^i} \tilde{\eta}^\dagger \ell_L^j + h.c.; \qquad \text{where } \tilde{\eta} = i\, \sigma_2 \eta^* \tag{3.28}$$

along with the right-handed neutrino majorana mass term generates the loop suppressed neutrino mass matrix (see Fig. 3.5).

To illustrate the radiative electroweak symmetry breaking mechanism, we adopted the scotogenic

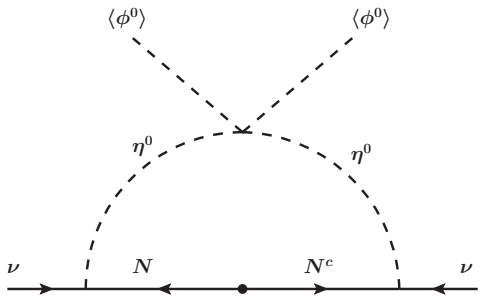

Figure 3.5: Diagrammatic representation of neutrino mass generation in the scotogenic model

version of the Inert doublet model [20]. The RGEs for the mass parameters are given by

$$\begin{aligned} 16\pi^2\frac{d\mu_1^2}{dt} =& 6\lambda_1\mu_1^2 + 2(2\lambda_3+\lambda_4)\mu_2^2 + \mu_1^2\left[2T - \frac{3}{2}(g_1^2+3g_2^2)\right]; \\ 16\pi^2\frac{d\mu_2^2}{dt} =& 6\lambda_2\mu_2^2 + 2(2\lambda_3+\lambda_4)\mu_1^2 + \mu_2^2\left[2T_\nu - \frac{3}{2}(g_1^2+3g_2^2)\right] - 4\sum_{i=1}^{3} M_i^2(\mathbf{h}\mathbf{h}^\dagger)_{ii}; \end{aligned} \tag{3.29}$$

where $T_\nu \equiv \mathrm{Tr}\left[\mathbf{h}^\dagger\mathbf{h}\right]$.

The complete set of RGEs is given in Sec. 3.4.3. The last term of the RGE for the mass parameter for scalar η namely μ_2^2 shows its dependency on the RH neutrino mass term. For a larger value, this becomes the dominating term and pulls down the mass parameter, ultimately making it negative at higher energy. This in turns breaks the precious $\mathbb{Z}_2$ symmetry spoiling the model completely.

3.4.3 Complete set of RGEs for Inert doublet model

The one loop RGEs for the Inert doublet model have already been computed. The SM gauge coupling RGEs are given by,

$$16\pi^2\frac{dg_i}{dt} = b_i g_i^3, \tag{3.30}$$

where $b_i = (-7, -3, \frac{21}{5})$ are the β-coefficients of the SM gauge couplings updated with the added particles.

The quark sector of the model remains unchanged, while the leptonic sector needs to be revisited. The RGEs for the leptonic Yukawa couplings are:

$$\begin{aligned} 16\pi^2\frac{d\mathbf{Y_e}}{dt} =& \mathbf{Y_e}\left\{\frac{3}{2}\mathbf{Y_e}^\dagger\mathbf{Y_e} + \frac{1}{2}\mathbf{h}^\dagger\mathbf{h} + T - \frac{9}{4}g_1^2 - \frac{9}{4}g_2^2\right\}; \\ 16\pi^2\frac{d\mathbf{h}}{dt} =& \mathbf{h}\left\{\frac{3}{2}\mathbf{h}^\dagger\mathbf{h} + \frac{1}{2}\mathbf{Y_e}^\dagger\mathbf{Y_e} + T_\nu - \frac{9}{20}g_1^2 - \frac{9}{4}g_2^2\right\}; \\ 16\pi^2\frac{d\mathbf{M}}{dt} =& \left\{(\mathbf{h}\mathbf{h}^\dagger)\mathbf{M} + \mathbf{M}(\mathbf{h}\mathbf{h}^\dagger)^*\right\}. \end{aligned} \tag{3.31}$$

For the quartic scalar coupling we find the following set of RGEs:

$$\begin{aligned}
16\pi^2\frac{d\lambda_1}{dt} =&12\lambda_1^2+4\lambda_3^2+4\lambda_3\lambda_4+2\lambda_4^2+2\lambda_5^2+\frac{3}{4}\left(\frac{9}{25}g_1^4+\frac{6}{5}g_1^2g_2^2+3g_2^4\right)\\
&-3\lambda_1\left(\frac{3}{5}g_1^2+3g_2^2\right)+4\lambda_1T-4H;\\
16\pi^2\frac{d\lambda_2}{dt} =&12\lambda_2^2+4\lambda_3^2+4\lambda_3\lambda_4+2\lambda_4^2+2\lambda_5^2+\frac{3}{4}\left(\frac{9}{25}g_1^4+\frac{6}{5}g_1^2g_2^2+3g_2^4\right)\\
&-3\lambda_2\left(\frac{3}{5}g_1^2+3g_2^2\right)+4\lambda_2T_\nu-4T_{4\nu};\\
16\pi^2\frac{d\lambda_3}{dt} =&2(\lambda_1+\lambda_2)(3\lambda_3+\lambda_4)+4\lambda_3^2+2\lambda_4^2+2\lambda_5^2+\frac{3}{4}\left(\frac{9}{25}g_1^4-\frac{6}{5}g_1^2g_2^2+3g_2^4\right)\\
&-3\lambda_3\left(\frac{3}{5}g_1^2+3g_2^2\right)+2\lambda_3(T+T_\nu)-4T_{\nu e};\\
16\pi^2\frac{d\lambda_4}{dt} =&2(\lambda_1+\lambda_2)\lambda_4+8\lambda_3\lambda_4+4\lambda_4^2+8\lambda_5^2+\frac{9}{5}g_1^2g_2^2\\
&-3\lambda_4\left(\frac{3}{5}g_1^2+3g_2^2\right)+2\lambda_4(T+T_\nu)+4T_{\nu e};\\
16\pi^2\frac{d\lambda_5}{dt} =&\lambda_5\left[2(\lambda_1+\lambda_2)+8\lambda_3+12\lambda_4-3\left(\frac{3}{5}g_1^2+3g_2^2\right)+2(T+T_\nu)\right].
\end{aligned} \tag{3.32}$$

$$\begin{aligned}
\text{where}\qquad T_\nu \equiv&\text{Tr}\left[\mathbf{h}^\dagger\mathbf{h}\right];\\
T_{4\nu} \equiv&\text{Tr}\left[\mathbf{h}^\dagger\mathbf{h}\mathbf{h}^\dagger\mathbf{h}\right];\\
T_{\nu e} \equiv&\text{Tr}\left[\mathbf{h}^\dagger\mathbf{h}\mathbf{Y}_\mathbf{e}^\dagger\mathbf{Y}_\mathbf{e}\right].
\end{aligned}$$

The RGEs for the mass parameters are given by Eq. (3.29). One notices from the set of RGEs that the evolution of Majorana Mass ($\mathbf{M}$), the new Yukawa coupling ($\mathbf{h}$) and the scalar quartic coupling λ_5 are proportional to the quantities themselves. The upshot of this setting is that these parameters remain small if they are small at any energy scale. This feature of the model becomes self-explanatory upon realization that if any of these parameters becomes zero, the neutrino becomes massless and global $U(1)$ symmetry conserving the lepton number is restored.

3.4.4 Solution to the RGEs

A sample point (given in the Table 3.3) generates the running of the mass parameters and the scalar quartic couplings shown in Fig. 3.6. The sample point maintains all the boundedness conditions at all energy scale.The decoupling of the three RH nautrino was only considered for the running of the mass parameter μ_2^2. As for all the other cases as the dependence on the RH neutrino mass is indirect, the decoupling effect is negligible.

In Fig. 3.6(a), below the energy level corresponding to the point where $\mu_1^2 = 0$ the electroweak symmetry is broken and the masses of the components of the scalar doublet η are splitted and the running of the masses of the charged and neutral component of the scalar η is shown. All the quartic couplings remain in the pertubative range and the all the new Yukawa couplings are chosen to be small $\mathbf{h}_{ij} \lesssim \mathcal{O}(.1)$.

Quartic couplings	values	Mass parameters	values
		$\mu_2^2(\mu_2)$	800^2 (GeV)^2
$\lambda_1(m_Z)$	0.258	M_1	900 GeV
$\lambda_1(\mu_2)$	0.173	M_2	1500 GeV
$\lambda_2(\mu_2)$	0.35	M_3	2000 GeV
$\lambda_3(\mu_2)$	0.38	$v(m_Z)$	174.10 GeV
$\lambda_4(\mu_2)$	-0.29	$v(\mu_2)$	170.36 GeV
$\lambda_5(\mu_2)$	-0.01	$\mu_1^2(m_Z)$	-88.72^2 (GeV)^2
		$\mu_1^2(\mu_2)$	-70.92^2 (GeV)^2

Table 3.3: Quartic coupling and mass parameter values for the sample point used for the Inert doublet model in Fig. 3.6

3.5 Extension of SM by a real scalar singlet

Perhaps the simplest extension of SM requires the existence of only a new heavy real scalar singlet of SM gauge group. The singlet under suitable conditions can serve as a candidate for dark matter.

3.5.1 The model

In this simplest extension of SM, the added singlet can be protected from decaying into SM particles by virtue of a symmetry - for example $\mathbb{Z}_2$ parity. This scenario can be well motivated from some higher symmetry at GUT scale where all the other additional particles lies above some intermediate scale. For example, such a stable dark matter can be easily incorporated in $SO(10)$ models. As a group of rank five, $SO(10)$ group includes an additional $U(1)$ symmetry which if broken by a 126 representation, a discrete $\mathbb{Z}_2$ symmetry is preserved at low energy. For such a case a scalar dark

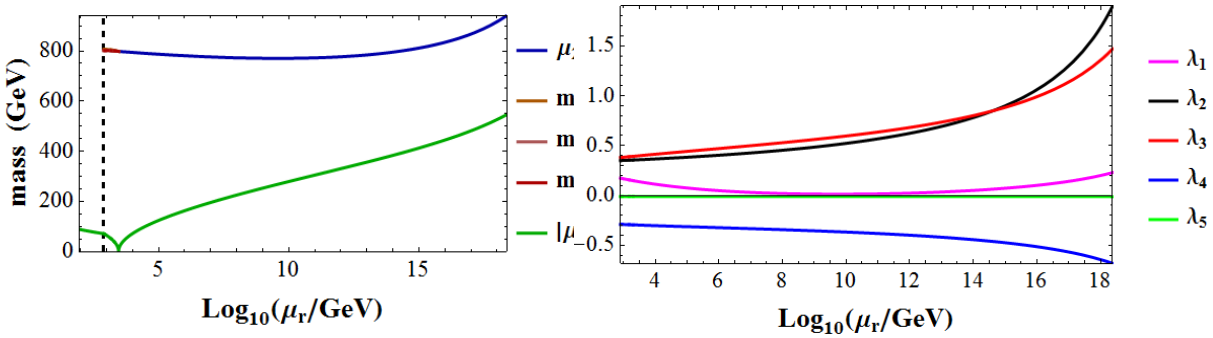

(a) Evolution of mass parameters

(b) Evolution of quartic couplings

Figure 3.6: One loop running of the parameters of Inert doublet model upto Planck scale. The black dashed line corresponds to the scale, $\mu_r = \mu_2$.

matter candidate can be easily stabilized if it comes from some $\mathbb{Z}_2$ odd representations (like 16-plet). In such cases, the low scale scalar potential becomes [21]:

$$V(\phi, s) = \mu_1^2 \phi^\dagger \phi + \frac{\mu_s^2}{2} s^2 + \frac{\lambda_1}{2}(\phi^\dagger \phi)^2 + \frac{\lambda_2}{8} s^4 + \frac{\lambda_3}{2}(\phi^\dagger \phi) s^2. \tag{3.33}$$

Below the energy scale corresponding to the mass of the singlet, the effective quartic coupling is given by

$$\lambda_1^{\text{eff}} = \lambda_1 - \frac{\lambda_3^2}{\lambda_2}. \tag{3.34}$$

And the mass of the observed Higgs particle is $m_h^2 = 2\lambda_1^{\text{eff}} v^2$ and the matching condition Eq.(3.34) is needed while one evolves the RGE for the Higgs quartic coupling.

3.5.2 The stability conditions and the evolution of the mass parameters

The parameters of the scalar potential must obey the boundeded constraints so that the potential remains bounded from below. The condition for this simple potential is given as,

$$\lambda_1 \geq 0; \qquad \lambda_2 \geq 0; \qquad \lambda_3 \geq -\sqrt{\lambda_1 \lambda_2}. \tag{3.35}$$

For this simple extension of SM, most of the RGEs of the SM remain the same. But one should update the RGEs for the Higgs quratic coupling (λ_1) and the Higgs mass parameters (μ_1^2) along with the newly introduced quartic couplings (λ_2, λ_3) and mass parameter (μ_s^2). The full set of new and updated RGEs is given in Sec. 3.5.3. The RGEs of the mass parameters are given as

$$\begin{aligned} 16\pi^2 \frac{d\mu_1^2}{dt} &= \left[6\lambda_1 + 2T - \frac{9}{10} g_1^2 - \frac{9}{2} g_2^2\right] \mu_1^2 + \lambda_3 \mu_s^2; \\ 16\pi^2 \frac{d\mu_s^2}{dt} &= 3\lambda_2 \mu_s^2 + 4\lambda_3 \mu_1^2. \end{aligned} \tag{3.36}$$

From the RGEs of the mass parameters, one immediately notices that the coupling λ_3 has the potential to turn the mass parameter of SM Higgs negative at low energy while it remains positive at high energy. And one also notices that one needs a lower bound on coupling λ_3 to perform such a mechanism. The quartic coupling λ_3 is also the coupling that keeps the dark matter in thermal equilibrium. So a lower limit needed for the radiative electroweak symmetry breaking can be trasnlated into a lower limit on the dark matter mass if one assumes that the thermal relic abundance of the dark matter is in agreement with the observed density, $\Omega_{DM}h^2 \simeq 0.1186$. Here Ω_{DM} is the critical mass density for dark matter and h is the Hubble constant in units of 100 km.(s.Mpc). The mass of the dark matter candidate is given by $m_s^2 = m_{DM}^2 = \frac{\lambda_3}{2}v^2 + \mu_s^2$ and also assuming standard thermal freeze-out, we get $m_{DM} \simeq 3.3\ \lambda_3$ TeV.

Furthermore, according to Eq. (3.37) the contribution of the quartic couplings λ_3 to the SM Higgs quartic coupling is just perfect to make the electroweak vaccum stable.

3.5.3 Complete set of RGEs for Extension of SM with a scalar singlet

While the RGEs for the mass parameters are given by Eq. (3.36), the RGEs for the quartic couplings are given by

$$\begin{aligned}
16\pi^2\frac{d\lambda_1}{dt} &= 12\lambda_1^2 - 3\lambda_1\left(\frac{3}{5}g_1^2 + 3g_2^2\right) + \frac{3}{2}g_2^4 + \frac{3}{4}\left(g_2^2 + \frac{3}{5}g_1^2\right)^2 + 4\lambda_1 T - 4H + \frac{\lambda_3^2}{2};\\
16\pi^2\frac{d\lambda_2}{dt} &= 3\lambda_2^2 + \frac{4}{3}\lambda_3^2;\\
16\pi^2\frac{d\lambda_3}{dt} &= 6\lambda_3(\lambda_1 + \lambda_2).
\end{aligned} \tag{3.37}$$

RGEs for the Yukawa couplings and the gauge couplings remain the same as SM.

3.5.4 Solution to the RGEs

Like the previous cases, we evolved the SM couplings and parameters at two-loop level upto the energy scale corresponding to the mass of the singlet. From that point we evolved the new set of RGEs at one loop level upto Planck scale.

We randomly took a sample point to illustrate the Radiative Electroweak symmetry breaking scenario for this simple extension of SM. The running in Fig. 3.7a is from the mass of the singlet to the Planck scale, while Fig. 3.7b is from weak scale to planck scale. To show the evolution of the SM Higgs quartic coupling we evolved the λ_1^{eff} upto the singlet mass using two-loop SM RGEs then used the matching condition in Eq. (3.34) and the set of updated RGEs to run the coupling upto Planck scale (see Fig. 3.8). The figure also shows that the electroweak vacuum is perfectly stable for the selected sample point.

Quartic couplings	values	Mass parameters	values
$\lambda_1^{\text{eff}}(m_Z)$	0.258	μ_s^2	559^2 (GeV)^2
$\lambda_1^{\text{eff}}(\mu_s)$	0.1887	$v(m_Z)$	174.10 GeV
$\lambda_1(\mu_s)$	0.247	$v(\mu_s)$	171.05 GeV
$\lambda_2(m_s)$	0.5	$\mu_1^2(m_Z)$	-88.72^2 (GeV)^2
$\lambda_3(m_s)$	0.17	$\mu_1^2(\mu_s)$	-74.48^2 (GeV)^2

Table 3.4: Quartic coupling and mass parameter values for the sample point used for the extension of SM by a real scalar singlet in Fig. 3.7

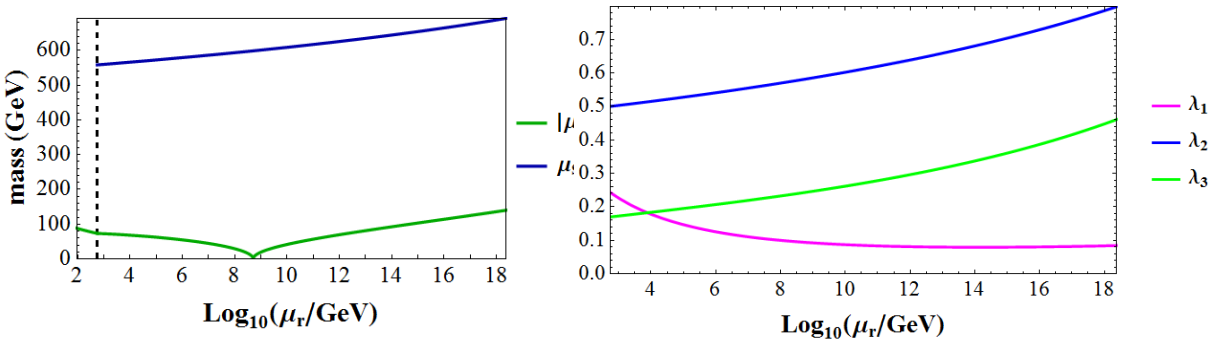

(a) Evolution of mass parameters

(b) Evolution of quartic couplings

Figure 3.7: One loop running of the parameters of SM with an extension by a real scalar singlet upto Planck scale. The black dashed line corresponds to the scale, $\mu_r = \mu_s$.

3.6 Vector-like fermion model

At the end of last year, the ATLAS and CMS collaborations of LHC presented the first data obtained at the Run 2 with proton-proton collisions at the center of mass energy of 13 TeV. Most interesting part of the data was the excess in the distribution of events containing two photons at the diphoton ($\gamma\gamma$) invariant mass approximately 750 GeV with a 3.9σ significance for ATLAS and 2.6σ for CMS [25, 26]. The signal cross section is reported to be (6 ± 3) fb by CMS and (10 ± 3) fb by ATLAS. In the updated analysis ATLAS has reported that it has observed a diphoton invariant mass around 750 GeV with local significances of 3.8 and 3.9 standard deviations in the searches optimized for a spin-2 and spin-0 particle. The global significances are estimated to be 2.1 standard deviation for both analysis [27]. For CMS the local significance of the excess is ~ 3.4 standard deviations. The

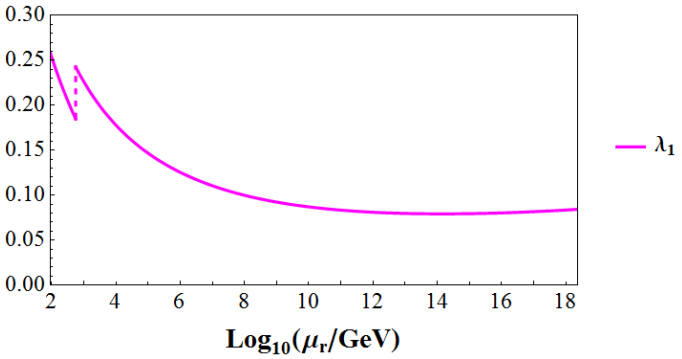

Figure 3.8: Running of the SM Higgs quatic coupling in the extension of SM by a real scalar singlet.

significance is reduced to 1.6 standard deviation when the effect of searching under multiple signal hypotheses is considered [4]. Even though the incident needs more data to rule out the possibility of a statistical fluctuation, it created a major out-pour of publications mentioning many possible interpretations and concerns regarding the phenomenon. Here we present a possible interpretation of this diphoton excess in a quark seesaw model with TeV scale vector-like fermions.

3.6.1 The model

The model uses the seesaw mechanism for quarks and leptons and is based upon the assumption that there exists a set of TeV scale vector-like fermions. These vector-like heavy fermions along with the SM fermions create the universal seesaw picture which naturally leads to small masses for the quarks like $u, d \cdots$ and leptons like e, μ. The CP violation for the model has been discussed and it was noted that the model provides a solution of the strong CP problem as the $\overline{\theta}$ parameter of strong CP problem only has non-zero value ($\overline{\theta} \sim 10^{-12}$) at two-loop level [22, 23, 24].

The original version of the model was constructed in the context of a left-right symmetric model. Here we will study a variant of the model which is based on an extension of the SM gauge sector by an $U(1)_X$, where all the left-handed fermions of SM are neutral under the new gauge group while the TeV scale vector-like fermions which are responsible for the seesaw masses for quarks and charged leptons are charged. The model requires two more additional scalar bosons (S_1 and S_2) along with the SM Higgs doublet and the quantum charge assignment for all the particles of the model is listed in the Table 3.5.

The vev of the singlet S_2 gives masses to the vector-like fermions and the vev of S_1 along with the electroweak vev mixes the right and left-handed quarks (and leptons) with the vector-like quarks

Particle	$(SU(3)_C \times SU(2)_L \times U(1)_Y \times U(1)_X)$
$\mathcal{Q}$	$(3, 2, 1/6, 0)$
$\mathcal{L}$	$(1, 2, -1/2, 0)$
u^c	$(3, 1, 2/3, -2)$
d^c	$(3, 1, -1/3, 2)$
e^c	$(1, 1, -1, 2)$
U, U^c	$(3, 1, -2/3, 1)$
D, D^c	$(3, 1, 1/3, -1)$
E, E^c	$(1, 1, 1, -1)$
ϕ	$(1, 2, 1/2, -1)$
S_1	$(1, 1, 0, 1)$
S_2	$(1, 1, 0, -2)$

Table 3.5: Particle content of the vector-like fermion model

(and leptons) while the $U(1)_X$ symmetry forbids the bare mass terms of any of the vector-like fermions.

Note that, the setup is anomaly free. As the added fermions are of vector-like, most of the anomalies cancel trivially. The only non-trivial cancellation are for the cases : $U(1)_Y \left[U(1)_X\right]^2$ and $\left[U(1)_Y\right]^2 U(1)_X$. A straightforward calculation using Table 3.5 shows that the anomalies for these two cases are also zero.

The Yukawa sector of the Lagrangian for this model is given by

$$\begin{aligned}\mathcal{L}_Y = &\mathbf{Y_u}\mathcal{Q}U^c\phi + \mathbf{F_u}Uu^cS_1 + \mathbf{G_u}UU^cS_2 \\ &- \mathbf{Y_d}\mathcal{Q}D^c\tilde{\phi} + \mathbf{F_d}Dd^cS_1^* + \mathbf{G_d}DD^cS_2^* \\ &- \mathbf{Y_e}\mathcal{L}E^c\tilde{\phi} + \mathbf{F_e}Ee^cS_1^* + \mathbf{G_e}EE^cS_2^* + h.c.\end{aligned} \tag{3.38}$$

where

$$\begin{aligned}\mathbf{Y_u}\mathcal{Q}U^c\phi =&(\mathbf{Y_u})_{ij}(u_iU_j^c\phi^0 - d_iU_j^c\phi_u^+); \\ -\mathbf{Y_d}\mathcal{Q}D^c\tilde{\phi} =&(\mathbf{Y_d})_{ij}(u_iD_j^c\phi^- + d_iD_j^c\overline{\phi}^0); \\ -\mathbf{Y_e}\mathcal{L}E^c\tilde{\phi} =&(\mathbf{Y_e})_{ij}(\nu_iE_j^c\phi^- + e_iE_j^c\overline{\phi}^0);\end{aligned} \tag{3.39}$$

and

$$\phi = \begin{pmatrix}\phi^+ \\ \phi^0\end{pmatrix}; \qquad \tilde{\phi} = \begin{pmatrix}\overline{\phi}^0 \\ \phi^-\end{pmatrix} \tag{3.40}$$

When the electroweak doublet and both the scalar singlets get vevs, one acquires the fermion (both quark and lepton) mass matrix $\mathcal{M}_f$ in the seesaw form as,

$$\mathcal{M}_f = \begin{pmatrix} 0 & \frac{1}{\sqrt{2}}\mathbf{Y_f}v \\ \mathbf{F_f}v_{s1} & \mathbf{G_f}v_{s2} \end{pmatrix} \tag{3.41}$$

where $\mathbf{f} = \mathbf{u}, \mathbf{d}, \mathbf{e}$. For such a case the mass of the light quark (or lepton) becomes $\mathbf{m_f} \simeq \dfrac{\mathbf{Y_f}\mathbf{F_f}vv_{s1}}{\sqrt{2}\mathbf{G_f}v_{s2}}$.

The scalar potential of the model can be written as

$$\begin{aligned} V(\phi, S_1, S_2) = \mu_\phi^2\phi^\dagger\phi + \mu_1^2 S_1^* S_1 + \mu_2^2 S_2^* S_2 - \left(\mu S_1^2 S_2 + h.c.\right) + \frac{\lambda_1}{2}(\phi^\dagger\phi)^2 + \frac{\lambda_2}{2}(S_1^* S_1)^2 \\ + \frac{\lambda_3}{2}(S_2^* S_2)^2 + \lambda_4(\phi^\dagger\phi)(S_1^* S_1) + \lambda_5(\phi^\dagger\phi)(S_2^* S_2) + \lambda_6(S_1^* S_1)(S_2^* S_2). \end{aligned} \tag{3.42}$$

Here μ can be taken as real without any loss of generality by the redefinition of the complex scalar S_2 .

When the scalar S_1 develops a vev v_{s1} via radiative corrections, the S_2 develops an induced vev due to the linear term in S_2 in the potential. For such a case, the imaginary part of the complex scalar S_1 is absorbed by the broken generator of $U(1)_X$ and the mass matrix for the scalar becomes:

$$\mathcal{M}_s^2 = \begin{pmatrix} 2\lambda_1 v^2 & 2\lambda_4 v v_{s1} & 0 & 0 \\ 2\lambda_4 v v_{s1} & 2\lambda_2 v_{s1}^2 & -2\mu v_{s1} & 0 \\ 0 & -2\mu v_{s1} & \lambda_5 v^2 + \lambda_6 v_{s1}^2 + \mu_2^2 & 0 \\ 0 & 0 & 0 & \lambda_5 v^2 + \lambda_6 v_{s1}^2 + \mu_2^2 \end{pmatrix} \tag{3.43}$$

Here the basis of the matrix $\mathcal{M}_s^2$ is $\{m_h, m_{S_1}, m_{S_{2R}}, m_{S_{2I}}\}$, where m_h is the SM Higgs, and m_{S_1} is the mass of the singlet S_1 and the $m_{S_{2R}}, m_{S_{2I}}$ are the masses of the real and imaginary part of the S_2 scalar. From the potential we find that the induced vev for the scalar S_2 is given by,

$$v_{s2} = \frac{\sqrt{2}\mu v_{s1}^2}{\lambda_5 v^2 + \lambda_6 v_{s1}^2 + \mu_2^2}. \tag{3.44}$$

3.6.2 The stability condition and the evolution of the mass parameters

From the stability point of view, the scalar potential of the vector-like fermion model and the two-loop neutrino mass model are identical. So, the stability condition given by Eq. (3.16) is applicable here too.

The RGEs for the mass parameters are

$$\begin{aligned}
16\pi^2\frac{d\mu_\phi^2}{dt} &= \mu_\phi^2\left[6\lambda_1 - \frac{9}{10}g_1^2 - \frac{9}{2}g_2^2 - 6g_4^2 + 2T\right] + 2\lambda_4\mu_1^2 + 2\lambda_5\mu_2^2;\\
16\pi^2\frac{d\mu_1^2}{dt} &= \mu_1^2\left[4\lambda_2 - 6g_4^2 + 2T_F\right] + 4\lambda_4\mu_\phi^2 + 2\lambda_6\mu_2^2 + 8\mu^2;\\
16\pi^2\frac{d\mu_2^2}{dt} &= \mu_2^2\left[4\lambda_3 - 24g_4^2 + 2T_G\right] + 4\lambda_5\mu_\phi^2 + 4\lambda_6\mu_1^2 + 4\mu^2;\\
16\pi^2\frac{d\mu}{dt} &= \mu\left[2\lambda_2 + 2\lambda_6 - 18g_4^2 + 2T_F + T_G\right].
\end{aligned} \tag{3.45}$$

The complete set of RGEs are given in the next section.

3.6.3 Complete set of RGEs for vector-like fermion model

The RGEs for the mass parameters are given by Eq. (3.45). The RGEs for the gauge couplings are given by

$$16\pi^2\frac{dg_i}{dt} = b_i g_i^3, \tag{3.46}$$

where $b_i = \left\{-3, \frac{-19}{6}, \frac{105}{10}, \frac{259}{3}\right\}$

The set of RGEs for all the Yukawa couplings is given by

$$\begin{aligned}
16\pi^2\frac{d\mathbf{Y_u}}{dt} &= \mathbf{Y_u}\left[\frac{3}{2}\left(\mathbf{Y_u^\dagger Y_u} - \mathbf{Y_d^\dagger Y_d}\right) + \frac{1}{2}\mathbf{G_u^\dagger G_u} + T - \frac{17}{20}g_1^2 - \frac{9}{4}g_2^2 - 8g_3^2 - 3g_4^2\right];\\
16\pi^2\frac{d\mathbf{Y_d}}{dt} &= \mathbf{Y_d}\left[\frac{3}{2}\left(\mathbf{Y_d^\dagger Y_d} - \mathbf{Y_u^\dagger Y_u}\right) + \frac{1}{2}\mathbf{G_d^\dagger G_d} + T - \frac{1}{4}g_1^2 - \frac{9}{4}g_2^2 - 8g_3^2 - 3g_4^2\right];\\
16\pi^2\frac{d\mathbf{Y_e}}{dt} &= \mathbf{Y_e}\left[\frac{3}{2}\mathbf{Y_e^\dagger Y_e} + \frac{1}{2}\mathbf{G_e^\dagger G_e} + T - \frac{9}{4}g_1^2 - \frac{9}{4}g_2^2 - 3g_4^2\right];\\
16\pi^2\frac{d\mathbf{F_u}}{dt} &= \mathbf{F_u}\left[\mathbf{F_u^\dagger F_u} + T_F - \frac{8}{5}g_1^2 - 8g_3^2 - 15g_4^2\right] + \frac{1}{2}\mathbf{G_u G_u^\dagger F_u};\\
16\pi^2\frac{d\mathbf{F_d}}{dt} &= \mathbf{F_d}\left[\mathbf{F_d^\dagger F_d} + T_F - \frac{2}{5}g_1^2 - 8g_3^2 - 15g_4^2\right] + \frac{1}{2}\mathbf{G_d G_d^\dagger F_d};\\
16\pi^2\frac{d\mathbf{F_e}}{dt} &= \mathbf{F_e}\left[\mathbf{F_e^\dagger F_e} + T_F - \frac{18}{5}g_1^2 - 15g_4^2\right] + \frac{1}{2}\mathbf{G_e G_e^\dagger F_e};\\
16\pi^2\frac{d\mathbf{G_u}}{dt} &= \mathbf{G_u}\left[\mathbf{G_u^\dagger G_u} + \mathbf{Y_u^\dagger Y_u} + T_G - \frac{8}{5}g_1^2 - 8g_3^2 - 6g_4^2\right] + \frac{1}{2}\mathbf{F_u F_u^\dagger G_u};\\
16\pi^2\frac{d\mathbf{G_d}}{dt} &= \mathbf{G_d}\left[\mathbf{G_d^\dagger G_d} + \mathbf{Y_d^\dagger Y_d} + T_G - \frac{2}{5}g_1^2 - 8g_3^2 - 6g_4^2\right] + \frac{1}{2}\mathbf{F_d F_d^\dagger G_d};\\
16\pi^2\frac{d\mathbf{G_e}}{dt} &= \mathbf{G_e}\left[\mathbf{G_e^\dagger G_e} + \mathbf{Y_e^\dagger Y_e} + T_G - \frac{18}{5}g_1^2 - 6g_4^2\right] + \frac{1}{2}\mathbf{F_e F_e^\dagger G_e}.
\end{aligned} \tag{3.47}$$

The RGEs for scalar quartic couplings are given by

$$
\begin{aligned}
16\pi^2\frac{d\lambda_1}{dt} &= 12\lambda_1^2 + 2\lambda_4^2 + 2\lambda_5^2 - 3\lambda_1\left(\frac{3}{5}g_1^2 + 3g_2^2 + 4g_4^2\right) + \left(\frac{27}{100}g_1^4 + \frac{9}{4}g_2^4 + \frac{9}{10}g_1^2g_2^2\right) \\
&\quad + 12g_4^2 + 6g_2^2g_4^2 + \frac{18}{5}g_1^2g_4^2 + 4\lambda_1 T - 4H; \\
16\pi^2\frac{d\lambda_2}{dt} &= 10\lambda_2^2 + 4\lambda_4^2 + 2\lambda_6^2 - 12\lambda_2 g_4^2 + 12g_4^4 + \lambda_2 T_F - 4H_F; \\
16\pi^2\frac{d\lambda_3}{dt} &= 10\lambda_3^2 + 4\lambda_5^2 + 2\lambda_6^2 - 48\lambda_3 g_4^2 + 48g_4^4 + 4\lambda_3 T_G - 4H_G; \\
16\pi^2\frac{d\lambda_4}{dt} &= 6\lambda_1\lambda_4 + 2\lambda_2\lambda_4 + 2\lambda_5\lambda_6 + 4\lambda_4^2 - \lambda_4\left(\frac{9}{2}g_2^2 + \frac{9}{10}g_1^2 + 12g_4^2\right) + 12g_4^4 + 2\lambda_4(T + T_F); \\
16\pi^2\frac{d\lambda_5}{dt} &= 6\lambda_1\lambda_5 + 4\lambda_3\lambda_5 + 2\lambda_4\lambda_6 + 4\lambda_5^2 - \lambda_5\left(\frac{9}{2}g_2^2 + \frac{9}{10}g_1^2 + 30g_4^2\right) + 48g_4^4 + 2\lambda_5(T + T_G) - 4H_{YG}; \\
16\pi^2\frac{d\lambda_6}{dt} &= 4\lambda_2\lambda_6 + 4\lambda_3\lambda_6 + 4\lambda_4\lambda_5 + 4\lambda_6^2 - 30\lambda_6 g_4^2 + 48g_4^4 + 2\lambda_6(T_F + T_G) - 4H_{FG}.
\end{aligned}
\tag{3.48}
$$

where

$$
\begin{aligned}
T &= \mathrm{Tr}\left[\mathbf{Y_e^\dagger Y_e} + 3\mathbf{Y_d^\dagger Y_d} + 3\mathbf{Y_u^\dagger Y_u}\right]; \\
T_F &= \mathrm{Tr}\left[\mathbf{F_e^\dagger F_e} + 3\mathbf{F_d^\dagger F_d} + 3\mathbf{F_u^\dagger F_u}\right]; \\
T_G &= \mathrm{Tr}\left[\mathbf{G_e^\dagger G_e} + 3\mathbf{G_d^\dagger G_d} + 3\mathbf{G_u^\dagger G_u}\right]; \\
H &= \mathrm{Tr}\left[\mathbf{Y_e^\dagger Y_e Y_e^\dagger Y_e} + 3\mathbf{Y_d^\dagger Y_d Y_d^\dagger Y_d} + 3\mathbf{Y_u^\dagger Y_u Y_u^\dagger Y_u}\right]; \\
H_F &= \mathrm{Tr}\left[\mathbf{F_e^\dagger F_e F_e^\dagger F_e} + 3\mathbf{F_d^\dagger F_d F_d^\dagger F_d} + 3\mathbf{F_u^\dagger F_u F_u^\dagger F_u}\right]; \\
H_G &= \mathrm{Tr}\left[\mathbf{G_e^\dagger G_e G_e^\dagger G_e} + 3\mathbf{G_d^\dagger G_d G_d^\dagger G_d} + 3\mathbf{G_u^\dagger G_u G_u^\dagger G_u}\right]; \\
H_{YG} &= \mathrm{Tr}\left[\mathbf{Y_e^\dagger Y_e G_e^\dagger G_e} + 3\mathbf{Y_d^\dagger Y_d G_d^\dagger G_d} + 3\mathbf{Y_u^\dagger Y_u G_u^\dagger G_u}\right]; \\
H_{FG} &= \mathrm{Tr}\left[\mathbf{F_e^\dagger F_e G_e^\dagger G_e} + 3\mathbf{F_d^\dagger F_d G_d^\dagger G_d} + 3\mathbf{F_u^\dagger F_u G_u^\dagger G_u}\right].
\end{aligned}
\tag{3.49}
$$

3.6.4 Solution to the RGEs

To find the solution of the set of RGEs, we took a more simplified case where we kept all the Yukawa coupling $\mathbf{F}$ to be small and negligible and Yukawa coupling $\mathbf{G} \simeq \mathcal{O}(1)$. The numerical solution was hunted for the case where one of the eigenvalue of the scalar mass matrix $\mathcal{M}_s$ corresponds to the SM Higgs boson and another one corresponds to the possible newly discovered scalar boson of mass ~ 750 GeV. The vector-like fermion mass was kept around TeV scale where the mass is approximated by $\sim \mathbf{G}v_{s2}$. One such sample point is given by the Table 3.6. As the first new particle in this model is at $\mu_s = 750$ GeV, the SM RGEs were evolved at two-loop level upto the scale μ_s and then the new set of RGEs was deployed to do the evolution of the couplings and mass parameters. Fig. 3.9 shows

Quartic couplings	values	mass parameters	values
$\lambda_1(m_Z)$	0.258	$\mu_1^2(\mu_s)$	-1800^2 (GeV)^2
$\lambda_1(\mu_s)$	0.175	$\mu_2^2(\mu_s)$	2550^2 (GeV)^2
$\lambda_2(\mu_s)$	0.25	$\mu_\phi^2(\mu_s)$	-71.37^2 (GeV)^2
$\lambda_3(\mu_s)$	0.24	$\mu(m_s)$	850 GeV
$\lambda_4(\mu_s)$	0.02	$\mu_\phi^2(m_Z)$	-88.72^2 (GeV)^2
$\lambda_5(\mu_s)$	0.1	$(G_u)_{ii}(M_z) \sim (G_d)_{ii}(M_z) \sim (G_e)_{ii}(M_z)$	0.45
$\lambda_6(\mu_s)$	0.09	v_{s1}	3.60 TeV
		v_{s2}	2.26 TeV

Table 3.6: Quartic coupling and mass parameter values for the sample point used for the vector-like fermion model in Fig. 3.9

that the both the vevs (electroweak vev and vev for the single S_1) can be generated by radiative correction.

3.7 Conclusion

We presented various extensions of SM where electroweak symmetry breaking was triggered by radiative loop corrections. Even though such symmetry breaking fails to occur in SM, the simplest extensions are able to incorporate the mechanism. Extensions like Type-II seesaw models, loop induced neutrino modelsm scalar dark matter models all have this built-in feature. For such cases, we found that TeV scale scalars are the best scenario as they can major effect on the evolution of the mass parameters. These TeV scale scalars may be detected in the upcoming LHC run.

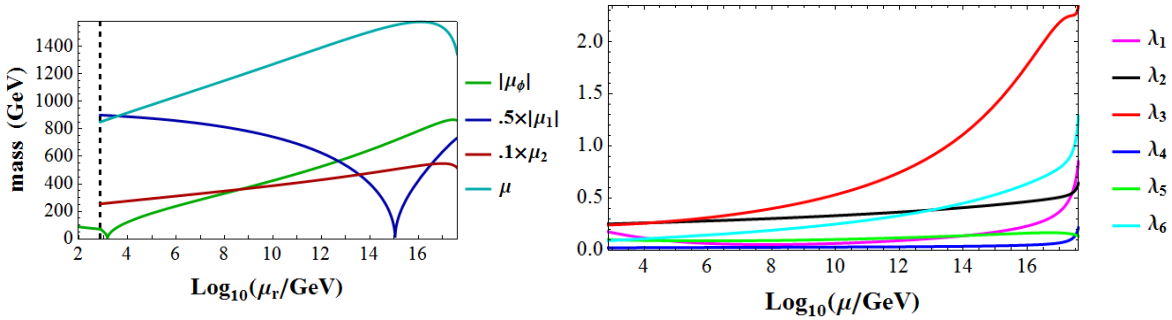

(a) Evolution of mass parameters

(b) Evolution of quartic couplings

Figure 3.9: One loop running of the couplings and mass parameters of vector-like fermion model. The black dashed line corresponds to the scale, $\mu_r = \mu_s$.

REFERENCES

[1] S. Chatrchyan *et al.* [CMS Collaboration], Phys. Lett. B **716**, 30 (2012) [arXiv:1207.7235 [hep-ex]]; G. Aad *et al.* [ATLAS Collaboration], Phys. Lett. B **716**, 1 (2012) [arXiv:1207.7214 [hep-ex]]; G. Aad *et al.* [ATLAS and CMS Collaborations], Phys. Rev. Lett. **114**, 191803 (2015) [arXiv:1503.07589 [hep-ex]].

[2] P. Minkowski, Phys. Lett. B **67**, 421 (1977); O. Sawada and A. Sugamoto, Tsukuba, Japan: Natl.Lab.High Energy Phys.(1979) 109 P.and Japan Natl Lab High Energy - KEK-79-18 (79,REC.JAN 80) 109p; S. Glashow, In *Cargese 1979, Proceedings, Quarks and Leptons* M. Gell-Mann, P. Ramond and R. Slansky, Conf. Proc. C **790927**, 315 (1979) [arXiv:1306.4669 [hep-th]];

[3] R. N. Mohapatra and G. Senjanovic, Phys. Rev. Lett. **44**, 912 (1980).

[4] M. Magg and C. Wetterich, Phys. Lett. B **94**, 61 (1980). doi:10.1016/0370-2693(80)90825-4

[5] G. Lazarides, Q. Shafi and C. Wetterich, Nucl. Phys. B **181**, 287 (1981). doi:10.1016/0550-3213(81)90354-0

[6] R. Foot, H. Lew, X. G. He and G. C. Joshi, Z. Phys. C **44**, 441 (1989). doi:10.1007/BF01415558

[7] A. Zee, Phys. Lett. B **93**, 389 (1980) Erratum: [Phys. Lett. B **95**, 461 (1980)]. doi:10.1016/0370-2693(80)90349-4, 10.1016/0370-2693(80)90193-8 K. S. Babu, Phys. Lett. B **203** (1988) 132. doi:10.1016/0370-2693(88)91584-5

[8] G. R. Farrar and P. Fayet, Phys. Lett. B **76**, 575 (1978). doi:10.1016/0370-2693(78)90858-4

[9] H. C. Cheng, K. T. Matchev and M. Schmaltz, Phys. Rev. D **66**, 036005 (2002) doi:10.1103/PhysRevD.66.036005 [hep-ph/0204342].

[10] H. C. Cheng and I. Low, JHEP **0309**, 051 (2003) doi:10.1088/1126-6708/2003/09/051 [hep-ph/0308199]. H. C. Cheng and I. Low, JHEP **0408**, 061 (2004) doi:10.1088/1126-6708/2004/08/061 [hep-ph/0405243]. I. Low, JHEP **0410**, 067 (2004) doi:10.1088/1126-6708/2004/10/067 [hep-ph/0409025].

[11] N. G. Deshpande and E. Ma, Phys. Rev. D **18**, 2574 (1978). doi:10.1103/PhysRevD.18.2574

[12] E. Ma, Phys. Rev. D **73**, 077301 (2006) doi:10.1103/PhysRevD.73.077301 [hep-ph/0601225].

[13] T. W. B. Kibble, G. Lazarides and Q. Shafi, Phys. Lett. B **113**, 237 (1982). doi:10.1016/0370-2693(82)90829-2 L. M. Krauss and F. Wilczek, Phys. Rev. Lett. **62**, 1221 (1989). doi:10.1103/PhysRevLett.62.1221 L. E. Ibanez and G. G. Ross, Phys. Lett. B **260**, 291 (1991). doi:10.1016/0370-2693(91)91614-2 L. E. Ibanez and G. G. Ross, Nucl. Phys. B **368**, 3 (1992). doi:10.1016/0550-3213(92)90195-H S. P. Martin, Phys. Rev. D **46**, 2769 (1992) doi:10.1103/PhysRevD.46.R2769 [hep-ph/9207218]. M. Kadastik, K. Kannike and M. Raidal, Phys. Rev. D **81**, 015002 (2010) doi:10.1103/PhysRevD.81.015002 [arXiv:0903.2475 [hep-ph]]. M. Kadastik, K. Kannike and M. Raidal, Phys. Rev. D **80**, 085020 (2009) Erratum: [Phys. Rev. D **81**, 029903 (2010)] doi:10.1103/PhysRevD.80.085020, 10.1103/PhysRevD.81.029903 [arXiv:0907.1894 [hep-ph]]. M. Frigerio and T. Hambye, Phys. Rev. D **81**, 075002 (2010) doi:10.1103/PhysRevD.81.075002 [arXiv:0912.1545 [hep-ph]]. T. Hambye, PoS IDM **2010**, 098 (2011) [arXiv:1012.4587 [hep-ph]]. L. J. Hall, K. Jedamzik, J. March-Russell and S. M. West, JHEP **1003**, 080 (2010) doi:10.1007/JHEP03(2010)080 [arXiv:0911.1120 [hep-ph]]. J. McDonald, Phys. Rev. Lett. **88**, 091304 (2002) doi:10.1103/PhysRevLett.88.091304 [hep-ph/0106249]. X. Chu, T. Hambye and M. H. G. Tytgat, JCAP **1205**, 034 (2012) doi:10.1088/1475-7516/2012/05/034 [arXiv:1112.0493 [hep-ph]]. C. E. Yaguna, JCAP **1202**, 006 (2012) doi:10.1088/1475-7516/2012/02/006 [arXiv:1111.6831 [hep-ph]].

[14] L. E. Ibanez and G. G. Ross, Phys. Lett. B **110**, 215 (1982). doi:10.1016/0370-2693(82)91239-4 K. Inoue, A. Kakuto, H. Komatsu and S. Takeshita, Prog. Theor. Phys. **68**, 927 (1982) Erratum: [Prog. Theor. Phys. **70**, 330 (1983)]. doi:10.1143/PTP.68.927 L. E. Ibanez, Phys. Lett. B **118**, 73 (1982). doi:10.1016/0370-2693(82)90604-9 J. R. Ellis, D. V. Nanopoulos and K. Tamvakis, Phys. Lett. B **121**, 123 (1983). doi:10.1016/0370-2693(83)90900-0 J. R. Ellis, J. S. Hagelin, D. V. Nanopoulos and K. Tamvakis, Phys. Lett. B **125**, 275 (1983). doi:10.1016/0370-2693(83)91283-2 L. Alvarez-Gaume, J. Polchinski and M. B. Wise, Nucl. Phys. B **221**, 495 (1983). doi:10.1016/0550-3213(83)90591-6

[15] K. S. Babu, B. Bajc and S. Saad, arXiv:1605.05116 [hep-ph].

[16] K. S. Babu, I. Gogoladze, P. Nath and R. M. Syed, Phys. Rev. D **72**, 095011 (2005) doi:10.1103/PhysRevD.72.095011 [hep-ph/0506312].

[17] M. A. Schmidt, Phys. Rev. D **76**, 073010 (2007) Erratum: [Phys. Rev. D **85**, 099903 (2012)] doi:10.1103/PhysRevD.85.099903, 10.1103/PhysRevD.76.073010 [arXiv:0705.3841 [hep-ph]].

[18] W. Chao and H. Zhang, Phys. Rev. D **75**, 033003 (2007) doi:10.1103/PhysRevD.75.033003 [hep-ph/0611323].

[19] K. S. Babu and J. Julio, AIP Conf. Proc. **1604**, 134 (2014). doi:10.1063/1.4883422

[20] A. Merle and M. Platscher, Phys. Rev. D **92**, no. 9, 095002 (2015) doi:10.1103/PhysRevD.92.095002 [arXiv:1502.03098 [hep-ph]].

[21] Y. Mambrini, N. Nagata, K. A. Olive and J. Zheng, Phys. Rev. D **93**, no. 11, 111703 (2016) doi:10.1103/PhysRevD.93.111703 [arXiv:1602.05583 [hep-ph]].

[22] K. S. Babu and R. N. Mohapatra, Phys. Rev. Lett. **62**, 1079 (1989). doi:10.1103/PhysRevLett.62.1079

[23] K. S. Babu and R. N. Mohapatra, Phys. Rev. D **41**, 1286 (1990). doi:10.1103/PhysRevD.41.1286

[24] P. S. B. Dev, R. N. Mohapatra and Y. Zhang, JHEP **1602**, 186 (2016) doi:10.1007/JHEP02(2016)186 [arXiv:1512.08507 [hep-ph]].

[25] CMS Collaboration [CMS Collaboration], collisions at 13TeV," CMS-PAS-EXO-15-004.

[26] The ATLAS collaboration, ATLAS-CONF-2015-081.

[27] M. Aaboud *et al.* [ATLAS Collaboration], arXiv:1606.03833 [hep-ex].

[28] V. Khachatryan *et al.* [CMS Collaboration], arXiv:1606.04093 [hep-ex].

CHAPTER 4

An $O(3)_L \times O(3)_R$ FLAVOR GAUGE SYMMETRY NEAR TEV SCALE

4.0 Short Review of SM Flavor Physics

In particle physics, the term "flavors" is used to describe several copies of the particle with the same gauge representation. So, when several particles have same quantum charges under the gauge group of the model and only differ by their masses, they are known as same type of particle with different "flavors". The term "flavor physics" refers to interaction that distinguishes between flavors. The gauge interaction related to unbroken symmetries and mediated by massless gauge bosons do not distinguish among the flavor and thus cannot be a part of the flavor physics. On the contrary, weak interaction mediated by massive gauge bosons ($W^{\pm}, Z$) do discriminate among particles with different flavors.

Type of particles	Gauge representation $SU(3)_C \times U(1)_{EM}$	List of flavors
Up-type quarks	$(3, +2/3)$	(i) up, (u) (ii) charm, (c) (iii) top, (t)
Down-type quarks	$(3, -1/3)$	(i) down, (d) (ii) strange, (s) (iii) bottom, (b)
Charged leptons	$(1, -1)$	(i) electron, (e) (ii) muon, (μ) (iii) tau, (τ)
Neutrinos	$(1, 0)$	(i) electron neutrino, (ν_e) (ii) muon neutrino, (ν_μ) (iii) tau neutrino, (ν_τ)

Table 4.1: List of flavored fermions of SM

Within SM, in terms of the unbroken gauge group $SU(3)_C \times U(1)_Q$ there are four different types

of particles and each type comes in three flavors. All the SM "flavored" fermions are enlisted in Table 4.1.

The term "flavor changing processes" refers to the processes where the total number of certain flavor does not remain constant. Here a particle of certain flavor is counted as $+1$ and the antiparticle is counted as -1. In flavor changing charged current (FCCC) the flavor changing process is mediated by a charged particle (within SM, the mediator is $W^{\pm}$-boson) while the flavor changing neutral current (FCNC) is mediated by a neutral one (within SM, the mediator is Z-boson). In FCCC, both up-type and down-type quarks and/or charged lepton and neutrinos are involved. Examples of such processes are: (i) $\mu \to e\ \overline{\nu}_e\ \nu_\mu$; (ii) $K^-(s\overline{u}) \to \mu^-\ \overline{\nu}_\mu$. In FCNC, either up-type or down-type quarks but not both and either charged leptons or neutrinos but not both are involved. Example of such processes are: (i) $\mu \to e\gamma$ (ii) $K_L(s\overline{d}) \to \mu^+\mu^-$. The most important feature of FCNC in SM is that FCNC in SM only happens at loop-level while FCCC in SM happens at tree level. This situation about FCNC makes it particularly sensitive to new physics beyond SM (BSM). If the FCNC in the new physics fails to have a suppression (like loop suppression in the case of SM) its contribution to FCNC might become comparable to SM one even if the new physics scale is much higher than the weak scale. This sensitivity of flavor physics about new physics is one of the primary reasons for the experimental endeavor for precise measurement of flavor data and theoretical effort to interpret them. So, any realistic flavor model will have to satisfy all the constraints imposed by such experimental data.

In SM, there are three generations for fermions, each consisting of five representations of SM gauge group $SU(3)_C \times SU(2)_L \times U(1)_Y$:

$$Q_{iL}(1,2,{}^1\!/_6);\ \ L_{iL}(1,2,-{}^1\!/_2);\ \ u_{iR}(\overline{3},1,-{}^2\!/_3);\ \ d_{iR}(\overline{3},1,{}^1\!/_3);\ \ e_{iR}(1,1,1); \tag{4.1}$$

In SM, the source of all flavor physics is in Yukawa sector of the Lagrangian as the weak interaction eigenstates and the mass eigenstates are not aligned. The Yukawa sector of the Lagrangian is given as:

$$\mathcal{L}_Y = \mathbf{Y}^u_{ij}\overline{Q^i_L}\tilde{\phi}u^j_R + \mathbf{Y}^d_{ij}\overline{Q^i_L}\phi d^j_R + \mathbf{Y}^e_{ij}\overline{\ell^i_L}\phi e^j_R + h.c. \tag{4.2}$$

where $\tilde{\phi} = i\ \sigma_2\phi^\dagger$. This is the flavor dependent and Charge-Parity (CP)-violating part of the Lagrangian where $\mathbf{Y} \not\propto \mathbb{1}$. In the absence of the Yukawa matrices $\mathbf{Y_u}$, $\mathbf{Y_d}$, $\mathbf{Y_e}$ the SM has a larger $U(3)^5$ global symmetry:

$$G_{global}(\mathbf{Y_{u,d,e}} = 0) = SU(3)^3_q \times SU(3)^2_\ell \times U(1)^5 \tag{4.3}$$

The non-Abelian part of the global symmetry is recognized as:

$$\begin{aligned} SU(3)_q^3 =& SU(3)_Q \times SU(3)_U \times SU(3)_D; \\ SU(3)_\ell^2 =& SU(3)_L \times SU(3)_E; \end{aligned} \tag{4.4}$$

This non-Abelian part is particularly relevant to the flavor physics as under these flavor symmetries:

$$Q_L \to V_Q Q_L; \;\; U_R \to V_U U_R; \;\; D_R \to V_D D_R; \;\; L_L \to V_L L_L; \;\; E_R \to V_E E_R; \tag{4.5}$$

where V_i's are the unitary matrix associated with the $SU(3)_i$ global groups. The Yukawa sector breaks the global symmetry and the remainder of the symmetry can be identified as:

$$G_{global}(\mathbf{Y_{u,d,e}} \neq 0) = U(1)_B \times U(1)_e \times U(1)_\mu \times U(1)_\tau \tag{4.6}$$

where baryon number is denoted by B. And $U(1)_Y$ (hypercharge) which is gauged in SM is also a good symmetry. So, the term "flavor violation" can be redefined as the interaction that breaks this $G_{global}(\mathbf{Y_{u,d,e}} = 0)$ group. For example, in SM the Yukawa interaction is flavor violating sector.

To identify the minimized number of parameters associated with the flavor violation in SM, one uses the quark Yukawa matrices in a basis where:

$$\mathbf{Y_d} = \lambda_\mathbf{d}; \qquad\qquad \mathbf{Y_u} = \mathbf{V_{CKM}^\dagger} \lambda_\mathbf{u}; \tag{4.7}$$

where $\lambda_{\mathbf{d,u}}$ are diagonal matrices and $\lambda_\mathbf{d} = \text{diag}\,(y_d, y_s, y_b)$ and $\lambda_\mathbf{u} = \text{diag}\,(y_u, y_c, y_t)$ while $\mathbf{V_{CKM}}$ is the unitary matrix known as Cabibo-Kobayashi-Maskawa (CKM) matrix which contains information on the strength of the flavor changing weak decays and has three real angles and one complex phase. So, in the quark flavor sector we end up having 10 parameters: 9 real ones and a single phase. In the mass basis, six of them are identified as six quark masses while three of them are mixing angles and last one being the complex phase and appears in the $\mathbf{V_{CKM}}$ matrix. Any flavor model of BSM also needs to be able to reproduce the CKM matrix which has been experimentally measured upto an excellent degree of precision.

4.1 Introduction

At the end of last year, the ATLAS and CMS collaborations of Large Hadron Collider (LHC) presented the first data obtained at the Run 2 with proton-proton collisions at the center of mass energy of 13 TeV. Most interesting part of the data was the excess in the distribution of events containing two photons at the diphoton ($\gamma\gamma$) invariant mass approximately 750 GeV with a 3.9σ significance

for ATLAS and 2.6σ for CMS. The signal cross section is reported to be (6 ± 3) fb by CMS and (10 ± 3) fb by ATLAS [1, 2]. In the updated analysis ATLAS has reported that it has observed a diphoton invariant mass around 750 GeV with local significance of 3.8 and 3.9 standard deviations in the searches optimized for a spin-2 and spin-0 particle. The global significance is estimated to be 2.1 standard deviation for both analysis [3]. For CMS the local significance of the excess is ~ 3.4 standard deviations. The significance is reduced to 1.6 standard deviation when the effect of searching under multiple signal hypotheses is considered [4]. Even though the incident needs more data to rule out the possibility of a statistical fluctuation, it created a major out-pour of publications mentioning many possible interpretations and concerns regarding the phenomenon. Unfortunately almost all the apparent explanations lack complete and consistent underlying structure behind the proposed explanations.

We propose a model with flavor structure based upon gauging one of the maximal subgroup of $[U(3)]^5$ which is the global flavor symmetry of SM, following the dictum that any symmetry that is anomaly-free must be gauged. Such a gauged symmetry provides an organizing principle for the SM fermions and can explain their masses and mixings. One can find out the set of maximal subgroup of the global flavor symmetry by determining the anomalies of the groups especially the G^3 and $G^2 \times Y$ anomalies, where G is the gauged flavor symmetry. From the anomaly cancellation calculation one finds out that the maximal groups that can be gauged are:

- $O(3)_{L\{Q,L\}} \times O(3)_{R\{u^c,d^c,e^c\}}$
- $O(3)_{\{Q,u^c,e^c\}} \times O(3)_{\{L,d^c\}}$
- $O(3)_{\{Q,u^c,d^c\}} \times O(3)_{\{L,e^c\}}$

For the first case, the left-handed $SU(2)_L$ doublet fermions (Q, L) are the triplets of $O(3)_L$ while the conjugate right-handed singlet fermions (u^c, d^c, e^c) are triplets of $O(3)_R$. So the fermions group structure under this flavor maximal sub group is:

$$Q(3,1); \quad L(3,1); \quad u^c(1,3); \quad d^c(1,3); \quad e^c(1,3); \tag{4.8}$$

The SM Higgs doublet field ϕ^a that generate fermion masses and mixings must then transform as $(3,3)$ of $O(3)_L \times O(3)_R$ and the Yukawa couplings of the SM are thus promoted to dynamic field ϕ^a_{ij} with a singlet unified coupling for each type of fermions.

Now, $O(3)_L \times O(3)_R$ group symmetry is sponetaneously broken down to $D_{3L} \times D_{3R}$ symmetry by the vacuum expectation values (vevs) of left-handed 7-plet (T^L) and right-handed 7-plet (T^R) while the $D_{3L} \times D_{3R}$ symmetry is completely broken down by either a scalar bi-fundamental $\psi(3,3)$ or a

pair of scalar fundamentals ($\psi_L(3,1)+\psi_R(1,3)$). The electroweak symmetry of the SM is broken by the complex bi-fundamental ($\phi(3,3)$) which is also a doublet under $SU(2)_L$ group.The neutral component of the ϕ_{33} element acquires the required electroweak vev to perform the electroweak symmetry breaking and generates masses for the third generation fermions. In this model, the Higgs particle discovered in the LHC is primarily this scalar component with an admixture of other neutral components from both ϕ and $\psi(\psi_{L/R})$. The other neutral components of the bi-fundamental ϕ provide masses and mixture for the other generations of fermions by vevs induced by the ψ vevs and the ϕ_{33} vev. In such a scenario, a scalar of 750 GeV mass which comprised mostly a scalar component from the bi-fundamental ψ can decay to two photons via loop diagram with some charged scalar from the doublet ϕ running in the loop.

4.2 The model(s)

We extend the gauge symmetry of the SM by the symmetry group $O(3)_L \times O(3)_R$, which is a maximal subgroup of the flavor symmetry possessed by the fermion contents of the SM. Due to anomaly cancellation the symmetry group $O(3)_L \times O(3)_R$ is one of the maximal subgroups of $[U(3)]^5$ that can be gauged. Under this symmetry group, the SM fermions belong to the $Q(3,1)+L(3,1)+u^c(1,3)+d^c(1,3)+e^c(1,3)$ representations. The scalar sector of the model contains $T^L(7,1)+T^R(1,7)+\phi(3,3)$ representations and either a real bi-fundamental $\psi(3,3)$ or a pair of real fundamentals $\psi_L(3,1)+\psi_R(1,3)$. All the Higgs fields except ϕ are singlets under the SM. And the electroweak (EW) symmetry is broken by the bi-fundamental of the flavor group $\phi(3,3)$ which is also a doublet under the SM gauge group $SU(2)_L$. The ϕ field is responsible for generating the fermion masses and mixings by performing electroweak symmetry breaking and mixing with the other scalar fields.

The 7-plet of $O(3)_{L/R}$ group is a symmetric traceless third ranked tensor $T^{L/R}_{abc}$, with $a,b,c=1-3$. Both the left-handed and right-handed 7-plet $T^{L/R}_{abc}$ can be written as [5]

$$
\begin{aligned}
T_{112} &= -\frac{1}{2}\chi_2 + \frac{1}{2\sqrt{15}}\chi_6; & T_{113} &= -\frac{1}{\sqrt{6}}\chi_3 + \frac{1}{\sqrt{10}}\chi_7;\\
T_{122} &= \frac{1}{2}\chi_1 + \frac{1}{2\sqrt{15}}\chi_5; & T_{223} &= \frac{1}{\sqrt{6}}\chi_3 + \frac{1}{\sqrt{10}}\chi_7;\\
T_{133} &= -\frac{2}{\sqrt{15}}\chi_5; & T_{233} &= -\frac{2}{\sqrt{15}}\chi_6.\\
T_{123} &= -\frac{1}{\sqrt{6}}\chi_4.
\end{aligned}
\tag{4.9}
$$

And the traceless conditions implies that:

$$\begin{aligned} T_{111} + T_{122} + T_{133} &= 0; \\ T_{112} + T_{222} + T_{233} &= 0; \\ T_{113} + T_{223} + T_{333} &= 0. \end{aligned} \tag{4.10}$$

For the group $O(3)_L$ ($O(3)_R$) we use the group indices to be a, b, c (α, β, γ).

Here we consider two different cases:

- **Model with a bi-fundamental:** Scalar sector contains: Left-handed 7-plet, $T^L(7,1)$ + Right-handed 7-plet, $T^R(1,7)$ + Bi-fundamental, $\psi(3,3)$ + Bi-fundamental which is also a $SU(2)_L$ doublet, $\phi(3,3)$
- **Model with fundamentals:** Scalar sector contains: Left-handed 7-plet, $T^L(7,1)$ + Right-handed 7-plet, $T^R(1,7)$ + Left-handed fundamental, $\psi_L(3,1)$ + Right-handed fundamental, $\psi_R(1,3)$ + Bi-fundamental which is also a $SU(2)_L$ doublet, $\phi(3,3)$.

Both the possibilities have been analyzed from the point of view of symmetry breaking, fermion masses and mixings, flavor constraints and possible candidate for 750 GeV scalar which can decay via diphoton channel.

4.3 Model with a bi-fundamental

As mentioned earlier, the scalar sector of this version of the model contains $T^L_{abc}, T^R_{\alpha\beta\gamma}, \phi^\rho_{a\alpha}$ and $\psi_{a\alpha}$. The complete Lagrangian with these scalar multiplets can be written as:

$$V = V_\psi + V_\chi + V_\phi + V_{\psi\phi} + V_m. \tag{4.11}$$

where

$$\begin{aligned}
V_\psi =& -\mu_\psi^2\ \psi_{a\alpha}\psi_{a\alpha} + \frac{1}{6}\,\boldsymbol{\mu_\psi}\ \epsilon_{abc}\epsilon_{\alpha\beta\gamma}\psi_{a\alpha}\psi_{b\beta}\psi_{c\gamma} + \lambda_{\psi 1}\psi_{a\alpha}\psi_{a\alpha}\psi_{b\beta}\psi_{b\beta} + \boldsymbol{\lambda_{\psi 2}}\psi_{a\alpha}\psi_{b\alpha}\psi_{a\beta}\psi_{b\beta}; \\
V_\chi =& -\nu_L^2\ T^L_{abc}\ T^L_{abc} + \xi_1\ (T^L_{abc}\ T^L_{abc})^2 + \boldsymbol{\xi_2}\ T^L_{abc}\ T^L_{bcd}\ T^L_{def}\ T^L_{efa} \\
& -\nu_R^2\ T^R_{\alpha\beta\gamma}\ T^R_{\alpha\beta\gamma} + \xi_3\ (T^R_{\alpha\beta\gamma}\ T^R_{\alpha\beta\gamma})^2 + \boldsymbol{\xi_4}\ T^R_{\alpha\beta\gamma}\ T^R_{\beta\gamma\delta}\ T^R_{\delta\mu\nu}\ T^R_{\mu\nu\alpha} + \xi_5\ T^L_{abc}\ T^L_{abc}\ T^R_{\alpha\beta\gamma}\ T^R_{\alpha\beta\gamma}; \\
V_\phi =& -\mu^2\phi^\rho_{a\alpha}\ \phi^{*\,\rho}_{a\alpha} + \boldsymbol{\lambda_1}\phi^\rho_{a\alpha}\ \phi^\sigma_{a\alpha}\ \phi^{*\,\rho}_{b\beta}\ \phi^{*\,\sigma}_{b\beta} + \boldsymbol{\lambda_2}\phi^\rho_{a\alpha}\ \phi^\sigma_{b\alpha}\ \phi^{*\,\rho}_{a\beta}\ \phi^{*\,\sigma}_{b\beta} + \boldsymbol{\lambda_3}\phi^\rho_{a\alpha}\ \phi^\sigma_{b\alpha}\ \phi^{*\,\rho}_{b\beta}\ \phi^{*\,\sigma}_{a\beta} \\
& + \boldsymbol{\lambda_4}\phi^\rho_{a\alpha}\ \phi^\sigma_{a\beta}\ \phi^{*\,\rho}_{b\alpha}\ \phi^{*\,\sigma}_{b\beta} + \boldsymbol{\lambda_5}\phi^\rho_{a\alpha}\ \phi^\sigma_{a\beta}\ \phi^{*\,\rho}_{b\beta}\ \phi^{*\,\sigma}_{b\alpha} + \lambda_6\phi^\rho_{a\alpha}\ \phi^\sigma_{b\beta}\ \phi^{*\,\rho}_{a\alpha}\ \phi^{*\,\sigma}_{b\beta} + \boldsymbol{\lambda_7}\phi^\rho_{a\alpha}\ \phi^\sigma_{b\beta}\ \phi^{*\,\rho}_{a\beta}\ \phi^{*\,\sigma}_{b\alpha} \\
& + \boldsymbol{\lambda_8}\phi^\rho_{a\alpha}\ \phi^\sigma_{b\beta}\ \phi^{*\,\rho}_{b\alpha}\ \phi^{*\,\sigma}_{a\beta} + \boldsymbol{\lambda_9}\phi^\rho_{a\alpha}\ \phi^\sigma_{b\beta}\ \phi^{*\,\rho}_{b\beta}\ \phi^{*\,\sigma}_{a\alpha};
\end{aligned}$$

$$
\begin{aligned}
V_{\psi\phi} = \; & \zeta_1 \phi^{\;\rho}_{a\alpha}\; \phi^{*\,\rho}_{a\alpha} \psi_{b\beta}\psi_{b\beta} + \boldsymbol{\zeta_2} \phi^{\;\rho}_{a\alpha}\; \phi^{*\,\rho}_{b\alpha} \psi_{a\beta}\psi_{b\beta} + \boldsymbol{\zeta_3} \phi^{\;\rho}_{a\alpha}\; \phi^{*\,\rho}_{a\beta} \psi_{b\alpha}\psi_{b\beta} + \boldsymbol{\zeta_4} \phi^{\;\rho}_{a\alpha}\; \phi^{*\,\rho}_{b\beta} \psi_{a\alpha}\psi_{b\beta} + \boldsymbol{\zeta_5} \phi^{\;\rho}_{a\alpha}\; \phi^{*\,\rho}_{b\beta} \psi_{a\beta}\psi_{b\alpha} \\
& + \boldsymbol{\mu_\zeta}\;\; \epsilon_{abc}\epsilon_{\alpha\beta\gamma} \phi^{\;\rho}_{a\alpha}\; \phi^{*\,\rho}_{b\beta} \psi_{c\gamma}; \\
V_m = \; & \kappa_1\; \phi^{\;\rho}_{a\alpha}\; \phi^{*\,\rho}_{a\alpha} T^L_{bcd} T^L_{bcd} + \boldsymbol{\kappa_2}\; \phi^{\;\rho}_{a\alpha}\; \phi^{*\,\rho}_{b\alpha} T^L_{acd} T^L_{bcd} + \kappa_3\; \phi^{\;\rho}_{a\alpha}\; \phi^{*\,\rho}_{a\alpha} T^R_{\delta\beta\gamma} T^R_{\delta\beta\gamma} + \boldsymbol{\kappa_4}\; \phi^{\;\rho}_{a\alpha}\; \phi^{*\,\rho}_{b\alpha} T^R_{\alpha\gamma\delta} T^R_{\beta\gamma\delta} \\
& + \; \kappa_5\; \psi_{a\alpha}\psi_{a\alpha} T^L_{bcd} T^L_{bcd} + \boldsymbol{\kappa_6}\; \psi_{a\alpha}\psi_{b\alpha} T^L_{acd} T^L_{bcd} + \kappa_7\; \psi_{a\alpha}\psi_{a\alpha} T^R_{\delta\beta\gamma} T^R_{\delta\beta\gamma} + \boldsymbol{\kappa_8}\; \psi_{a\alpha}\psi_{a\beta} T^R_{\alpha\gamma\delta} T^R_{\beta\gamma\delta} \\
& + \; i\; \boldsymbol{\lambda_L} \epsilon_{\alpha\beta\gamma} \phi^{\;\rho}_{a\alpha}\; \phi^{*\,\rho}_{b\beta} \psi_{c\gamma} T^L_{abc} + \; i\; \boldsymbol{\lambda_R} \epsilon_{abc} \phi^{\;\rho}_{a\alpha}\; \phi^{*\,\rho}_{b\beta} \psi_{c\gamma} T^R_{\alpha\beta\gamma}.
\end{aligned}
$$

Here the non-trivial couplings are denoted in bold. a, b, c, d, e, f are $O(3)_L$ indices, $\alpha, \beta, \gamma, \delta, \mu, \nu$ are $O(3)_R$ indices and ρ, σ are $SU(2)_L$ indices.

4.3.1 The $O(3)_L \times O(3)_R$ flavor symmetry and the EW symmetry breaking

To break the $O(3)_L \times O(3)_R$ flavor symmetry we chose the vevs of the 7-plets as $\langle \chi^L_1 \rangle = v_L$ and $\langle \chi^R_1 \rangle = v_R$. This choice of vevs breaks the symmetry as follows:

$$
O(3)_L \times O(3)_R \to D_{3L} \times D_{3R}. \tag{4.12}
$$

We chose this symmetry breaking scale to be $v_L \sim v_R \sim 10$ TeV. Since $T^{L,R}$ and ψ fields are the SM singlets, so the SM gauge group can only be broken by the doublet field ϕ. We assume that the ϕ_{33} component of the doublet field acquires a vev, $\langle \phi_{33} \rangle = v_{\rm ew}$ which can be taken to be real. This vev $v_{\rm ew} = 174$ GeV breaks the SM symmetry group :

$$
SU(2)_L \times U(1)_Y \to U(1)_{\rm Q}. \tag{4.13}
$$

This vev structure corresponds to the following stationary equations :

$$
\begin{aligned}
& \kappa_1 v^2_{\rm ew} - 2\nu^2_L + 2\,(2\xi_1 + \xi_2)\, v^2_L + 2\xi_5 v^2_R = 0; \\
& \kappa_3 v^2_{\rm ew} + 2\xi_5 v^2_L - 2\nu^2_R + 2\,(2\xi_3 + \xi_4)\, v^2_R = 0; \\
& \lambda_\phi v^2_{\rm ew} - \mu^2 + \kappa_1 v^2_L + \kappa_3 v^2_R = 0.
\end{aligned} \tag{4.14}
$$

with $\lambda_\phi = \sum_{i=1}^{9} \lambda_i$. These equation set has the solution:

$$
\begin{aligned}
\nu^2_L &= \frac{1}{2}\kappa_1 v^2_{\rm ew} + (2\xi_1 + \xi_2)\, v^2_L + \xi_5 v^2_R, \\
\nu^2_R &= \frac{1}{2}\kappa_3 v^2_{\rm ew} + \xi_5 v^2_L + (2\xi_3 + \xi_4)\, v^2_R, \\
\mu^2 &= \lambda_\phi v^2_{\rm ew} + \kappa_1 v^2_L + \kappa_3 v^2_R.
\end{aligned} \tag{4.15}
$$

Using the solution set of the stationary equations, we examine the mass spectrum of the scalars. We write the doublet fields as:

$$
\phi_{ij} = \begin{pmatrix} \phi^+_{ij} \\ \frac{H^0_{ij} + i\, A^0_{ij}}{\sqrt{2}} \end{pmatrix}. \tag{4.16}
$$

Due to the aforementioned symmetry breaking the fields χ_1^L, χ_1^R and H_{33}^0 mix with each other and the mass matrix in the basis $\left\{\chi_1^L, \chi_1^R, H_{33}^0\right\}$ is given by:

$$\mathcal{M}_{s1} = \begin{pmatrix} 4v_L^2\left(2\xi_1+\xi_2\right) & 4v_L v_R \xi_5 & 2v_{\rm ew} v_L \kappa_1 \\ 4v_L v_R \xi_5 & 4v_R^2\left(2\xi_3+\xi_4\right) & 2v_{\rm ew} v_R \kappa_3 \\ 2v_{\rm ew} v_L \kappa_1 & 2v_{\rm ew} v_R \kappa_3 & 2v_{\rm ew}^2 \lambda_\phi \end{pmatrix}. \tag{4.17}$$

The mixing between the $\chi_1^{L,R}$ and H_{33}^0 fields is of the order of $\sim v_{ew}/v_{L,R} \sim 174\text{GeV}/10^4\text{GeV} \sim 10^{-2}$ which is pretty small. Then only term that mixes χ_1^L and χ_1^R fields is the trivial coupling ξ_5.

The fields $\chi_2^{L,R}$ remain massless and are the Goldstone bosons. The components $\chi_{5,6,7}^{L,R}$ do not mix with other fields and acquire masses given by:

$$\begin{aligned} m^2_{\chi^L_{5,6}} =& \frac{8}{15}\kappa_2 v_{\rm ew}^2 - \frac{4}{5}\xi_2 v_L^2; \\ m^2_{\chi^L_7} =& \frac{3}{5}\left(\kappa_2 v_{\rm ew}^2 - 2\xi_2 v_L^2\right). \\ m^2_{\chi^R_{5,6}} =& \frac{8}{15}\kappa_4 v_{\rm ew}^2 - \frac{4}{5}\xi_4 v_R^2; \\ m^2_{\chi^R_7} =& \frac{3}{5}\left(\kappa_4 v_{\rm ew}^2 - 2\xi_4 v_R^2\right). \end{aligned} \tag{4.18}$$

$\chi_{5,6}^{L,R}$ are degenerate in mass as they form a doublet (2) under the symmetry $D_{3L,R}$ and $\chi_7^{L,R}$ is an odd singlet ($1'$) under $D_{3L,R}$.

In addition, χ_3^L mix with H_{13}^0. The mass matrix for the fields χ_3^L and H_{13}^0 in the basis $\left\{\chi_3^L, H_{13}^0\right\}$ is given by:

$$\mathcal{M}_{s2} \begin{pmatrix} \frac{1}{3}v_{\rm ew}^2\kappa_2 & \frac{v_{\rm ew}v_L\kappa_2}{\sqrt{6}} \\ \frac{v_{\rm ew}v_L\kappa_2}{\sqrt{6}} & \frac{1}{2}v_L^2\kappa_2 \end{pmatrix} \tag{4.19}$$

which has a Goldstone state. One can Diagonalize the mass matrix by the similarity transformation $O^T M O$, where the orthogonal matrix can be written as

$$O = \begin{pmatrix} \cos\theta_L & -\sin\theta_L \\ \sin\theta_L & \cos\theta_L \end{pmatrix}, \text{ with } \theta_L = \frac{1}{2}\tan^{-1}\left(\frac{2v_{\rm ew}v_L/\sqrt{6}}{v_{\rm ew}^2/3 - v_L^2/2}\right). \tag{4.20}$$

Then the Goldstone state is given by $\chi_3^{'L} = \cos\theta_L\, \chi_3^L - \sin\theta_L\, H_{13}^0$ and the orthogonal state is given by $H_{13}^{'0} = \sin\theta_L\, \chi_3^L + \cos\theta_L\, H_{13}^0$ which has the mass, $m^2_{H^{'0}_{13}} = \frac{1}{6}\kappa_2\left(2v_{\rm ew}^2 + 3v_L^2\right)$. The mixing is small since $\theta_L \sim O(\tan^{-1}[v_{ew}/v_L]) \sim 10^{-2}$ and the Goldstone is mostly composed of χ_3^L.

Similarly, the fields χ_4^L and H_{23}^0 gets mixed and the mass matrix is similar to the one given in Eq. (4.19) except the off-diagonal terms have an additional negative sign. So the states $H_{13}^{'0}, H_{23}^{'0}$ form a doublet under D_{3L} group (more specifically $(2,1)$ representation under $D_{3L}\times D_{3R}$). For χ^R one needs to make the replacements $v_L \to v_R$ and $\kappa_2 \to \kappa_4$. So the Goldstone bosons due to the

$O(3)_L$ symmetry breaking are χ_2^L and $\chi_{3,4}^{'L}$ and due to the $O(3)_R$ symmetry breaking the Goldstone states are χ_2^R and $\chi_{3,4}^{'R}$ where:

$$\begin{aligned}
\chi_3^{'L} &= \cos\theta_L\, \chi_3^L - \sin\theta_L\, H_{13}^0; \\
\chi_4^{'L} &= \cos\theta_L\, \chi_4^L - \sin\theta_L\, H_{23}^0; \\
\chi_3^{'R} &= \cos\theta_R\, \chi_3^R - \sin\theta_R\, H_{31}^0; \\
\chi_4^{'R} &= \cos\theta_R\, \chi_4^R - \sin\theta_R\, H_{32}^0;
\end{aligned} \tag{4.21}$$

with

$$\begin{aligned}
\theta_L &= \frac{1}{2}\tan^{-1}\left(\frac{2v_{\rm ew}v_L/\sqrt{6}}{v_{\rm ew}^2/3 - v_L^2/2}\right); \\
\theta_R &= \frac{1}{2}\tan^{-1}\left(\frac{2v_{\rm ew}v_R/\sqrt{6}}{v_{\rm ew}^2/3 - v_R^2/2}\right).
\end{aligned}$$

The field ψ_{11} mixes with H_{22}^0 and the mass matrix in the basis $\left\{\psi_{11}, H_{22}^0\right\}$ is given by:

$$\mathcal{M}_{s3} = \begin{pmatrix} \zeta_1 v_{\rm ew}^2 - 2\mu_\psi^2 + v_L^2\,(2\kappa_5+\kappa_6) + v_R^2\,(2\kappa_7+\kappa_8) & v_{\rm ew}\mu_\zeta \\ v_{\rm ew}\mu_\zeta & \frac{1}{2}\left(-2\,(\lambda_\phi - \lambda_1 - \lambda_6)\, v_{\rm ew}^2 + v_L^2\kappa_2 + v_R^2\kappa_4\right) \end{pmatrix}. \tag{4.22}$$

Naturally the off-diagonal term is much smaller than the diagonal terms. In addition, assuming the coupling μ_ζ small, one can treat the states ψ_{11} and H_{22}^0 to be almost purely mass eigenstate. The mass matrix for the fields ψ_{12} and H_{21}^0, ψ_{21} and H_{12}^0 and ψ_{22} and H_{11}^0 are also given by Eq. (4.22). The reason for such degeneracy becomes obvious when one realizes that with the vevs v_L, v_R the decomposition of bi-fundamental of $O(3)_L \times O(3)_R$ in the $D_{3L} \times D_{3R}$ is given by:

$$(3,3) \to (2,2) + (1,2) + (2,1) + (1',1') \tag{4.23}$$

As the electroweak breaking is triggered by the vev of ϕ_{33} which is an odd singlet $(1')$ of $D_{3L} \times D_{3R}$, it does not break the $D_{3L} \times D_{3R}$ symmetry.

The $\psi_{13,23}$ components of the bi-fundamental field ψ form a doublet under D_{3L} whereas $\psi_{31,32}$ is a doublet under D_{3R} while ψ_{33} is the odd singlet. The masses of these $(2,1)$, $(1,2)$ and $(1',1')$ multiplets of $D_{3L} \times D_{3R}$ are,

$$\begin{aligned}
m_{\psi_{13,23}}^2 &= (\zeta_1+\zeta_3)\, v_{\rm ew}^2 - 2\mu_\psi^2 + (2\kappa_5+\kappa_6)\, v_L^2 + 2\kappa_7 v_R^2, \\
m_{\psi_{31,32}}^2 &= (\zeta_1+\zeta_2)\, v_{\rm ew}^2 - 2\mu_\psi^2 + 2\kappa_5 v_L^2 + (2\kappa_7+\kappa_8)\, v_R^2, \\
m_{\psi_{33}}^2 &= \zeta_\psi v_{\rm ew}^2 + 2\left(-\mu_\psi^2 + \kappa_5 v_L^2 + \kappa_7 v_R^2\right),
\end{aligned} \tag{4.24}$$

with $\zeta_\psi = \zeta_1 + \zeta_2 + \zeta_3 + \zeta_4 + \zeta_5$.

The imaginary parts of the doublets A_{ij}'s do not mix with the ψ fields. $A^0_{11,12,21,22}$, $A^0_{13,23}$, and $A^0_{31,32}$ belong to the representations $(2,2)$, $(2,1)$ and $(1,2)$ of $D_{3L} \times D_{3R}$ respectively. The charged scalars $\phi^{\pm}_{ij}$ form similar multiplets whereas, Goldstones A^0_{33} and $\phi^{\pm}_{33}$ are eaten-up by the SM gauge bosons. The masses of these multiplets are given below :

$$\begin{aligned} m^2_{A^0_{11,12,21,22}} &= \frac{1}{2}\left(-2\left(\lambda_\phi + \lambda_1 - \lambda_6\right) v^2_{\rm ew} + \kappa_2 v^2_L + \kappa_4 v^2_R\right), \\ m^2_{A^0_{13,23}} &= \frac{1}{2}\kappa_2 v^2_L - 2\left(\lambda_1 + \lambda_4 + \lambda_5\right) v^2_{\rm ew}, \\ m^2_{A^0_{31,32}} &= \frac{1}{2}\kappa_4 v^2_R - 2\left(\lambda_1 + \lambda_2 + \lambda_3\right) v^2_{\rm ew}, \end{aligned} \tag{4.25}$$

and,

$$\begin{aligned} m^2_{\phi^{\pm}_{11,12,21,22}} &= \frac{1}{2}\left(-2\left(\lambda_\phi - \lambda_6\right) v^2_{\rm ew} + \kappa_2 v^2_L + \kappa_4 v^2_R\right), \\ m^2_{\phi^{\pm}_{13,23}} &= \frac{1}{2}\kappa_2 v^2_L - \left(\lambda_\phi - \lambda_2 - \lambda_6 - \lambda_7\right) v^2_{\rm ew}, \\ m^2_{\phi^{\pm}_{31,32}} &= \frac{1}{2}\kappa_4 v^2_R - \left(\lambda_\phi - \lambda_4 - \lambda_6 - \lambda_8\right) v^2_{\rm ew}. \end{aligned} \tag{4.26}$$

4.3.2 The $D_{3L} \times D_{3R}$ flavor symmetry breaking

In the previous sub-section, the mass spectrum of the scalars were analyzed in details in the $D_{3L} \times D_{3R}$ symmetric case. From the expressions of the masses one sees that with couplings being $\sim O(1)$, all the scalar fields (except H^0_{33} which is the SM doublet) tend to have masses $\sim O(v_{L,R}) \sim 10$ TeV. But for phenomenological interest, by appropriately fixing the quartic couplings we will keep the masses of the bi-fundamentals ($\psi_{a\alpha}$, $\phi_{a\alpha}$) at the sub-TeV range ($\sim 0.5 - 1$ TeV). From the expressions of the masses it is clear that, to have the scalars $\phi_{a\alpha}$ at the sub-TeV range, one needs to have $v_L \kappa_2^{1/2}, v_R \kappa_4^{1/2} \sim O(0.5 - 1\text{TeV})$. For similar reason, the couplings $\kappa_{5,6,7,8}$ needs to be fixed in Eq. (4.24) for the bi-fundamental field $\psi_{a\alpha}$.

$D_{3L} \times D_{3R}$ is a good flavor symmetry and only needs to be broken at some lower scale ($\sim$ several GeV) for flavor considerations. So one can work in the decoupling limit, where the heavy 7-plet fields, $\chi_i^{L,R}$ can be integrated out. Then at the lower scale, one can only concentrate on the effective potential of the bi-fundamentals. In Fig. 4.1 it is shown that the quartic couplings for the ψ field get modified due to the presence of such feynman diagrams.

To take into account such modification, the relevant terms of the original potential is of the form,

$$V \supset \lambda v \chi_i \psi\psi + \chi_i^2 m^2_{\chi_i}. \tag{4.27}$$

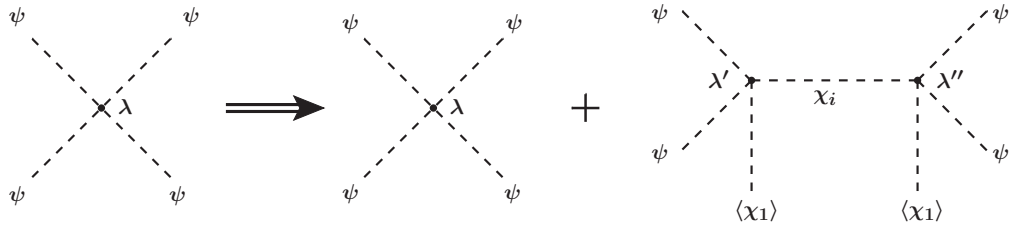

Figure 4.1: Feynman diagram for effective quartic coupling

By taking the derivative with respect to the heavy fields, one can solve for these fields as,

$$\frac{\partial V}{\partial \chi_i} = 0, \tag{4.28}$$

$$\chi_i = -\frac{\lambda v}{2m_{\chi_i}^2}\psi\psi. \tag{4.29}$$

Then the original quartic couplings for the bi-fundamental field get modified as,

$$V_{eff} \supset \left(\lambda - c\lambda'\lambda'' \frac{\langle\chi\rangle^2}{m_{\chi_i}^2}\right)\psi^4. \tag{4.30}$$

where c is some constant. Similarly one needs to update the quatric couplings of terms involving $\psi^2|\phi|^2$ and also $|\phi|^4$. $\chi_{1,5,6}$ fields are integrated out as they become massive and for χ_7 field, no term like $\lambda v\chi_i\psi\psi$ exist in the original potential. Also recall that the fields χ_2 and $\chi'_{3,4}$ are the Goldstone bosons. For any calculations from now on, we will be dealing with the effective potential involving fields ψ and ϕ and show the explicit form of these effective couplings in terms of the original couplings. And also the primes ($'$) on the fields $H'^0_{13,23,31,32}$ will be suppressed.

Now to break the $D_{3L} \times D_{3R}$ flavor symmetry, some components of the ψ field needs to acquire vevs. From the analysis above, ψ field decomposes as $(2,2)+(1,2)+(2,1)+(1',1')$ under $D_{3L} \times D_{3R}$ group. We assume a vev structure ($v_{a\alpha}$) for $\psi_{a\alpha}$ where $(2,2)$ vev is diagonal and the rest of the multiplets get all non-zero vevs. Such a vev structure will break the $D_{3L} \times D_{3R}$ symmetry and the mass degeneracies will be broken as well.

The consequence of this symmetry breaking is that all the neutral components of $\psi_{a\alpha}$ and $\phi_{a\alpha}$ will mix with each other. In this second stage of symmetry breaking, we assume none of the components of ϕ gets any explicit vev (recalling that ϕ_{33} vev already broke the EW symmetry). The other components of ϕ also get induced vevs through ϕ_{33} and ψ vevs and generate all the fermion masses and mixings. The off-diagonal vevs $v_{a\alpha}$ must be small like $\sim$ 10 GeV to avoid FCNC. Since the diagonal vevs do not induce mixings among all the components of $\phi_{a\alpha}$, these vevs can be $\sim$ 100 GeV (diagonal ψ vevs introduce mixings among $\{\phi_{11}, \phi_{22}, \phi_{33}\}$; between $\{\phi_{12}, \phi_{21}\}$; between $\{\phi_{13}, \phi_{31}\}$; between $\{\phi_{23}, \phi_{32}\}$). The phenomenologically relevant mixings among different scalar fields due to

such breaking pattern will be discussed in the next section in details. Also the induced vevs of ϕ will be analysed in the next subsection where we discuss the fermion mass generation.

4.3.3 The Yukawa Lagrangian

The SM fermions belong to the $Q(3,1)+L(3,1)+u^c(1,3)+d^c(1,3)+e^c(1,3)$ representations under the $O(3)_L \times O(3)_R$ group. In our model, the only Higgs field that is responsible for generating the fermions masses and mixings is $\phi(3,3)$ which is a SM doublet with $Y = 1/2$. Fermion masses arise from the Yukawa Lagrangian

$$\mathcal{L}_y = y_u Q_a u^c_\alpha \phi_{a\alpha} + y_d Q_a d^c_\alpha \phi^*_{a\alpha} + y_l L_a e^c_\alpha \phi^*_{a\alpha} + h.c. \tag{4.31}$$

where $y_{u,d,l}$ are the single unified Yukawa couplings in each sector. And the fermion mass matrices are then given by

$$M^u_{a\alpha} = y_u \langle \phi_{a\alpha} \rangle,\ M^d_{a\alpha} = y_d \langle \phi^*_{a\alpha} \rangle,\ M^l_{a\alpha} = y_l \langle \phi^*_{a\alpha} \rangle. \tag{4.32}$$

Since the EW symmetry is broken by the 33 component of ϕ, $y_u \sim m_t/v_{\rm ew}$, $y_d \sim m_b/v_{\rm ew}$ and $y_l \sim m_\tau/v_{\rm ew}$ where $y_u \sim O(1)$ and $y_{d,l} \ll y_u$. As explained above, the $D_{3L} \times D_{3R}$ breaking vevs of ψ will induce ϕ VEVS that are responsible for fermion mass and mixing generations. In general scalars with O(1) Yukawa couplings with the up-quarks must have mass $\gtrsim O(100)$ TeV due to flavor constraints. However, such constraints are not valid in this model due to the presence of the approximate $D_{3L} \times D_{3R}$ flavor symmetry and these scalars can be relatively light. In this model we assume the masses of $\phi_{a\alpha} \sim O(0.5-1)$ TeV for phenomenological requirements.

We write down the expressions of the induced vevs of the ϕ field due to the $D_{3L} \times D_{3R}$ symmetry breaking. After this symmetry breaking the masses of the scalars $H^0_{a\alpha}$ and the pseudoscalars $A^0_{a\alpha}$ will get modified. These corrections will be proportional to the D_3 breaking vevs and we denote them as $\delta m^2_{H^0_{a\alpha}}$ and $\delta m^2_{A^0_{a\alpha}}$ respectively. In the following expressions we only keep the leading order terms for simplicity.

$$\begin{aligned}
\langle \phi_{11} \rangle =& \frac{\zeta_4 v_{11} v_{33} v_{\rm ew}}{m^2_{H^0_{11}} + \delta m^2_{H^0_{11}}} + \frac{\frac{i}{2}\left(v^2_{11} - v^2_{22}\right) v_{\rm ew} \left(\frac{\kappa_6 v_{32} \lambda_L}{3\xi_2 v_L} + \frac{\kappa_8 v_{23} \lambda_R}{3\xi_4 v_R}\right)}{m^2_{A^0_{11}} + \delta m^2_{A^0_{11}}} \\
\langle \phi_{12} \rangle =& \frac{\zeta_5 v_{13} v_{32} v_{\rm ew}}{m^2_{H^0_{12}} + \delta m^2_{H^0_{12}}} + \frac{\frac{i\kappa_6 \left(v^2_{22} - v^2_{11}\right) v_{31} v_{\rm ew} \lambda_L}{6\xi_2 v_L}}{m^2_{A^0_{12}} + \delta m^2_{A^0_{12}}} \\
\langle \phi_{13} \rangle =& \frac{\frac{c_1 \cos\theta_L + c_2 \sin\theta_L}{24\xi_2(2\xi_1+\xi_2) v^4_L}}{m^2_{H^0_{13}} + \delta m^2_{H^0_{13}}} + \frac{-\frac{i\kappa_8 v_{22} v_{31} v_{32} v_{\rm ew} \lambda_R}{3\xi_4 v_R}}{m^2_{A^0_{13}} + \delta m^2_{A^0_{13}}}
\end{aligned}$$

$$
\begin{aligned}
\langle\phi_{21}\rangle =& \frac{\zeta_5 v_{23} v_{31} v_{\rm ew}}{m^2_{H^0_{21}} + \delta m^2_{H^0_{21}}} + \frac{-\frac{1}{6} i v_{13} v_{\rm ew} \left(\frac{2\kappa_6 v_{23} v_{32} \lambda_L}{\xi_2 v_L} + \frac{\kappa_8 \left(v_{11}^2 - v_{22}^2\right) \lambda_R}{\xi_4 v_R} \right)}{m^2_{A^0_{21}} + \delta m^2_{A^0_{21}}} \\
\langle\phi_{22}\rangle =& \frac{\zeta_4 v_{22} v_{33} v_{\rm ew}}{m^2_{H^0_{22}} + \delta m^2_{H^0_{22}}} + \frac{\frac{1}{3} i v_{13} v_{31} v_{\rm ew} \left(\frac{\kappa_6 v_{23} \lambda_L}{\xi_2 v_L} + \frac{\kappa_8 v_{32} \lambda_R}{\xi_4 v_R} \right)}{m^2_{A^0_{22}} + \delta m^2_{A^0_{22}}} \\
\langle\phi_{23}\rangle =& \frac{\frac{c_3 \cos\theta_L + c_4 \sin\theta_L}{24\xi_2 (2\xi_1 + \xi_2) v_L^3}}{m^2_{H^0_{23}} + \delta m^2_{H^0_{23}}} + \frac{\frac{i\kappa_8 v_{11} \left(v_{22}^2 - v_{11}^2\right) v_{\rm ew} \lambda_R}{6\xi_4 v_R}}{m^2_{A^0_{23}} + \delta m^2_{A^0_{23}}} \\
\langle\phi_{31}\rangle =& \frac{\frac{c_5 \cos\theta_R + c_6 \sin\theta_R}{24\xi_4 (2\xi_3 + \xi_4) v_R^4}}{m^2_{H^0_{31}} + \delta m^2_{H^0_{31}}} + \frac{-\frac{i\kappa_6 v_{13} v_{22} v_{23} v_{\rm ew} \lambda_L}{3\xi_2 v_L}}{m^2_{A^0_{31}} + \delta m^2_{A^0_{31}}} \\
\langle\phi_{32}\rangle =& \frac{\frac{c_7 \cos\theta_R + c_8 \sin\theta_R}{24\xi_4 (2\xi_3 + \xi_4) v_R^4}}{m^2_{H^0_{32}} + \delta m^2_{H^0_{32}}} + \frac{\frac{i\kappa_6 v_{11} \left(-v_{11}^2 + v_{22}^2\right) v_{\rm ew} \lambda_L}{6\xi_2 v_L}}{m^2_{A^0_{32}} + \delta m^2_{A^0_{32}}}
\end{aligned}
\tag{4.33}
$$

with the dimensionful quantities c_i's are given by:

$$
\begin{aligned}
c_1 =& 24\xi_2 \left(2\xi_1 + \xi_2\right) v_L^4 v_{\rm ew} \left(\zeta_2 v_{11} v_{31} + \left(\zeta_2 + \zeta_4 + \zeta_5\right) v_{13} v_{33}\right) \\
c_2 =& -24\sqrt{\frac{2}{3}} \xi_2 \kappa_6 \left(2\xi_1 + \xi_2\right) v_L^5 \left(v_{11} v_{31} + v_{13} v_{33}\right) \\
c_3 =& 24\xi_2 \left(2\xi_1 + \xi_2\right) v_L^3 v_{\rm ew} \left(\zeta_2 v_{22} v_{32} + \left(\zeta_2 + \zeta_4 + \zeta_5\right) v_{23} v_{33}\right) \\
c_4 =& -8\sqrt{6} \xi_2 \kappa_6 \left(2\xi_1 + \xi_2\right) v_L^4 \left(v_{22} v_{32} + v_{23} v_{33}\right) \\
c_5 =& 24\xi_4 \left(2\xi_3 + \xi_4\right) v_{\rm ew} v_R^4 \left(\zeta_3 v_{11} v_{13} + \left(\zeta_3 + \zeta_4 + \zeta_5\right) v_{31} v_{33}\right) \\
c_6 =& -8\sqrt{6} \kappa_8 \xi_4 \left(2\xi_3 + \xi_4\right) \left(v_{11} v_{13} + v_{31} v_{33}\right) v_R^5 \\
c_7 =& 24\xi_4 \left(2\xi_3 + \xi_4\right) v_{\rm ew} v_R^4 \left(\zeta_3 v_{22} v_{23} + \left(\zeta_3 + \zeta_4 + \zeta_5\right) v_{32} v_{33}\right) \\
c_8 =& -8\sqrt{6} \kappa_8 \xi_4 \left(2\xi_3 + \xi_4\right) \left(v_{22} v_{23} + v_{32} v_{33}\right) v_R^5
\end{aligned}
\tag{4.34}
$$

One also needs to notice that the masses of the quarks (for example strange quark) will receive finite correction from the relations given in the Eq. (4.31). The correction to the mass comes from the diagram given by Fig. 4.2.

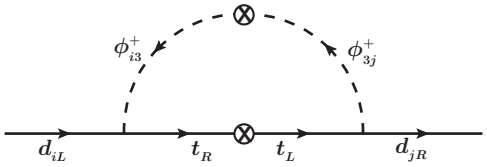

Figure 4.2: Feynman diagram for the correction of strange and bottom quark masses

4.4 Explaining the 750 GeV di-photon signal

As in the model the field ψ_{11} gets mixed with ϕ_{11}, and we identify this admixture as the 750 GeV scalar, $\boldsymbol{S} = \cos\theta\ \psi_{11} + \sin\theta\ \phi_{11}$. So ψ_{11} can be produced through ϕ_{11} field. The corresponding Feynman diagram is shown in Fig. 4.3.

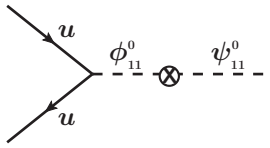

Figure 4.3: Production of 750 GeV scalar.

As mentioned earlier, the $D_{3L} \times D_{3R}$ symmetry needs to be broken at the few GeV range due to flavor constraints. One can break $D_3 \times D_3$ symmetry by a certain vev structure of the bi-fundamental field, ψ. The EW symmetry is broken by the $\langle\phi_{33}\rangle = v_{ew}$ that we have taken to be real. This is the only component of the doublet field that gets explicit vev. But to generate the fermion masses and mixing, the other components of ϕ needs to get vev too. These components can in principle get induced vevs due to breaking of $D_3 \times D_3$ symmetry by the ψ field. For such purpose, we assume a general vev structure $\langle\psi_{ij}\rangle \neq 0$ for all i, j. The off-diagonal vevs must be small due to flavor constraints ~ 10 GeV, but the diagonal vevs can be ~ 100 GeV. After the symmetry breaking all the neutral scalar fields in ψ and ϕ will mix with each other. We assume that ψ_{11} and ϕ_{11} mix well and the mixings of these fields with rest of the neutral scalars are relatively small. Then the part of the potential that contain this mixing is

$$\begin{bmatrix}\psi_{11} & \phi_{11}\end{bmatrix}\begin{bmatrix}a_1 & a_3\\ a_3^* & a_2\end{bmatrix}\begin{bmatrix}\psi_{11}\\ \phi_{11}^*\end{bmatrix}, \tag{4.35}$$

From the potential one sees that, ψ_{11} can decay into two photon since it has coupling to the charged fields $\phi^{\pm}_{ij}$. This mixing arises from the term of the form:

$$\begin{aligned}\lambda Tr[\psi^2]Tr[\phi^\dagger\phi] &\to \lambda\langle\psi_{11}\rangle\psi_{11}Tr[\phi^*\phi] \\ &\supset \langle\psi_{11}\rangle\psi_{11}(\lambda_{13}\phi^+_{13}\phi^-_{13} + \lambda_{23}\phi^+_{23}\phi^-_{23} + \lambda_{31}\phi^+_{31}\phi^-_{31} + \lambda_{32}\phi^+_{32}\phi^-_{32}).\end{aligned} \tag{4.36}$$

Such decay of 750 GeV scalar to di-photon is shown in Fig. 4.4. These charged scalars can be light ~ 400 GeV. It is clear that more terms can in principle contribute to this process, such as $\phi^+_{ii}\phi^-_{ii}$. But these scalars will be directly produced at LHC and their masses can not be too light and needs to be $\gtrsim 1$ TeV from phenomenological constraints. The effective couplings in Eq. (4.36) in terms of the original couplings are given by:

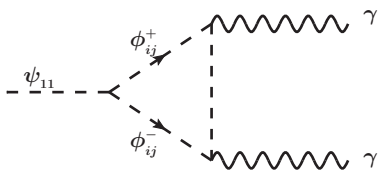

Figure 4.4: Decay of ψ_{11} field to di-photon.

$$\begin{aligned}
\lambda_{13} &= 2\zeta_1 + 2\zeta_2 - \frac{8\kappa_1\kappa_5 v_1^2}{m^2_{\chi_1^L}} - \frac{4\kappa_2\kappa_5 v_1^2}{m^2_{\chi_1^L}} - \frac{4\kappa_1\kappa_6 v_1^2}{m^2_{\chi_1^L}} - \frac{2\kappa_2\kappa_6 v_1^2}{m^2_{\chi_1^L}} - \frac{2\kappa_2\kappa_6 v_1^2}{15m^2_{\chi_5^L}} - \frac{8\kappa_3\kappa_7 q_1^2}{m^2_{\chi_1^R}} - \frac{4\kappa_3\kappa_8 q_1^2}{m^2_{\chi_1^R}}, \\
\lambda_{23} &= 2\zeta_1 - \frac{8\kappa_1\kappa_5 v_1^2}{m^2_{\chi_1^L}} - \frac{4\kappa_2\kappa_5 v_1^2}{m^2_{\chi_1^L}} - \frac{4\kappa_1\kappa_6 v_1^2}{m^2_{\chi_1^L}} - \frac{2\kappa_2\kappa_6 v_1^2}{m^2_{\chi_1^L}} + \frac{2\kappa_2\kappa_6 v_1^2}{15m^2_{\chi_5^L}} - \frac{8\kappa_3\kappa_7 q_1^2}{m^2_{\chi_1^R}} - \frac{4\kappa_3\kappa_8 q_1^2}{m^2_{\chi_1^R}}, \\
\lambda_{31} &= 2\zeta_1 + 2\zeta_3 - \frac{8\kappa_1\kappa_5 v_1^2}{m^2_{\chi_1^L}} - \frac{4\kappa_1\kappa_6 v_1^2}{m^2_{\chi_1^L}} - \frac{8\kappa_3\kappa_7 q_1^2}{m^2_{\chi_1^R}} - \frac{12\kappa_4\kappa_7 q_1^2}{m^2_{\chi_1^R}} - \frac{4\kappa_3\kappa_8 q_1^2}{m^2_{\chi_1^R}} - \frac{6\kappa_4\kappa_8 q_1^2}{m^2_{\chi_1^R}} - \frac{2\kappa_4\kappa_8 q_1^2}{5m^2_{\chi_5^R}}, \\
\lambda_{32} &= 2\zeta_1 - \frac{8\kappa_1\kappa_5 v_1^2}{m^2_{\chi_1^L}} - \frac{4\kappa_1\kappa_6 v_1^2}{m^2_{\chi_1^L}} - \frac{8\kappa_3\kappa_7 q_1^2}{m^2_{\chi_1^R}} - \frac{4\kappa_3\kappa_8 q_1^2}{m^2_{\chi_1^R}}.
\end{aligned} \tag{4.37}$$

We estimate the production cross section of $\boldsymbol{S}$ at the 13 TeV LHC as [6]:

$$\sigma(pp \to \boldsymbol{S}) \sim 125 K y^2 \text{ pb}, \tag{4.38}$$

and the decay width to be

$$\Gamma(\boldsymbol{S} \to u\overline{u}) \sim 45 y^2 \text{ GeV}. \tag{4.39}$$

We take $K = 2$ and $y = 1/3$ for numerical computations. For such a case the production cross section is about 20pb while the decay width turns out to be 5 GeV. For such a scenario the branching ratio for two photon decay should be about 10^{-4} so that $\sigma \times \text{Br} = 2 \sim 3$fb. Naive estimation without any enhancement for the diphoton channel is about $\left(\frac{\alpha}{4\pi}\right) \equiv 10^{-6}$. An enhancement of few hundreds can come from the fact that in the term given by Eq. (4.36) the vev of ψ_{11} can be of the order of 100 GeV as the diagonal vev does not induce mixing between ϕ_{ij}'s which in turn could have caused FCNC.

Again for the decay channel, from the diagram in Fig. 4.4, one realizes that the presence of multiple charged scalar particles introduces another factor of enhancement. As there are nine charged scalars in the bi-fundamental ϕ, an enhancement of $(9 \times 3)^2 \approx 10^3$ can be there, if the effective quartic is about 3. One also needs to consider the masses of the charged scalars. The off-diagonal charged scalars can be as light as $400 \sim 500$ GeV while if we consider the diagonal charged scalar, they needs to at the TeV range. We analyzed both the case when the four off-diagonal charged

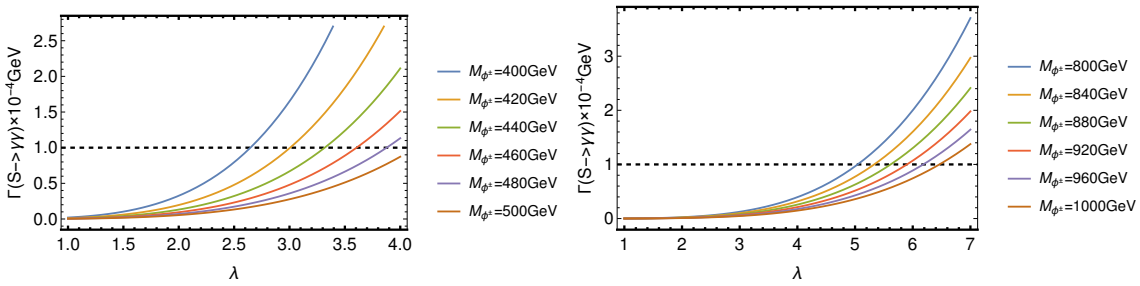

Figure 4.5: Decay width for the process $\boldsymbol{S} \to \gamma\gamma$ for the cases (i) when four charged scalars contribute in Eq. (4.36) (left) and (ii) when all the charged scalars contribute (right). The vev of ψ_{11} is fixed to 100 GeV.

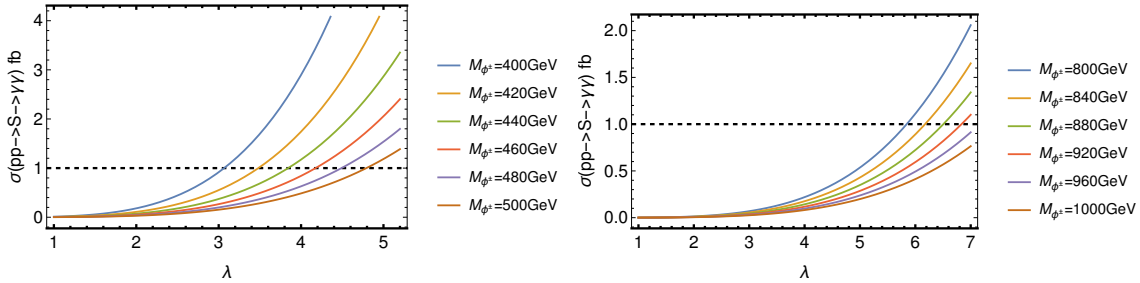

Figure 4.6: Production cross section $\times$ the branching ratio for the cases (i) when four charged scalars contribute in Eq. (4.36) (left) and (ii) when all the charged scalars contribute (right). The vev of ψ_{11} is fixed to 100 GeV.

scalars are light and all the charged scalar are at the TeV scale (see Fig. 4.5, Fig. 4.6). From the plots one realizes that if the four off-diagonal charged scalars are as light as 400 GeV, then with effective quartic coupling of ~ 3 one can get the production crosssection $\times$ Branching ratio ≈ 3fb.

4.5 Model with the fundamentals

The scalar sector of this version of the model contains $T^L_{abc}, T^R_{\alpha\beta\gamma}, \psi^L_a, \psi^R_\alpha$ and $\phi^\rho_{a\alpha}$. The complete Lagrangian with these scalar multiplets can be written as:

$$V = V_\psi + V_\chi + V_\phi + V_{\psi\phi} + V_m. \tag{4.40}$$

where

$$
\begin{aligned}
V_\psi =& -\mu_{_L}^2\ \psi_i^L\psi_i^L + \xi_1(\psi_i^L\psi_i^L)^2 - \mu_{_R}^2\ \psi_\alpha^R\psi_\alpha^R + \zeta_1(\psi_\alpha^R\psi_\alpha^R)^2 + \eta_1(\psi_\alpha^R\psi_\alpha^R)(\psi_i^L\psi_i^L)\\
V_\chi =& -\nu_{_L}^2\ T^L_{ijk}\ T^L_{_{ijk}} + \xi_2\ (T^L_{_{ijk}}\ T^L_{_{ijk}})^2 + \boldsymbol{\xi_3}\ T^L_{_{ijk}}\ T^L_{jkl}\ T^L_{lmn}\ T^L_{mni}\\
&-\nu_{_R}^2\ T^R_{\alpha\beta\gamma}\ T^R_{\alpha\beta\gamma} + \zeta_2\ (T^R_{\alpha\beta\gamma}\ T^R_{\alpha\beta\gamma})^2 + \boldsymbol{\zeta_3}\ T^R_{\alpha\beta\gamma}\ T^R_{\beta\gamma\delta}\ T^R_{\delta\mu\nu}\ T^R_{_{\mu\nu\alpha}} + \eta_2\ T^L_{ijk}\ T^L_{ijk}\ T^R_{\alpha\beta\gamma}\ T^R_{\alpha\beta\gamma}\\
V_{\psi\chi} =&\ \xi_4\ \psi_i^L\psi_i^L\ T^L_{lmn}\ T^L_{lmn} + \boldsymbol{\xi_5}\ \psi_i^L\psi_j^L\ T^L_{imn}\ T^L_{jmn} + \boldsymbol{\xi_6}\ \psi_i^L\psi_j^L\psi_k^L\ T^L_{ijk} + \boldsymbol{\xi_7}\ \psi_i^L\ T^L_{ijk}T^L_{jmn}T^L_{kmn}\\
&+\zeta_4\ \psi_\alpha^R\psi_\alpha^R\ T^R_{\beta\mu\nu}\ T^R_{\beta\mu\nu} + \boldsymbol{\zeta_5}\ \psi_\alpha^R\psi_\beta^R\ T^R_{\alpha\mu\nu}\ T^R_{\beta\mu\nu} + \boldsymbol{\zeta_6}\ \psi_\alpha^R\psi_\beta^R\psi_\gamma^R\ T^R_{\alpha\beta\gamma} + \boldsymbol{\zeta_7}\ \psi_\alpha^R\ T^R_{\alpha\beta\gamma}\ T^R_{\beta\mu\nu}\ T^R_{\gamma\mu\nu}\\
&+\eta_3\ \psi_\alpha^R\psi_\alpha^R\ T^L_{ijk}\ T^L_{_{ijk}} + \eta_4\ \psi_i^L\psi_i^L\ T^R_{\alpha\beta\gamma}\ T^R_{\alpha\beta\gamma}\\
V_\phi =& -\mu^2\phi^\rho_{i\alpha}\ \phi^{*\,\rho}_{i\alpha} + \lambda_1(\phi^\rho_{i\alpha}\ \phi^{*\,\rho}_{i\alpha})^2 + \boldsymbol{\lambda_2}\epsilon^{\rho\rho'}\epsilon^{\sigma\sigma'}\phi^\rho_{i\alpha}\ \phi^{*\,\sigma}_{i\alpha}\phi^{\rho'}_{j\beta}\ \phi^{*\,\sigma'}_{j\beta} + \boldsymbol{\lambda_3}\phi^\rho_{i\alpha}\ \phi^{*\,\rho}_{j\beta}\phi^\sigma_{i\alpha}\ \phi^{*\,\sigma}_{j\beta} + \boldsymbol{\lambda_4}\phi^\rho_{i\alpha}\ \phi^{*\,\sigma}_{i\beta}\phi^\sigma_{j\alpha}\ \phi^{*\,\rho}_{j\beta}\\
&+\boldsymbol{\lambda_5}\epsilon^{\rho\rho'}\epsilon^{\sigma\sigma'}\phi^\rho_{i\alpha}\ \phi^{*\,\sigma'}_{i\beta}\phi^{\rho'}_{j\alpha}\ \phi^{*\,\sigma}_{j\beta} + \boldsymbol{\lambda_6}\phi^\rho_{i\alpha}\ \phi^{*\,\rho}_{j\alpha}\phi^\sigma_{j\beta}\ \phi^{*\,\sigma}_{i\beta} + \boldsymbol{\lambda_7}\epsilon^{\rho\rho'}\epsilon^{\sigma\sigma'}\phi^\rho_{i\alpha}\ \phi^{*\,\sigma}_{j\alpha}\phi^{\rho'}_{j\beta}\ \phi^{*\,\sigma'}_{i\beta} + \boldsymbol{\lambda_8}\phi^\rho_{i\alpha}\ \phi^{*\,\rho}_{j\alpha}\phi^\sigma_{i\beta}\ \phi^{*\,\sigma}_{j\beta}\\
&+\boldsymbol{\lambda_9}\epsilon^{\rho\rho'}\epsilon^{\sigma\sigma'}\phi^\rho_{i\alpha}\ \phi^{*\,\sigma}_{j\alpha}\phi^{\rho'}_{i\beta}\ \phi^{*\,\sigma'}_{j\beta}\\
V_{\psi\phi} =&\ \xi_8\ \psi_i^L\psi_i^L\phi^\rho_{i\alpha}\ \phi^{*\,\rho}_{i\alpha} + \boldsymbol{\xi_9}\ \psi_i^L\psi_j^L\phi^\rho_{i\alpha}\ \phi^{*\,\rho}_{j\alpha} + \boldsymbol{\mu_{LH}}\epsilon_{ijk}\ \phi^\rho_{i\alpha}\ \phi^{*\,\rho}_{j\alpha}\ \psi_k^L\\
&+\ \ \zeta_8\ \psi_{_R}^\alpha\psi_{_R}^\alpha\phi_\rho^{i\beta}\ \phi_\rho^{i\beta *} + \boldsymbol{\zeta_9}\ \psi_\alpha^R\psi_\beta^R\phi^\rho_{i\alpha}\ \phi^{*\,\rho}_{i\beta} + \boldsymbol{\mu_{RH}}\epsilon_{\alpha\beta\gamma}\phi^\rho_{i\alpha}\ \phi^{*\,\rho}_{i\beta}\psi_\gamma^R + \boldsymbol{\eta_H}\epsilon_{ijk}\epsilon_{\alpha\beta\gamma}\phi^\rho_{i\alpha}\ \phi^{*\,\rho}_{j\beta}\psi_k^L\psi_\gamma^R\\
V_m =&\ \kappa_1\ T^L_{lmn}\ T^L_{lmn}\phi^\rho_{i\alpha}\phi^{*\,\rho}_{i\alpha} + \boldsymbol{\kappa_2}\ T^L_{ijk}\ \psi_i^L\phi^\rho_{j\alpha}\phi^{*\,\rho}_{k\alpha} + \boldsymbol{\kappa_3}\ T^L_{imn}\ T^L_{jmn}\phi^\rho_{i\alpha}\phi^{*\,\rho}_{j\alpha}\\
&+\ \ \kappa_4\ \ T^R_{\beta\gamma\delta}\ T^R_{\beta\gamma\delta}\phi^\rho_{i\alpha}\phi^{*\,\rho}_{i\alpha} + \boldsymbol{\kappa_5}\ T^R_{\alpha\beta\gamma}\ \psi_\alpha^R\phi^\rho_{i\beta}\phi^{*\,\rho}_{i\gamma} + \boldsymbol{\kappa_6}\ T^R_{\alpha\gamma\delta}\ T^R_{\beta\gamma\delta}\phi^\rho_{i\alpha}\phi^{*\,\rho}_{i\beta}
\end{aligned}
$$

Here, $a, b, c\cdots$ are $O(3)_L$ indices, $\alpha, \beta, \gamma\cdots$ are $O(3)_R$ indices and ρ, σ are $SU(2)_L$ indices.

Let us assume the D_3 preserving vev to be 10^3 TeV. $\chi_{_{L1,R1}}$ are the singlets of $D_{3L,R}$ and acquires the vev to break the $O(3)_L \times O(3)_R$ group.

$$
\begin{aligned}
\chi_{_{L1}} &\leftarrow \chi_{_{L1}} + v_{_{L1}}\\
\chi_{_{R1}} &\leftarrow \chi_{_{R1}} + v_{_{R1}}
\end{aligned}
\tag{4.41}
$$

The vev equation becomes:

$$
\langle V\rangle = -\nu_{_L}^2 v_{_{L1}}^2 + \xi_2 v_{_{L1}}^4 + \frac{1}{2}\xi_3 v_{_{L1}}^4 - \nu_{_R}^2 v_{_{R1}}^2 + \zeta_2 v_{_{R1}}^4 + \frac{1}{2}\zeta_3 v_{_{R1}}^4 + \eta_2 v_{_{L1}}^2 v_{_{R1}}^2 \tag{4.42}
$$

Minimizing the equation, we get:

$$
\begin{aligned}
\nu_{_L}^2 &= 2\ \xi_2 v_{_{L1}}^2 + \xi_3 v_{_{L1}}^2 + \eta_2 v_{_{R1}}^2\\
\nu_{_R}^2 &= 2\ \zeta_2 v_{_{R1}}^2 + \zeta_3 v_{_{R1}}^2 + \eta_2 v_{_{L1}}^2
\end{aligned}
\tag{4.43}
$$

The mass matrices are at this stage:

$$M^2(\chi_{_L}^1,\chi_{_R}^1)=\begin{pmatrix} 8\,\xi_{_2}v_{_{L1}}^2+4\,\xi_{_3}v_{_{L1}}^2 & 4\,\eta_{_2}v_{_{L1}}v_{_{R1}} \\ 4\,\eta_{_2}v_{_{L1}}v_{_{R1}} & 8\,\zeta_{_2}v_{_{R1}}^2+4\,\zeta_{_3}v_{_{R1}}^2 \end{pmatrix};$$

$$M^2(\chi_{_L}^5,\psi_{_L}^1)=\begin{pmatrix} -\frac{4}{5}\,\xi_{_3}v_{_{L1}}^2 & \frac{2}{\sqrt{15}}\,\xi_{_7}v_{_{L1}}^2 \\ \frac{2}{\sqrt{15}}\,\xi_{_7}v_{_{L1}}^2 & 2\,\xi_{_4}v_{_{L1}}^2+\xi_{_5}v_{_{L1}}^2+2\,\eta_{_4}v_{_{R1}}^2-2\mu_{_L}^2 \end{pmatrix};$$

$$M^2(\chi_{_L}^6,\psi_{_L}^2)=\begin{pmatrix} -\frac{4}{5}\,\xi_{_3}v_{_{L1}}^2 & \frac{2}{\sqrt{15}}\,\xi_{_7}v_{_{L1}}^2 \\ \frac{2}{\sqrt{15}}\,\xi_{_7}v_{_{L1}}^2 & 2\,\xi_{_4}v_{_{L1}}^2+\xi_{_5}v_{_{L1}}^2+2\,\eta_{_4}v_{_{R1}}^2-2\mu_{_L}^2 \end{pmatrix};$$

$$M^2(\chi_{_L}^7,\psi_{_L}^3)=\begin{pmatrix} -\frac{6}{5}\,\xi_{_3}v_{_{L1}}^2 & \frac{1}{\sqrt{10}}\,\xi_{_7}v_{_{L1}}^2 \\ \frac{1}{\sqrt{10}}\,\xi_{_7}v_{_{L1}}^2 & 2\,\xi_{_4}v_{_{L1}}^2+2\,\eta_{_4}v_{_{R1}}^2-2\mu_{_L}^2 \end{pmatrix};$$

$$M^2(\chi_{_R}^5,\psi_{_R}^1)=\begin{pmatrix} -\frac{4}{5}\,\zeta_{_3}v_{_{R1}}^2 & \frac{2}{\sqrt{15}}\,\zeta_{_7}v_{_{R1}}^2 \\ \frac{2}{\sqrt{15}}\,\zeta_{_7}v_{_{R1}}^2 & 2\,\zeta_{_4}v_{_{R1}}^2+\zeta_{_5}v_{_{R1}}^2+2\,\eta_{_3}v_{_{L1}}^2-2\mu_{_R}^2 \end{pmatrix};$$

$$M^2(\chi_{_R}^6,\psi_{_R}^2)=\begin{pmatrix} -\frac{4}{5}\,\zeta_{_3}v_{_{R1}}^2 & \frac{2}{\sqrt{15}}\,\zeta_{_7}v_{_{R1}}^2 \\ \frac{2}{\sqrt{15}}\,\zeta_{_7}v_{_{R1}}^2 & 2\,\zeta_{_4}v_{_{R1}}^2+\zeta_{_5}v_{_{R1}}^2+2\,\eta_{_3}v_{_{L1}}^2-2\mu_{_R}^2 \end{pmatrix};$$

$$M^2(\chi_{_R}^7,\psi_{_R}^3)=\begin{pmatrix} -\frac{6}{5}\,\zeta_{_3}v_{_{R1}}^2 & \frac{1}{\sqrt{10}}\,\zeta_{_7}v_{_{R1}}^2 \\ \frac{1}{\sqrt{10}}\,\zeta_{_7}v_{_{R1}}^2 & 2\,\zeta_{_4}v_{_{R1}}^2+2\,\eta_{_3}v_{_{L1}}^2-2\mu_{_R}^2 \end{pmatrix};$$

Now, $\left\{\chi_{_L}^5,\psi_{_L}^1\right\}$ or $\left\{\chi_{_L}^6,\psi_{_L}^2\right\}$ can be diagonalized by the diagonalization matrix:

$$R_L=\begin{pmatrix} \cos\theta_L & \sin\theta_L \\ -\sin\theta_L & \cos\theta_L \end{pmatrix} \tag{4.44}$$

where,

$$\theta_L=\frac{2\sqrt{15}\,\xi_{_7}}{30\,\xi_{_4}+15\,\xi_{_5}+30\,\eta_{_4}r^{-2}-30\,\mu_{_r}^2+12\,\xi_{_3}} \tag{4.45}$$

where,

$$r=\frac{v_{_{L1}}}{v_{_{R1}}};\qquad\qquad \mu_{_r}=\frac{\mu_{_L}}{v_{_{L1}}} \tag{4.46}$$

To have the D_3 doublet $\chi_d=\left\{\chi_{_L}^5,\chi_{_L}^6\right\}$ in the range of 30 TeV and D_3 doublet $\psi_d=\left\{\psi_{_L}^1,\psi_{_L}^2\right\}$ in the range of 1 TeV with very little mixing, we need $\xi_{_7}\approx 10^{-6}$ and $\xi_{_3}\approx 10^{-3}$ along with the fine tune $\left\{2\,\xi_{_4}v_{_{L1}}^2+\xi_{_5}v_{_{L1}}^2+2\,\eta_{_4}v_{_{R1}}^2-2\mu_{_L}^2\right\}\approx -1$ Tev which makes $\theta_L\approx 10^{-6}$. This makes the eigenvalues of the matrix $M^2(\chi_d,\psi_d)$ as $\approx\{1000,1\}$, ie. the D_3 doublet χ_d will have a mass around 30 TeV and the D_3 doublet ψ_d will have a mass around 1 TeV.

If the mixing is not small, Then

$$\theta_L = \arctan\left[\frac{\sqrt{15}}{4\,\xi_{_7}}\left(\xi_{_5} + 2\,\eta_{_4} r^{-2} + 2\,\xi_{_4} + \frac{4}{5}\xi_{_3} + \sqrt{\frac{16}{15}\xi_{_7}^2 + \left\{\xi_{_5} + 2\,\eta_{_4} r^{-2} + 2\,\xi_{_4} + \frac{4}{5}\xi_{_3} - \mu_{_r}^2\right\}^2} - 2\mu_{_r}^2\right)\right]$$
$$= \arctan\left[\frac{\sqrt{15}}{4\,\xi_{_7}}\left(\xi_{_c} + \sqrt{\frac{16}{15}\xi_{_7}^2 + \left\{\xi_{_c} - \mu_{_r}^2\right\}^2} - 2\mu_{_r}^2\right)\right]$$

where,

$$\xi_{_c} = \xi_{_5} + 2\,\eta_{_4} r^{-2} + 2\,\xi_{_4} + \frac{4}{5}\xi_{_3}$$

In this case, we need $\xi_{_7} \approx 10^{-3}$ and $\xi_{_3} \approx 10^{-3}$ along with the previous fine tuning of $\left\{2\,\xi_{_4} v_{_{L1}}^2 + \xi_{_5} v_{_{L1}}^2 + 2\,\eta_{_4} v_{_{R1}}^2 - 2\mu_{_L}^2\right\} \approx -1$ Tev. This makes the eigenvalues of the matrix $M^2(\chi_d, \psi_d)$ as $\approx \{1000, 1\}$, ie. the D_3 doublet χ_d will have a mass around 30 TeV and the D_3 doublet ψ_d will have a mass around 1 TeV.

Here,

$$R_L M^2(\chi_d, \psi_d) R_L^T = D^2(\chi_d, \psi_d) \tag{4.47}$$

And we define:

$$\Psi_D = \begin{pmatrix} \psi_D \\ \chi_D \end{pmatrix} = R_L \begin{pmatrix} \psi_d \\ \chi_d \end{pmatrix} \tag{4.48}$$

where,

$$\psi_D = \begin{pmatrix} \psi_1 \\ \psi_2 \end{pmatrix}; \qquad \chi_D = \begin{pmatrix} \chi_5 \\ \chi_6 \end{pmatrix} \tag{4.49}$$

So, the conversion becomes

$$\begin{aligned} \psi_1 &= \cos\theta_L \psi_L^1 + \sin\theta_L \chi_L^5 \\ \psi_2 &= \cos\theta_L \psi_L^2 + \sin\theta_L \chi_L^6 \\ \chi_5 &= -\sin\theta_L \psi_L^1 + \cos\theta_L \chi_L^5 \\ \chi_6 &= -\sin\theta_L \psi_L^2 + \cos\theta_L \chi_L^6 \end{aligned} \tag{4.50}$$

The Lagrangian for the two D_3 doublet can be written as:

$$
\begin{aligned}
V_{2D} = & -a_L\left(\psi_{L1}^2+\psi_{L2}^2\right)+b_L\left(\psi_{L1}^2+\psi_{L2}^2\right)^2+c_L\left(3\psi_{L1}\psi_{L2}^2-\psi_{L1}^3\right)+d_L\left(\chi_{L5}^2+\chi_{L6}^2\right)+e_L\left(\chi_{L5}^2+\chi_{L6}^2\right)^2 \\
& +f_L\left(3\chi_{L5}\chi_{L6}^2-\chi_{L5}^3\right)+g_L\left[\chi_{L5}\left(\psi_{L2}^2-\psi_{L1}^2\right)+2\psi_{L1}\psi_{L2}\chi_{L6}\right]+h_L\left[\psi_{L1}\left(\chi_{L6}^2-\chi_{L5}^2\right)+2\psi_{L2}\chi_{L5}\chi_{L6}\right] \\
& +i_L\left[\left(\psi_{L1}^2-\psi_{L2}^2\right)\left(\chi_{L5}^2-\chi_{L6}^2\right)+4\psi_{L1}\psi_{L2}\chi_{L5}\chi_{L6}\right]+j_L\left(\psi_{L1}^2+\psi_{L2}^2\right)\left(\chi_{L5}^2+\chi_{L6}^2\right) \\
& +k_L\left(\psi_{L1}^2+\psi_{L2}^2\right)\left(\psi_{L1}\chi_{L5}+\psi_{L2}\chi_{L6}\right)+l_L\left(\chi_{L5}^2+\chi_{L6}^2\right)\left(\psi_{L1}\chi_{L5}+\psi_{L2}\chi_{L6}\right) \\
& -a_R\left(\psi_{R1}^2+\psi_{R2}^2\right)+b_R\left(\psi_{R1}^2+\psi_{R2}^2\right)^2+c_R\left(3\psi_{R1}\psi_{R2}^2-\psi_{R1}^3\right)+d_R\left(\chi_{R5}^2+\chi_{R6}^2\right)+e_R\left(\chi_{R5}^2+\chi_{R6}^2\right)^2 \\
& +f_R\left(3\chi_{R5}\chi_{R6}^2-\chi_{R5}^3\right)+g_R\left[\chi_{R5}\left(\psi_{R2}^2-\psi_{R1}^2\right)+2\psi_{R1}\psi_{R2}\chi_{R6}\right]+h_R\left[\psi_{R1}\left(\chi_{R6}^2-\chi_{R5}^2\right)+2\psi_{R2}\chi_{R5}\chi_{R6}\right] \\
& +i_R\left[\left(\psi_{R1}^2-\psi_{R2}^2\right)\left(\chi_{R5}^2-\chi_{R6}^2\right)+4\psi_{R1}\psi_{R2}\chi_{R5}\chi_{R6}\right]+j_R\left(\psi_{R1}^2+\psi_{R2}^2\right)\left(\chi_{R5}^2+\chi_{R6}^2\right) \\
& +k_R\left(\psi_{R1}^2+\psi_{R2}^2\right)\left(\psi_{R1}\chi_{R5}+\psi_{R2}\chi_{R6}\right)+l_R\left(\chi_{R5}^2+\chi_{R6}^2\right)\left(\psi_{R1}\chi_{R5}+\psi_{R2}\chi_{R6}\right) \\
& +a_M\left(\psi_{L1}^2+\psi_{L2}^2\right)\left(\psi_{R1}^2+\psi_{R2}^2\right)+b_M\left(\psi_{L1}^2+\psi_{L2}^2\right)\left(\chi_{R5}^2+\chi_{R6}^2\right)+c_M\left(\psi_{R1}^2+\psi_{R2}^2\right)\left(\chi_{L5}^2+\chi_{L6}^2\right) \\
& +d_M\left(\chi_{L5}^2+\chi_{L6}^2\right)\left(\chi_{R5}^2+\chi_{R6}^2\right)
\end{aligned}
$$

Comparing the two doublet potential with the complete potential, we get

$$
\begin{aligned}
a_L = & -\frac{2}{5}\,\xi_3 v_{L1}^2\sin^2\theta_L+\xi_4 v_{L1}^2\cos^2\theta_L+\frac{1}{2}\,\xi_5 v_{L1}^2\cos^2\theta_L+\frac{2}{\sqrt{15}}\,\xi_7 v_{L1}^2\cos\theta_L\sin\theta_L+\eta_4 v_{R1}^2\cos^2\theta_L-\mu_L^2\cos^2\theta_L \\
b_L = & \ \xi_1\cos^4\theta_L+\xi_2\sin^4\theta_L+\frac{71}{150}\,\xi_3\sin^4\theta_L+\xi_4\cos^2\theta_L\sin^2\theta_L+\frac{13}{30}\,\xi_5\cos^2\theta_L\sin^2\theta_L+\frac{\sqrt{3}}{2\sqrt{5}}\,\xi_6\cos^3\theta_L\sin\theta_L \\
& -\frac{2}{5\sqrt{15}}\,\xi_7\cos\theta_L\sin^3\theta_L \\
c_L = & \ \frac{4}{5\sqrt{15}}\,\xi_3 v_{L1}\sin^3\theta_L+\frac{1}{\sqrt{15}}\,\xi_5 v_{L1}\cos^2\theta_L\sin\theta_L+\frac{1}{2}\,\xi_6 v_{L1}\cos^3\theta_L+\frac{4}{15}\,\xi_7 v_{L1}\cos\theta_L\sin^2\theta_L \\
d_L = & -\frac{2}{5}\,\xi_3 v_{L1}^2\cos^2\theta_L+\xi_4 v_{L1}^2\sin^2\theta_L+\frac{1}{2}\,\xi_5 v_{L1}^2\sin^2\theta_L-\frac{2}{\sqrt{15}}\,\xi_7 v_{L1}^2\cos\theta_L\sin\theta_L+\eta_4 v_{R1}^2\sin^2\theta_L-\mu_L^2\sin^2\theta_L \\
e_L = & \ \xi_1\sin^4\theta_L+\xi_2\cos^4\theta_L+\frac{71}{150}\,\xi_3\cos^4\theta_L+\xi_4\cos^2\theta_L\sin^2\theta_L+\frac{13}{30}\,\xi_5\cos^2\theta_L\sin^2\theta_L-\frac{\sqrt{3}}{2\sqrt{5}}\,\xi_6\cos\theta_L\sin^3\theta_L \\
& +\frac{2}{5\sqrt{15}}\,\xi_7\cos^3\theta_L\sin\theta_L \\
f_L = & \ \frac{4}{5\sqrt{15}}\,\xi_3 v_{L1}\cos^3\theta_L+\frac{1}{\sqrt{15}}\,\xi_5 v_{L1}\cos\theta_L\sin^2\theta_L-\frac{1}{2}\,\xi_6 v_{L1}\sin^3\theta_L-\frac{4}{15}\,\xi_7 v_{L1}\cos^2\theta_L\sin\theta_L \\
g_L = & \ \frac{4\sqrt{3}}{5\sqrt{5}}\,\xi_3 v_{L1}\cos\theta_L\sin^2\theta_L+\frac{1}{4\sqrt{15}}\xi_5 v_{L1}\left(\cos\theta_L+\cos 3\theta_L\right)-\frac{3}{2}\,\xi_6 v_{L1}\cos^2\theta_L\sin\theta_L-\frac{1}{15}\,\xi_7 v_{L1}\left(\sin\theta_L-\sin 3\theta_L\right) \\
h_L = & \ \frac{4\sqrt{3}}{5\sqrt{5}}\,\xi_3 v_{L1}\cos^2\theta_L\sin\theta_L+\frac{1}{4\sqrt{15}}\xi_5 v_{L1}\left(\sin\theta_L-\sin 3\theta_L\right)+\frac{3}{2}\,\xi_6 v_{L1}\cos\theta_L\sin^2\theta_L+\frac{1}{15}\,\xi_7 v_{L1}\left(\cos\theta_L+\cos 3\theta_L\right) \\
i_L = & \ 2\,\xi_1\cos^2\theta_L\sin^2\theta_L+2\,\xi_2\cos^2\theta_L\sin^2\theta_L+\frac{71}{75}\,\xi_3\cos^2\theta_L\sin^2\theta_L-2\,\xi_4\cos^2\theta_L\sin^2\theta_L+\frac{1}{120}\,\xi_5\left(11+13\cos 4\theta_L\right) \\
& -\frac{1\sqrt{3}}{8\sqrt{5}}\,\xi_6\sin 4\theta_L-\frac{1}{10\sqrt{15}}\,\xi_7\sin 4\theta_L \\
j_L = & \ 4\,\xi_1\cos^2\theta_L\sin^2\theta_L+4\,\xi_2\cos^2\theta_L\sin^2\theta_L+\frac{142}{75}\,\xi_3\cos^2\theta_L\sin^2\theta_L+\ \xi_4\cos^2 2\theta_L+\frac{1}{60}\,\xi_5\left(1+13\cos 4\theta_L\right) \\
& -\frac{1\sqrt{3}}{4\sqrt{5}}\,\xi_6\sin 4\theta_L-\frac{1}{5\sqrt{15}}\,\xi_7\sin 4\theta_L
\end{aligned}
$$

$$
\begin{aligned}
k_L =& -4\,\xi_1\cos^3\theta_L\sin\theta_L + 4\,\xi_2\cos\theta_L\sin^3\theta_L + \frac{142}{75}\,\xi_3\cos\theta_L\sin^3\theta_L + \frac{1}{2}\,\xi_4\sin 4\theta_L + \frac{13}{60}\,\xi_5\sin 4\theta_L \\
&+ \frac{\sqrt{3}}{4\sqrt{5}}\,\xi_6\,(\cos 2\theta_L + \cos 4\theta_L) + \frac{1}{5\sqrt{15}}\,\xi_7\,(-\cos 2\theta_L + \cos 4\theta_L) \\
l_L =& -4\,\xi_1\cos\theta_L\sin^3\theta_L + 4\,\xi_2\cos^3\theta_L\sin\theta_L + \frac{142}{75}\,\xi_3\cos^3\theta_L\sin\theta_L - \frac{1}{2}\,\xi_4\sin 4\theta_L - \frac{13}{60}\,\xi_5\sin 4\theta_L \\
&+ \frac{\sqrt{3}}{2\sqrt{5}}\,\xi_6\,(1+2\cos 2\theta_L)\sin^2\theta_L - \frac{1}{5\sqrt{15}}\,\xi_7\,(\cos 2\theta_L + \cos 4\theta_L)
\end{aligned}
\tag{4.51}
$$

$$
\begin{aligned}
a_R =& -\frac{2}{5}\,\zeta_3 v_{R1}^2\sin^2\theta_R + \zeta_4 v_{R1}^2\cos^2\theta_R + \frac{1}{2}\,\zeta_5 v_{R1}^2\cos^2\theta_R + \frac{2}{\sqrt{15}}\,\zeta_7 v_{R1}^2\cos\theta_R\sin\theta_R + \eta_3 v_{L1}^2\cos^2\theta_R - \mu_R^2\cos^2\theta_R \\
b_R =& \ \zeta_1\cos^4\theta_R + \zeta_2\sin^4\theta_R + \frac{71}{150}\,\zeta_3\sin^4\theta_R + \zeta_4\cos^2\theta_R\sin^2\theta_R + \frac{13}{30}\,\zeta_5\cos^2\theta_R\sin^2\theta_R + \frac{\sqrt{3}}{2\sqrt{5}}\,\zeta_6\cos^3\theta_R\sin\theta_R \\
&- \frac{2}{5\sqrt{15}}\,\zeta_7\cos\theta_R\sin^3\theta_R \\
c_R =& \ \frac{4}{5\sqrt{15}}\,\zeta_3 v_{R1}\sin^3\theta_R + \frac{1}{\sqrt{15}}\,\zeta_5 v_{R1}\cos^2\theta_R\sin\theta_R + \frac{1}{2}\,\zeta_6 v_{R1}\cos^3\theta_R + \frac{4}{15}\,\zeta_7 v_{R1}\cos\theta_R\sin^2\theta_R \\
d_R =& -\frac{2}{5}\,\zeta_3 v_{R1}^2\cos^2\theta_R + \zeta_4 v_{R1}^2\sin^2\theta_R + \frac{1}{2}\,\zeta_5 v_{R1}^2\sin^2\theta_R - \frac{2}{\sqrt{15}}\,\zeta_7 v_{R1}^2\cos\theta_R\sin\theta_R + \eta_3 v_{L1}^2\sin^2\theta_R - \mu_R^2\sin^2\theta_R \\
e_R =& \ \zeta_1\sin^4\theta_R + \zeta_2\cos^4\theta_R + \frac{71}{150}\,\zeta_3\cos^4\theta_R + \zeta_4\cos^2\theta_R\sin^2\theta_R + \frac{13}{30}\,\zeta_5\cos^2\theta_R\sin^2\theta_R - \frac{\sqrt{3}}{2\sqrt{5}}\,\zeta_6\cos\theta_R\sin^3\theta_R \\
&+ \frac{2}{5\sqrt{15}}\,\zeta_7\cos^3\theta_R\sin\theta_R \\
f_R =& \ \frac{4}{5\sqrt{15}}\,\zeta_3 v_{R1}\cos^3\theta_R + \frac{1}{\sqrt{15}}\,\zeta_5 v_{R1}\cos\theta_R\sin^2\theta_R - \frac{1}{2}\,\zeta_6 v_{R1}\sin^3\theta_R - \frac{4}{15}\,\zeta_7 v_{R1}\cos^2\theta_R\sin\theta_R \\
g_R =& \ \frac{4\sqrt{3}}{5\sqrt{5}}\,\zeta_3 v_{R1}\cos\theta_R\sin^2\theta_R + \frac{1}{4\sqrt{15}}\zeta_5 v_{R1}\,(\cos\theta_R + \cos 3\theta_R) - \frac{3}{2}\,\zeta_6 v_{R1}\cos^2\theta_R\sin\theta_R - \frac{1}{15}\,\zeta_7 v_{R1}\,(\sin\theta_R - \sin 3\theta_R) \\
h_R =& \ \frac{4\sqrt{3}}{5\sqrt{5}}\,\zeta_3 v_{R1}\cos^2\theta_R\sin\theta_R + \frac{1}{4\sqrt{15}}\zeta_5 v_{R1}\,(\sin\theta_R - \sin 3\theta_R) + \frac{3}{2}\,\zeta_6 v_{R1}\cos\theta_R\sin^2\theta_R + \frac{1}{15}\,\zeta_7 v_{R1}\,(\cos\theta_R + \cos 3\theta_R) \\
i_R =& \ 2\,\zeta_1\cos^2\theta_R\sin^2\theta_R + 2\,\zeta_2\cos^2\theta_R\sin^2\theta_R + \frac{71}{75}\,\zeta_3\cos^2\theta_R\sin^2\theta_R - 2\,\zeta_4\cos^2\theta_R\sin^2\theta_R + \frac{1}{120}\,\zeta_5\,(11 + 13\cos 4\theta_R) \\
&- \frac{1\sqrt{3}}{8\sqrt{5}}\,\zeta_6\sin 4\theta_R - \frac{1}{10\sqrt{15}}\,\zeta_7\sin 4\theta_R \\
j_R =& \ 4\,\zeta_1\cos^2\theta_R\sin^2\theta_R + 4\,\zeta_2\cos^2\theta_R\sin^2\theta_R + \frac{142}{75}\,\zeta_3\cos^2\theta_R\sin^2\theta_R + \ \zeta_4\cos^2 2\theta_R + \frac{1}{60}\,\zeta_5\,(1 + 13\cos 4\theta_R) \\
&- \frac{1\sqrt{3}}{4\sqrt{5}}\,\zeta_6\sin 4\theta_R - \frac{1}{5\sqrt{15}}\,\zeta_7\sin 4\theta_R \\
k_R =& -4\,\zeta_1\cos^3\theta_R\sin\theta_R + 4\,\zeta_2\cos\theta_R\sin^3\theta_R + \frac{142}{75}\,\zeta_3\cos\theta_R\sin^3\theta_R + \frac{1}{2}\,\zeta_4\sin 4\theta_R + \frac{13}{60}\,\zeta_5\sin 4\theta_R \\
&+ \frac{\sqrt{3}}{4\sqrt{5}}\,\zeta_6\,(\cos 2\theta_R + \cos 4\theta_R) + \frac{1}{5\sqrt{15}}\,\zeta_7\,(-\cos 2\theta_R + \cos 4\theta_R) \\
l_R =& -4\,\zeta_1\cos\theta_R\sin^3\theta_R + 4\,\zeta_2\cos^3\theta_R\sin\theta_R + \frac{142}{75}\,\zeta_3\cos^3\theta_R\sin\theta_R - \frac{1}{2}\,\zeta_4\sin 4\theta_R - \frac{13}{60}\,\zeta_5\sin 4\theta_R \\
&+ \frac{\sqrt{3}}{2\sqrt{5}}\,\zeta_6\,(1+2\cos 2\theta_R)\sin^2\theta_R - \frac{1}{5\sqrt{15}}\,\zeta_7\,(\cos 2\theta_R + \cos 4\theta_R)
\end{aligned}
\tag{4.52}
$$

and finally:

$$\begin{aligned}
a_M &= \left(\eta_3 \cos^2\theta_R + \eta_2 \sin^2\theta_R\right)\sin^2\theta_L + \left(\eta_1 \cos^2\theta_R + \eta_4 \sin^2\theta_R\right)\cos^2\theta_L \\
b_M &= \left(\eta_4 \cos^2\theta_R + \eta_1 \sin^2\theta_R\right)\cos^2\theta_L + \left(\eta_2 \cos^2\theta_R + \eta_3 \sin^2\theta_R\right)\sin^2\theta_L \\
c_M &= \left(\eta_3 \cos^2\theta_R + \eta_2 \sin^2\theta_R\right)\cos^2\theta_L + \left(\eta_1 \cos^2\theta_R + \eta_4 \sin^2\theta_R\right)\sin^2\theta_L \\
d_M &= \left(\eta_4 \cos^2\theta_R + \eta_1 \sin^2\theta_R\right)\sin^2\theta_L + \left(\eta_2 \cos^2\theta_R + \eta_3 \sin^2\theta_R\right)\cos^2\theta_L
\end{aligned} \tag{4.53}$$

Setting $\partial_{\chi_5} V_{2D} = 0$ and $\partial_{\chi_6} V_{2D} = 0$, we get upto first order in χ_5 and χ_6, one finds that one needs to do the following replacement to find the effective potential at TeV scale:

$$\begin{aligned}
\chi_{L5} \to & \frac{g_L}{2d_L}\psi_{L1}^2 + \frac{g_L h_L}{2d_L^2}\psi_{L1}^3 - \frac{k_L}{2d_L}\psi_{L1}^3 - \frac{g_L}{2d_L}\psi_{L2}^2 + \frac{g_L h_L}{2d_L^2}\psi_{L1}\psi_{L2}^2 - \frac{k_L}{2d_L}\psi_{L1}\psi_{L2}^2 \\
\chi_{L6} \to & -\frac{g_L}{d_L}\psi_{L1}\psi_{L2} + \frac{g_L h_L}{2d_L^2}\psi_{L1}^2\psi_{L2} - \frac{k_L}{2d_L}\psi_{L1}^2\psi_{L2} + \frac{g_L h_L}{2d_L^2}\psi_{L2}^3 - \frac{k_L}{2d_L}\psi_{L2}^3 \\
\chi_{R5} \to & \frac{g_R}{2d_R}\psi_{R1}^2 + \frac{g_R h_R}{2d_R^2}\psi_{R1}^3 - \frac{k_R}{2d_R}\psi_{R1}^3 - \frac{g_R}{2d_R}\psi_{R2}^2 + \frac{g_R h_R}{2d_R^2}\psi_{R1}\psi_{R2}^2 - \frac{k_R}{2d_R}\psi_{R1}\psi_{R2}^2 \\
\chi_{R6} \to & -\frac{g_R}{d_R}\psi_{R1}\psi_{R2} + \frac{g_R h_R}{2d_R^2}\psi_{R1}^2\psi_{R2} - \frac{k_R}{2d_R}\psi_{R1}^2\psi_{R2} + \frac{g_R h_R}{2d_R^2}\psi_{R2}^3 - \frac{k_R}{2d_R}\psi_{R2}^3
\end{aligned} \tag{4.54}$$

One can use these equation to solve for χ_5 and χ_6 for both the left-handed and right-handed cases and use them to remove the χ_5 and χ_6 from the low energy theorem and rewrite the potential in terms of ψ_L and ψ_R.

The effective potential becomes:

$$\begin{aligned}
V_{eff} = & -a_L\left(\psi_{L1}^2 + \psi_{L2}^2\right) + b_L\left(\psi_{L1}^2 + \psi_{L2}^2\right)^2 + c_L\left(3\psi_{L1}\psi_{L2}^2 - \psi_{L1}^3\right) \\
& + \alpha_L\left(\psi_{L1}^2 + \psi_{L2}^2\right)^2 + \beta_L\left(\psi_{L1}^2 + \psi_{L2}^2\right)^3 + \gamma_L\left(\psi_{L1}^2 + \psi_{L2}^2\right)\left(3\psi_{L1}\psi_{L2}^2 - \psi_{L1}^3\right) + \delta_L\left(3\psi_{L1}\psi_{L2}^2 - \psi_{L1}^3\right)^2 \\
& - a_R\left(\psi_{R1}^2 + \psi_{R2}^2\right) + b_R\left(\psi_{R1}^2 + \psi_{R2}^2\right)^2 + c_R\left(3\psi_{R1}\psi_{R2}^2 - \psi_{R1}^3\right) \\
& + \alpha_R\left(\psi_{R1}^2 + \psi_{R2}^2\right)^2 + \beta_R\left(\psi_{R1}^2 + \psi_{R2}^2\right)^3 + \gamma_R\left(\psi_{R1}^2 + \psi_{R2}^2\right)\left(3\psi_{R1}\psi_{R2}^2 - \psi_{R1}^3\right) + \delta_R\left(3\psi_{R1}\psi_{R2}^2 - \psi_{R1}^3\right)^2
\end{aligned} \tag{4.55}$$

where:

$$\begin{aligned}
\alpha_L = & -\frac{g_L}{4d_L} \\
\beta_L = & \frac{f_L g)L^3}{8d_L^3} - \frac{g_L^2 h_L^2}{4d_L^3} - \frac{g_L^2 i_L}{4d_L^2} + \frac{g_L^2 j_L}{4d_L^2} + \frac{g_L h_L k_L}{2d_L^2} - \frac{k_L^2}{4d_L} \\
\gamma_L = & \frac{g_L^2 h_L}{4d_L^2} - \frac{g_L k_L}{2d_L} \\
\delta_L = & -\frac{f_L g_L^3}{4d_L^3} + \frac{g_L^2 i_L}{2d_L^2}
\end{aligned} \tag{4.56}$$

$$
\begin{aligned}
\alpha_R =& -\frac{g_R}{4d_R} \\
\beta_R =& \frac{f_R g) R^3}{8d_R^3} - \frac{g_R^2 h_R^2}{4d_R^3} - \frac{g_R^2 i_R}{4d_R^2} + \frac{g_R^2 j_R}{4d_R^2} + \frac{g_R h_R k_R}{2d_R^2} - \frac{k_R^2}{4d_R} \\
\gamma_R =& \frac{g_R^2 h_R}{4d_R^2} - \frac{g_R k_R}{2d_R} \\
\delta_R =& -\frac{f_R g_R^3}{4d_R^3} + \frac{g_R^2 i_R}{2d_R^2}
\end{aligned}
\tag{4.57}
$$

One needs to be careful about writing done such effective theory as one needs to include both the left and right-handed part and also the trivial mixed terms. With this $d = 6$ dimensional effective potential one can show that when the non-trivial $d = 6$ dimensional term becomes comparable to the $d = 4$ terms, one can essentially break the left-over $\mathbb{Z}_2$ symmetry with the D_3 doublet vevs. In such a case, the relation between the doublet vevs are no longer valid and vev of each component can be treated as an independent parameter. Such a freedom is an absolute necessity to satisfy the FCNC constraints as this vev structure induces the vevs of all the components of ϕ except ϕ_{33} which gets an explicit vev.

With the electroweak vev $\langle\phi_{33}\rangle$, the vev structure of the complex bi-fundamental becomes:

$$
\mathcal{M} = \frac{\langle\phi_{33}\rangle}{M_\phi^2}
\begin{pmatrix}
\langle\psi_{L2}\rangle\langle\psi_{R2}\rangle & \langle\psi_{L2}\rangle\langle\psi_{R1}\rangle & \mu_L\langle\psi_{L2}\rangle \\
\langle\psi_{L1}\rangle\langle\psi_{R2}\rangle & \langle\psi_{L1}\rangle\langle\psi_{R1}\rangle & \mu_L\langle\psi_{L1}\rangle \\
\mu_R\langle\psi_{R2}\rangle & \mu_R\langle\psi_{R1}\rangle & \approx \langle\phi_{33}\rangle^2
\end{pmatrix}
\tag{4.58}
$$

The matrix $\mathcal{M}$ can satisfy all the flavor constraints if $\mathcal{M}_{31} \approx \mathcal{M}_{32} \approx \mathcal{M}_{21} \approx 0$ and $\mathcal{M}_{12} < \mathcal{M}_{22}$ and $\mathcal{M}_{13} < \mathcal{M}_{23}$. In the previous analysis, we were able to show that $\langle\psi_{L1}\rangle, \langle\psi_{L2}\rangle, \langle\psi_{R1}\rangle$ and $\langle\psi_{R2}\rangle$ can all be made independent of each other as the broken down model does not carry $\mathbb{Z}_2$ symmetry anymore. Also in the fundamental case, μ_L and μ_R are free massive parameters. So, we can easily make $\mathcal{M}_{31} \approx \mathcal{M}_{32} \approx \mathcal{M}_{21} \approx 0$. But due to structure of $\mathcal{M}$ the relation $\mathcal{M}_{12} < \mathcal{M}_{22}$ cannot be satisfied.

One can consider two types of solution to this problem:

- One can consider the situation where the D_3 doublet χ_5, χ_6 are also getting explicit vevs. In this scenario one can analyze the full symmetry breaking sector. As both the D_3 doublets are getting vevs, the $\mathbb{Z}_2$ symmetry will be broken and the induced vev structure will also be modified.

- One can also include a bi-fundamental along with the pair of fundamentals where the bi-fundamental gets a diagonal vev structure. In that case, current induced vev structure will be modified and all the flavor constraints can be satisfied. One extra advantage of this scenario is that even though the model is not minimal it will also have a candidate for 750 GeV scalar.

4.6 Conclusion

We have presented a flavor model based on the maximal subgroup of the global flavor symmetry of the fermions of SM. The gauged flavor group $O(3)_L \times O(3)_R$ is spontaneously broken down to $D_{3L} \times D_{3R}$ group by a pair of left and right-handed 7-plet. In this D_3 preserving limit, the first and the second generations of fermions are treated in an identical manner making the flavor structure specifically attractive. The electroweak symmetry is broken by the bi-fundamental ϕ which is a doublet under $SU(2)_L$. For the last stage of symmetry breaking, one can introduce a real bi-fundamental ψ with a off-diagonal vevs of the order of few GeV while the constraints is much more relaxed for the diagonal vevs. The $\langle\psi\rangle$ along with the electroweak vev $\langle\phi_{33}\rangle$ induces vevs for all the elements of ϕ fields. In turn, these induced vevs generate all the masses and mixings for the fermions of SM. Similar scenario can be portrayed with a pair of fundamentals.

For the model where the $D_{3L} \times D_{3R}$ symmetry gets broken by the bi-fundamental ψ field, the scalar field ψ_{11} with an admixture of mainly ϕ_{11}, can have a mass of 750 GeV. Even though in this case the decay width turns out to be 5 GeV, the Production crosssection $\times$ Branching ratio $\approx$ 3fb can be achieved.

REFERENCES

[1] CMS Collaboration [CMS Collaboration], collisions at 13TeV," CMS-PAS-EXO-15-004.

[2] The ATLAS collaboration, ATLAS-CONF-2015-081.

[3] M. Aaboud *et al.* [ATLAS Collaboration], arXiv:1606.03833 [hep-ex].

[4] V. Khachatryan *et al.* [CMS Collaboration], arXiv:1606.04093 [hep-ex].

[5] M. Koca, R. Koc and H. Tutunculer, "Explicit breaking of SO(3) with Higgs fields in the representations l = 2 and l = 3," Int. J. Mod. Phys. A **18**, 4817 (2003) [hep-ph/0410270].

[6] D. Aloni, K. Blum, A. Dery, A. Efrati and Y. Nir, arXiv:1512.05778 [hep-ph].

CHAPTER 5

DARK MATTER IN SO(10) GUTs

5.1 Introduction

A plethora of astrophysical and cosmological observations has established the existence of dark matter (DM) beyond any reasonable doubt. Its prevalence in the universe has been measured to be at a much higher rate than that of ordinary baryonic matter. The total mass-energy of the known universe contains 4.9% ordinary matter, 26.8% dark matter and the rest is contributed by dark energy [1]. The currently most accurate determination of critical density of dark matter, Ω_{DM} comes from global fits of cosmological parameters to a variety of observations. Using measurements of the anisotropy of the cosmic microwave background (CMB) and of the partial distribution of galaxies, we find that the density of cold, non-baryonic dark matter is:

$$\Omega_{DM} \sim 0.1186 \pm 0.0020 \tag{5.1}$$

where h is the Hubble constant in units of 100km/(s.Mpc) [2]. The baryonic matter (BM) density is given by

$$\Omega_{BM} \sim 0.02226 \pm 0.00023 \tag{5.2}$$

Even though more than 80% of the energy density of matter in the universe is composed of such non-baryonic dark matter, the Standard Model (SM) of particle physics cannot explain this observation as it lacks any candidate for such (dark) matter.

One of the most promising class of DM candidates is weakly interacting massive particle or WIMP. These neutral and colorless particles couple to SM particles via weak interactions and have weak scale masses. The fact that the thermal relic abundance of such particles can well explain the current energy density of the DM is known as WIMP miracle. Such WIMP particles are predicted by many well studied models. In most of the supersymmtric (SUSY) models the lightest supersymmetric particle (LSP) is a well known candidate for WIMP DM. For example, in minimal SUSY SM (MSSM), R-parity makes the lightest SUSY particle stable and thus becomes a well motivated dark matter candidate [3].

To be a competent dark matter candidate, the particle should be stable or have sufficiently long lifetime compared to the age of the universe. Simple discrete symmetries like R-parity can perform an excellent job of preventing the particle from decaying. Kaluza-Klein parity [4] in universal extra dimension models and T-parity [5] in Littlest Higgs models can also stabilize the lightest particle; turning them into promising dark matter candidate. Similar role is played by a $\mathbb{Z}_2$ symmetry for the case of Inert doublet models [6] or Scotogenic models [7].

$SO(10)$ representation	Type of representation	$\mathbb{Z}_2$ charge
1	rank 0 tensor	+
10	rank 1 tensor	+
45	rank 2 tensor	+
54	rank 2 tensor	+
210	rank 4 tensor	+
16	pure spinor	−
144	vector-spinor	−
126	rank 5 tensor	+

Table 5.1: List of irreducible representation of $SO(10)$

5.2 Discrete symmetries in $SO(10)$

Grand Unified Theories (GUTs) like $SO(10)$ have a lot of attractive features (see Chap. 2). Unlike many of the previously mentioned cases where the stabilizing symmetries are imposed by hand on the low energy theories, GUTs can provide a natural framework where unbroken discrete $\mathbb{Z}_N$ symmetries can be generated in a plausible way [8]. This phenomenon happens when any extra gauged $U(1)$ Abelian factors are only broken by order parameters carrying N units of the $U(1)$ charge. $SO(10)$ is a rank- five group and has an extra $U(1)$ symmetry beyond the SM gauge group.

In general, suppose a GUT Lie group contains an extra $U(1)$ with all of the fields ϕ_i have integer charges Q_i while a Higgs field ϕ_H has a non-zero charge Q_H. If $Q_H = 0 \mod N$ a vacuum expectation value (vev) of H will break the $U(1)$ factor but will imply an effective model still invariant under the gauge transformation $\phi_i \to e^{i2\pi Q_i/N}\phi_i$, where $e^{i2\pi Q_H/N} = 1$, which is defined as $\mathbb{Z}_N$ discrete symmetry. If $\langle H_N \rangle$ breaks the extra $U(1)$ of $SO(10)$ while leaving unbroken a $\mathbb{Z}_N$ discrete symmetry. The smallest irreducible representation containing H_N has highest weight

$$\Lambda_N = (0\ 0\ 0\ 0\ N) \tag{5.3}$$

and dimension

$$dimension\ \Lambda_N = (1+N)\left(1+\frac{N}{2}\right)\left(1+\frac{N}{3}\right)^2\left(1+\frac{N}{4}\right)^2\left(1+\frac{N}{5}\right)^2\left(1+\frac{N}{6}\right)\left(1+\frac{N}{7}\right) \quad (5.4)$$

Thus, SO(10) GUT can account for the stability of DM in terms of the remnant $\mathbb{Z}_N$ symmetry originating from the extra $U(1)$ gauge symmetry. To realize discrete symmetry corresponding to $N = 1, 2, 3, \cdots$ the dimension of the irreducible representation for the needed Higgs field needs to be $\mathbf{16}, \mathbf{126}, \mathbf{672}, \cdots$. As long as we consider relatively small representation **126** is the only candidate and $\mathbb{Z}_2$ is the corresponding discrete symmetry. The $\mathbb{Z}_2$ charge of various $SO(10)$ multiplets are given in Table 5.1.

5.3 DM candidates in $SO(10)$ GUTs

Stable $SO(10)$ scalar DM candidates must be odd$(-)$ under the $\mathbb{Z}_2$ symmetry, while the fermion candidates must be even$(+)$. Therefore fermions must originate in a $\mathbf{10}, \mathbf{45}, \mathbf{54}, \mathbf{120}, \mathbf{126}, \mathbf{210}$ or $\mathbf{210'}$ representation, while the scalars are restricted to either **16** or **144** of $SO(10)$ [9, 10]. For a TeV scale DM, one requires explicit fine-tuning mechanism. It has been shown that if one requires gauge coupling unification at a sufficient high scale to ensure proton stability compatible with experiments, a unification scale greater than the intermediate scale and elastic cross sections compatible with direct detection experiments, despite the long list of possible candidates, only a handful survives. The details of such models of DM has already been analyzed in Ref. [9, 10].

Let us consider the case of $(1, 3, 0)$ fermion under $SU(3)_c \times SU(2)_L \times U(1)_Y$. This may emerge from $\mathbf{45_F}, \mathbf{54_F}$ or $\mathbf{210_F}$ of fermions, the simplest case being $\mathbf{45_F}$. As mentioned in the work done in Ref. [9, 10] one needs fine-tuning to make the mass of this DM particle 2.7 TeV which is needed for correct relic abundance. A bare mass term $(\mathbf{45_F})^2$ and a coupling with $\mathbf{54_H}$ as $(\mathbf{45_F})^2\mathbf{54_H}$ will allow for this. No other fragment of $\mathbf{45_F}$ fermion will remain light.

The problem with this scenario is that gauge boson loop corrections will generate mass for the DM $(1, 3, 0)$ multiplet. $\overline{X'}$ gauge boson which is $(\overline{3}, 2, -1/6)$ under SM will have a vertex: $(1, 3, 0)(3, 2, 1/6)(\overline{3}, 2, -1/6)$ where $(1, 3, 0)$ is DM fermion, $(3, 2, 1/6)$ is a fragment of $\mathbf{45_F}$ fermion and $(\overline{3}, 2, -1/6)$ is $\overline{X'}$ gauge boson. Since $(3, 2, 1/6)$ fragment from the $\mathbf{45_F}$ fermion has a GUT scale mass, the one-loop induced mass for DM $(1, 3, 0)$ is proportional to the GUT scale (see Fig. 5.1). So to keep the DM in the TeV range, one needs to fine-tune the fermion mass order by order. While this can be done, the level of tuning is much more unnatural than fine-tuning only at the tree-level. On the contrary to the first impression, it is not true that due to chiral symmetry fermion mass will

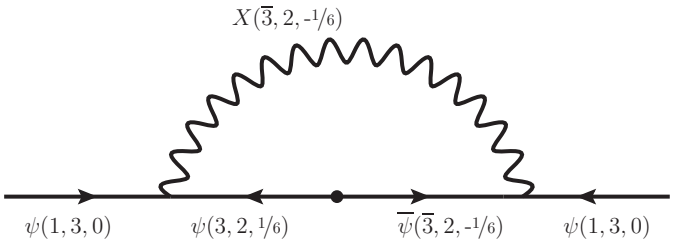

Figure 5.1: Feynman diagram for loop correction to the mass of $\psi(1,3,0)$ from $\mathbf{45_F}$

be protected in this case. Chiral symmetry only protects the mass up to the mass of other members of the same GUT multiplet.

If we allow fine-tuning order by order then some of the constraints mentioned in Ref. [9, 10] are not really needed. For example, it is noted by them that the $(1,3,0)$ DM arising from 54_F will form a Pati-Salam multiplet $(3,3,1)$ under $SU(2)_L \times SU(2)_R \times SU(4)_c$. So making the $(1,3,0)$ DM light may also make other hypercharged triplets $(1,3,1)$ under SM light. This is not quite correct. Left-right symmetry would imply that the entire $(3,3,1)$ should have the same mass. However, the 126_H has broken $SO(10)$ down to $SU(5)$. So in the gauge boson sector left-right symmetry is broken. The gauge boson loops mentioned above will split the masses of the various $(3,3,1)$ submultiplets. So, accepting order by order fine-tuning, technically there is no problem with getting just the $(1,3,0)$ component light as DM in these models as well.

One of the most simplest version of dark matter namely fermionic singlet has been ignored from the analysis. We propose a generic mechanism to incorporate dark matter into an arbitrary $SO(10)$ GUT with an unbroken $B-L$ parity. Due to the gauge-singlet nature of the DM candidate and its supporting interactions this does not interfere with any of the gauge unification, proton lifetime and other constraints obtained prior to the addition of such a dark sector.

5.4 The fermionic singlet DM in SO(10) GUTs

The idea here is to use the fact that there is a $\mathbb{Z}_2$ symmetry left behind the $U(1)_{B-L}$ whenever the latter is broken by the vev of a **126**-dimensional scalar. It is clear that the combination of its fermionic nature with the even $\mathbb{Z}_2^{B-L}$ parity will make a fermionic singlet $\mathbf{1_F}$ absolutely stable. The allowed interactions of $\mathbf{1_F}$ are thus:

$$\mathcal{L} \supset M_1 \mathbf{1_F 1_F} + \frac{\lambda}{\Lambda} \mathbf{1_F 1_F 126_S 126_S^*} + \frac{\rho}{\Lambda} \mathbf{1_F 1_F 45_S}^2 + \frac{\sigma}{\Lambda} \mathbf{1_F 1_F 10_S}^2 + \frac{\gamma}{\Lambda} \mathbf{1_F 1_F 120_S}^2 \tag{5.5}$$

SO(10) multiplet	Statistics	Z_2^{B-L}	Note
$\mathbf{16_F}$	$-$	$-$	SM matter
$\mathbf{126_S}$	$+$	$+$	the $U(1)_{B-L}$ breaker
$\mathbf{45_S}$ and/or $\mathbf{54_S}$ and/or 210	$+$	$+$	GUT-breaking scalars
$\mathbf{10_S}$ and/or $\mathbf{120_S}$	$+$	$+$	extra EWSB scalars
...	...	...	...
$\mathbf{1_F}$	$-$	$+$	the DM candidate

Table 5.2: The $SO(10)$, Lorentz and the $B-L$ parity quantum numbers in the simple $SO(10)$ GUT models under consideration. The matter singlet at the bottom is the DM candidate as the combination of the statistics with the $\mathbb{Z}_2^{B-L}$ parity make it absolutely stable.

where for simplicity, we assumed the $SO(10)$ symmetry is broken by the vev of $\mathbf{45_S}$ (one may employ $\langle\mathbf{54_S}\rangle$ and/or $\langle\mathbf{210_S}\rangle$ instead), Λ denotes the cut-off of the theory (above the GUT scale).

5.4.1 The thermal abundance of singlet fermionic dark matter

The Lagrangian (5.5) gives rise to the processes given in Table 5.3 in the very hot ($T \gtrsim M_{GUT}$) early Universe. In order to avoid the GUT monopole problem in what follows we shall assume that

#	Process	effective coupling	Note
(a)	$\mathbf{45_S 45_S} \leftrightarrow \mathbf{1_F 1_F}$	ρ/Λ	DM production/annihilation
(b)	$\mathbf{45_S 1_F} \leftrightarrow \mathbf{45_S 1_F}$	ρ/Λ	DM scattering
(c)	$\mathbf{45_S} \leftrightarrow \mathbf{1_F 1_F}$	$\rho\langle 45_S\rangle/\Lambda$	DM production/annihilation
(d)	$\mathbf{1_F} \leftrightarrow \mathbf{45_S 1_F}$	$\rho\langle 45_S\rangle/\Lambda$	Scalar bremmstrahlung
(e)	$\mathbf{126_S 126_S^*} \leftrightarrow \mathbf{1_F 1_F}$	λ/Λ	DM production/annihilation
(f)	$\mathbf{126_S 1_F} \leftrightarrow \mathbf{126_S 1_F}$	λ/Λ	DM scattering
(g)	$\mathbf{126_S} \leftrightarrow \mathbf{1_F 1_F}$	$\lambda\langle 126_S^*\rangle/\Lambda$	DM production/annihilation
(h)	$\mathbf{1_F} \leftrightarrow \mathbf{126_S 1_F}$	$\lambda\langle 126_S^*\rangle/\Lambda$	Scalar bremmstrahlung

Table 5.3: The basic scattering/annihilation processes underwent by 1_F in the early Universe under the supervision of the Lagrangian (5.5).

the inflation occurred after the GUT phase transition and, hence, the reheating temperature T_R was significantly smaller than the GUT scale. Under these circumstances, however, the thermal population of $\mathbf{45_S}$ with masses of the order of M_{GUT} shall be negligible and, hence, the reactions (a) - (d) from Table 5.3 will be incapable of maintaining the $\mathbf{1_F}$ DM population (that might have been also created upon the inflaton decay) in thermal equilibrium with the rest of the world below

T_R.

Concerning the reactions (e) - (h) from Table 5.3 the singlet of $\mathbf{126_S}$ (i.e., the one responsible for the seesaw scale) should live at an intermediate-scale and, hence, may develop a thermal population if T_R was bigger than the seesaw scale. There are two basic scenarios here:

- If the intermediate symmetry broken by $\langle \mathbf{126_S} \rangle$ contains the full $SU(4)_C$ this phase transition would again produce monopoles which, though not as abundant as the GUT-scale ones, are unwanted; in such a case the inflation should occur even later. However, for a yet lower T_R the RH neutrinos might not be populated enough to provide a successful leptogenesis.

- On the other hand, if the intermediate symmetry breaking does not suffer from the monopole issue, i.e., T_R may be higher than the mass of the singlet in 126_S entering the processes (e) - (h) (and thus also large enough to excite a thermal population of RH neutrinos) the reaction (e)[1] would maintain the $\mathbf{1_F}$'s in thermal equilibrium as long as

$$\Gamma_{ann.} = n_{\mathbf{1_F}}(T) \langle \sigma_{\mathbf{1_F 1_F} \leftrightarrow \mathbf{126_S 126_S^*}} |v| \rangle > H(T) = 1.66 \times g_*^{1/2} \frac{T^2}{M_P} \tag{5.6}$$

from where we would like to get a condition for the relic to be cold and the abundance to be roughly correct, i.e., $\Omega_{DM} h_0^2 \sim 0.1$. The latter condition yields following the classical "WIMP miracle" reasoning and assuming the current temperature of the DM gas is not parametrically different from that of the photons.

$$\Omega_{DM} h_0^2 \approx 10^4 \frac{x_{FO}}{g_{*S}/\sqrt{g_*}} \frac{1}{M_P \sigma_0} \mathrm{eV}^{-1} \approx 0.1 \tag{5.7}$$

with

$$x_{FO} \equiv \frac{m_{1_F}}{T_{FO}} \approx \log K - \frac{1}{2} \log (\log K) \tag{5.8}$$

for

$$K \approx 0.04 \frac{g}{\sqrt{g_*}} M_P m_{\mathbf{1_F}} \sigma_0 \tag{5.9}$$

where for simplicity, we assumed the thermally-averaged cross-section behaves as an s-wave (i.e., $\langle \sigma |v| \rangle \approx \sigma_0 (T/m_{1_F})^n$ with $n = 0$) and, given the relevant couplings above,

$$\sigma_0 = \sigma_{\mathbf{1_F 1_F} \to \mathbf{126_S 126_S^*}} \approx \frac{1}{64\pi} \left(\frac{\lambda}{\Lambda} \right)^2 . \tag{5.10}$$

This yields the desired CDM value of the freezout parameter (i.e., $x_{FO} \gg 1$) iff $K \gg 1$ and, hence,

$$0.04 \frac{g}{\sqrt{g_*}} M_P m_{1_F} \frac{1}{64\pi} \left(\frac{\lambda}{\Lambda} \right)^2 \gg 1 \tag{5.11}$$

which for $|\lambda| < 4\pi$ and $\Lambda \approx M_P$, is never satisfied for m_{1_F} smaller than M_P.

[1] Actually, (g) is likely to be irrelevant because the effective coupling is suppressed by $\langle \mathbf{126_S} \rangle / \Lambda$.

Hence, we conclude that without other interactions than those in Eq. (5.5) the 1_F can not be a cold relic and, thus, irrespective of what its abundance turns out, it is not a viable CDM candidate in the scenarios of our interest. This is rather intuitive as a species with only feeble couplings to the thermal bath tends to decouple soon, i.e., when it is still very relativistic.

5.4.2 The extra scalar singlet

Obviously, the way out is to ensure a much stronger (i.e., renormalizable) coupling with the visible sector in some way. Perhaps the simplest option here is to add an extra scalar $SO(10)$ singlet 1_S which, by its very nature, is Z_2^{B-L} even. As such, it may couple not only to the DM singlet 1_F, but via the Higgs portal coupling, also to the SM:

$$\mathcal{L} \supset M_S \mathbf{1_S}^2 + y\, \mathbf{1_F 1_F 1_S} + \kappa\, \mathbf{1_S} H^\dagger H + \beta\, \mathbf{1_S}^2 H^\dagger H \tag{5.12}$$

Note that in this case the Boltzmann equations encompass two different processes that may keep 1_F in thermal equilibrium to much lower scales, namely

- case i) :

$$H H^\dagger \leftrightarrow \mathbf{1_S 1_S} \quad \text{together with} \quad \mathbf{1_S} \leftrightarrow \mathbf{1_F 1_F} \tag{5.13}$$

  This set of reactions should be capable of keeping 1_F in thermal equilibrium with the SM fields (through their couplings to H) in an extended range of m_{1_F}, m_{1_S} and the relevant couplings.

- case ii) :

$$\mathbf{1_F 1_F} \leftrightarrow A A^\dagger \tag{5.14}$$

  Here A stands for the SM quarks, leptons and gauge bosons, which is due to the Higgs/$\mathbf{1_S}$ exchange and, thus, requires a non-negligible mixing among the two. Clearly, this situation corresponds to $m_{\mathbf{1_S}}$ not very far from the electroweak scale (otherwise H and $\mathbf{1_S}$ would not mix sufficiently).

In such a minimal extension of the SM one can include one Majorana fermion χ which is the $\mathbf{1_F}$, and one real scalar S which is the $\mathbf{1_S}$. Then excluding the kinetic part the Lagrangian for the dark matter χ can be written as:

$$\mathcal{L}_\chi = -\frac{1}{2}\, (M_\chi \overline{\chi}\chi + g_s S \overline{\chi}\chi + i\, S \overline{\chi}\gamma_5 \chi) \tag{5.15}$$

where M_χ is the dark matter mass, g_s is the scalar coupling and g_p is the pseudo-scalar one. The scalar potential becomes:

$$V(\phi, S) = -\mu_\phi^2 \phi^\dagger \phi + \frac{\lambda}{2}(\phi^\dagger \phi)^2 - \frac{\mu_s^2}{S^2} + \frac{\lambda_s}{4} S^4 + \frac{\lambda_m}{2} S^2 (\phi^\dagger \phi) + \mu_1^3 S + \frac{\mu_3}{3} S^3 + \mu S (\phi^\dagger \phi) \tag{5.16}$$

where ϕ is the SM Higgs doublet that breaks the electroweak symmetry after acquiring a vev. In unitary gauge we can write:

$$\phi = \frac{1}{\sqrt{2}} \begin{pmatrix} 0 \\ v_{ew} + h \end{pmatrix} \qquad \text{and} \qquad \langle \phi \rangle = \frac{1}{\sqrt{2}} \begin{pmatrix} 0 \\ v_{ew} \end{pmatrix} \tag{5.17}$$

In principle S can also get a vev, but it is always possible to choose a basis where vev of S is zero. In this basis, μ_1 is not free but given by $\mu_1^3 = \mu v_{ew}^2/2$. In this new basis:

$$V(h, S) = -\frac{\mu_\phi^2}{2} h^2 + \frac{\lambda}{8} h^4 - \frac{\mu_s^2}{S^2} + \frac{\lambda_s}{4} S^4 + \frac{\lambda_m}{4} S^2 h^2 + \frac{\mu_3}{3} S^3 + \mu S h^2 \tag{5.18}$$

The $S - h$ mixing term (μ term) provides the portal between the dark matter sector and the SM. The mass eigenstates of two scalars can be written as:

$$\begin{aligned} H_1 &= h \cos\alpha + S \sin\alpha \\ H_2 &= S \cos\alpha - h \sin\alpha \end{aligned} \tag{5.19}$$

where α is the mixing angle. So, via the Higgs portal such a dark matter can have LHC signature (see Fig. 5.2). The phenomenology of such a model has been studied extensively by many groups [11].

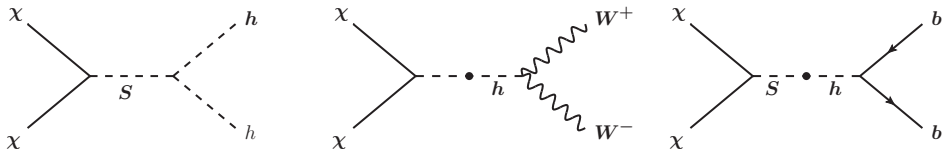

Figure 5.2: Feynman diagram of DM decaying into SM particles

5.5 The fermionic 10-plet DM in SO(10) GUTs

If DM is inside $\mathbf{10_F}$ of fermion, and if $SO(10)$ is broken by $\mathbf{45_H}$ and $\mathbf{126_H}$, then there is no renormalizable coupling of $\mathbf{10_F}$ fermion with a Higgs that acquires GUT VEV. One can choose the bare mass of $\mathbf{10_F}$ to be at TeV scale. This would mean that the color triplet partner of DM will also have TeV mass. For DM mass of 1.1 TeV (appropriate for doublet fermion DM from relic density), the mass of color triplet partner is 3 TeV as the radiative correction to the doublet mass will be proportional to the triplet mass (see Fig. 5.3). This GUT partner of DM will be observable at

LHC. Current limit on long-lived gluino is of order 1.2 TeV from ATLAS, and the limit on the GUT partner color triplet is similar.

In this model, there are other constraints. The color triplet partner of DM will be unstable, but its

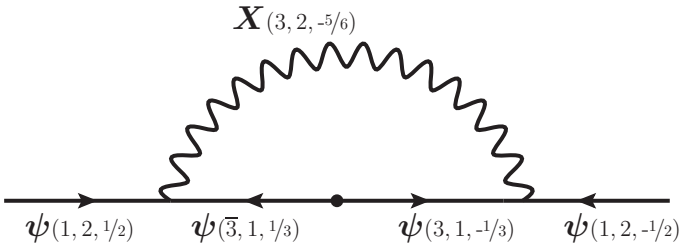

Figure 5.3: Feynman diagram of radiative correction to dark matter mass, where dark matter is a fermionic weak doublet

lifetime will be 10^{17} years if the decay is mediated by $SO(10)$ gauge bosons of mass 10^{15} GeV. This is not cosmologically viable. If there is an intermediate scale, the lifetime can be < 1 s (shorter than BBN start) with intermediate scale being 10^9 GeV. The effective operator is $(\mathbf{10_F 16_F})(\mathbf{10_F 16_F})^*$ where $\mathbf{10_F}$ is the DM multiplet and $\mathbf{16_F}$ is SM fermion. This can be obtained by integrating out a **16**-scalar which does not acquire a VEV. Take the ν^c like member of **16**-scalar as the intermediate state. It will couple to $\psi(3,1,-1/3), d^c$ and $\psi(1,2,1/2), \ell$ where $\psi(3,1,-1/3)$ and $\psi(1,2,1/2)$ are parts of $\mathbf{10_F}$. Here $\psi(1,2,1/2)$ contains the DM particle. Thus this diagram will lead to $\psi(3,1,-1/3) \to d + \ell +$ DM decay (see Fig. 5.4). Note that the color triplet partner of DM has no symmetry protecting it from decaying into DM particle as above.

Finally, to be consistent with direct detection limit, the doublet fermion DM must have Majorana

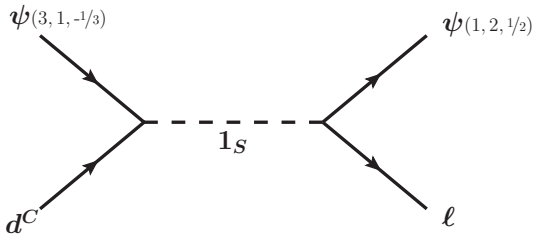

Figure 5.4: Feynman diagram of color triplet from 10_F decaying into DM

character. That is, there must be a splitting in mass of the two neutral members by at least 100 keV. This can also be achieved by an effective term $(\mathbf{10_F 10_F})(\phi.\phi)$ where ϕ is the SM Higgs doublet. This can be obtained by exchanging singlet fermion with mass of order 10^9 GeV to generate 100

keV Majorana mass via the "seesaw" mechanism. The $SO(10)$ level effective operator is $(\mathbf{10_F 10_S})^2$.

An alternative remains when the entire $\mathbf{10_F}$ and a $\mathbf{1_F}$ is at the TeV scale. This case has been studied by various authors [12] under the name doublet-singlet DM. Here there is no need for a singlet scalar. But if no fine-tuning is allowed, the color triplet partner of DM doublet will be at around 2 TeV mass.

In such an extension of the SM, we include a gauge singlet fermion S which is $\mathbf{1_F}$ and a pair of fermionic electroweak doublets D, D^c which come from $\mathbf{10_F}$. So the doublets have a vector-like mass term and the neutral components of the doublets mix with the singlet hrough renormalizabel couplings to the Higgs boson. Again the $\mathbb{Z}_2$ symmetry ensures the stability of the DM. The doublets are given as:

$$D = \begin{pmatrix} \nu \\ E \end{pmatrix}; \qquad D^c \begin{pmatrix} -E^c \\ \nu^c \end{pmatrix}; \tag{5.20}$$

where ν and E carries the corresponding SM quantum numbers. So, the Lagrangian is given by:

$$\mathcal{L}_{DM} \supset -\lambda D\phi S - \lambda' D^c \tilde{\phi} S - M_D D D^c - \frac{M_S}{2} S^2 + h.c. \tag{5.21}$$

where $\tilde{\phi} = i\,\sigma_2\,\phi$.

The three physical mass eigenstates for the neutral particles are a linear combination of singlet and doublet states:

$$\nu_i = \theta_i S + \alpha_i \nu + \beta_i \nu^c, \qquad i = 1, 2, 3 \tag{5.22}$$

We assume that ν_1 is the lightest Majorana neutral state and is the dark matter candidate. Due to the λ, λ' couplings in the Lagrangian this ν_1 has a Higgs portal and can decay into SM particles. Both the spin-dependent and spin-independent cases have been studied extensively from the phenomenological point of view. For a strict WIMP, the possibilities for avoiding direct and indirect detection are pretty constrained and the prospects for detection or exclusion in the near future are extremely promising.

This exhausts all the possibilities consistent with the assumption that DM fermion mass is not to be tuned order by order to TeV scale. For example, if we try to make $\mathbf{45_F}$ entirely light at the TeV scale, renormalization would make the $(1, 1, 0)$ member lighter than the $(1, 3, 0)$ component. It may be possible to get the correct relic density, but the theory might be very much tuned. Also, there will be too many exotica at the TeV scale.

5.6 Conclusion

Despite the colossal success of Standard Model, the physics beyond SM has become an absolutely necessity. Many extensions of SM manages to explain the origin and smallness of neutrino mass, baryon asymmetry, dark matter and so on. But seldom one single extension can explain multiple issues of SM. $SO(10)$ Grand Unified Theory is one of such rare extension which has the potential to solve all such conundrums.

In this work, we managed to show that one can easily incorporate dark matter in a class $SO(10)$ models where the $B-L$ has been broken by **126**-plet. In such a case, the model has a remnant $\mathbb{Z}_2$ symmetry which can ensure the stability of dark matter. The dark matter candidate can be the singlet of SM coming from different sources. Fermionic DMs must originate from $\mathbf{1}$, $\mathbf{10}, \mathbf{45}, \mathbf{54}, \mathbf{120}, \mathbf{126}, \mathbf{210}$ or $\mathbf{210'}$ representation, while the scalars are restricted to either **16** or **144** of $SO(10)$. One particular advantage of using $\mathbf{1_F}$ besides being the most simplest case is that it does not interfere with other features of the $SO(10)$ model like unification of gauge couplings. Unfortunately, the singlet fermion alone fails to be a viable dark matter candidate and one needs to extend the model with a singlet scalar which acts as a Higgs portal. One also has other options like including multiplets like $\mathbf{10_F}$ along with or without $\mathbf{1_F}$ to address the issue of dark matter in a $SO(10)$ model. Such scenarios are also promising as they possess rich phenomenology and possibilities of having TeV scale dark matter which can be detected in direct or indirect detection experiments.

REFERENCES

[1] P. A. R. Ade *et al.* [Planck Collaboration], Astron. Astrophys. **571**, A1 (2014) doi:10.1051/0004-6361/201321529 [arXiv:1303.5062 [astro-ph.CO]].

[2] K. A. Olive *et al.* [Particle Data Group Collaboration], Chin. Phys. C **38**, 090001 (2014). doi:10.1088/1674-1137/38/9/090001

[3] G. R. Farrar and P. Fayet, Phys. Lett. B **76**, 575 (1978). doi:10.1016/0370-2693(78)90858-4

[4] H. C. Cheng, K. T. Matchev and M. Schmaltz, Phys. Rev. D **66**, 036005 (2002) doi:10.1103/PhysRevD.66.036005 [hep-ph/0204342].

[5] H. C. Cheng and I. Low, JHEP **0309**, 051 (2003) doi:10.1088/1126-6708/2003/09/051 [hep-ph/0308199]. H. C. Cheng and I. Low, JHEP **0408**, 061 (2004) doi:10.1088/1126-6708/2004/08/061 [hep-ph/0405243]. I. Low, JHEP **0410**, 067 (2004) doi:10.1088/1126-6708/2004/10/067 [hep-ph/0409025].

[6] N. G. Deshpande and E. Ma, Phys. Rev. D **18**, 2574 (1978). doi:10.1103/PhysRevD.18.2574

[7] E. Ma, Phys. Rev. D **73**, 077301 (2006) doi:10.1103/PhysRevD.73.077301 [hep-ph/0601225].

[8] T. W. B. Kibble, G. Lazarides and Q. Shafi, Phys. Lett. B **113**, 237 (1982). doi:10.1016/0370-2693(82)90829-2 L. M. Krauss and F. Wilczek, Phys. Rev. Lett. **62**, 1221 (1989). doi:10.1103/PhysRevLett.62.1221 L. E. Ibanez and G. G. Ross, Phys. Lett. B **260**, 291 (1991). doi:10.1016/0370-2693(91)91614-2 L. E. Ibanez and G. G. Ross, Nucl. Phys. B **368**, 3 (1992). doi:10.1016/0550-3213(92)90195-H S. P. Martin, Phys. Rev. D **46**, 2769 (1992) doi:10.1103/PhysRevD.46.R2769 [hep-ph/9207218]. M. Kadastik, K. Kannike and M. Raidal, Phys. Rev. D **81**, 015002 (2010) doi:10.1103/PhysRevD.81.015002 [arXiv:0903.2475 [hep-ph]]. M. Kadastik, K. Kannike and M. Raidal, Phys. Rev. D **80**, 085020 (2009) Erratum: [Phys. Rev. D **81**, 029903 (2010)] doi:10.1103/PhysRevD.80.085020, 10.1103/PhysRevD.81.029903 [arXiv:0907.1894 [hep-ph]]. M. Frigerio and T. Hambye, Phys. Rev. D **81**, 075002 (2010) doi:10.1103/PhysRevD.81.075002 [arXiv:0912.1545 [hep-ph]]. T. Hambye, PoS IDM **2010**, 098 (2011) [arXiv:1012.4587 [hep-ph]]. L. J. Hall, K. Jedamzik, J. March-Russell

and S. M. West, JHEP **1003**, 080 (2010) doi:10.1007/JHEP03(2010)080 [arXiv:0911.1120 [hep-ph]]. J. McDonald, Phys. Rev. Lett. **88**, 091304 (2002) doi:10.1103/PhysRevLett.88.091304 [hep-ph/0106249]. X. Chu, T. Hambye and M. H. G. Tytgat, JCAP **1205**, 034 (2012) doi:10.1088/1475-7516/2012/05/034 [arXiv:1112.0493 [hep-ph]]. C. E. Yaguna, JCAP **1202**, 006 (2012) doi:10.1088/1475-7516/2012/02/006 [arXiv:1111.6831 [hep-ph]].

[9] Y. Mambrini, N. Nagata, K. A. Olive, J. Quevillon and J. Zheng, Phys. Rev. D **91**, no. 9, 095010 (2015) doi:10.1103/PhysRevD.91.095010 [arXiv:1502.06929 [hep-ph]].

[10] N. Nagata, K. A. Olive and J. Zheng, JHEP **1510**, 193 (2015) doi:10.1007/JHEP10(2015)193 [arXiv:1509.00809 [hep-ph]].

[11] S. Esch, M. Klasen and C. E. Yaguna, Phys. Rev. D **88**, 075017 (2013) doi:10.1103/PhysRevD.88.075017 [arXiv:1308.0951 [hep-ph]].

[12] T. Cohen, J. Kearney, A. Pierce and D. Tucker-Smith, Phys. Rev. D **85**, 075003 (2012) doi:10.1103/PhysRevD.85.075003 [arXiv:1109.2604 [hep-ph]].

CHAPTER 6

SUMMARY AND CONCLUSIONS

This dissertation has been dedicated to the studies of the physics beyond the Standard Model (SM) of particle physics. One particular focus of the study was towards a class of extension of SM known as $SO(10)$ grand unified theory (GUT). Such a model can unify all the gauge couplings at a large enough scale compatible with the existing bounds on the proton life-time, deliver a realistic Yukawa sector in agreement with all data on flavor physics, can explain the origin and the smallness of neutrino masses as well as the origin of the baryon asymmetry of the universe either via leptogenesis or post-spheleron baryogenesis. $SO(10)$ models can provide viable dark matter candidate through breaking of a global PQ $U(1)$ symmetry in the form of axions or dark matter can be a SM singlet residing inside a $SO(10)$ multiplet stabilized by a remnant $\mathbb{Z}_2$ symmetry of $B-L$ breaking by **126**-plet.

In Chapter 2, a minimal renormalizable non-supersymmetric $SO(10)$ grand unified model with a symmetry breaking sector consisting of Higgs fields in the $\mathbf{54_H} + \mathbf{126_H} + \mathbf{10_H}$ representations was studied. This model admits a single intermediate scale associated with Pati-Salam symmetry along with a discrete parity. Spontaneous symmetry breaking, the unification of gauge couplings and proton lifetime estimates were studied in details in this framework. Including threshold corrections self-consistently, obtained from a full analysis of the Higgs potential, we showed that the model is compatible with the current experimental bound on proton lifetime. The model generally predicts an upper bound of few times 10^{35} yrs for proton lifetime, which is not too far from the present Super-Kamiokande limit of $\tau_p \gtrsim 1.4 \times 10^{34}$ yrs. With the help of a Pecci-Quinn symmetry and the resulting axion, the model provides a suitable dark matter candidate while also solving the strong CP problem. The intermediate scale, $M_I \approx (10^{13} \sim 10^{14})$ GeV which is also the $B-L$ scale, is of the right order for the right-handed neutrino mass which enables a successful description of light neutrino masses and oscillations. The Yukawa sector of the model consists of only two matrices in family space and leads to a predictive scenario for quark and lepton masses and mixings. The branching ratios for proton decay are calculable with the leading modes being $p \to e^+\pi^0$ and $p \to \overline{\nu}\pi^+$. Even though the model predicts no new physics within the reach of LHC, the next generation proton decay detectors and axion search experiments have the capability to pass verdict on this minimal

scenario.

In Chapter 3, we presented a general mechanism of electroweak symmetry breaking by evolution of the Higgs mass parameter of the theory known as "Radiative Electroweak Symmetry Breaking". Even though the mechanism fails to work in SM due to the dominance of gauge coupling contributions to the evolution of Higgs mass parameter, the mechanism is quite successful in various extensions of SM. The work is based on the fact that with suitable terms in the renormalization group equations (RGEs), one can evolve the mass parameters in such a way that the mass parameter corresponding to the electroweak symmetry breaking scalar can be negative in low energy while it starts off being positive at high energy scale. If such a solution exists one must also ensure the boundedness of the potential and the perturbitivity of the theory. We showed that such a radiative electroweak symmetry breaking can occur for SM extensions like Type-II seesaw model, radiative neutrino mass model and the inert doublet model. Even the simplest extension of SM by a real scalar singlet can perform such a radiative symmetry breaking and under suitable condition the electroweak vacuum becomes stable upto planck scale. We have also analyzed a variant of quark seesaw model which was originally based on a left-right symmetric model and introduces TeV scale vector-like fermions. The model can accommodate a scalar of 750 GeV which is the potential candidate particle for the recently reported excess at around 750 GeV diphoton invariant mass, but with a signal strength lower than initially reported down.

In Chapter 4, one of the maximal subgroup, namely $O(3)_L \times O(3)_R$ of flavor group of SM fermions, namely $[U(5)]^5$ was gauged and subsequently broken by the vacuum expectation values (vevs) of 7-plets ($\chi^{L,R}$) of $O(3)_{L,R}$ and electroweak symmetry by the scalar ϕ which is a complex bi-fundamental of the flavor group and doublet of $SU(2)_L$. This scalar breaks the flavor gauge group to $D_{3L} \times D_{3R}$ which is nicely supported by the flavor constrains if this structure further gets broken by vevs of the order of few GeV. This last stage of symmetry breaking can be done by $\psi(3,3)$ which is a real bi-fundamental of the gauged flavor group with a particular vev structure or by a pair of fundamentals $\psi_L + \psi_R$ along with a bi-fundamental with diagonal vev structure. Such models can provide a scalar particle of 750 GeV mass which can be a suitable candidate for the recently reported excess in the diphoton channel. For the bi-fundamental case, it has been shown that the model can produce the right order of production crosssection $\times$ Branching ratio ≈ 3 fb while the decay width is of the order of 5 GeV.

In Chapter 5, we have studied the possible dark matter candidate in the context of $SO(10)$ grand unified theories (GUTs). Motivated by the long list of attractive features of such class of models, we have studied all the possible TeV scale dark matter candidates in $SO(10)$ GUTs. Being

a rank-five group $SO(10)$ has an extra diagonal generator which can be identified as the $B-L$ generator. It has been shown that if the $B-L$ is broken by **126**-plet, a discrete group $\mathbb{Z}_2$ remains and can ensure the stability of appropriate dark matter candidate. A lot of possibilities have been considered and the simplest case - dark matter being a fermionic singlet- has been proposed and studied extensively. Even though this simple case has the benefit of not spoiling the other features of $SO(10)$ like gauge coupling unification, such a dark matter has no renormalizable coupling to SM particle and gets frozen out when it is very relativistic. Again the simplest solution is adding a singlet scalar that ensure renormalizable coupling with the SM Higgs boson via Higgs portal. Other possibilities include $\mathbf{10_F}$ with or without the fermionic singlet. One important consequence of using particles from $\mathbf{10_F}$ as dark matter candidate is that the multiplet also contains color triplet which is not protected by any symmetry. Such a color triplet will decay leading to detectable signature in LHC and one can either establish or exclude the model in near future. Higher representation of fermions and scalars can also be introduced as DM candidate if the desired component is protected by the aforementioned $\mathbb{Z}_2$ symmetry, but usually requires quite a bit extra fine-tuning and one also needs to be careful about the effects of such multiplets in the gauge couplings evolution.

Thus the dissertation presents various well motivated extension of SM emphasizing on the feature commonly known as "unification". We ended up not having detectable signature in LHC for all the cases studied, but with the help of other wonderful experiments namely proton decay detectors like Super-Komiakande, Hyper-Komiakande (in future), DUNE(in future), various dark matter and axion detectors like XENON, LUX, ADMX can provide a verdict on such models. Even though one might feel uncomfortable in the absence of a definite experimental guidance, one should also realize that we have enough experimental evidence of physics beyond SM. One needs to continue investigating theoretically well motivated yet phenomenologically realistic models following the footsteps of Paul Dirac, who said "If you are receptive and humble, mathematics will lead you by the hand.". Yet the model needs to be able to explain all the experimental evidences. Such a model should also be able to predict certain outcomes in the current or upcoming experiments all around the world as "In reality, a theory in natural science cannot be without experimental foundations; physics, in particular, comes from experimental work." - Samual C. C. Ting

VITA

Saki Ahmed Khan

Candidate for the Degree of

Doctor of Philosophy

Dissertation: UNIFICATION AND PHYSICS BEYOND THE STANDARD MODEL

Major Field: Physics

Biographical:

Education:

Completed the requirements for the degree of Doctor of Philosophy with a major in Physics at Oklahoma State University in July, 2016.
Recieved Diploma in High Energy Physics (Equivalent to M.Sc.), The Abdus Salam International Centre for Theoretical Physics (ICTP), Trieste, Italy in 2009
Received B.Sc. (Hons.), Department of Physics, University of Dhaka, Dhaka, Bangladesh in 2007.

Recognition:

PITT PACC travel award, Phenomenology Symposium 2015, University of Pittsburgh.
Outstanding Research Assistant (2015), Department of Physics, Oklahoma State University.
Outstanding Teaching Assistant (2014), Department of Physics, Oklahoma State University.
Doctoral Excellence Award (2009-11), Department of Physics, Oklahoma State University.
Professor Ali Imam Memorial Gold Medal, 2004 for the highest achievement in BSc. (Hons.) in Physics, Physics Department, University of Dhaka.

Professional Memberships:

American Physical Society